Modeling Effects of Habitat Change and Restoration Alternatives on Salmon in the Chehalis River Basin Using a Salmonid Life-Cycle Model

Phase 1 Report for Contracts **WDFW #15-03970** and **RCO #17-1477**

April 2021

NOAA Contract Report Series NMFS-NWFSC-CR

Modeling Effects of Habitat Change and Restoration Alternatives on Salmon in the Chehalis River Basin Using a Salmonid Life-Cycle Model

Timothy J. Beechie,[1] Colin Nicol,[1] Caleb Fogel,[1] Jeff Jorgensen,[1] Jamie Thompson,[1] Gus Seixas,[1] Josh Chamberlin,[1] Jason Hall,[1] Britta Timpane-Padgham,[1] Peter Kiffney,[1] Spencer Kubo,[2] and Jenna Keaton[1]

April 2021

[1]Fish Ecology Division
Northwest Fisheries Science Center
2725 Montlake Boulevard East
Seattle, Washington 98112

[2]School of Aquatic and Fishery Sciences
University of Washington
1122 Northeast Boat Street
Seattle, Washington 98195

U.S. DEPARTMENT OF COMMERCE

National Oceanic and Atmospheric Administration
National Marine Fisheries Service
Northwest Fisheries Science Center

Contents

List of Acronyms

7-DADM: 7-day average daily maximum (temperature)
ADA: average of daily averages (temperature)
ADM: average daily maximum (temperature)
AIC: Akaike's Information Criterion
ASEP: Aquatic Species Enhancement Plan
ASRP: Aquatic Species Restoration Plan
AugADA: August average of daily averages (temperature)
BIP: beaver intrinsic potential
BLM: Bureau of Land Management
C-CAP: Coastal Change Analysis Program (NOAA landcover data)
CFS: cubic feet per second
CVS: Continuous Vegetation Survey
DEM: Digital Elevation Model (digital elevation topographic data)
DHSVM: Distributed Hydrologic Soil Vegetation Model
EDR: Ecological Diversity Region
EDT: Ecosystem Diagnosis and Treatment
EFC: Environmental Flow Components
GIS: Geographic Information System
GLO: General Land Office
GSU: geospatial unit
IHA: Indicators of Hydrologic Alteration (a set of hydrologic metrics for evaluating changes in stream flows)
IPCC: International Panel on Climate Change
LAS: LASer file format for lidar point cloud data
LCM: life-cycle model
LR: large river
NHD: National Hydrologic Dataset
NLCD: National Land Cover Dataset
NOAA: National Oceanic and Atmospheric Administration
NorWeST: North West Stream Temperature
NPGO: North Pacific Gyre Oscillation
NSD: Natural Systems Design
NWIFC: Northwest Indian Fisheries Commission
PDO: Pacific Decadal Oscillation
PRISM: Parameter-elevation Regressions on Independent Slopes Model
PSU: Portland State University
PVA: population viability analysis
RCO: Recreation and Conservation Office
RCP: Representative Concentration Pathway

RCW: Revised Code of Washington
SAR: smolt-to-adult return
SC: side channel
SOI: Southern Oscillation Index
SRC: standardized regression coefficient
SRT: Science Review Team
SS: small stream
SST: Sea Surface Temperature
SWIFD: Statewide Integrated Fish Distribution
UGA: Urban Growth Area
USGS: United States Geological Survey
UWI: Coastal Upwelling Index
VIC: Variable Infiltration Capacity
VSP: viable salmon population
WDF: Washington Department of Fisheries
WDFW: Washington Department of Fish and Wildlife
WDNR: Washington Department of Natural Resources

Acknowledgments

Executive Summary

A key element of the *Aquatic Species Restoration Plan* (ASRP) for the Chehalis Basin is habitat restoration for anadromous salmonids of economic and cultural significance, including spring and fall Chinook salmon (*Oncorhynchus tshawytscha*), coho salmon (*O. kisutch*), steelhead (*O. mykiss*), and chum salmon (*O. keta*). The chum model results will be released in 2020. To assist with development of the Chehalis basin ASRP, the National Oceanic and Atmospheric Administration (NOAA) Northwest Fisheries Science Center developed a suite of analyses and models to assess habitat changes from historical (pre-EuroAmerican settlement or natural potential) conditions to present. The results of those habitat assessments were then used in a salmonid Life-Cycle Model (LCM) with nine diagnostic scenarios to determine which types of habitat changes most limit rebuilding of salmon populations within the Chehalis Basin, and how those limitations vary by subbasin. This identification of habitat constraints is intended to help identify key restoration actions for salmon populations in the basin. In addition to modeling the diagnostic scenarios, three restoration scenarios developed by the Science and Review Team (SRT) and Steering Committee (including climate change and future development) were modeled to evaluate potential improvements in salmon and steelhead populations in the future. This modeling completes Phase 1 of the NOAA modeling process. Additional modeling will occur in Phase 2 of developing the ASRP.

Model Overview

The NOAA analysis uses three separate models to take raw GIS data and ultimately produce life-cycle model results for each salmonid species under each diagnostic or restoration scenario (Figure 1). The three components of the model are the spatial analysis, the habitat analysis, and the life-cycle model (blue circles in Figure 1). We refer to this suite of models as the NOAA Model. The spatial analysis processes the raw data files and produces five habitat data layers that contain current habitat areas and conditions, which are the inputs to the habitat analysis. In the habitat analysis, the five habitat data layers are used to estimate both historical and current life-stage capacities and productivities for each species and sub-basin in each diagnostic or restoration scenario. That is, the outputs of the habitat analysis are individual data files for each diagnostic or habitat restoration scenario, with each file containing the life-stage and species-specific capacities and productivities used as the inputs to the LCM.

The LCM is then run with each diagnostic scenario for each species to diagnose which past habitat changes most limit rebuilding of each species, as well as with each restoration scenario to assess potential improvements in each species in the future (including climate change and future development). The model is run without harvest for all species and scenarios. The model outputs include estimates of the equilibrium spawner abundance during the last 50 years of each model run (N_{eq}), as well as cumulative life-cycle productivity (P_n) and cumulative life-cycle capacity (C_n). The species currently modeled are

Raw data layers:
USGS 10-m DEM
C-CAP land cover raster
PRISM mean annual precip
Washington roads
Ecological Diversity Regions
SWIFD streamlines
WDFW Migration barriers
WDFW Thermalscape
Riparian files
Floodplain habitat polygons
Large river edge habitat
Large river backwaters
Spawning riffles

Final habitat layers:
Large river edge habitat
Large river backwaters
Large river spawning riffles
Floodplain habitats
Attributed streamline

Diagnostic scenarios:
Migration barriers
Fine sediment
Wood loading
Shade (temperature)
Bank armor
Channel straightening
Beaver ponds
Floodplain habitats

Restoration scenarios:
Restoration actions
Climate change effects
Future development

LCM results
-Coho
-Spring Chinook
-Fall Chinook
-Steelhead

Figure 1. Illustration of the analysis steps, proceeding from the raw data layers, to habitat data layers, to habitat scenarios, and finally to the life-cycle model (LCM) outputs. C-CAP is NOAA's Coastal Change Analysis Program; SWIFD is the Washington Department of Fish and Wildlife (WDFW) Statewide Integrated Fish Distribution.

fall Chinook salmon, spring Chinook salmon, coho salmon, and steelhead. Results in this report are from Version 13 of the NOAA model.

Life-cycle Models

The NOAA Chehalis salmonid life-cycle models are population dynamics models driven by demographic rates, productivities, and capacities, where cohorts are tracked through time and space in an age-structured, stage-based approach. The spatial units in the life-cycle models are 63 individual subbasins or mainstem reaches (Section 3.1.1), each of which is treated as a separate population with some percentage of juveniles interacting in the mainstem as they move downstream. Through a series of computational loops, cohorts are moved through the life stages and ages, with corresponding life-stage capacity and productivity parameters for each subbasin. Each loop iteration represents a one-year time step, transitioning fish from one age class to the next and applying as many intermediate life stages as necessary within a time step. That is, each time step in the model represents one year, and that year may include multiple life stages (e.g., fry colonization, summer rearing, and winter rearing).

The freshwater life-stages are modeled in a sequence of either density-dependent or density-independent stages. Density-dependent stages use either the Beverton-Holt function or a hockey stick function, applying the life-stage capacities and productivities produced in the habitat analysis. Density independent stages have no capacity limits. The number and structure of life stages varies among species, but all of the salmon and

steelhead modeled for the Chehalis basin share certain stages or parameters in common, such as spawning, egg incubation, juvenile rearing, delta-bay rearing, ocean rearing, and upstream migration (Section 3.3). The largest differences among species are in length and locations of juvenile rearing, length of ocean rearing, and age structure of returns. Details of the life-cycle models for each species are in Section 4.

Diagnostic Scenarios

The diagnostic scenarios include scenarios for historical and current habitat conditions, as well as nine scenarios in which each habitat factor is set to historical conditions independently (keeping all other factors in current conditions). The diagnostic scenarios that set one habitat component at a time to historical conditions help determine which types of habitat restoration will most benefit salmon and steelhead populations. In these scenarios, we evaluate the separate influences of changes in the following processes and habitat factors:

1. Migration barriers
2. Fine sediment in spawning gravels
3. Wood abundance change in small streams and large rivers
4. Shade (temperature) changes in small streams and large rivers
5. Bank armor in large rivers
6. Large river channel straightening
7. Beaver pond changes in small streams
8. Floodplain habitat change (including side channels, ponds, marshes, lakes, and temperature effect)
9. Wood abundance and floodplain habitat change combined

The diagnostic scenario results indicate that restoration of shade, wood, beaver ponds and floodplain habitat provide the greatest opportunities to increase spawner abundances for the four species modeled in the Chehalis River basin (Table 1, Section 5.1). Removal of migration barriers provides only a modest potential increase in coho salmon in the Chehalis River basin, and only in a few areas of the basin where barriers are concentrated (Table 1, Section 5.2). The largest modeled restoration potentials for coho salmon are from restoring overwinter habitats such as beaver ponds and floodplain habitats, whereas the largest modeled restoration potentials for spring Chinook come from restoring wood abundance, shade, and floodplain habitats. The largest modeled restoration potentials for fall Chinook and steelhead is the combination of restoring wood abundance and floodplain habitats. Floodplain restoration opportunities are greatest in the Black River, Cascade Mountain, and Mainstem EDRs, as well as in the Satsop River subbasin (Section 5.2). Shade restoration opportunities are greatest in the Cascade Mountains, Central Lowlands, Black River, and Lower Chehalis Mainstem EDRs. Opportunities for wood and beaver pond restoration are relatively evenly distributed across all EDRs, but particularly in small streams (<20m bankfull width). Reduction of fine sediment may also be important, but uncertainty in reach-specific fine sediment levels and sources of fine sediment require further field inventory to identify and prioritize sediment reduction actions.

Table 1. Modeled number of spawners (N_{eq}, without harvest) in each diagnostic scenario for coho, spring Chinook, fall Chinook, and steelhead for the Chehalis basin (percent change in parentheses). Abundance cells (columns 2-5) with changes >25% are dark blue, and abundance cells with changes 10-25% are shaded light blue. Scenarios (column 1) with 3 or more species with abundance values >25% are dark blue, 2 species >25% are medium blue, and 1 species >25% are light blue. Gray cells are current and historical conditions.

Scenario	Coho	Spring Chinook	Fall Chinook	Steelhead
Current conditions	90,625	1,035	31,746	16,092
No barriers	98,645 (9%)	1,035 (0%)	32,388 (2%)	16,577 (3%)
Historical fine sediment	104,514 (15%)	1,618 (56%)	42,227 (33%)	18,166 (13%)
Historical wood	113,230 (25%)	1,363 (32%)	39,096 (23%)	20,949 (30%)
Historical shade	109,092 (20%)	1,454 (40%)	32,341 (2%)	17,399 (8%)
Historical bank conditions	90,712 (0%)	1,062 (3%)	32,346 (2%)	16,181 (1%)
Historical large river length	91,048 (0%)	1,108 (7%)	33,128 (4%)	16,795 (4%)
Historical beaver ponds	181,202 (100%)	1,042 (1%)	32,596 (3%)	16,064 (0%)
Historical floodplain habitat	145,702 (61%)	1,394 (35%)	36,439 (15%)	18,822 (17%)
Historical wood and floodplain	172,209 (90%)	1,797 (74%)	44,733 (41%)	24,285 (51%)
All historical conditions	396,226 (337%)	3,551 (243%)	67,570 (113%)	29,867 (86%)

Coho Salmon

Modeled coho salmon spawner abundance increased by 100% in the historical beaver pond scenario and 61% in the historical floodplain scenario (Figure 2). The historical wood scenario increased modeled spawner abundance by 25%, whereas the historical wood + floodplain scenario increased modeled spawner abundance by 90%. Historical shade, migration barriers, and fine sediment increased spawner abundance by 9-20%, and all other scenarios produced less than 1% change. The diagnostic scenario with all historical conditions had a modeled spawner abundance more than 300% higher than the modeled current abundance.
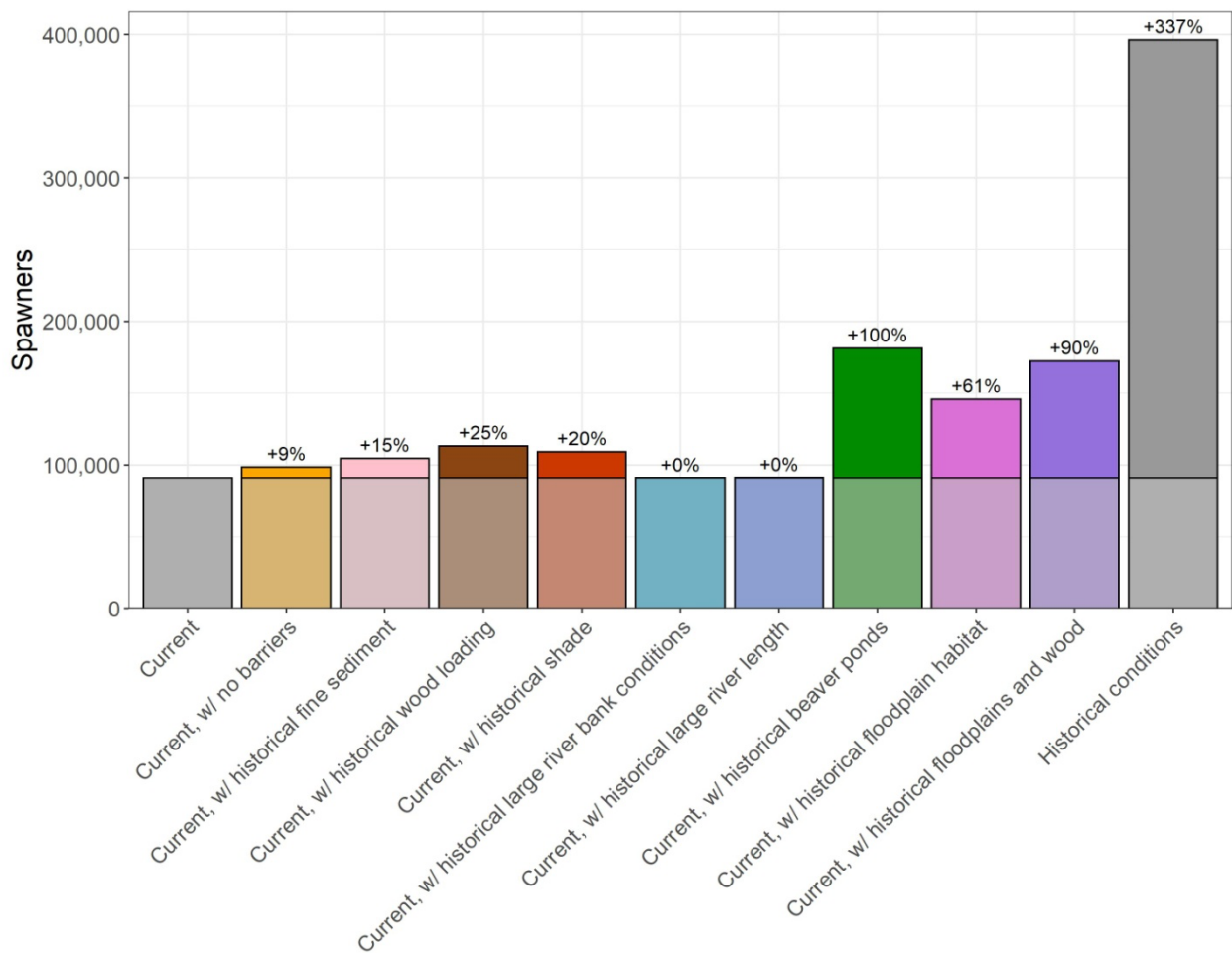
Figure 2. Modeled difference in spawner abundance (N_{eq}, without harvest) among diagnostic scenarios for coho salmon.

Spring Chinook Salmon

Modeled spring Chinook spawner abundance increased by 41% and 35% in the historical shade and floodplain scenarios, respectively, primarily due to reduced temperatures. Abundance increased by 57% in the historical fine sediment scenario, and by 32% in the historical wood abundance scenario (Figure 3). The historical wood and floodplain combination scenario produced a 74% increase in modeled spawner abundance. All other scenarios produced a change in spawner abundance of 7% or less (no barriers, historical beaver ponds, historical large river bank conditions, and historical large river length). The diagnostic scenario with all historical conditions had a spawner abundance of about 3,500 compared to modeled abundance under current conditions of about1,000 (an increase of 243%).

Model version = v13
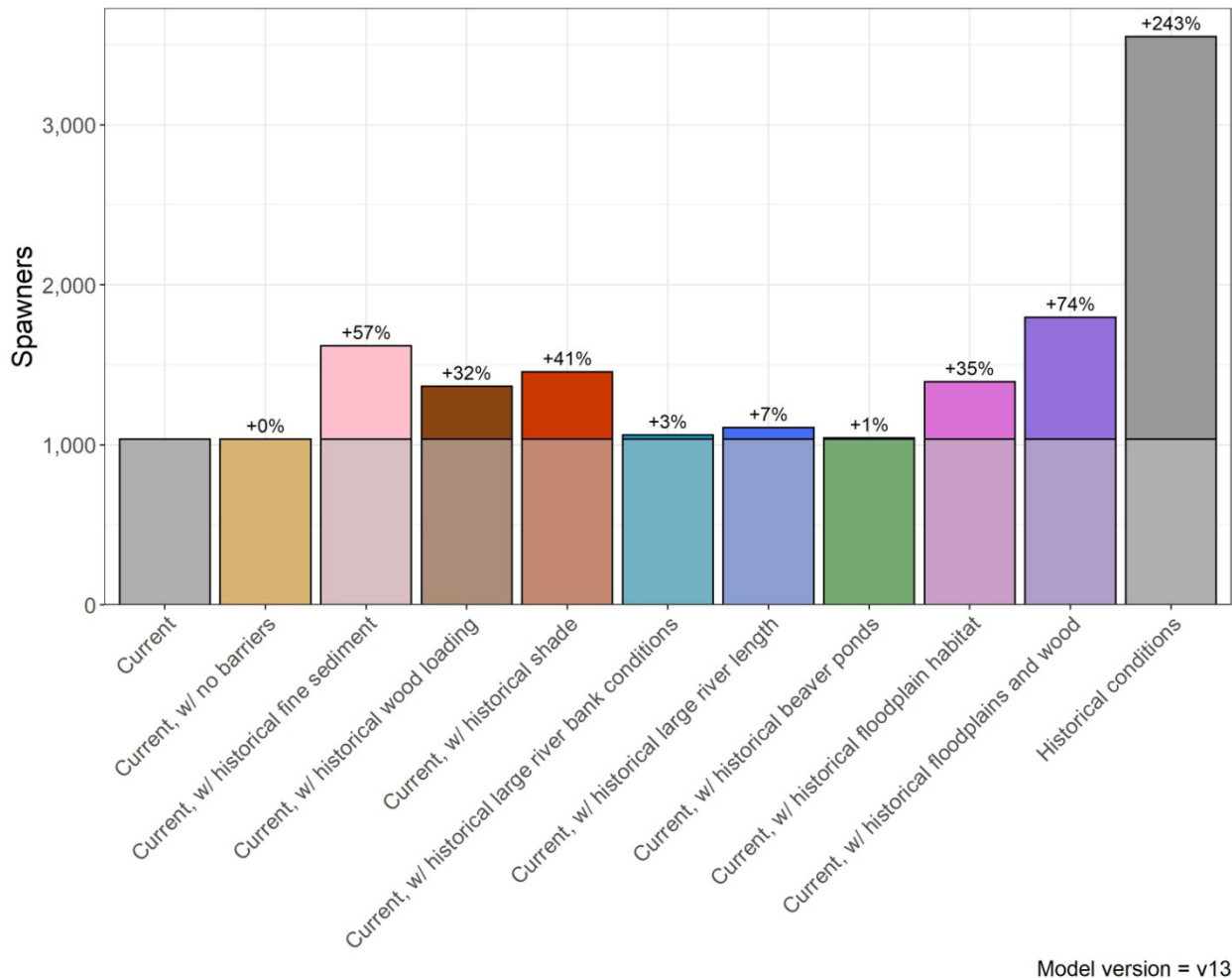
Figure 3. Modeled difference in spawner abundance (N_{eq}, without harvest) among diagnostic scenarios for spring Chinook salmon.

Fall Chinook Salmon

Modeled fall Chinook spawner abundance increased by 41% in the historical wood and floodplain combination scenario, but most of that increase was apparently from wood abundance (23% in the wood abundance scenario alone) (Figure 4). Modeled spawner abundance increased 33% in the historical fine sediment scenario, suggesting that fine sediment may be a significant issue, particularly for the fry migrant component of the population. All other scenarios produced a change in spawner abundance of 15% or less (no barriers, historical beaver ponds, historical large river bank conditions, historical large river length, historical shade, and historical floodplain habitat). The diagnostic scenario with all historical conditions had a spawner abundance of about 67,000 compared to modeled abundance under current conditions of about 32,000 (an increase of 113%).
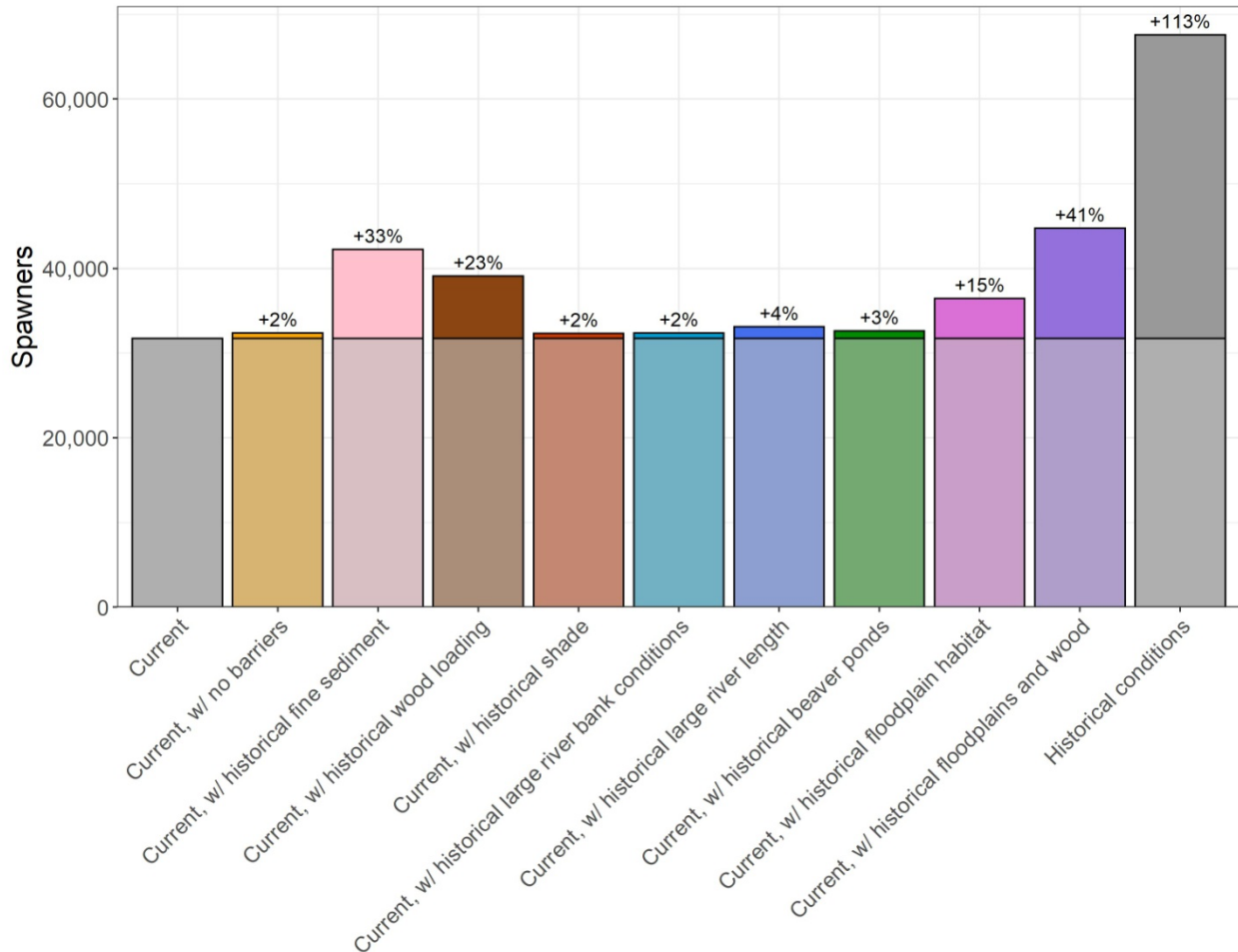
Model version = v13

Figure 4. Modeled difference in spawner abundance (N_{eq}, without harvest) among diagnostic scenarios for fall Chinook salmon.

Steelhead

Modeled steelhead spawner abundance increased by about 30% in the historical wood abundance scenario and 13 to 17% in the fine sediment and floodplain habitat scenarios (Figure 5). The historical wood + floodplain scenario increased modeled spawner abundance by 51%. All other scenarios produced less than 5% change in abundance. The diagnostic scenario with all historical conditions had a modeled spawner abundance 86% higher than the modeled current abundance.

Model version = v13
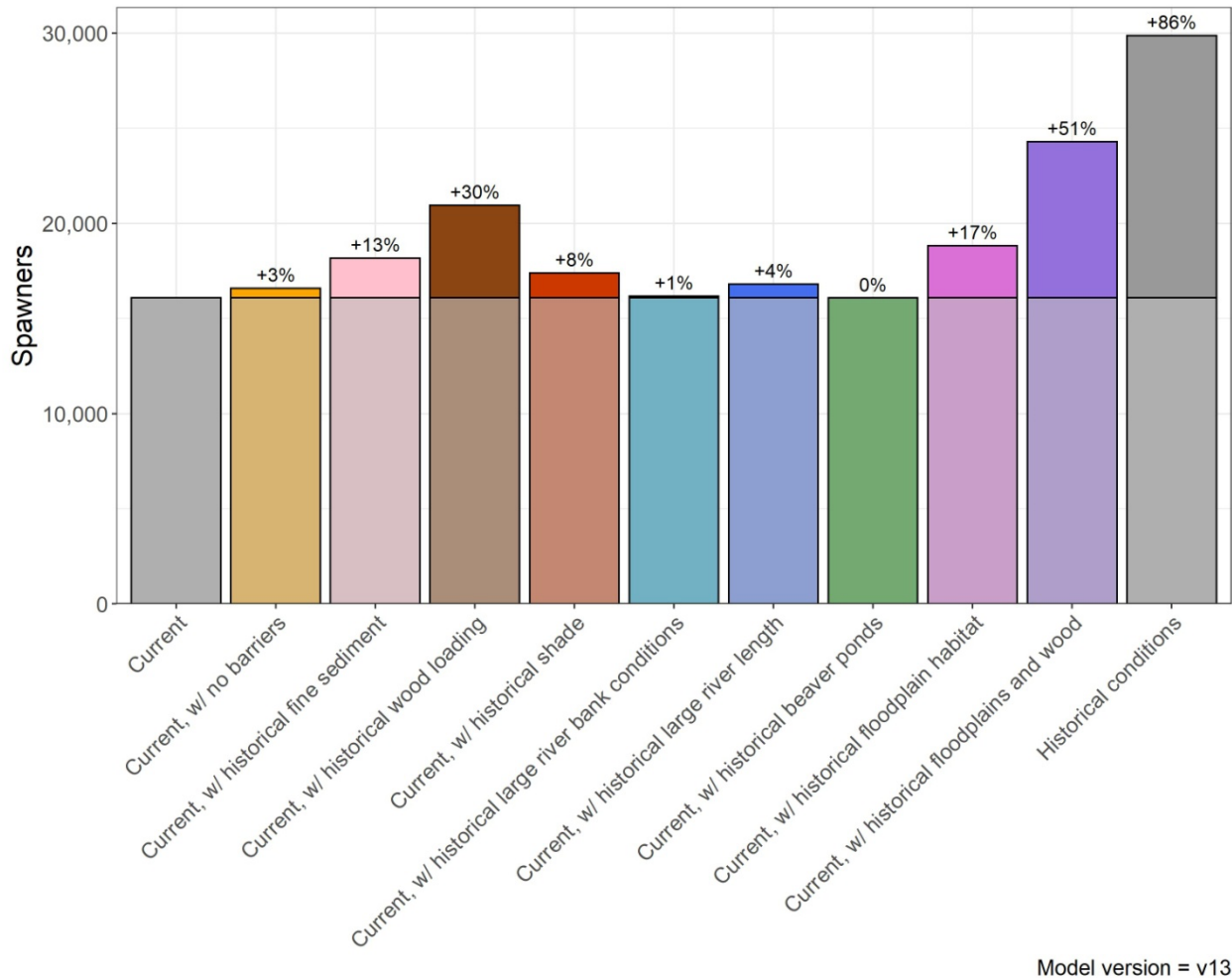
Figure 5. Modeled difference in spawner abundance (N_{eq}, without harvest) among diagnostic scenarios for steelhead.

Potential Restoration Actions

The diagnostic scenarios suggest that five types of habitat changes have had significant effects on salmon populations in the Chehalis basin and therefore afford the largest restoration opportunities: loss of floodplain habitat, loss of wood from streams and rivers, loss of beaver ponds, loss or reduction of riparian forests, and, in some locations, migration

barriers. Restoration of these habitats or habitat attributes is likely to substantially increase salmon spawner abundance of each species. Moreover, there are sufficient data to indicate where and what types of restoration actions are most needed for these habitat changes. A sixth potentially important habitat change—increased fine sediment and reduced incubation survival—requires further field inventory to identify and prioritize restoration actions. A summary of the actions and important locations is in Table 2.

Table 2. Summary of potential restoration actions indicated by the diagnostic scenario results.

Restoration action	Summary
Floodplain reconnection	Reconnection of floodplain habitats provides overwintering habitat for coho salmon, as well as decreasing stream temperature and increasing side channel spawning and rearing areas for Chinook and steelhead. Among subbasins, the Lower Mainstem Chehalis, Skookumchuck, Black, Humptulips, and Satsop have large floodplain restoration potential (Section 6). Each of those areas had significant historical marsh habitat that has been lost or degraded (Appendix F).
Wood placement	Wood restoration is likely to modestly benefit all species. Larger habitat changes are likely in small, moderate-slope reaches where wood substantially increases pool and spawning gravel area. The potential benefits of wood restoration are relatively evenly distributed across the subbasins, and the analysis does not indicate strong spatial priorities for wood restoration.
Beaver pond restoration	Restoring beaver ponds to small streams is likely to significantly benefit coho salmon (more than doubling the population in the historical beaver pond scenario), with relatively small effects on the other three species. The potential for recovery of beaver ponds and beaver populations is greatest the Olympic Mountains, Grays Harbor Tributaries, Willapa Hills, Black Hills, Cascade Mountains, Black River and Central Lowlands EDRs.
Riparian restoration	Riparian restoration includes both riparian planting and protection. It is likely to significantly increase shade and reduce stream temperature in a few areas, some of which are very important to spring Chinook. Riparian restoration should also increase wood recruitment in the future, although wood abundance in streams typically does not begin to increase until riparian forests are well over 60 years old.
Barrier removal	While the potential for barrier removals to benefit species is small overall (especially for spring Chinook, which have only one barrier within their range), local benefits can be large (e.g., in subbasins such as the Skookumchuck, Cloquallum, Newaukum, and South Fork Chehalis).
Fine sediment reduction	The diagnostic scenario for historical fine sediment indicates that spring and fall Chinook subpopulations are very sensitive to fine sediment levels, however we are unsure of where and what types of restoration actions are needed. This suggests that field assessments of fine sediment levels and sources of fine sediment should be conducted to identify the most important sources of sediment to address through restoration actions.

Habitat Restoration Scenarios

We ran a No Action future scenario and three restoration scenarios developed and agreed upon by the Science Review Team (SRT), which are intended to help evaluate the potential biological benefits of habitat restoration for each species modeled. These scenarios are listed as the No Action alternative and Scenarios 1, 2, and 3. Each scenario includes estimated improvement in life-stage capacities and density-independent productivities for mid-century and late-century. The No Action alternative includes riparian tree growth, removal of certain barriers, future development, and climate change. The three restoration scenarios represent low, moderate, and high levels of restoration effort:

1. Scenario 1 focuses restoration effort in 38 geospatial units (GSUs); within each targeted GSU barriers are removed and 20% to 50% of the stream length is treated.
2. Scenario 2 adds to Scenario 1 by restoring segments in 10 additional GSUs (48 GSUs total); within each targeted GSU barriers are removed and 20% to 50% of the stream length is treated.
3. Scenario 3 adds to Scenario 2 by restoring segments in 19 additional GSUs (67 GSUs total); within each targeted GSU barriers are removed and 20% to 75% of the stream length is treated.

In addition to barrier removal, the proposed restoration actions are wood addition, riparian plantings, and floodplain reconnection. In all scenarios, riparian and floodplain restoration are applied only in GSUs outside managed forest lands. Barrier removal and wood placement are applied in GSUs both inside and outside managed forest lands. In GSUs inside managed forest lands, we also model passive recovery of riparian conditions as forested buffer zones mature. Each restoration scenario includes improvement in life-stage capacities and productivities, based on a percentage of improvement from the current to the historical condition within a treated reach.

The restoration scenario results indicate that restoration actions increase abundance and productivity for all species, but also that impacts from climate change diminish those increases in the future. Fall Chinook salmon and steelhead are least sensitive to increasing temperatures due to climate change, and all three restoration scenarios increased fall Chinook spawner abundance despite mid- and late-century temperature increases. Spring Chinook and coho salmon are most sensitive to climate change effects on stream temperature and low flows, and without restoration their projected abundances decrease more than 25% by late century in the No Action alternative.

Coho Salmon

Modeled future coho salmon spawner abundance decreased in both of the No Action scenarios, by 10% in the mid-century scenario and 28% in the late century scenario (Figure 6). Mid-century spawner abundance ranged from an increase of 10% in Scenario 1 to an increase of 26% in Scenario 3. Late-century spawner abundance ranged from a decrease of 10% in Scenario 1 to an increase of 2% in Scenario 3.
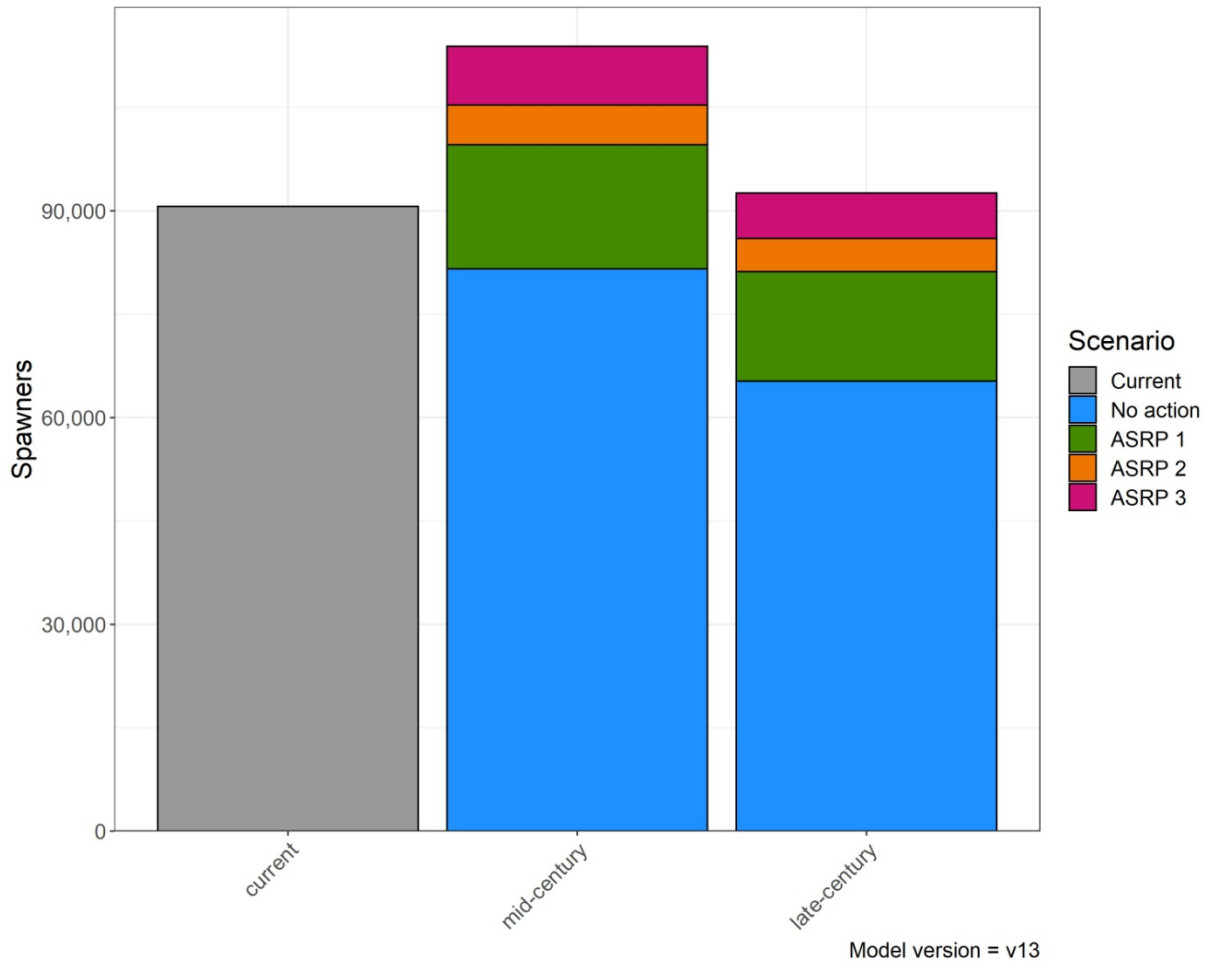
Figure 6. Projected coho spawner abundance (N_{eq}, without harvest) for the No Action alternative and three future restoration scenarios.

Spring Chinook Salmon

Spring Chinook are most sensitive to future temperature changes, and modeled future spring Chinook spawner abundance decreased in the No Action scenarios, by 9% in the mid-century scenario and 39% in the late century scenario (Figure 7). Mid-century spawner abundance ranged from an increase of 15% in Scenario 1 to an increase of 21% in Scenario 3. Late-century spawner abundance decreased in all three scenarios, by 18% in Scenarios 1 and 2 and 13% in Scenario 3.
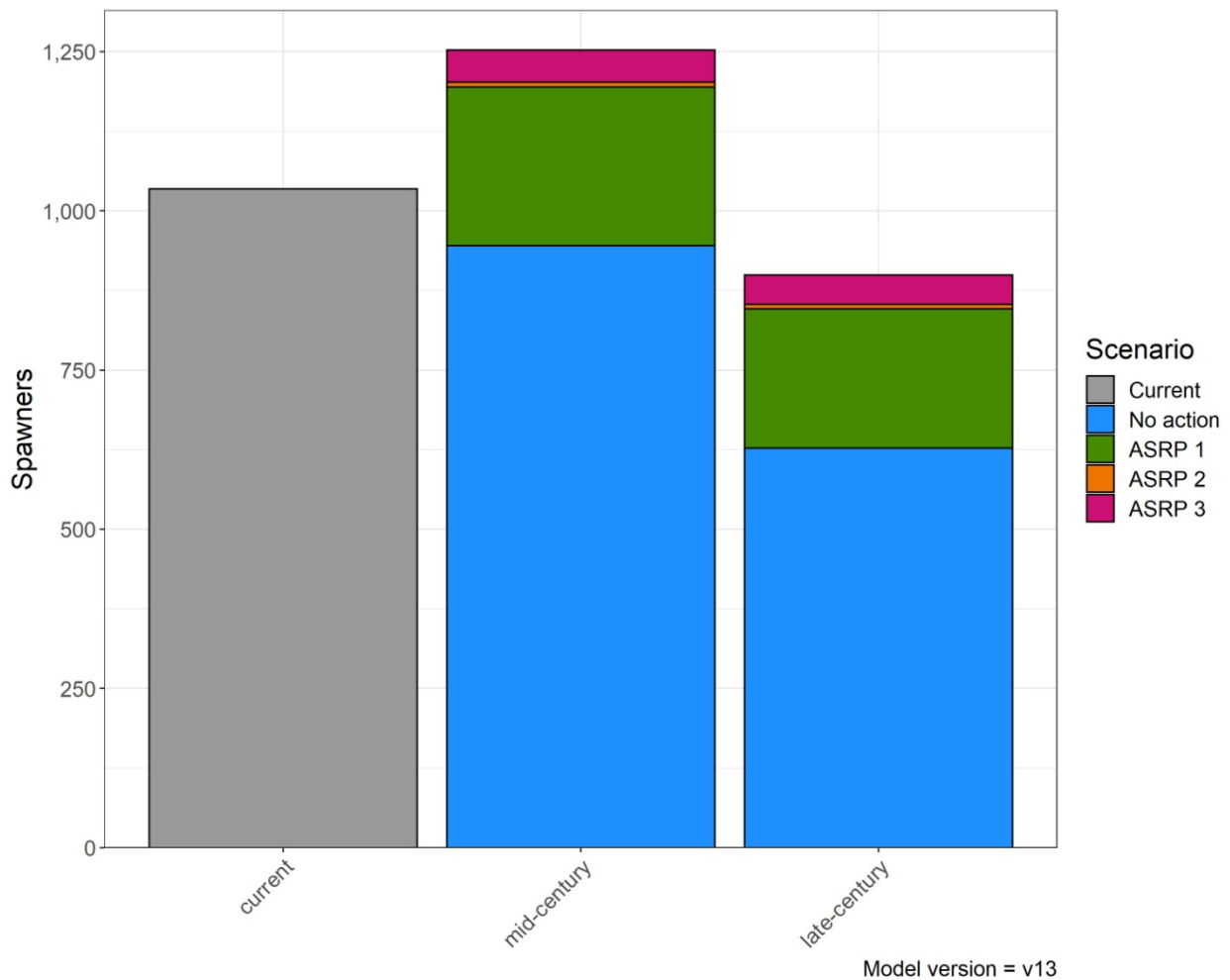
Figure 7. Projected spring Chinook spawner abundance (N_{eq}, without harvest) for the No Action alternative and three future restoration scenarios.

Fall Chinook Salmon

Modeled future fall Chinook spawner abundance decreased by 3% in the mid-century No Action scenario, and by 4% in the late century No Action scenario, indicating that fall Chinook are much less sensitive to stream temperature change than coho salmon or spring Chinook. Modeled abundance increased in all future restoration scenarios (Figure 8). Mid-century spawner abundance increased by 8% in Scenario 1, by 10% in Scenario 2, and by 14% in Scenario 3. Late-century spawner abundance increased by 7% in Scenario 1, 8% in Scenario 2, and 12% in Scenario 3.
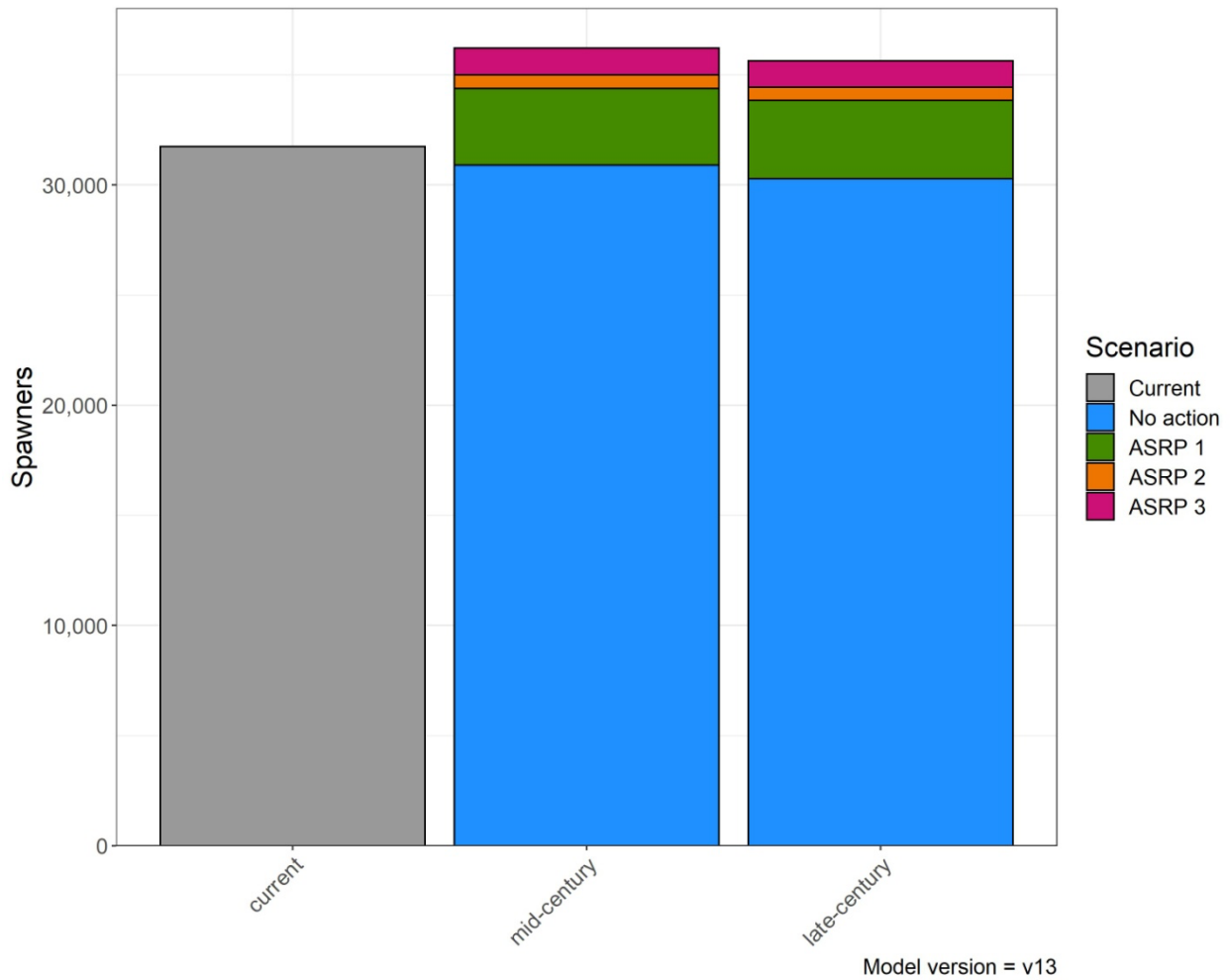
Figure 8. Projected fall Chinook spawner abundance (N_{eq}, without harvest) for the No Action alternative and three future restoration scenarios.

Steelhead

Modeled future steelhead spawner abundance decreased by 5% in the mid-century No Action scenario, and by 18% in the late century No Action scenario, indicating that steelhead are somewhat less sensitive to stream temperature and low flow change than coho salmon or spring Chinook. Modeled abundance increased in all future restoration scenarios (Figure 9). Mid-century spawner abundance increased by 8% in scenario 1, by 11% in scenario 2, and by 14% in scenario 3. Late-century spawner abundance changed by -5% in scenario 1, by -2% in scenario 2, and by +2% in scenario 3.
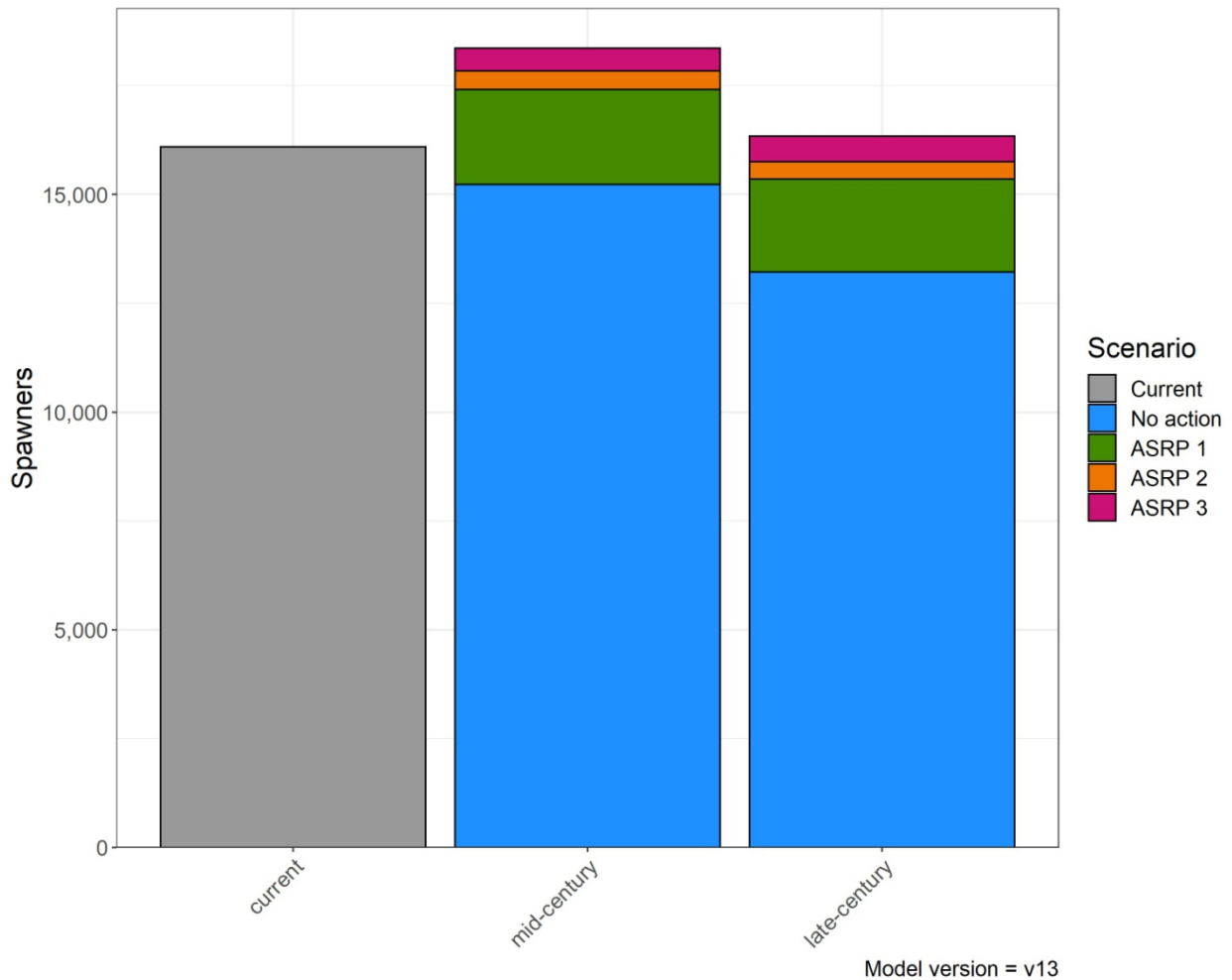
Figure 9. Projected steelhead spawner abundance (N_{eq}, without harvest) for the No Action alternative and three future restoration scenarios.

Summary

The NOAA Model was used to evaluate nine diagnostic scenarios, along with three restoration scenarios. The model results for these scenarios indicate that population declines for coho, spring Chinook, fall Chinook salmon, and steelhead are most attributable to loss of beaver ponds, loss of floodplain habitats, loss of in-stream wood, reduced stream shade in some locations, and potentially increased fine sediment. Migration barriers are a significant cause of decline in only a few subbasins, and primarily for coho salmon and steelhead. These diagnoses highlight that important restoration actions for salmon include:

1. Reconnection of floodplain habitats (side-channels, marshes, and ponds) via levee setback and/or re-aggradation of channels using in-stream wood or beaver dam analogs.
2. Restoration of instream wood to increase spawning and rearing habitat availability (i.e., increase gravel retention and pool formation).
3. Riparian restoration to increase stream shading and reduce stream temperature, as well as to provide long-term wood recruitment in the future.
4. Restoration of beaver populations to increase beaver pond abundance, or potentially use beaver dam analogs to mimic those features.
5. Targeted removal of migration barriers that block access to significant amounts of habitat.
6. Confirm or identify areas with high fine sediment levels, identify sediment sources for those areas, and address sediment sources through restoration actions (e.g., by forest road reduction or remediation, or by reducing other sediment inputs such as agricultural or urban sources).

The restoration scenario results indicate that fall Chinook are least sensitive to future temperature changes, and that restoration actions may increase fall Chinook abundance under all three restoration scenarios even in the late-century period. Spring Chinook, coho salmon, and steelhead are more sensitive to future temperature change. All three scenarios project increases in spawner abundance in mid-century for these three species, but continued temperature increases into the late-century period reduce spawner abundances to near current levels. Scenario 3 projects a slight increase in coho and steelhead spawner abundances in late century, and Scenario 3 keeps spring Chinook spawner abundance slightly below current levels in late century.

1. Introduction

To assist aquatic habitat restoration planning in the Chehalis River basin, the Northwest Fisheries Science Center was contracted to assess changes in key watershed processes, assess habitat changes from historical (or natural potential) conditions to present, and use a salmonid life-cycle model to evaluate which habitat changes most limit the potential rebuilding of salmon populations. The watershed process and habitat change assessments focus on changes in sediment supply, hydrology, riparian functions, floodplain habitat, large river habitat, and small stream habitat. Results of these assessments are used in the spatial model to create reach-specific habitat attributes throughout the Chehalis basin. These habitat attributes are the inputs to the habitat model, which creates input files of subbasin-specific life stage capacities and productivities for the life-cycle models for each diagnostic or restoration scenario. Finally, the life-cycle models integrate habitat losses or improvements across all life stages of salmon and steelhead to determine which losses or improvements will most improve abundance and productivity of each population evaluated. We collectively refer to these three model components (spatial model, habitat model, and life-cycle models) as the NOAA Model. All results in this report were produced using Version 13 of the NOAA Model. This modeling completes Phase 1 of the NOAA modeling process. Additional modeling will occur in Phase 2 of developing the Aquatic Species Restoration Plan (ASRP).

Using the NOAA Model, we created and evaluated a series of nine diagnostic scenarios. The diagnostic scenarios are intended to help understand the relative importance of each type of habitat degradation on each species (e.g., loss of riparian shade, loss of wood, loss of floodplain habitats). We also model a set of restoration scenarios developed by the Science Review Team (SRT) to assess the potential outcomes of restoration balanced against the effects of climate change and future development. These analyses are intended to help inform development of the Aquatic Species Restoration Plan (ASRP) for the Chehalis River basin. The ASRP describes a suite of restoration actions aimed at improving habitats for three "guilds" of aquatic species (1) anadromous salmonids, (2) other fish species, and (3) non-fish species. A key element of the ASRP is habitat restoration for anadromous salmonids of economic and cultural significance, including spring and fall Chinook salmon (*Oncorhynchus tshawytscha*), coho salmon (*O. kisutch*), steelhead (*O. mykiss*), and chum salmon (*O. keta*). Therefore, substantial efforts have been made to understand where and which types of restoration actions will most benefit those species, including development of restoration alternatives and modeling the likely outcomes of each alternative using the Ecosystem Diagnosis and Treatment (EDT) model (ASEP 2014, and current revised EDT model runs).

This report begins with a brief description of the process-based restoration approach and the analyses needed to follow this approach (Section 2). An overview of all of the model components is in Section 3, and Section 4 describes details of the individual species models. Sections 5 through 7 present model results, and Section 8 is a discussion of model uncertainty and sensitivity.

2. A Process-based Assessment Approach

The NOAA Model is designed to diagnose the relative importance of historical changes to salmon habitats and habitat-forming processes, and to evaluate the potential effectiveness of alternative process-based restoration strategies. Process-based restoration focuses on restoring natural rates of physical, chemical, and biological process that sustain river ecosystems (Beechie and Bolton 1999, Kondolf et al. 2006, Beechie et al. 2010). Examples of landscape processes included here are erosion and sediment supply, riparian processes, and channel-floodplain interactions. These processes influence habitat conditions, which in turn influence biological responses (in this case salmon abundance and life-cycle productivity). The main premise is that degradation of driving processes has caused habitat loss or degradation, and therefore that restoration of watershed processes will restore and sustain habitats and salmon populations over the long term.

Beechie et al. (2010) proposed four fundamental process-based principles to guide restoration planning:

1. Target root causes of habitat degradation,
2. Tailor restoration actions to local potential,
3. Match the scale of restoration to the scale of the problem, and
4. Be explicit about expected outcomes.

The core principle is that restoration should address root causes of degradation rather than the symptoms of it (Beechie and Bolton 1999, Kondolf et al. 2006). This principle is intended to help focus restoration on those actions that will be most cost-effective and sustainable. The second and third principles are intended to guide restoration designs to have a high chance of success. That is, a restoration action should be suited to a site's physical and biological potential so that projects do not fail because they attempt to create habitat conditions that a site cannot support over the long term (Kondolf et al. 2001, Brierly and Fryirs 2009). Moreover, actions should be at a scale commensurate with the problem, so that actions are large enough or numerous enough to have the desired effect. Finally, the last principle is intended to help set realistic expectations for what can be achieved through restoration.

It is important to note that natural processes cannot always be fully restored, and that partial process restoration or habitat creation will also be necessary in some cases (Beechie et al. 2010). Especially for habitat creation, the first principle is not applied because habitat creation by definition addresses symptoms rather than root causes. However, the second and third principles should guide the design of habitat creation projects to assure that constructed habitat features persist and function as intended. That is, created habitats should be consistent with a site's potential so that other un-restored processes do not destroy or diminish the effectiveness of the project, and the size of the project is large enough to realize the intended restoration benefit.

2.1 Assessment Questions

Our assessment approach focuses on answering three key questions (Figure 2.1) (see Beechie et al. 2003, 2008a, 2010, 2013a):

1. How have specific habitat features changed from historical conditions and altered salmon populations?
2. What are the causes of those habitat changes?
3. Which restoration actions will likely provide the greatest benefit to salmon populations?

These questions guide the analysis so that model outputs help evaluate likely outcomes of various restoration alternatives for the Chehalis River basin, focusing on identifying restoration strategies that will most cost-effectively improve salmon populations.
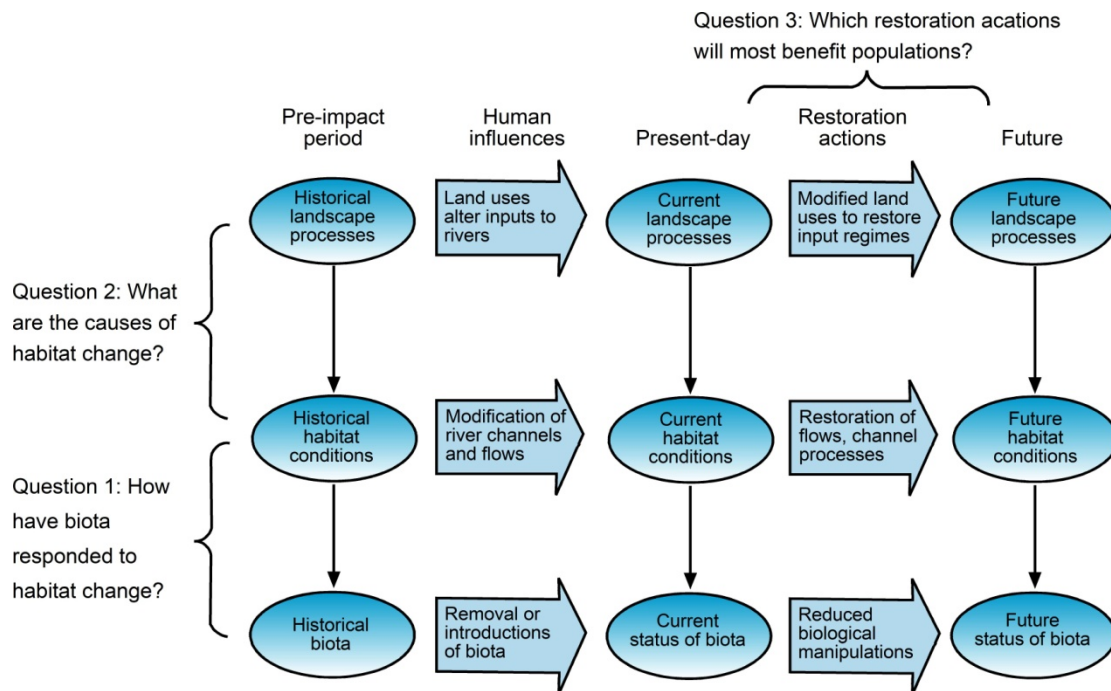
Figure 2.1. Schematic diagram of process linkages and analysis questions that guide our analysis. Figure from modified from Beechie et al. (2010).

2.2 Assessment Components

This assessment addresses three watershed process components, and eight habitat change components (Table 2.1). The watershed process assessments focus on quantifying the difference between historical process rates or conditions and current process rates or conditions for sediment supply, hydrology, and riparian functions (Beechie et al. 2003, 2013a). The habitat change assessments focus on quantifying the difference between historical habitat availability or condition and the current habitat availability or condition (Beechie et al. 1994, Beechie and Bolton 1999). The three habitat strata assessed are small streams (<20 m bankfull width, see map in Appendix A), large rivers (>20m bankfull width, see map in Appendix A), and floodplains (relatively flat areas adjacent to the channel at approximately bankfull elevation, see map in Appendix F). In each stratum, understanding the natural or background rate or condition is essential for understanding whether habitats or habitat–forming processes are degraded or not, and therefore whether restoration is needed. That is, some landscapes or reaches have low potential habitat value, and a low current habitat value may simply reflect the natural potential rather than degradation. By contrast, landscapes or reaches with high natural potential and poor current condition indicate areas where restoration may be beneficial.

The analysis components are linked through a conceptual model in which each driver of habitat change influences habitat conditions and capacities or productivities for each life stage in the life-cycle model (Figure 2.2) (Moussalli and Hilborn 1986, Beechie et al. 1994, Green and Beechie 2004, Scheuerell et al. 2006, Beechie et al. 2015). The main purpose of this modeling is to understand which habitat changes have had the most influence on population declines (Beechie et al. 1994), and also which restoration strategies or actions will have the greatest biological benefit (Scheuerell et al. 2006, Beechie et al. 2015). These results then help decision makers understand how habitat conditions affect salmon populations, and assist them in developing strategies and priorities for restoration. The habitat scenarios used to evaluate past habitat changes are the *diagnostic scenarios*, and the scenarios evaluating future restoration alternatives are the *restoration scenarios*. In the following sections, we describe methods and results for each habitat, causal process, and life-cycle model analysis presented in this report.

This analysis approach has been used in river basins where the natural condition provides a useful assessment benchmark (e.g., Beechie et al. 1994, Bartz et al. 2006, Scheuerell et al. 2006), as well as in rivers where management constraints are so severe that an alternative process-based benchmark is needed (Beechie et al. 2015). Climate change considerations have also been included in such assessments (Battin et al. 2007), and there are new methods available for considering climate change in restoration planning without explicit modeling of climate change effects (Beechie et al. 2013b, Perry et al. 2015). In this study, we include climate change effects on stream temperature and low flows in modeling restoration scenarios into the future. Modeling of future peak flows is discussed in Appendix J, and will be incorporated in Phase 2.

Table 2.1. Brief description of assessment components for the Chehalis River basin watershed analysis and life-cycle model. More detailed methods and results for watershed and habitat assessments are in Appendices A through J.

Assessment Component	Description
Watershed process assessments	
Riparian functions	Assess riparian vegetation conditions and effects on stream shading and wood supply (Appendix A)
Hydrology	Assess effects of changing land cover, existing dams, and climate change on peak and low flows (Appendix B)
Sediment supply	Assess logging road effects on surface erosion and fine sediment in spawning gravels (Appendix C)
Habitat change assessments	
Migration barriers	Quantify area of habitat that is inaccessible due to man-made barriers (Appendix D), and influence on habitat capacity and productivity (Appendix I)
Fine sediment	Assess influence of change in fine sediment in spawning gravels on incubation productivity (Appendices C and I)
Wood abundance	Assess influence of changes in wood abundance on habitat capacity and productivity (Appendix I)
Stream temperature	Assess changes in stream temperature due to altered riparian condition (Appendix A), and influence on habitat capacity and productivity (Appendix I and J)
Bank armoring	Assess influence of changes in bank armoring on habitat capacity and productivity (Appendices E and I)
Channel straightening	Assess influence of changes in main channel length on habitat capacity and productivity (Appendix I)
Beaver ponds	Assess influence of changes in beaver pond areas on habitat capacity and productivity (Appendix I)
Floodplain habitats	Assess loss of floodplain habitats relative to historical or natural potential (Appendix F), and influence on habitat capacity and productivity (Appendix I)
Salmon and steelhead life-cycle modeling	
Estimating population declines due to habitat losses (diagnostic scenarios)	Evaluate population changes for spring and fall Chinook salmon, coho salmon, and steelhead due to habitat changes
Estimating potential population responses to climate change, development, and restoration (restoration scenarios)	Evaluate population changes for spring and fall Chinook salmon, coho salmon, and steelhead under alternative restoration scenarios
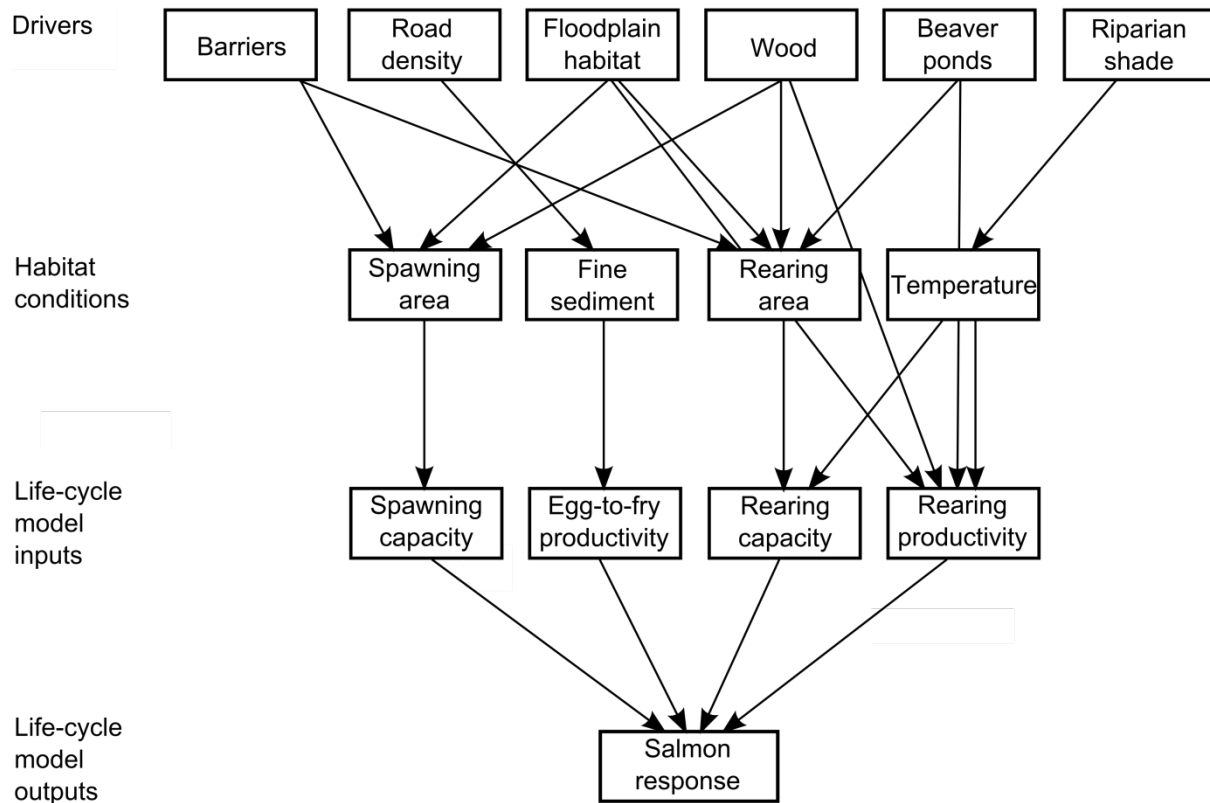
Figure 2.2. Simplified schematic diagram of linkages among drivers of habitat change, life stage capacities and productivities, and salmon response in the NOAA Model for the Chehalis River basin. Effects on life-cycle model (LCM) inputs in this example are based on coho salmon. Note that not all potential linkages are shown. Figure modified from Beechie et al. (2003).

3. Overview of the NOAA Model

The NOAA analysis uses three separate models to take the raw GIS data and ultimately produce life-cycle model results for each species under each diagnostic or restoration scenario (Figure 3.1). The three components of the model are the spatial analysis, the habitat analysis, and the life-cycle model (blue circles in Figure 3.1). We refer to this suite of models as the NOAA Model. The spatial data inputs to the spatial analysis include raw data files such as digital elevation models, land cover, precipitation, roads, riparian data, SWIFD stream lines, historical and current small stream habitat area, floodplain habitat areas, and large river edge habitats. The spatial analysis code processes the raw data files and produces five habitat data layers that contain the current habitat areas and conditions used in the NOAA analysis: large river edge habitat, large river backwaters, large river spawning riffles, floodplain habitat, and an attributed stream line that contains all remaining reach parameters (e.g., channel slope, bankfull width, fine sediment level, stream temperature). A more detailed description of the spatial analysis is in Section 3.1.

In the habitat analysis, we use the five habitat data layers to estimate historical and current life-stage capacities and productivities for each species, subbasin, and diagnostic scenario, which are used in the life-cycle model to estimate density-dependent survival of eggs or fish through each life stage (e.g., Moussalli and Hilborn 1986). These capacities and

Raw data layers:
USGS 10-m DEM
C-CAP land cover raster
PRISM mean annual precip
Washington roads
Ecological Diversity Regions
SWIFD streamlines
WDFW Migration barriers
WDFW Thermalscape
Riparian files
Floodplain habitat polygons
Large river edge habitat
Large river backwaters
Spawning riffles

Final habitat layers:
Large river edge habitat
Large river backwaters
Large river spawning riffles
Floodplain habitats
Attributed streamline

Diagnostic scenarios:
Migration barriers
Fine sediment
Wood loading
Shade (temperature)
Bank armor
Channel straightening
Beaver ponds
Floodplain habitats

Restoration scenarios:
Restoration actions
Climate change effects
Future development

LCM results
-Coho
-Spring Chinook
-Fall Chinook
-Steelhead

Figure 3.1. Illustration of the analysis steps, proceeding from the raw data layers, to habitat data layers, to habitat scenarios, and finally to the life-cycle model (LCM) outputs. C-CAP is NOAA's Coastal Change Analysis Program; SWIFD is the Washington Department of Fish and Wildlife (WDFW) State-Wide Integrated Fish Distribution.

productivities are derived from physical habitat, and therefore vary by subbasin. The outputs of the habitat analysis are subbasin- and species-specific life-stage capacities and productivities (1) for each diagnostic habitat scenario for evaluating effects of past habitat changes, and (2) for each habitat restoration scenario for evaluating potential response of each species to alternative habitat restoration actions.

The diagnostic scenarios include scenarios for historical and current habitat conditions, as well as scenarios in which each habitat factor is set to historical conditions independently (keeping all other factors in current conditions). The purpose of the diagnostic scenarios is to help understand the relative importance of each type of habitat degradation in limiting potential rebuilding of each species. These scenarios are described in more detail in Section 3.2, and in the life-cycle model descriptions for each species (Section 4).

The restoration scenarios include various combinations of restoration actions agreed upon by the Science Review Team (SRT). The SRT was formed to provide scientific guidance for the development of the ASRP, and it includes scientists associated with WDFW, Quinault Indian Nation, Confederated Tribes of the Chehalis Reservation, NOAA Fisheries, ICF International, and Anchor QEA. These restoration scenarios are intended to help evaluate the potential biological benefits of habitat restoration alternatives for each species. Because the restoration scenarios estimate habitat conditions into the future, climate change effects on life-stage capacities and productivities for each species are also included in the restoration scenarios. These scenarios are described in more detail in Section 3.2.3 and Appendix J.

Finally, the life-cycle model is run with each habitat scenario for each species to diagnose the relative influences of past habitat changes on each species, and to assess which habitat restoration options will likely have the greatest benefit for each species (Section 3.3). The life-cycle model inputs are the life-stage capacities and productivities for each species, which are unique to each scenario. The outputs reported include the equilibrium spawner abundance in the absence of fishing (N_{eq}), as well as other metrics such as intrinsic productivity (P_n) and cumulative life-cycle capacity (C_n) (Moussalli and Hilborn 1986). We provide a general description of the life-cycle model in Section 3.3, and detailed descriptions of the life-cycle model for each species in Section 4.

3.1 Spatial Analysis

The spatial analysis uses 14 geospatial data layers as inputs, and produces five habitat data layers that are used later in the habitat analysis. In this part of the analysis process, the geospatial input data layers are analyzed to produce the physical habitat attributes used to estimate life-stage capacities and productivities in the subsequent habitat analysis. The input layers to the spatial analysis include data layers produced from the NOAA watershed process assessment components (e.g., the riparian change analysis in Appendix A), the habitat change assessment components (e.g., the floodplain habitat analysis in Appendix F), as well as a number of other data layers from various sources (Table 3.1.1). The output data layers contain the habitat quantity and quality data for each subbasin; these data layers then become the inputs for the habitat analysis described in Section 3.2.

8

Table 3.1.1. Input data layers for the spatial analysis.

Input data layer	Description
National Elevation Dataset (NED) (10-m digital elevation model)	From USGS, used for channel slope calculations, and for flow accumulation processes to calculate drainage areas, road density, and mean annual precipitation above each reach in the SWIFD streams.
Land cover	NOAA C-CAP land cover (forested, bare, wetland, agriculture, developed), used in pool area calculations in small streams.
Land use	Washington State Land Use 2010; used in road density calculations, and in developing restoration scenarios for managed forest lands.
Mean annual precipitation	From PRISM (Oregon State University), used in estimating bankfull width.
Unpaved roads	From Washington Department of Natural Resources, used in calculating road density for estimating percent fines in spawning gravel.
Subbasin boundaries (including Ecological Diversity Regions)	From the ASRP Science Review Team, contains spatial units for habitat analysis and life-cycle modeling.
SWIFD stream lines	From WDFW and NWIFC (line work based on National Hydrography Dataset); this is the base stream layer for analysis, and contains salmon and steelhead distributions.
Migration barrier points	From WDFW, modifies spawning and rearing area availability based on culvert passability ratings.
Stream temperature	Current summer stream temperature modeled in the WDFW Thermalscape and by Portland State University
NOAA riparian condition dataset (Appendix A)	Tree height and canopy opening angles used to model stream temperature (historical, current, 2040s and 2080s).
NOAA large river edge habitats (Appendix E)	Hand mapped from aerial photography, used for estimating historical and current rearing habitat availability.
NOAA large river backwaters (Appendix E)	Hand mapped from aerial photography, used for estimating historical and current rearing habitat availability.
NOAA floodplain habitats (Appendix F)	Hand mapped marshes and ponds from General Land Office surveys and National Hydrography Dataset, used for estimating historical and current rearing habitat availability.
NOAA large river spawning riffles (Appendix H)	Hand mapped from aerial photography, used for estimating historical and current spawning habitat availability.

3.1.1 Input Datasets

Five of the geospatial inputs are publically available data sets that provide topography, land cover, precipitation, and road locations. The National Elevation Dataset (NED) from USGS is a 10-m resolution digital elevation model, which is used for channel slope calculations and to estimate drainage areas and densities for various parameters (https://lta.cr.usgs.gov/NED). The Coastal Change Analysis Program (C-CAP) land cover dataset is a NOAA 30-m resolution raster dataset produced in 2016 (https://coast.noaa.gov/digitalcoast/data/). For land use, we used the Washington Department of Ecology Land Use 2010 layer (https://ecology.wa.gov/Research-Data/Data-resources/Geographic-Information-Systems-GIS/Data#l).

Land cover types (e.g., forest, agriculture, developed) are used at several points in the analyses to alter habitat quantity or quality, and land use type (e.g., commercial forest) is used to identify managed forest lands for road density calculations and creating restoration scenarios. The mean annual precipitation dataset is also at 30-m resolution, and was obtained from the PRISM Climate Group at Oregon State University (http://www.prism.oregonstate.edu/). The precipitation data were used primarily for estimating bankfull width of each stream reach. Road data were obtained from the Washington Geospatial Open Data Portal (http://geo.wa.gov/), and were used in the prediction of percent fine sediment in spawning gravels in each reach.

Four of the geospatial data sets we used have been produced or updated specifically for use in developing the Chehalis River basin Aquatic Species Restoration Plan. Spatial units defined for the salmon and steelhead models include 63 subbasins, which were then grouped into 10 Ecological Diversity Regions by the Science Review Team (Figure 3.1.1). The 63 subbasins are either independent tributaries entering the mainstem Chehalis (which vary in size from small streams to large tributary rivers), or sub-reaches of the mainstem EDRs. Each subbasin is treated as a subpopulation in each life-cycle model, and each subpopulation is modeled independently of the others with interactions among subpopulations only occurring in the mainstem reaches when juveniles move downstream from their natal subbasins. Washington Department of Fish and Wildlife (WDFW) and the Northwest Indian Fisheries Commission (NWIFC) have produced an updated State-Wide Integrated Fish Distribution (SWIFD) dataset, which contains updated fish distributions for each salmon and steelhead species. The stream lines for this dataset have been modified slightly from their original (which was the National Hydrography Dataset, or NHD) by WDFW and Northwest Indian Fisheries Commission. Migration barriers are contained in a WDFW database of migration barriers, which has also been recently updated. This data set is used for estimating reductions in spawning and rearing capacities for salmon and steelhead due to restricted access by the barriers. The summer stream temperature data sets are from WDFW (tributaries) and Portland State University (the mainstem from Crim Creek to Porter Creek).

Five geospatial datasets were produced by NOAA's Northwest Fisheries Science Center for this project. The first is the NOAA riparian condition dataset, which contains tree heights
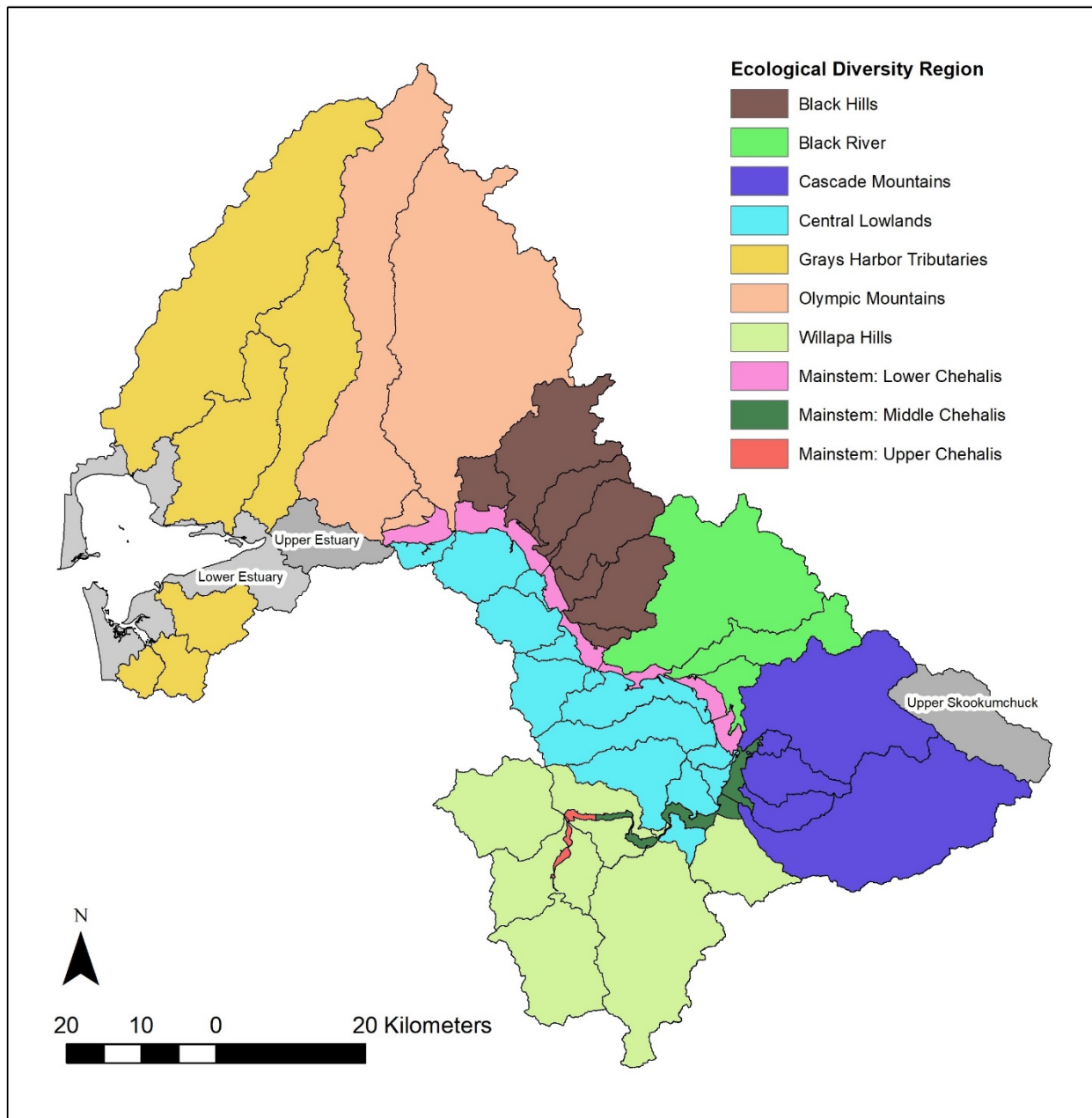
Figure 3.1.1. Map of the 63 subbasins modeled with the NOAA life-cycle models (black boundaries) and Ecological Diversity Regions defined by the Science Review Team (colored regions). Subbasins are each modeled as individual subpopulations in the life-cycle models, EDRs are unique geographic areas identified to help ensure that the spatial distribution of restoration effort addresses multiple species, life histories, and spatial structure of populations. Gray subbasins are not included in EDRs (upper Skookumchuck above the dam has no spawners currently, upper and lower estuary are predominantly tidal rearing habitats).

and forested buffer widths for each reach in the SWIFD anadromous species fish distribution (i.e., we do not include reaches with resident fish only). This data set is used mainly for estimating canopy opening angles and modeling stream temperature (Appendix A). Data sets two and three contain large river edge habitats and backwaters (Appendix E). The NOAA large river edge habitat dataset contains hand-digitized lengths of bank and bar edge units (from recent aerial photography), which are later converted to habitat areas using empirical functions to estimate the width of each unit type. The NOAA large river backwater dataset contains hand-digitized polygons of backwater units (from recent aerial photography). Data set four is the NOAA floodplain habitat dataset, which contains hand-digitized polygons of historical and current floodplain ponds, marshes and lakes, based on the General Land Office surveys of 1853 to 1901 (Appendix F), as well as mapped ponds, marshes and lakes in the National Hydrography Dataset. Finally, dataset five, the NOAA large river spawning riffle dataset, contains spawning riffle polygons which were hand-digitized from recent aerial photography, which are used in estimating current spawning capacity for each species that uses those portions of the river network (Appendix H).

3.1.2 Analyses and Output Datasets

The first step in the spatial analysis is to generate physical attributes for each 200-m reach in the SWIFD stream network. Drainage area upstream of each reach is calculated using flow accumulation with the 10-m NED. Mean annual precipitation upstream of each reach is then calculated using a weighted flow accumulation of the mean annual precipitation grid. Bankfull width is then predicted for each reach based on empirical equations developed specifically for the Chehalis River basin. Reach-specific wetted widths were provided by ICF International. Finally, channel slope is calculated for each reach based on reach length and the difference between upstream and downstream elevations.

A riparian analysis module then uses the NOAA riparian condition files to calculate the canopy opening angle at each analysis point. Canopy opening angle was calculated in two ways, using lidar where it was available, and using aerial photography where lidar was not available. In both cases, canopy opening angle is calculated using the canopy opening width and tree heights on each side of the stream (Appendix A). Analysis points are at 10-meter spacing where we use lidar, and 200 to 300 meter spacing where we use aerial photography. Historical canopy opening angle was calculated using the current canopy opening width and separate reference tree heights for small stream and large river segments (Appendix A). A stream temperature model then uses the drainage area and change in canopy opening angle at each analysis point to estimate the change in summer stream temperatures from historical to current conditions and from current to mid-century (2040s) and late-century (2080s) conditions in the restoration scenarios.

Fish passage ratings for each reach are calculated based on the passability ratings assigned to each barrier in the WDFW barrier database. Most barriers have a passage rating assigned by WDFW (usually 0, 0.33, 0.67, or 1.0). For those barriers with no passage rating (~10%), the data base assumes a passage rating of 0.5 based on the recommendation of WDFW. We calculate reduced spawning capacity in all SWIFD reaches upstream of a barrier based on these passage ratings (details in Appendix D and for each species in

Section 4). Where there are multiple barriers in sequence on a stream, the passability ratings are multiplicative, so that the proportion of returning spawners is successively reduced with each barrier. For example, for two barriers with a passage rating of 0.33, reaches upstream of the first barrier have a passage rating of 0.33, and reaches upstream of the second barrier have a passage rating of 0.11 (0.33 × 0.33). These reduced capacities also influence subbasin average productivities through weighting of reach-level productivities for prespawning and incubation life stages. Barriers do not influence juvenile movements in the model, as most juvenile movements are in the downstream direction.

The land cover class adjacent to stream reaches influences percent pool area (rearing habitat conditions) and spawner densities, which is a surrogate for the influence of wood abundance on pool area and spawning gravel area (Montgomery et al. 1999, Beechie et al. 1994, 2001, 2006a). To do this, the C-CAP land-cover layer was reclassified into forest, agriculture, developed, water, bare/shrub/grass, and wetland, and land cover was assigned to each 200-m reach in a 30-m buffer on either side of each reach (Appendix E).

An estimate of fine sediment in each reach of the basin was calculated from the slope-width index and road density (Appendix C). Using the USGS DEM and our slope estimates for each reach, reaches with slope-width index <0.05 were assigned a high percent fines based on local data (Mobrand Biometrics, Inc. 2003). In reaches with slope-width index >0.05, we used a Washington Department of Natural Resources roads layer and a Washington State Department of Ecology land use layer to create a layer of unpaved roads in forest lands. Using that roads layer, road density draining to each 200 m segment was calculated, and road density was then related to percent fine sediment in the spawning gravels. Finally, percent fine sediment was related to incubation productivity for each reach (Appendix I). It is important to note that this approach does not incorporate the influence of other sediment sources on fine sediment levels, so fine sediment levels in many locations will differ from modeled fine sediment levels based on road density alone.

In the final steps of the spatial analysis, subbasin designations and Ecological Diversity Region designations are assigned to each reach in the attributed SWIFD stream line. The relevant physical attributes from the intermediate data layers are then transferred to the attributed SWIFD reaches. Other necessary attributes are retained in the attributed SWIFD stream layer (Table 3.1.2). The five datasets produced by the spatial analysis contain the small stream, large river (3 datasets), and floodplain habitat data (Table 3.1.2), which then become the input data for the habitat analysis (Section 3.2). The NOAA large river edge habitat and backwater datasets contain areas of edge habitat types, as well as other relevant habitat quality attributes such as stream temperature. The NOAA floodplain habitat dataset includes areas of all floodplain habitat types.

Finally, the attributed SWIFD streamline contains the reach-specific current areas of all habitat types in small streams (pools, riffles, ponds), as well as channel slope, bankfull width, wetted width, and habitat quality attributes such as the 7-day average daily maximum temperature or percent fines in spawning gravels. The non-habitat parameters

Table 3.1.2. Output habitat data layers and examples of attributes contained in each layer.

Habitat data layer	Habitat attributes
Large river edge habitat	Historical and current edge habitat types and areas (bank edge and bar edge units), spatial units, and fish distributions.
Large river backwaters	Current backwater areas, with habitat quality attributes (e.g., temperature), spatial units, and fish distributions.
Large river spawning riffles	Current spawning gravel area, plus habitat quality attributes (e.g., temperature, fine sediment), spatial units, and fish distributions.
Floodplain habitat	Historical and current floodplain marsh and pond areas, with spatial units and fish distributions.
Attributed stream line	Channel slope, bankfull width, wetted width, stream temperature, land cover, percent fine sediment, fish distribution.

(e.g., slope) influence some aspects of the habitat analysis, such as differences in current and historical pool areas in small streams (details in Appendix E). These five datasets are used in the habitat analysis to estimate historical and current life-stage capacities and productivities for each species and scenario.

3.2 Habitat Analysis

The habitat analysis produces the historical and current habitat capacity and productivity values for each species, life-stage, habitat change, and subbasin (Section 3.2.1), and then creates both diagnostic and restoration scenarios using various combinations of the historical and current values (Sections 3.2.2 and 3.2.3). Capacities for each life stage define the maximum number of fish that can be produced at the end of a life stage, and productivities are the density independent productivities for a life stage (i.e., survival at very low abundance). These parameters are used to define density-dependent (Beverton-Holt or hockey stick) or density-independent functions for life stages in the life-cycle models (e.g., Moussalli and Hilborn 1986, Scheuerell et al. 2006) (described further in Section 3.3). The diagnostic scenarios are intended to help understand the relative importance of each type of habitat degradation on each species, and the restoration scenarios are intended to help evaluate the potential biological benefits of ASRP habitat restoration actions for each species, including the influence of climate change.

The habitat analysis uses the five output files from the spatial analysis to estimate current and historical life-stage capacities and productivities for each species and scenario (Figure 3.1). Each habitat attribute from the spatial analysis influences one or more life stage capacities or productivities in the life-cycle models, so that the influence of each habitat change on a salmon population can be evaluated in either diagnostic or restoration scenarios. That is, habitat parameters selected for use in the model were chosen because they can be altered by land use, restoration, or climate change, and because changes in those parameters can be quantitatively linked to changes in life-stage capacities or productivities.

3.2.1 Modeling Life-stage Capacities and Productivities

The life-stage capacities are modeled based on end-of life stage densities for each habitat type (details of calculations in Appendix H), multiplied by the total area of a habitat type in each subbasin. Capacities of all habitat types are then summed at the subbasin level, yielding a total life-stage capacity for each subbasin for each species and scenario. Changes in capacity can result from changes in habitat area or changes in density. Where there are empirical data to estimate changes in habitat areas from current to historical habitat conditions, the change in habitat area influences the change in habitat capacity. In addition to changes in habitat area, a change in habitat quality can also influence capacity via a change in density. For example, a decrease in stream temperature between the current and historical scenarios will reduce rearing capacity via a change in end-of-stage density (Appendix I). The densities used for each species under current conditions are explained in detail for each species in Section 4.

Productivity (or fecundity in the case of the spawning life stage) is a function of either habitat type or habitat quality (or species in the case of fecundity). In the case of habitat type, empirical data often indicate that different habitat types have different productivity values. For example, over winter productivities for coho salmon are relatively low in tributary channels (mean survival = 0.35, Ogston et al. 2014), but much higher in beaver ponds (mean survival = 0.78, Ogston et al. 2014). In these cases, the estimated life-stage productivity for a subbasin is calculated as the average of the two productivities, weighted by the capacity of each habitat type (Appendix H). To evaluate changes in habitat quality, we calculate a difference in productivity or create a productivity multiplier as a function of the change in the habitat quality attribute. For example, incubation productivity is calculated as a function of percent fine sediment (Appendix I), whereas summer rearing productivity is modified as a function of stream temperature (Appendix I).

3.2.2 Diagnostic Scenarios

The purpose of the diagnostic scenarios is to help understand the relative restoration potential of each type of habitat degradation on each species. Using the historical and current life-stage capacities and productivities, we developed a current condition scenario and nine diagnostic habitat scenarios to evaluate influences of habitat changes on coho salmon, spring and fall Chinook salmon, and steelhead. In the nine diagnostic scenarios, one habitat factor at a time is set to historical conditions while keeping all others at current conditions (Table 3.2.1). We also produce one scenario representing all historical conditions. Detailed descriptions of the scenarios and parameters for each species are in Section 4 and Appendix I.

The current conditions scenario sets all habitats to current conditions, and therefore uses all of the current life-stage capacities and productivities for each species. The historical scenario sets all habitats to historical conditions, and therefore uses all of the historical life-stage capacities and productivities for each species. The scenarios that use all current conditions except setting one habitat component at a time to historical conditions are used to help determine which types of habitat losses most constrain recovery of salmon and

Table 3.2.1. Description of the current condition scenario and the nine diagnostic habitat scenarios evaluated with the life-cycle models.

Scenario	Description
Current	Current conditions for all habitat variables
No barriers	Current conditions for all habitats but no migration barriers
Historical fine sediment	Current conditions with historical fine sediment and incubation productivity
Historical wood abundance	Current conditions with historical wood abundance in small streams and large rivers (current temperatures)
Historical shade	Current conditions with historical shade and temperature in small streams and large rivers
Historical large river bank conditions	Current conditions with no rip-rap in large river
Historical large river length	Current conditions with historical large river length
Historical beaver ponds	Current conditions with historical beaver pond areas in small streams
Historical floodplain habitat	Current conditions with historical side channel, marsh, and pond habitats in floodplains
Historical wood and floodplain habitat	Current conditions with historical wood abundance and side channel, marsh, and pond habitats in floodplains
Historical (all historical conditions)	Historical conditions for all habitat variables

steelhead populations in each Ecological Diversity Region and subbasin. In these scenarios, we evaluate the separate influences of:

1. Migration barriers
2. Fine sediment in spawning gravels
3. Wood abundance change in small streams and large rivers
4. Shade (temperature) changes in small streams and large rivers
5. Bank armor in large rivers
6. Large river channel straightening
7. Beaver pond changes in small streams
8. Floodplain habitat change (including side channels, ponds, marshes, and lakes)
9. Wood abundance and floodplain habitat change combined

In the NOAA model, the barrier component influences upstream migration of all salmon and steelhead, which is reflected in reduced spawning capacity above barriers according to the passage factor for each barrier. For example, spawning capacity above a barrier with a passage rating of 0.33 is 1/3 of its full capacity. We also assume barriers affect upstream migration productivity of adults in the model, weighted by egg capacity. Rearing habitat above barriers is unchanged, except that rearing habitat capacity above complete blockages is considered zero because no fish have access to that habitat.

Fine sediment affects density-independent incubation productivity in redds for all species.

The historical wood abundance scenario examines the effect of changing wood abundance alone, without a concomitant influence of the riparian zone on stream temperature. Wood abundance influences spawning capacity in small streams for all species, incubation productivity (reduces redd scour), and summer and winter rearing capacity and productivity for juvenile coho and steelhead in small streams and large rivers (Appendix I). It also affects Chinook parr migrant capacity and productivity in large rivers.

The shade change scenario affects productivity of adult spring Chinook salmon on their migration upriver, as well as capacity and productivity of juvenile coho salmon, steelhead, and spring and fall Chinook rearing during the summer.

Bank armoring affects the density of rearing salmonids, and therefore the rearing capacity of large rivers for all species. Large river channel straightening reduces both spawning and rearing habitat areas, and therefore spawning and rearing capacities of all species.

Beaver ponds in small streams have strong influences on overwintering capacity and productivity of coho salmon in particular, but have less effect on rearing capacities and productivities for other species and life stages. Similarly, floodplain habitat change also has a strong influence on overwintering capacities and productivities for juvenile coho salmon.

Bay and marine productivities are estimated separately in the life-cycle model. When multiplied together they produce a productivity value in the range of empirical estimates of smolt-to-adult returns (SAR). Marine productivities are taken from literature, and bay productivities are back-calculated from empirical SAR values divided by the total marine productivity.

3.2.3 Restoration and Climate Change Scenarios

We also ran a series of restoration scenarios agreed upon by the Science Review Team (SRT Memo #2, December 11, 2017), which are intended to help evaluate the potential biological benefits of habitat restoration for each species modeled. These scenarios are listed as the No Action alternative and Scenarios 1, 2, and 3 by the SRT (Table 3.2.2). Each scenario includes estimated improvement in life-stage capacities and density-independent productivities for mid-century and late century. The no action alternative includes riparian tree growth, removal of certain barriers, future development, and climate change. The three restoration scenarios represent low, moderate, and high levels of restoration effort. Scenario 1 focuses restoration effort in 38 geospatial units (GSUs), and within each targeted GSU barriers are removed and 20% to 50% of the stream length is treated (details in Table 3.2.1). Scenario 2 focuses restoration effort in 48 GSUs, and within each targeted GSU barriers are removed and 20% to 50% of the stream length is treated. Scenario 3 focuses restoration effort in 67 GSUs, and within each targeted GSU barriers are removed and 20% to 75% of the stream length is treated. The primary restoration actions proposed are barrier removal, wood addition, riparian restoration, and floodplain reconnection. In all scenarios, riparian and floodplain restoration are applied only in GSUs outside managed forest lands. Barrier removal and wood placement are applied in GSUs both inside and

Table 3.2.2. Summary of restoration and climate change scenarios identified by the Science Review Team. Recovery of stream shading via tree growth is also included in all managed forest scenarios, regardless of other treatments. GSU refers to Geospatial Units.

Scenario	Mid Century	Late Century
No action	Tree growth: increases shade	Tree growth: increases shade
	Climate change: increases temperature 1°C	Climate change: increases temperature 2°C
	Development: increases impervious area	Development: increases impervious area
Scenario 1	Restoration + tree growth, climate change, and development	Restoration + tree growth, climate change, and development
	Restoration focused in 39 GSUs, 226 miles of stream restored and 356 barrier culverts removed (out of 1790)	Riparian recovery continues in restored areas and managed forests, increasing shade and reducing stream temperature
Scenario 2	Restoration + tree growth, climate change, and development	Restoration + tree growth, climate change, and development
	Restoration focused in 48 GSUs, 315 miles of stream restored and 605 barrier culverts removed (out of 1790)	Riparian recovery continues in restored areas and managed forests, increasing shade and reducing stream temperature
Scenario 3	Restoration + tree growth, climate change, and development	Restoration + tree growth, climate change, and development
	Restoration focused in 67 GSUs, 449 miles of stream restored and 668 barrier culverts removed (out of 1790)	Riparian recovery continues in restored areas and managed forests, increasing shade and reducing stream temperature

outside managed forest lands. In GSUs inside managed forest lands, we also model passive recovery of riparian conditions as forested buffer zones mature.

Each restoration scenario includes improvement in life-stage capacities and productivities, based on a percentage of improvement from the current to the historical condition within a treated reach. For example, a wood restoration component may indicate that we add enough wood to close 50% of the gap between current and historical conditions in a treated reach, and the life stage capacities and productivities are increased accordingly. This percentage value is termed the intensity scalar. The intensity scalars modeled are listed in Table 3.2.3. Note that we used intensity scalars for the effects of large wood addition and floodplain reconnection, but for the riparian shade change we used modeled changes in canopy opening angle based on tree growth from current conditions. Also, inside managed forest we assumed that floodplain habitats are reconnected as a function of wood addition (floodplain restoration scalar set at 1.0).

Table 3.2.3. Intensity scalars or modeling used in the NOAA model for the three restoration scenarios. Zeros in late century indicate that no additional restoration is implemented after mid-century, but benefits of prior restoration persist.

Restoration action	Mid Century	Late Century
Outside managed forest		
Barriers	Selected barriers fixed	NA
Large wood	1.0	0 (continue at 1.0)
Beaver ponds	1.0[a]	0 (continue at 1.0)
Riparian	0.75	0.75 (continued tree growth)
Floodplain reconnection	1.0 (assumed reconnection as a function of riparian restoration)	0 (continue at 1.0)
Inside managed forest		
Barriers	Selected barriers fixed	NA
Large wood	1.0	0 (continue at 1.0)
Beaver ponds	0.1 (assumed recovery of beaver in forest lands)	0 (continue at 0.1)
Riparian	NA, no riparian planting in managed forest	NA, no riparian planting in managed forest
Floodplain reconnection	1.0 (assumed reconnection as a function of large wood placement)	0 (continue at 1.0)

a. Where wood placement is included in a scenario outside managed forest, we assume beaver dam analogues may be used in place of wood structures for small streams.

We modeled future water temperature scenarios using estimated temperature increases due to climate change, along with riparian and floodplain restoration scenarios to estimate future temperature reduction due to increased shade or hyporheic exchange. For the climate change increases, we used the NorWeST stream temperature database (Isaak et al. 2017). The NorWeST future stream temperature changes are estimated from the A1B emissions scenario in IPCC (2013) for mid-century (2030-2069, midpoint 2045) and late-century periods (2070-2099, midpoint 2085). Estimated increases were 1.4°C for mid-century and 2.4°C for late-century. However, the baseline period for these estimates is 1993-2011 (midpoint 2002), whereas the new Chehalis Thermalscape data are based on temperature data from 2014-2016 (midpoint 2015). Therefore, we adjusted the temperature changes to account for a change in the baseline year from 2002 to 2015 (details in Appendices A and J), resulting in final estimated changes of +1.0°C for mid-century and +2.0°C for late-century for the August ADA. The riparian and floodplain

restoration scenarios modeled can reduce stream temperatures, but in many cases the temperature reductions do not offset projected increases. Hence, the future temperatures in the model are often warmer than current temperatures despite restoration actions.

Future urban development is included in the scenarios as a projected change in impervious area, which is detailed in Appendix J. In the NOAA model, this change only affects prespawn productivity for coho salmon (Appendix I). Climate change is also expected to increase peak flows in the Chehalis River basin, but this effect is currently not included in the model because it is a stochastic effect and the Life-Cycle Model Workgroup recommended not including stochastic model elements in this model version.

3.3 Life-cycle Models

In this section, we briefly describe the structure and methods used in the life-cycle models, focusing on model aspects that are common across all species. An overview of the life histories of Chehalis basin salmon and steelhead is in Appendix K of this report, and details of the life-cycle models for each species are in Section 4.

3.3.1 Life-cycle Model Structure

The NOAA Chehalis salmonid life-cycle models are population dynamics models driven by demographic rates, productivities, and capacities, where cohorts are tracked through time and space in an age-structured, stage-based approach. The life-cycle models are written in R and are very flexible so that alternative parameterizations and assumptions can be compared. The main objective of the modeling is to compare effects of differing habitat losses and the relative effectiveness of alternative suites of management actions to inform decision-makers for development of the ASRP.

The life-cycle models are age-structured, stage-based stochastic matrix-type population dynamics models that move cohorts through time and space. The array of abundance, $\mathbf{N}$, evolves at each time step, t:

$$\mathbf{N}(t) = \begin{bmatrix} n_1 \\ n_2 \\ n_3 \\ n_4 \\ n_5 \end{bmatrix}.$$

In this model illustration, the 5 × 1 array tracks abundance for five age classes: parr (n_1), smolts (n_2), ocean residence (from one to three years, n_3-n_5), and spawners (four and five year old fish that spent two and three years, respectively, in the ocean, n_4 and n_5; see, for example, Zabel et al. 2006). Each age class represents a one-year time step in the model, and each year may include multiple life stages (e.g., egg incubation, fry colonization, and summer rearing may be included in the parr age class, n_2). This array varies by species and can be shortened or lengthened to encompass age classes older than 5 years (e.g., for steelhead repeat spawners).

For the Chehalis life-cycle models we split the single column array depicted in the simple illustration above into multiple columns, with each column corresponding to a spatial unit (subbasin or mainstem segment, see Figure 3.1.1) (e.g., Jorgensen et al. 2017). Juvenile production in each simulation year in each spatial unit is generated from spawners that return to that spatial unit. That is, each column of the array represents a natal subbasin of juvenile production and to which adult recruits will return. In the Chehalis basin, we have an abundance array with dimensions $n \times 63$, with the n rows corresponding to the age classes, and the columns corresponding to the 63 spatial units:

$$\mathbf{N}(t) = \begin{bmatrix} n_{1,1} & n_{1,2} \cdots & n_{1,63} \\ n_{2,1} & n_{2,2} \cdots & n_{2,63} \\ \vdots & \vdots \ddots & \vdots \\ n_{5,1} & n_{5,2} \cdots & n_{5,63} \end{bmatrix}.$$

The spatial units include both tributary and mainstem subbasins, and the spatial extent of spawning and rearing for each species as determined by the co-managers and codified in the Statewide Integrated Fish Distribution (SWIFD) GIS database. As fish from each spatial unit transition across life stages, they may remain in the same subbasin or move to a new location, such as with downstream migration to mainstem, delta, bay, or ocean environments. In some cases, the movement is modeled as volitional or density-independent, and in other cases we use a density-dependent movement function (e.g., Greene and Beechie 2004). When fish move downstream to the mainstem they interact with fish from other subbasins in a density-dependent rearing stage (except Chinook and chum fry migrants, which only experience density-independent productivity in the mainstem). Upon maturation, fish that have moved out of their natal subbasin and reared in another one are assumed to return to and reproduce in their natal subbasin.

Because we modified the $\mathbf{N}(t)$ abundance array to account for production from each spatial unit (j) separately, we developed individual habitat capacity and productivity parameters for each unit. In some cases, parameters applied to each spatial unit were the same (e.g., maturation schedule, fecundity, estuary and ocean productivities). In other cases, parameters differed among spatial units to capture the unique habitat characteristics of each subbasin (e.g., spawning, incubation, and juvenile rearing capacities and productivities). We summarize model results at the subbasin level, for each of the 10 Ecological Diversity Regions, and for the entire Chehalis basin.

Through a series of computational loops, cohorts are moved through the life stages and ages (rows) with corresponding parameters for each spatial unit (columns) that regulate demographic rates. Each loop iteration represents a one-year time step, transitioning fish from one age class to the next and applying as many intermediate life stages as necessary within a time step. That is, each time step in the model represents one year, and that year may include multiple life stages.

The freshwater life-stages are modeled in a sequence of either density-dependent or density-independent stages. Density-dependent stages use either the Beverton-Holt

function or a hockey stick function, applying the life-stage capacities and productivities produced in the habitat analysis. The Beverton-Holt function is:

$$N_{stage+1} = \frac{p \cdot N_{stage}}{1 + \left(\frac{p}{c}\right) \cdot N_{stage}} \quad ,$$

where N_{stage} is abundance of eggs or fish at the beginning of the stage, p is the density-independent productivity for the life stage, c is the capacity at the end of the stage, and $N_{stage+1}$ is abundance of fish at the end of the stage (sensu Moussalli and Hilborn 1986). The hockey stick function is:

$$N_{stage+1} = p \cdot N_{stage} \quad ,$$

up to the capacity (c) for the life-stage, and thereafter is equal to the end-of-stage capacity. Density-independent functions are simply:

$$N_{stage+1} = p \cdot N_{stage} \quad ,$$

with no capacity limit. The delta-bay and marine stages are all modeled with density-independent productivity only, with cumulative productivity rates through the bay and ocean calibrated to be in the range of empirical smolt-to-adult return (SAR) rates. Annual marine productivity rates are taken from literature, and we back-calculate the delta-bay productivity by dividing the SAR by the annual ocean productivity rates. Details for all calculations for each species are in Section 4.

3.3.2 Overview of Life Stages and Life-cycle Model Parameters

The number and structure of life stages varies among species, but all of the salmon and steelhead modeled for the Chehalis basin share certain stages or parameters in common. Here we describe parameters shared across most of the life-cycle models, and provide a brief summary in Table 3.3.1. Specific calculations and parameter values for each species are included in Section 4, as well as in Appendices H and I.

Spawning and Fecundity

In the spawning life stage, we use a hockey stick function that scales linearly (female spawner abundance multiplied by fecundity) up to each spatial unit's egg capacity threshold (based on redd capacity and fecundity, details for each species in Section 4).

Table 3.3.1. Overview of common life stages and calculations used in the life-cycle models of Chehalis River spring and fall Chinook salmon, coho salmon, and steelhead. Note that additional stages and/or fish movement steps are included as needed for each species (e.g., steelhead repeat spawners, or density-dependent movement of Chinook fry migrants). Details of life stages and parameter values for each species are in Section 4, and methods for calculation of parameter values are in Appendices H and I.

Life Stage	Model Calculation
Spawning/eggs	Modeled with a hockey function, using empirically estimated spawning capacities and fecundity values from literature. Varies with wood abundance.
Incubation	Modeled using density-independent incubation productivity values. Varies with peak flow (Phase 2 model), fine sediment.
Fry colonization	Modeled with Beverton-Holt function using estimated fry rearing capacity and density independent productivity, or as density independent productivity where capacity could not be estimated (e.g., coho salmon). Varies with wood abundance.
Juvenile rearing: fry-parr	Modeled with a Beverton-Holt function, using empirically estimated rearing capacities and productivities. Varies with wood abundance, floodplain connectivity, temperature, beaver pond abundance, and other factors.
Juvenile rearing: parr-smolt	Modeled with a Beverton-Holt function, using empirically estimated rearing capacities and productivities. Varies with wood abundance, floodplain connectivity, beaver pond abundance, and other factors
Outmigration	Density independent, in some cases combined with delta-bay rearing. Affected by temperature for spring and fall Chinook.
Delta-bay rearing	Density independent; varies by species and age at estuary entry.
Ocean rearing	Density independent; can vary by age and can be stochastic or fixed.
Maturation	Adults in the ocean have age-specific maturation rates (i.e., a specified proportion of adults at each age return to spawn).
Harvest	Optional. Harvest rates are currently not included.
Upstream migration/holding	Density independent, empirical prespawn productivities based on literature values/functions for each species. Affected by temperature for spring Chinook and impervious area for coho salmon.

Incubation

We assume that there is no density dependence during the incubation stage, and that eggs experience only density-independent mortality. We model density-independent incubation productivity for each spatial unit as a function of fine sediment levels (Appendices C and I).

Rearing: Fry-to-parr

We model subsequent freshwater rearing stages sequentially with a Beverton-Holt function that accounts for density-dependent effects at particular life stages. We use the following form,

$$N_{stage+1} = \frac{p \cdot N_{stage}}{1 + \left(\frac{p}{c}\right) \cdot N_{stage}} \quad ,$$

where $N_{stage+1}$ is abundance at the beginning of the next life stage, N_{stage} is abundance at the beginning of the life stage, p is productivity to the next life stage, and c is capacity for the end of the stage (Moussalli and Hilborn 1986). A single rearing capacity is calculated for each spatial unit (subbasin or mainstem unit), by summing the areas of each habitat type and multiplying each total habitat area by the type-specific density (Appendix H). To produce a single productivity value for the Beverton-Holt equation for each spatial unit, productivity values are calculated as the weighted average productivity across all reaches in a subbasin based on the proportion of rearing capacity in each habitat area (Appendix H).

Rearing: Parr-to-smolt

We use the Beverton-Holt equation as above, with a unique capacity and productivity calculated for each spatial unit for summer rearing. Notably, the weighted average winter

rearing productivity can change among scenarios in two primary ways: a change in the productivity of fish within a habitat type, or a change in the proportions of fish rearing in each habitat type (a function of changes in habitat area or type-specific density).

Delta-bay rearing

This is the beginning of the ocean phase for each species. We model delta-bay rearing as density-independent for all species. Delta-bay productivities are back-calculated for each species using estimated smolt-to-adult return rates (M. Zimmerman, WDFW, personal communication) divided by previously published annual ocean productivities.

Ocean rearing

We model ocean rearing with annual density-independent productivity rates for each year of ocean residency. Ocean productivity can either be constant or assumed to be stochastic on an annual basis. When it varies annually we sample according to a random uniform

distribution around an annual estimated ocean productivity (Ricker 1976, Greene and Beechie 2004). For the model runs presented in this report we model ocean productivity as constant.

Maturation

Ocean maturing adult fish have spawning propensities (or maturation rates) derived from age composition data (WDFW, unpublished data). The respawn rate for steelhead includes a kelt probability, ocean reconditioning and productivity, and the propensity to return to spawn.

Harvest

Harvest may be turned on or off in the model. For this report we have run the models without harvest. When harvest is included, it is modeled as a density-independent function.

Upstream migration and holding

We did not have data to estimate holding capacities for any species, so this stage was modeled as a density-independent life stage for each species (i.e., we used only a productivity value). For steelhead and fall Chinook salmon, we included a fixed prespawn productivity value (including the upstream migration and holding periods) (Kareiva et al. 2000). For spring Chinook, we used a functional relationship relating prespawning productivity to summer water temperatures, including upstream migration through holding periods prior to spawning. This functional relationship was adopted from a life-cycle model for spring Chinook salmon in the Willamette River basin (see Appendix I). For coho salmon, we modeled reach-specific prespawn productivity values based on percent impervious area in the watershed upstream of each reach (Feist et al. 2011, details in Appendix I).

3.3.3 Model Outputs and Interpretation of Results

For each life-cycle model and each scenario, we produced three metrics of population performance: equilibrium spawner abundance without harvest (N_{eq}), cumulative life-cycle capacity (C_n), and cumulative life-cycle productivity (P_n). We produce these results by subbasin, EDR, and for the Chehalis basin. However, the results for the 63 subbasins are too long for inclusion in the report. Output files of subbasin results will be made available on the NOAA watershed program web page. Equilibrium spawner abundance (N_{eq}) is the geometric mean of the total number of spawners over the last 50 years of a model run. We estimated cumulative life-cycle productivity (P) empirically by modeling the number of recruits produced by one fish after one generation. This value is equal to the slope of the Beverton-Holt curve at the origin, and is related to resilience of populations. We then calculate the cumulative life-cycle capacity (C), using:

$$C_n = \frac{P_n N_{eq}}{P_n - 1}$$

We also estimated the relative change in equilibrium spawner abundance among EDRs or subbasins, calculated as the percent change relative to current conditions:

$$\% \, change = \frac{scenario - current}{current} \times 100$$

Note that in some cases a high percent change in abundance may represent a relatively small increase in total abundance. For example, a 50% increase in abundance could represent an increase from 100 to 150 spawners in one subbasin, or an increase from 10,000 to 15,000 spawners in another subbasin. Therefore, both measures should be examined to evaluate restoration potential among subbasins. Estimates of P_n values among subbasins indicate differences in life-cycle productivity.

Finally, we quantified the sensitivity of the model to individual life stage capacities and productivities. These sensitivities help identify which life stages most constrain population performance. Sensitivity analyses for the life-cycle model for each species are in Section 8 of this report.

We emphasize that the life-cycle model results should be interpreted as an indication of the relative magnitude of response to changes in habitat scenarios or life-stage parameters. These results highlight which habitat changes are most influential to a salmon population, and can help guide development of a restoration strategy. A restoration strategy should describe which types of habitat restoration will most likely improve population performance, and should generally identify where those restoration actions are most needed (e.g., EDRs or subbasins) (Beechie et al. 2008).

The NOAA life-cycle model outputs for alternative diagnostic and restoration scenarios are most useful as a relative ranking tool. That is, the models are not prescriptive in the sense that they do not predict the equilibrium spawner abundance for a given scenario. Rather, the results across scenarios or spatial units should be used to assess relative differences among alternative diagnostic or restoration scenarios or locations, and interpretations of the outputs should focus on the magnitude and direction of change and not in the numbers of fish.

The life-cycle model results can also help direct resources toward additional monitoring or research that is needed to better anticipate the likely outcomes of habitat restoration. For example, if particular parameters are found to be highly influential yet little data are informing their values, then targeted research and monitoring would be useful in reducing this uncertainty. Additionally, if a scenario suggests a large population response to a specific life-stage capacity or productivity, it may be important to further evaluate whether these model results are realistic and reflect the biology of the species. The model results may also suggest ideas for additional scenarios to be constructed and tested.

3.3.4 Model Accuracy and Quality Assurance

Throughout model development, we worked with the Life-cycle Model Workgroup (which included members associated with NOAA, Quinault Indian Nation, Washington Department

of Fish and Wildlife, and Anchor QEA) to evaluate and improve the structure of the life-cycle models, input parameters, and functional relationships used to modify those parameters as a function of habitat change. This process lasted more than a year, involving numerous meetings to review and revise elements of the models. As part of that process, we kept a log of all substantive model changes (Appendix L), and wrote more than 20 short memoranda documenting responses to issues raised or model revisions. All elements of those memoranda that have bearing on the methods and results have been incorporated into this report or its appendices. Proposed revisions that were ultimately rejected for various reasons are not included.

The first accuracy check of the life-cycle models was a comparison of model-generated spawner abundance with recent estimates of total run size, with all of the habitat parameter values set to current conditions. However, the observed total run size reflects the equilibrium population size with annual harvest influencing marine productivity, whereas the modeled spawner abundance reflects the equilibrium population size without a harvest effect on marine productivity. Therefore, one would expect modeled abundance to be in the high end of the range for observed abundance. Given this difference, this check only gives a general indication of model accuracy, and is most useful for evaluating whether relative abundances among subpopulations are similar to the pattern in observed subbasin run size estimates. The model also produces tables of subbasin cumulative life-cycle capacity and intrinsic productivity, which can be reviewed for consistency with results of other studies and models. As additional spawner or juvenile abundance observations become available for Chehalis River salmonids, more formal calibration procedures could be attempted in the future (e.g., Hartig et al. 2011).

We also use a number of quality assurance steps to ensure that each model component is providing reasonable results. These steps include numerical, graphical and map outputs of life stage capacities and productivities for each species and scenario (which help us evaluate performance of the spatial and habitat models), as well as graphing abundance of eggs or fish at the end of each life stage for each scenario (which helps us evaluate performance of the life-cycle models). We also plot abundance of eggs or fish at the end of each life stage for each Ecological Diversity Region and diagnostic scenario. These plots help assess whether the model outputs from each life stage appear to accurately reflect perceived spatial distributions of habitat capacity and productivity changes. Moreover, these plots allow us to view the progression of various habitat effects through successive life stages. This information not only allows us to check model performance, but also to gain insight into which life stages and habitats exert the largest constraints on a population.

Finally, we displayed the outputs of models results or capacity and productivity parameters in map or bar chart form to visually assess whether the scenarios produce life-cycle model input parameters that reflect perceived habitat differences for each subbasin and habitat scenario. In each set of maps or graphs, we displayed the difference in a single life-cycle parameter across all nine diagnostic scenarios. For example, we produced a panel of nine maps that shows the increase in winter rearing productivities between current conditions and each scenario setting one or more habitat features to historical conditions. That is, each of the nine maps is a heat map that shows the relative increase in winter rearing

productivity for each subbasin for that scenario. In this way, we can see if each scenario accurately reflects the perceived influence of a habitat change (e.g., setting summer temperature to historical conditions should have no effect on winter rearing productivity, whereas as setting wood abundance to historical levels should have a relatively large effect). Moreover, we can evaluate whether differences among subbasins reflect perceived habitat differences. For example, a few subbasins have relatively high summer temperatures relative to historical conditions, and we can examine whether differences in estimated density-independent summer rearing productivities reflect the spatial distribution of mapped temperature changes.

4. Life-cycle Model and Scenario Descriptions

For each species modeled (coho, spring Chinook, fall Chinook, steelhead), we describe details of the life-cycle model, and briefly describe the calculation of capacity and productivity parameters for each life stage under current conditions. We then describe the estimation of historical conditions for each diagnostic scenario for each species. Historical parameter values are a function of habitat changes that modify capacity or productivity, as described in Appendix I.

4.1 Coho Salmon Life-cycle Model

In this section, we first describe the coho salmon life-cycle model structure, including the life stages and parameter estimates for current conditions (Section 4.1.1). We then describe the diagnostic habitat scenarios (Section 4.1.2). Model results and interpretation are in Sections 5, 6, and 7.

4.1.1 Life-cycle Model Description and Parameters: Coho Salmon

The life-cycle model for coho salmon has six main freshwater life stages (upstream migration, spawning, egg incubation, fry colonization, summer rearing, and winter rearing) that are influenced by freshwater habitat conditions (Figure 4.1.1). Definitions of fish stage-location names in boxes of Figure 4.1.1 are in Table 4.1.1. Each life stage influences the abundance of salmon at the end of that time period (spawners, eggs, emergent fry, end-of-spring fry, end-of-summer parr, and end of winter smolts). Smolts then leave the basin, and experience emigration, delta-bay, and marine productivity. A simple overview of the life stages and how capacities and productivities are calculated is shown in Table 4.1.2. Additional details of capacity and productivity calculations are in Appendices H and I.

The parameter estimates for current conditions are summarized in Tables 4.1.3 (capacity) and 4.1.4 (productivity and fecundity). These parameter estimates define the baseline (current condition) scenario for the life-cycle model. In the next section (4.1.2 Diagnostic Scenarios), we describe how we modify these parameter estimates given a change in any of the eight habitat factors used in the diagnostic scenarios.

For upstream migration and holding, we model the stage as density-independent. Prespawn mortality of coho salmon is related to percent development, road density, and other indicators of human development (McCarthy et al. 2008, Feist et al. 2011, 2017). For this model, we estimate prespawn mortality as a function of percent impervious area, based on data in Feist et al. (2011). Details of the calculation are in Appendix I.

We model the spawning life stage with a hockey stick function, using estimated redd capacity and fecundity to calculate egg capacity (c) (Table 4.1.3). We use a density-independent productivity (F) of 2500 eggs per female (Salo and Bayliff 1958) (Table 4.1.4).
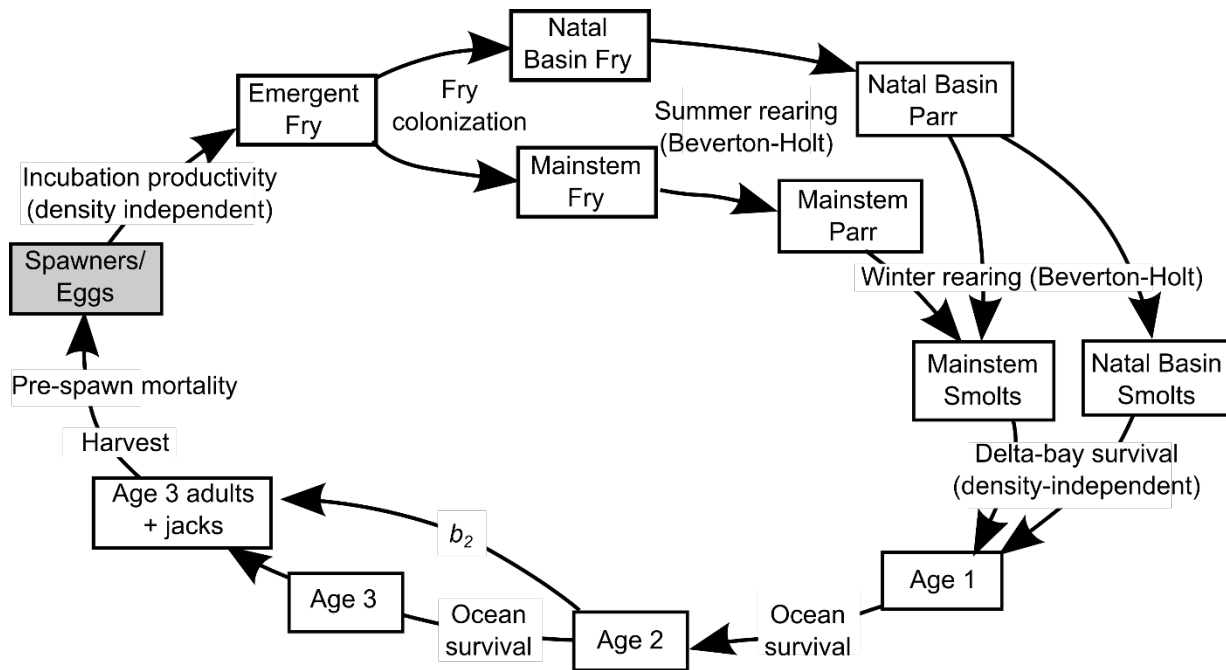
Figure 4.1.1. Schematic diagram of the life-cycle model for coho salmon in the Chehalis River basin.

Table 4.1.1. Definitions of fish stage-location names in Figure 4.1.1.

Term	Definition
Spawners/eggs	Spawners are adult coho that have returned to spawn and survived upstream migration; number of eggs is fecundity × number of females (females = spawners × 0.5)
Emergent fry	Fry emerging from the gravel (prior to fry colonization stage)
Natal basin fry	Post-colonization fry staying in their natal subbasin (prior to summer rearing)
Mainstem fry	Post-colonization fry that moved to the mainstem (prior to summer rearing)
Natal basin parr	Juveniles in natal subbasin at end of summer rearing
Mainstem parr	Juveniles in mainstem at end of summer rearing
Natal basin smolts	Juveniles leaving natal subbasin at end of winter rearing
Mainstem smolts	Juveniles leaving mainstem at end of winter rearing
Jacks	Age-2 fish returning to spawn
Adults	Age-3 adults returning to spawn

Table 4.1.2. Overview of life stages, functions, and parameters used in the coho salmon life-cycle model in the Chehalis River. See text and following tables for parameters and citations. DI = density independent, DD = density dependent. Gray highlight indicates freshwater life stages.

Life Stage	Function	Capacity	Productivity
Upstream migration and holding	DI	No capacity limit.	Varies as a function of land use.
Spawning	DD (Hockey stick)	Varies with wood abundance and barriers.	Constant among scenarios.
Incubation	DI	No capacity limit.	Varies with average percent fines and slope-width index.
Fry colonization	DI	No capacity limit.	Productivity remains constant among scenarios.
Summer rearing	DD (Beverton-Holt)	Varies with wood abundance, temperature, barriers.	Varies with wood abundance, temperature.
Winter rearing	DD (Beverton-Holt)	Varies with wood abundance, beaver ponds, floodplain habitat.	Varies with wood abundance, beaver ponds, floodplain habitat.
Delta-bay productivity	DI	No capacity limit.	Constant among scenarios.
Annual ocean productivity	DI	No capacity limit.	Constant among scenarios.

Table 4.1.3. Data used to estimate life-stage capacities in the coho salmon life-cycle model for the Chehalis River. Habitat Data Source refers to the source of the habitat areas used to estimate capacity (i.e. the outputs of the NOAA spatial analysis, see Section 3.1). Additional details are in Appendix H. Historical values are estimated using the functions described in Appendix I. Gray shading indicates freshwater life stages.

Life Stage (Equation Form)	Habitat Data Source	Data Used to Estimate Life-stage Capacities (current condition)
Upstream migration and holding (density independent)	NA	NA (we found no data to estimate holding capacity)
Spawning (hockey stick)	Large river riffle area, attributed stream layer	Egg capacity = number of redds multiplied by fecundity (2500 eggs/female, Salo and Bayliff 1958) *Number of redds in large rivers (>20 m bankfull width):* Digitized riffle area divided by redd area (6 m²) (Beechie et al. 2006a, redd area from Gallagher and Gallagher 2005) *Number of redds in small streams (<20 m bankfull width):* Redds/km (<1% slope) = 85 (Montgomery et al. 1999, streams <20 m width) Redds/km (1-3% slope, high wood abundance) = 274 (Montgomery et al. 1999, streams <20 m width) Redds/km (1-3% slope, low wood abundance) = 12 (Montgomery et al. 1999, streams <20 m width)
Incubation (density independent)	Attributed stream layer	NA (assumes that density dependence is in the spawning stage, and once eggs are in the gravel there is only density-independent productivity)
Fry colonization (density independent)	NA	NA (assumes that fry rearing and movement are density independent)
Summer rearing (Beverton-Holt)	Large river edge habitat, large river backwaters, floodplain habitat, attributed stream layer	*Density (fish/m²):* Bank (natural) = 1.96 (Beamer and Henderson 1998) Bank (modified) = 0.96 (Beamer and Henderson 1998) Bar (gravel or sand) = 0.0 (Beamer and Henderson 1998) Backwater = 1.86 (Beamer and Henderson 1998) Pool (sm. stream) = 1.7 (Nickelson 1998, density for scour pools, most common type) Riffle (sm. stream) = 0.3 (Nickelson 1998) Beaver pond = 1.2 (Nickelson 1998, weighted average of small and large ponds) Lake (>5 ha) = 0 (no data available) Side-channel pool = 1.7 (Nickelson 1998) Side-channel riffle = 0.3 (Nickelson 1998) Pond/Slough – small = 1.8 (Nickelson 1998) Pond/Slough – large = 0.9 (Nickelson 1998, reduced by half for large ponds as with winter pond densities in Reeves et al. 1989)

Table 4.1.3 (cont.). Data used to estimate life-stage capacities in the coho salmon life-cycle model.

Life Stage (Equation Form)	Habitat Data Source	Data Used to Estimate Life-stage Capacities (current condition)
Winter rearing (Beverton-Holt)	Large river edge habitat, large river backwaters, floodplain habitat, attributed stream layer	*Density (fish/m^2):* Bank (natural) = 0.32 (Beamer and Henderson 1998) Bank (modified) = 0.0 (Beamer and Henderson 1998) Bar = 0.0 (Beamer and Henderson 1998) Backwater = 0.64 (Beamer and Henderson 1998) Pool (sm. stream) = 0.4 (Nickelson 1998, density for scour pools, most common type) Riffle (sm. stream) = 0.01 (Nickelson 1998) Beaver pond = 1.2 (Nickelson 1998, weighted average of small and large ponds) Marsh = 0.32 (Henning 2004) Lake (>5 ha) = 0.0025 (Beechie et al. 1994) Side-channel pool = 0.4 (Nickelson 1998) Side-channel riffle = 0.01 (Nickelson 1998) Pond/Slough – small = 1.8 (Nickelson 1998) Pond/Slough – large = 0.9 (Nickelson 1998, reduced by half for large ponds as with winter pond densities in Reeves et al. 1989)
Delta-bay	NA	NA (modeled as density independent)
Ocean	NA	NA (modeled as density independent)

Table 4.1.4. Data used to estimate life-stage productivities in the coho salmon life-cycle model for the Chehalis River. Additional details are in Appendix I. Gray shading indicates freshwater life stages.

Life Stage (Equation Form)	Productivity or fecundity (current condition)
Upstream migration and holding (density independent)	Varies with percent impervious area (based on Feist et al. 2011, 2017).
Spawning (hockey stick)	Fecundity =2500 eggs/female (Salo and Bayliff 1958).
Incubation (density independent)	Slope-width index <0.05: p = 0.04 (based on data from Mobrand Biometrics Inc, 2003). Slope-width index >0.05: incubation productivity is a function of percent fine sediment <0.85 mm (Jensen et al. 2009, Appendix I).
Fry colonization (Beverton-Holt)	Current condition p = 0.78 (Reeves et al. 1989). Fixed in all scenarios.
Summer rearing (Beverton-Holt)	Current condition (low wood abundance, T < 18°C) p = 0.84 (Reeves et al. 1989). Varies with wood abundance and temperature (details in Section 4.1.2)
Winter rearing (Beverton-Holt)	Current condition: small stream with (low wood abundance p = 0.35, ponds and sloughs p = 0.78 (Ogston et al. 2014). Varies with wood abundance, beaver pond area, and floodplain habitat areas (details in Section 4.1.2).
Delta-bay productivity (includes outmigrant productivity)	Productivity p = 0.08. Back-calculated from SAR of 0.04 and annual ocean productivities (i.e., 0.08 * 0.7 * 0.7 = 0.04). Fixed in all scenarios.
Ocean age 1 productivity	Productivity, p = 0.7 (Ricker 1976). Fixed. Maturation rate = 0.033. (Godfrey 1969).
Ocean age 2 productivity	Productivity, p = 0.7 (Ricker 1976). Fixed. All adults return to spawn.
Harvest	Optional (currently modeled without harvest).

In large rivers (>20 m bankfull width), redd capacity is a function of spawning gravel area (digitized from aerial photography) and redd area (6 m^2, Gallagher and Gallagher 2005). In small streams, we estimated the number of redds per km of channel based on channel slope and adjacent land use (Beechie et al. 2006a, Montgomery et al. 1999). When the number of returning spawners is below capacity, the number of eggs is the number of adults × percent females × fecundity. Spawning capacity is influenced by migration barriers and wood abundance in the habitat scenarios (Appendices D and I).

The incubation stage is modeled using density-independent incubation productivity. We assume that density dependence occurs in the spawning stage (i.e., the number of eggs in the gravel is limited by the egg capacity), and that once eggs are in the gravel there is no additional density-dependent mortality. We assume that density-independent incubation productivity is 0.04 where the slope-width index is <0.05 due to very low sediment transport capacity (see Section 4.1.3 and Appendices C and I for more details). Where slope-width index >0.05, we model incubation productivity as a function of percent fine sediment <0.85 mm, which is a function of current road density (productivity equation from Jensen et al. 2009):

$$p = \frac{1}{1+e^{-(1.989-0.185 \cdot sed)}},$$

where p is productivity and sed is percent fine sediment in spawning gravel.

The fry colonization stage is modeled as density-independent, using density-independent spring rearing productivity as the input (Nickelson 1998, Reeves et al. 1989). We also model movement of fry downstream from tributaries to the mainstem, with a fixed percentage of fry leaving their natal subbasins and moving volitionally downstream to the mainstem (5%) (Larry Lestelle, email on July 26, 2018). Each tributary subbasin is connected to the mainstem, so any fry leaving a natal tributary encounter a mainstem subbasin as the first spatial unit downstream, and fry remain in the mainstem subbasin they first encounter through summer rearing (see Figure 3.1.1 for map of subbasins). Productivity for this stage is set at 0.78 (Reeves et al. 1989). We note that we did not use a density-dependent migration here because fry colonization survival is likely density independent (Lestelle 2007).

The summer rearing stage (fry-to-parr) is modeled as a Beverton-Holt function, using summer rearing capacity and density-independent summer rearing productivity as inputs. Summer rearing capacity (c) is a function of summer habitat areas by type in large rivers, small streams, and floodplains, multiplied by type- and season-specific densities to estimate rearing capacity. Habitat types and fish densities for summer rearing in large rivers are from reanalyzed data from Beamer and Henderson (1998) (Table 4.1.2). We used the 95th percentile of densities for each habitat type and month, using April for end of winter and September for end of summer. Summer coho densities are low in bar edge habitats (0 fish/m^2), but higher in bank and backwater habitats (0.96 to 1.96 fish/m^2). In small streams, densities are high in pools and low in riffles (1.7 and 0.3 fish/m^2) (Nickelson 1998). We treat side channels as small streams, using a density of 0.9 fish/m^2 (the average of pool and riffle densities). Floodplain ponds and sloughs are treated as beaver ponds, with small ponds or sloughs (<500 m^2) having a density of 1.8 fish/m^2 (Nickelson 1998), and large ponds or sloughs having a density of 0.9 fish/m^2 (half of the small pond density, based on and Reeves et al. 1989). Marshes are typically dry in the summer, so there is no summer rearing fish density for that habitat type. Productivity for this stage is initially set at 0.84 (Reeves et al. 1989) (Table 4.1.4), but it can be modified by wood abundance and stream temperature (details in Section 4.1.2 and Appendix I). Differences in summer rearing habitat capacity among scenarios are mainly a function of changes in stream temperature, wood abundance, floodplain habitat areas, and beaver pond areas.

After summer rearing, a percentage of coho parr move downstream to the nearest main stem reach, and then distribute to all downstream reaches for winter rearing. As noted above, each tributary subbasin is connected to the mainstem, so any parr leaving a natal tributary encounter a mainstem subbasin as the first spatial unit downstream. Under current conditions, we model 11% of parr leaving subbasins, and we assume that the percentage of fish leaving a subbasin decreases to 7% when we use historical wood abundance, and to 3% when we use historical beaver ponds or floodplain habitat (Cramer Associates, 2007). Our rationale is that as winter rearing habitat quantity and quality increase, fewer fish will migrate downstream to other habitats. That is, we assume fewer parr leave a subbasin as winter rearing habitat quality increases.

The winter rearing stage (parr-to-smolt) is modeled as a Beverton-Holt function, using winter rearing capacity and density-independent winter rearing productivity as inputs. For winter rearing in large rivers, 95th percentile coho densities are relatively low in all edge habitat types (0 to 0.64 fish/m^2) (Beamer and Henderson 1998) (Table 4.1.3). In small streams, densities are higher in pools and lower in riffles (0.4 and 0.01 fish/m^2) (Nickelson 1998). We treat side channels as small streams, using a density of 0.2 fish/m^2 (the average of pool and riffle densities). Floodplain ponds and sloughs are treated as beaver ponds, with small ponds or sloughs (<500 m^2) having a density of 1.8 fish/m^2 (Nickelson 1998), and densities in large ponds or sloughs are 0.9 fish/m^2 (half of the small pond density, based on and Reeves et al. 1989). Productivity for this stage is initially set at 0.35 for large rivers for small streams with low wood abundance (75th percentile from Ogston et al. 2014) and 0.78 for ponds (75th percentile from Ogston et al. 2014). Productivity in small streams and large rivers can be further modified by wood abundance (Quinn and Peterson 1996, McHugh et al. 2017).

Outside of freshwater, we modeled coho salmon productivity in the delta-bay and ocean with fixed productivity rates, followed by optional fixed rates of harvest and prespawn mortality (Table 4.1.4). We modeled delta-bay productivity with a productivity of 0.08, which was back-calculated to achieve a total SAR of ~0.04 (Zimmerman 2018). That is, we divided the SAR of 0.04 by 0.49 (two years of ocean productivity at 0.7), to estimate the

delta-bay component of SAR. This value currently includes emigration productivity, so the mortality of fish migrating to the bay is embedded in the delta-bay productivity value. Annual ocean productivity was set at 0.7 (Ricker 1976), and is density independent. We applied a maturation rate (b_2) of 0.033 at age 2 (Godfrey 1969). Jacks and all age 3 fish surviving the ocean return to spawn, with harvest rate and prespawn mortality applied prior to spawning. We currently run the model with harvest turned off, although the model can be run with any harvest rate applied prior to river entry. For comparisons of population size among scenarios and subbasins, we use equilibrium spawner abundance as our main metric.

4.1.2 Diagnostic Scenarios: Coho Salmon

The diagnostic scenarios are used to model effects of past habitat changes on coho salmon populations, given specific assumptions of how each change in habitat quantity or quality

affects life-stage capacities or productivities. Each scenario examines how a change in a single habitat factor affects coho salmon abundance and productivity in each EDR. The purpose of the diagnostic scenarios is to examine how the coho salmon population responds to each type of habitat change independently. In this section we describe the hypotheses and assumptions underlying how we model each habitat effect for coho salmon. The nine scenarios we model are:

1. Migration barriers
2. Fine sediment in spawning gravels
3. Wood abundance change in small streams and large rivers
4. Shade (temperature) changes in small streams and large rivers
5. Bank armor in large rivers
6. Large river channel straightening
7. Beaver pond changes in small streams
8. Floodplain habitat change (including side channels, ponds, marshes, and lakes)
9. Wood abundance and floodplain habitat change combined

Migration barriers: In the coho salmon life-cycle model, migration barriers reduce spawning capacity above barriers according to the passage ratings assigned by WDFW (Table 4.1.3), along with rearing capacity when the passage rating is 0 (no fish access the habitat, so the rearing capacity is excluded from the subbasin capacity) (details in Appendix I). In the diagnostic scenario that evaluates the effect of migration barriers on coho salmon abundance, we run a diagnostic scenario for "no barriers", in which we set all habitat conditions to current conditions with the exception that we remove all barriers.

Fine sediment in spawning gravels: For the historical fine sediment scenario, the road density is set to zero, and in reaches with slope-width index >0.05 incubation productivity is calculated from the equation of Jensen et al. (2009)

$$p = \frac{1}{1+e^{(-1.989+0.185 \cdot fine\ sed)}},$$

where *p* is density-independent incubation productivity and *fine sed* is percent fine sediment <0.85 mm (see Appendix H for more detail). At a road density of 0, *sed* = 5.7% and *p* = 0.72. In reaches with slope-width index <0.05, mean percent fines is 27% for both current and historical conditions (based on data from Mobrand Biometrics, Inc. 2003), and density-independent incubation productivity is 0.04 (using the equation from Jensen et al. 2009).

Wood abundance: The wood abundance scenario examines the effect of wood abundance alone, without a concomitant influence of wood on floodplain connection or of riparian shade on stream temperature. We model wood abundance influences on coho salmon spawning capacity in small streams, summer rearing capacity and productivity for juvenile coho in small streams and large rivers, and winter rearing capacity and productivity for juvenile coho in small streams and large rivers (Appendix I). For spawning capacity, wood abundance affects spawning capacity in small streams (Montgomery et al. 1999),

increasing redds per km from 85 in low-gradient, low-wood (pool-riffle) channels to 274 in low-gradient, high-wood (forced pool-riffle) channels, and from 12 in moderate-gradient low-wood (plane bed) channels to 274 in low-gradient, high-wood (forced pool-riffle) channels. Note that the forced pool riffle planform occurs in both low-gradient and moderate-gradient channels. In large rivers spawning capacity increases by 30% at high wood abundance, which reflects increased spawning gravel retention and holding pool formation.

Shade and stream temperature: Decreased shade increases stream temperature (temperature model described in Appendix A), which decreases coho salmon abundance and productivity via changes in summer rearing capacity and productivity. We first estimate a productivity multiplier based on stream temperature that decreases summer rearing productivity from its base value. At temperatures <18°C, the multiplier is 1, so there is no change in summer rearing productivity. From 18°C to 24°C, the multiplier decreases linearly from 1 to 0, and above 24°C the multiplier is 0 (based on ASEP 2014, Appendix C). We use the same multiplier for capacity that we used for productivity (details in Appendix I).

Bank armoring: Bank armoring affects the density of rearing salmonids, and therefore the rearing capacity of large rivers for all species. We digitized visible areas of rip-rap bank edge units (see Appendix E), and used coho salmon summer and winter rearing densities for rip-rap banks (reanalyzed from data in Beamer and Henderson 1998, see also Appendix H). For the historical condition we simply converted all rip-rap bank edge units to natural bank edge units, and used the higher summer and winter rearing density for natural banks to estimate rearing capacity for each unit (density data from Beamer and Henderson 1998). We did not estimate a productivity change for these unit type changes.

Main channel length (channel straightening): We hypothesize that large river channel straightening reduces both spawning and rearing habitat areas, and therefore spawning and rearing capacities of all species. We used reach-specific channel length multipliers developed by Natural Systems Design (Tim Abbe, Susan Dickerson-Lange) and NOAA (Tim Beechie) to modify large river habitat areas for the historical condition. The length multipliers ranged from 1 to 1.5, with the majority being ≤1.2. The channel length multipliers for each reach are listed in Appendix E.

Beaver pond changes in small streams: We assumed that rearing density of coho salmon in beaver ponds is the same under current and historical conditions, but that the area of beaver ponds was substantially greater historically (Pollock et al. 2004). Setting beaver pond density to historical conditions (6 ponds/km, Pollock et al. 2004) increases beaver pond area 10-fold over current conditions (current beaver pond density 0.55 ponds/km, Wampler et al. 1993).

Floodplain habitat change (side-channels, marshes, and ponds): Loss of floodplain habitats that were historically available (side-channels, marshes, and ponds) reduces spawning, summer rearing, and winter rearing habitat capacity and productivity for juvenile coho salmon. Loss of floodplain hyporheic connectivity also increases stream temperature

(Appendix J). The historical scenario includes historical side-channel area, historical pool and spawning areas in side channels, and historical areas of floodplain ponds, sloughs, and marshes. For coho salmon, these habitat types support higher juvenile densities and have higher juvenile productivities.

Delta-bay and marine productivities: Because the intent of the diagnostic scenarios is to evaluate the effect of changes in freshwater habitat conditions, we hold all of these values constant across scenarios (see Table 4.1.4).

4.2 Spring and Fall Chinook Salmon Life-cycle Models

This section includes a brief summary of the structure and parameters of the spring and fall Chinook salmon life-cycle models (Section 4.2.1), and a description of the how the diagnostic scenarios are modeled for Chinook salmon (Section 4.2.2). We describe the two species together because the life-cycle model structures are nearly identical. The major differences are their spawning distributions and spring Chinook experience temperature-related prespawn mortality because they enter the river in spring and find holding areas for the summer months. Fall Chinook enter the river after the summer high temperatures and do not experience temperature-related prespawn mortality.

4.2.1 Life-cycle Model Description and Parameters: Spring and Fall Chinook Salmon

The spring and fall Chinook models have five freshwater life-stages that are influenced by freshwater habitat conditions (upstream migration, spawning, egg incubation, fry colonization, and subyearling rearing) (Figure 4.2.1). Definitions of fish stage-location names in boxes of Figure 4.2.1 are in Table 4.2.1. Each life stage influences the abundance of salmon at the end of that time period (spawners, eggs, emergent fry, fry migrants, and subyearling migrants). In the models, fry colonize natal subbasin rearing habitats first, and fry exceeding the natal subbasin rearing capacity move downstream through the mainstem to the bay as fry migrants. Fry migrants are assumed to be in freshwater for one week in their natal basin, and subyearling migrants are in freshwater for twelve weeks (Mara Zimmerman, WDFW, personal communication). Fry migrants have additional migration mortality, but that mortality is absorbed in the delta-bay productivity value in the model. Fry and subyearlings are assigned different productivity rates in the delta-bay, and thereafter have similar ocean productivities. A description of the calculations and parameters for the life-stages is shown in Table 4.2.2.

The parameter estimates for current conditions are summarized in Tables 4.2.3 (capacity) and 4.2.4 (productivity). These parameter estimates define the current condition scenario for the life-cycle model. Both species share input parameters, however, in reaches where their distribution overlaps each species is assigned a share of the total capacity based on subbasin specific percentages of spring and fall Chinook spawners (WDFW, unpublished data). For mainstem rearing, 81% of the capacity goes to fall Chinook and 19% to spring Chinook based on the average ratio of spawner abundances. In the next section (4.2.2 Diagnostic Scenarios), we describe how we modify these parameter estimates given a change in any of eight habitat factors that we model in our diagnostic scenarios.

For upstream migration and holding, we model the life stage as density independent. Spring Chinook productivity is estimated as a function of stream temperature based on data from the Willamette River (Appendix I), and fall Chinook productivity is fixed at 0.9 to indicate that there is likely some mortality due to predation or poaching.
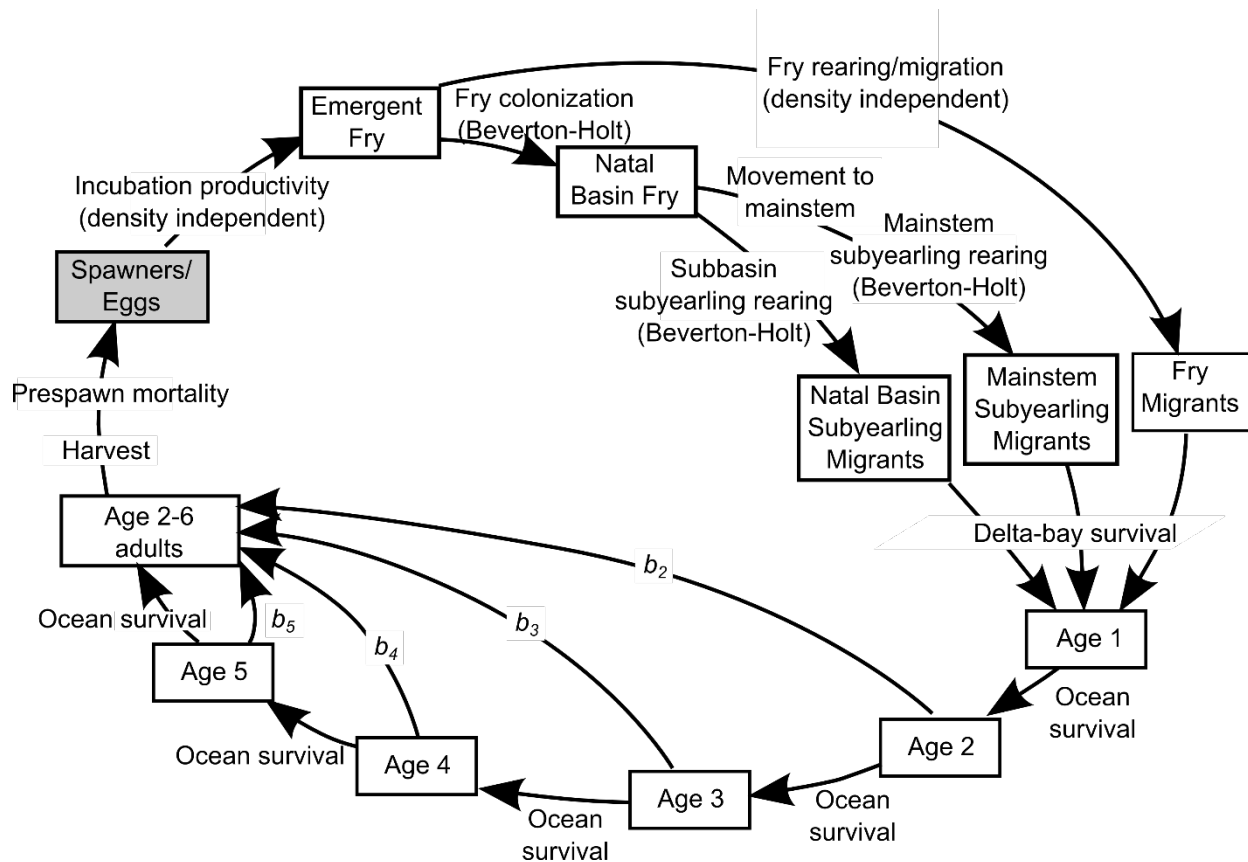
Figure 4.2.1. Schematic diagram of the life-cycle model for spring and fall Chinook salmon in the Chehalis River basin. Gray box indicates that we report results in number of spawners (or spawners + harvest, if harvest is turned on in the model).

Table 4.2.1. Definitions of fish stage-location names in Figure 4.2.1.

Term	Definition
Spawners/eggs	Spawners are adult Chinook that have returned to spawn and survived upstream migration; number of eggs is fecundity × number of females (females = spawners × 0.5)
Emergent fry	Fry emerging from the gravel (prior to fry colonization stage)
Natal basin fry	Post-colonization fry staying in their natal subbasin
Mainstem fry	Post-colonization fry that moved to the mainstem
Fry migrants	Fry entering the bay after 1 week of rearing
Natal basin subyearling migrants	Subyearlings from natal subbasin entering the bay after 12 weeks of rearing
Mainstem subyearling migrants	Subyearlings from mainstem entering the bay after 12 weeks of rearing
Adults	Age 2-6 adults in ocean prior to returning to spawn

For the spawning life stage (hockey stick form), we use a density-independent fecundity (F) of 5400 eggs per female for both spring and fall Chinook (Greene and Beechie 2004) (Table 4.2.4). Spawning capacity is expressed as egg capacity (c), which is the estimated maximum number of redds multiplied by the fecundity (Table 4.2.3). In large rivers (>20 m bankfull width), redd capacity is a function of spawning gravel area (digitized from aerial photography, Appendix H) and redd area (14.1 m^2, Beechie et al. 2006a). In small streams, we estimated the number of redds per km of channel based on channel slope and adjacent land use (Beechie et al. 2006a, Montgomery et al. 1999). When the number of returning spawners is below capacity, the number of eggs is number of spawners × percent females × fecundity. Spawning capacity is influenced by migration barriers and wood abundance in the habitat scenarios (Appendix I).

The incubation stage is modeled using density-independent incubation productivity. We assume that density dependence occurs in the spawning stage (i.e., the number of eggs in the gravel is limited by the egg capacity), and that there is no additional density-dependent mortality in the incubation stage. We estimate that density-independent incubation productivity is 0.04 where the slope-width index is <0.05 due to very low sediment transport capacity and average percent fines of 28% (see Appendices C and I for more details). Where slope-width index is >0.05, we model incubation productivity as a function of percent fine sediment <0.85 mm (Appendix I), which is a function of current road density (Appendix C). The productivity equation is from Jensen et al. (2009):

$$p = \frac{1}{1+e^{(-1.989+0.185 \cdot sed)}},$$

where p is productivity and sed is percent fine sediment in spawning gravels.

The fry colonization stage in natal subbasins is modeled with density-dependent movement using the Beverton-Holt function:

$$N_{stage+1} = \frac{p \cdot N_{stage}}{1 + \left(\frac{p}{c}\right) \cdot N_{stage}},$$

where N_{stage} is abundance of emergent fry at the beginning of the stage, p is the density independent productivity for the stage, and c is the fry rearing capacity (Figure 4.2.2). This function is applied during the first week of fry colonization. Fry below the Beverton-Holt curve remain in their natal stream, and fry above the curve move downstream to the bay. In the model, these movement rules create two outmigrant groups: fry migrants and subyearling migrants.

Fry migrants spend only one week in freshwater and subyearling migrants spend 12 weeks in freshwater. Fry rearing productivity is density independent and subyearling rearing productivity is density dependent (Anderson and Topping 2018). Additional density-independent mortality may accrue for fry migrants as they migrate to the bay, but all additional fry-migrant rearing mortality after the first week is absorbed in the density-independent delta-bay productivity value for fry migrants. After the first week, subyearling-migrants are redistributed in equal proportions across the natal basin and all mainstem reaches downstream of the subbasin. They then experience 11 more weeks of

Table 4.2.2. Overview of life stages, parameters, and functions used in the spring and fall Chinook salmon life-cycle models in the Chehalis River. Additional details are included in Appendices H and I. DI = density independent, DD = density dependent. Gray shading indicates freshwater life stages.

Life Stage	Function	Capacity	Productivity
Upstream migration and holding	DI	No capacity limit.	Varies as a function of summer temperature for spring Chinook. Fixed at 0.9 for fall Chinook.
Spawning	DD (Hockey stick)	Varies with wood abundance and barriers.	Constant among scenarios.
Incubation	DI	No capacity limit.	Varies with average percent fines and slope-width index.
Fry colonization (natal basin and mainstem)	DD (Beverton-Holt)	Varies with wood abundance, beaver ponds, and floodplain habitat.	Constant among scenarios.
Fry rearing (natal basin and mainstem)	DI	Varies with wood abundance, beaver ponds, and floodplain habitat.	Varies with wood abundance, beaver ponds, and floodplain habitat.
Subyearling rearing (natal basin)	DD (Beverton-Holt)	Varies with wood abundance, beaver ponds, and floodplain habitat.	Varies with wood abundance, beaver ponds, and floodplain habitat.
Subyearling rearing (mainstem reaches)	DD (Beverton-Holt)	Varies with wood abundance and floodplain habitat.	Varies with wood abundance and floodplain habitat.
Delta-bay	DI	No capacity limit.	Varies between fry and subyearling migrants.
Annual ocean	DI	No capacity limit.	Constant among scenarios.

density-dependent rearing in those reaches, giving subyearlings the average rearing experience of all reaches they pass through.

All rearing capacities are estimated at the subbasin scale using the sum of habitat areas of each habitat type multiplied by habitat-type-specific densities. For Chinook salmon, we estimate capacity as a function of daily maximum fish density, mean residence time, and the temporal extent of the rearing period to account for multiple groups of fish moving through habitats using:

$$c = d \cdot A \cdot \frac{t}{r}$$

where, c is capacity (# of fish), d is maximum daily density (fish/ha), A is habitat area (ha), t is the extent of the rearing period (weeks), and r is the mean residence time (weeks). In the Chehalis, we used a total rearing period (t) of 24 weeks and mean residence time in the natal subbasin (r) of 12 weeks, so c is $d \cdot A \cdot 2$.
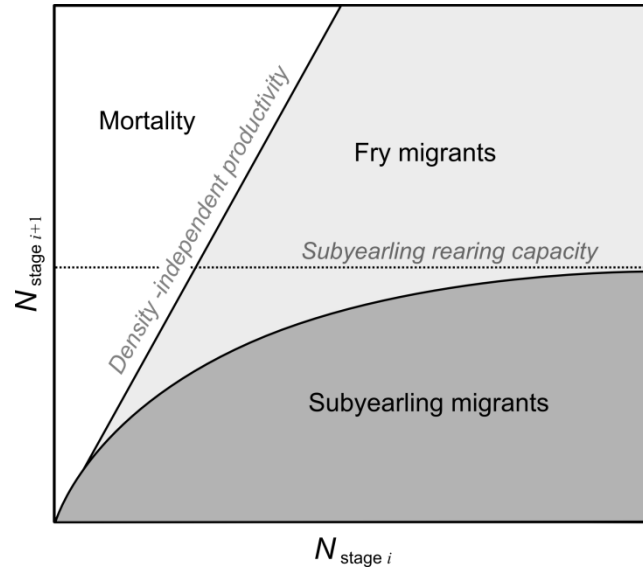
Figure 4.2.2. Illustration of the Beverton-Holt density-dependent movement calculations in the spring and fall Chinook models. Fry between the Beverton-Holt curve and the density independent productivity line (light gray) leave the river in the first week as fry migrants. Fry below the Beverton-Holt curve (dark gray) stay in the natal subbasin for one week, and then redistribute throughout the natal basin and downstream mainstem reaches to become subyearling migrants. Adapted from Greene and Beechie (2004).

Table 4.2.3. Chinook salmon data used to estimate freshwater life-stage capacities in the spring and fall Chinook life-cycle models for the Chehalis River. Habitat Data Source refers to the source of the habitat areas used to estimate capacity (i.e. the outputs of the NOAA spatial analysis, see Section 3.1). Additional details are in Appendix H. Historical values are estimated using the functions described in Appendix I. Gray shading indicates freshwater life stages.

Life Stage (Equation Form)	Habitat Data Source	Data Used to Estimate Life-stage Capacities (current condition)
Upstream migration and holding (density independent)	NA	NA (we found no data to estimate holding capacity)
Spawning (hockey stick)	Large river riffle area, attributed stream layer	Egg capacity = number of redds multiplied by fecundity (5400 eggs/female, Greene and Beechie 2004) *Number of redds in large rivers (>20 m bankfull width):* Digitized riffle area divided by redd area (14.1 m^2) (Beechie et al. 2006a) *Number of redds in small streams (<20 m bankfull width):* Redds/km (<1% slope) = 4.2 (Montgomery et al. 1999, streams <20 m width) Redds/km (1-3% slope, high wood abundance) = 8.8 (Montgomery et al. 1999, streams <20 m width) Redds/km (1-3% slope, low wood abundance) = 0 (Montgomery et al. 1999, streams <20 m width)
Incubation (density independent)	Attributed stream layer	NA (assumes that density dependence is in the spawning stage, and during incubation there is only density-independent productivity)
Fry colonization - natal basin and mainstem (density dependent, Beverton-Holt)	Large river edge habitat, large river backwaters, floodplain habitat, attributed stream layer	*Density (fish/m^2):* Bank (natural) = 1.27 (Beamer and Henderson 1998) Bank (modified) = 0.64 (Beamer and Henderson 1998) Bar (boulder) = 0.0 (Beamer and Henderson 1998) Bar (gravel) = 0.64 (Beamer and Henderson 1998) Bar (sand) = 0.32 (Beamer and Henderson 1998) Backwater = 1.91 (Beamer and Henderson 1998) Pool (sm. stream) = 0.05 (J. Thompson, unpublished data) Riffle (sm. stream) = 0.02 (J. Thompson, unpublished data) Pond (sm. stream) = 0.05 (no data, assumed same as pool density) Lake (>5 ha) = 0 (no data available) Side-channel pool = 0.05 (J. Thompson, unpublished data) Side channel riffle = 0.02 (J. Thompson, unpublished data) Slough = 0.05 (assumed same as ponds above) Floodplain pond = 0.05 (assumed same as ponds above) Marsh = 0 (no data)
Subyearling rearing - natal basin (density dependent, Beverton-Holt)	Same as fry colonization	Same as fry colonization

Table 4.2.3 (Cont.). Chinook salmon data used to estimate freshwater life-stage capacities in the spring and fall Chinook life-cycle models.

Life Stage (Equation Form)	Habitat Data Source	Data Used to Estimate Life-stage Capacities (current condition)
Subyearling rearing - main stem (density dependent, Beverton-Holt)	Same as fry colonization	Same as fry colonization
Delta-bay	NA	NA (modeled as density independent)
Ocean	NA	NA (modeled as density independent)

Table 4.2.4. Chinook salmon data used to estimate life-stage productivities in the spring and fall Chinook life-cycle models for the Chehalis River. Additional details are in Appendix I. Gray shading indicates freshwater life stages.

Life Stage (Equation Form)	Productivity or fecundity (current condition)
Upstream migration and holding (density independent)	Spring Chinook: Productivity decreases with increasing stream temperature (based on Wenatchee R. data, Bowerman et al. 2018) Fall Chinook: Productivity fixed at 0.9
Spawning (hockey stick)	Fecundity =5400 eggs/female (Greene and Beechie 2004)
Incubation (density independent)	Incubation productivity is a function of modeled percent fine sediment <0.85 mm. Productivity equation from Jensen et al. 2009. See Appendix C for estimates of percent fines. $$p = \frac{1}{1 + e^{(-1.989+0.185 \cdot sed)}}$$
Fry colonization and outmigration natal basin/ mainstem (density independent)	Current condition p = 0.894 (1 week)
Subyearling rearing - natal basin (density dependent, Beverton-Holt)	Stream and river, p = 0.29 (11 weeks) Floodplain habitats, p = 0.50 (Martens and Connolly 2014)
Subyearling rearing - main stem (density dependent, Beverton-Holt)	Stream and river, p = 0.29 (11 weeks) Floodplain habitats, p = 0.50 (Martens and Connolly 2014)
Delta-bay productivity	Fry migrants: p = 0.001 Subyearling migrants: p = 0.06 (back-calculated using SAR and percent fry migrants in adult returns)
Ocean productivity	Age 1: p = 0.6 (Greene and Beechie 2004) Age 2: p = 0.7 (Greene and Beechie 2004) Age 3: p = 0.8 (Greene and Beechie 2004) Age 4: p = 0.9 (Greene and Beechie 2004) Age 5: p = 0.9 (Greene and Beechie 2004)
Maturation rate	b_2 = 0.005 (modified from Greene and Beechie 2004) b_3 = 0.097 (modified from Greene and Beechie 2004) b_4 = 0.6 (modified from Greene and Beechie 2004) b_5 = 0.8 (modified from Greene and Beechie 2004) b_6 = 1 (modified from Greene and Beechie 2004)
Harvest (optional)	Spring Chinook: modeled without harvest Fall Chinook: modeled without harvest

For large river densities by habitat type, we used the 95th percentile of densities across the months of February through June from Skagit River data for estimating rearing capacity (data from Beamer and Henderson 1998). Density parameters are generally highest in mainstem edge habitats (1.27 and 1.91 fish/m^2 in natural banks and backwaters, respectively) (Beamer and Henderson 1998), and much lower in small streams, side channels, and floodplain habitats (<0.1 fish/m^2) (J. Thompson, unpublished data). All density parameters are shown in Table 4.2.3. Productivity for the fry colonization stage (first week) under current conditions is 0.894, which is the weekly productivity rate for Chinook salmon in fresh water (based on the 12-week productivity of 0.26, L. Lestelle, personal communication). After fry colonization, natal subbasin subyearlings and mainstem subyearlings then experience an additional 11 weeks of density dependent mortality before moving to the bay. The 12-week productivity for subyearling rearing under current conditions is 0.26 for streams and rivers and 0.50 for floodplain habitats, including the fry colonization stage) (Table 4.2.4) (L. Lestelle, personal communication, Martens and Connolly 2014).

Once in the delta-bay, fry and subyearling migrants experience different density-independent productivity rates, then all fish in the ocean receive the same fixed density-independent productivity rates, followed by harvest (optional, currently modeled with no harvest) (Table 4.2.4). For spring Chinook, we calculated a delta-bay subyearling productivity by trial and error to achieve a weighted average SAR near 2% for subyearling migrants (based on analysis from Gary Morishima). We then calculated fry migrant delta-bay productivity to have a weighted average SAR near 0.4% (the recommended SAR from WDFW) and ~5% fry-migrant origin fish in the adult return (Campbell et al. 2017). The resulting subyearling-migrant SAR is 2.05%, the weighted SAR across all ages is 0.43% and the percent of fry migrant origin fish in the adult return is 6.2%. For fall Chinook, we used the same process, calculating a delta-bay subyearling productivity by trial and error to achieve a weighted average SAR near 2% for subyearling migrants. We then used the same fry migrant delta-bay productivity as for spring Chinook. The resulting subyearling-migrant SAR is 1.96%, the weighted SAR across all ages is 0.19% and the percent of fry-migrant origin fish in the adult return is 15%, which is also consistent with Campbell et al. (2017).

Each age class of fish in the ocean also has a propensity to spawn (*b*), so some proportion of each age class leaves the ocean population each year. We began with the *b* parameters from Greene and Beechie (2004), and then modified them by trial and error until the model reproduced the age structure of recent spawning populations in the Chehalis River basin (WDFW unpublished data, compiled by E. Walther, email on 5/15/2017).

4.2.2 Diagnostic Scenarios: Spring and Fall Chinook Salmon

The diagnostic scenarios are used to model effects of past habitat changes on spring and fall Chinook salmon populations, given specific assumptions of how each change in habitat quantity or quality affects life-stage capacities or productivities. Each scenario examines how a change in a single habitat factor affects spring and fall Chinook salmon abundance and productivity in each subbasin. The purpose of the diagnostic scenarios is to examine how the spring and fall Chinook salmon populations respond to each type of habitat change

48

independently. In this section we describe the assumptions and data underlying how we model each habitat effect. The nine habitat changes we model are:

1. Migration barriers
2. Fine sediment in spawning gravels
3. Wood abundance change in small streams and large rivers
4. Shade (temperature) changes in small streams and large rivers
5. Bank armor in large rivers
6. Large river channel straightening
7. Beaver pond changes in small streams
8. Floodplain habitat change (including side channels, ponds, marshes, and lakes)
9. Wood abundance and floodplain habitat change combined

Migration barriers: In the spring and fall Chinook salmon life-cycle models, migration barriers reduce the abundance and productivity of spawning Chinook salmon via reduced prespawn productivity and spawning capacity above barriers according to the passage ratings assigned by WDFW (Table 4.2.3). To evaluate the influence of migration barriers on spring and fall Chinook salmon abundance and productivity under these assumptions, we run a diagnostic scenario for "no barriers", in which we set all habitat conditions to current conditions with the exception that we remove all barriers.

Fine sediment in spawning gravels: Density-independent incubation productivity in redds declines with increasing percent fine sediment in spawning gravels (Table 4.2.4). For the historical fine sediment scenario, the road density is set to zero, and incubation productivity in reaches with slope-width index <0.05 is 0.72 based on the empirical equation from Jensen et al. (2009) (see Appendix I for more detail). In reaches with slope-width index <0.05, mean percent fines is 27% for both current and historical conditions, and density-independent incubation productivity is 0.04 (based on data from Mobrand Biometrics, Inc. 2003).

Wood abundance: The wood abundance scenario examines the effect of wood abundance alone, without a concomitant influence of the riparian zone on stream temperature. The wood abundance scenario only modifies capacities and productivities in stream channels, and does not influence the amount of floodplain habitat available (Appendix I). A separate scenario examines the potential effect of wood abundance on both in-channel and floodplain habitat, assuming that higher wood abundance also reactivates floodplain habitat. Wood abundance influences spawning capacity in small streams and large rivers, and rearing capacity and productivity for juvenile spring and fall Chinook in small streams and large rivers (Table 4.2.2).

Shade and stream temperature: Decreased shade increases stream temperature (temperature model described in Appendix A), which decreases adult prespawn productivity in the spring Chinook model, but not in the fall Chinook model because they enter the river after peak summer temperatures. Stream temperature also influences late subyearling outmigrant productivity. The model uses the same temperature functions described above for current conditions, with the prespawn and subyearling productivity

multipliers decreasing with increases in temperature (e.g., Scheuerell et al. 2006, Honea et al. 2009). More details are in Appendix I.

Bank armoring: For the historical bank condition scenario, we simply converted all rip-rap bank edge units to natural bank edge units, and used the higher summer and winter rearing density for natural banks to estimate rearing capacity for each unit (density data from Beamer and Henderson 1998). We did not estimate a productivity change for these unit type changes.

Main channel length (channel straightening): Large river channel straightening reduces both spawning and rearing habitat areas, and therefore spawning and rearing capacities of all species. We used reach-specific channel length multipliers developed by Natural Systems Design (Tim Abbe, Susan Dickerson-Lange) and NOAA (Tim Beechie) to modify large river habitat areas for the historical condition. The large river multipliers ranged from 1 to 1.5, with the majority being ≤1.2.

Beaver pond changes in small streams: We found few data on Chinook rearing capacity as a function of beaver ponds, and we assumed that beaver ponds have Chinook densities similar to pools in small-streams (0.05 fish/m^2). Therefore, beaver ponds have a relatively small effect on Chinook rearing capacity. For rearing productivity, we found one study indicating higher productivity in off-channel habitats for rearing (0.50 compared to 0.29 in channels, Martens and Connolly 2014), so we also assigned the higher rearing productivity to beaver ponds.

Floodplain habitat change (side-channels, marshes, and ponds): Setting floodplain habitat area (side-channels, marshes, and ponds) to historical conditions increases spawning and rearing capacities and productivities for juvenile Chinook salmon, and also decreases stream temperature through increased floodplain hyporheic connectivity (Appendix J). Our historical scenario includes increases in side-channel area, high wood abundance in side channels, and increased floodplain ponds, sloughs, and marshes. Floodplain ponds and sloughs are given the same densities as beaver ponds. We found no studies with juvenile rearing densities in marshes, so we assigned marshes a density of zero. Productivity for rearing is assumed to be 0.50 across all floodplain habitat types (Martens and Connolly 2014).

Delta-bay and marine productivities: Because the intent of the diagnostic scenarios is to evaluate the effect of changes in freshwater habitat conditions, we hold all of these values constant across scenarios (see Table 4.2.4, method described in preceding section).

4.3 Steelhead Life-cycle Model

In this section, we first describe the steelhead life-cycle model structure, including the life stages and parameter estimates for current conditions (Section 4.3.1). We then describe the diagnostic habitat scenarios (Section 4.3.2). Model results are in Section 5.

4.3.1 Life-cycle Model Description and Parameters: Steelhead

The life-cycle model for steelhead has nine main freshwater life stages that are influenced by freshwater habitat conditions: upstream migration, spawning, egg incubation, age-0+ summer rearing, age-0+ winter rearing, age-1+ summer rearing, age-2 winter rearing, age-2+ summer rearing, and age-3 winter rearing (Figure 4.3.1). Definitions of fish stage-location names in boxes of Figure 4.3.1 are in Table 4.3.1. Habitat conditions for each life stage influence the abundance of steelhead at the end of that time period: spawners, eggs, emergent fry, end-of-spring fry, end-of-summer age-0+ parr, end of winter age-1 parr (or age-1 smolts for those that leave), end-of- summer age-1+ parr, and end of winter age-2
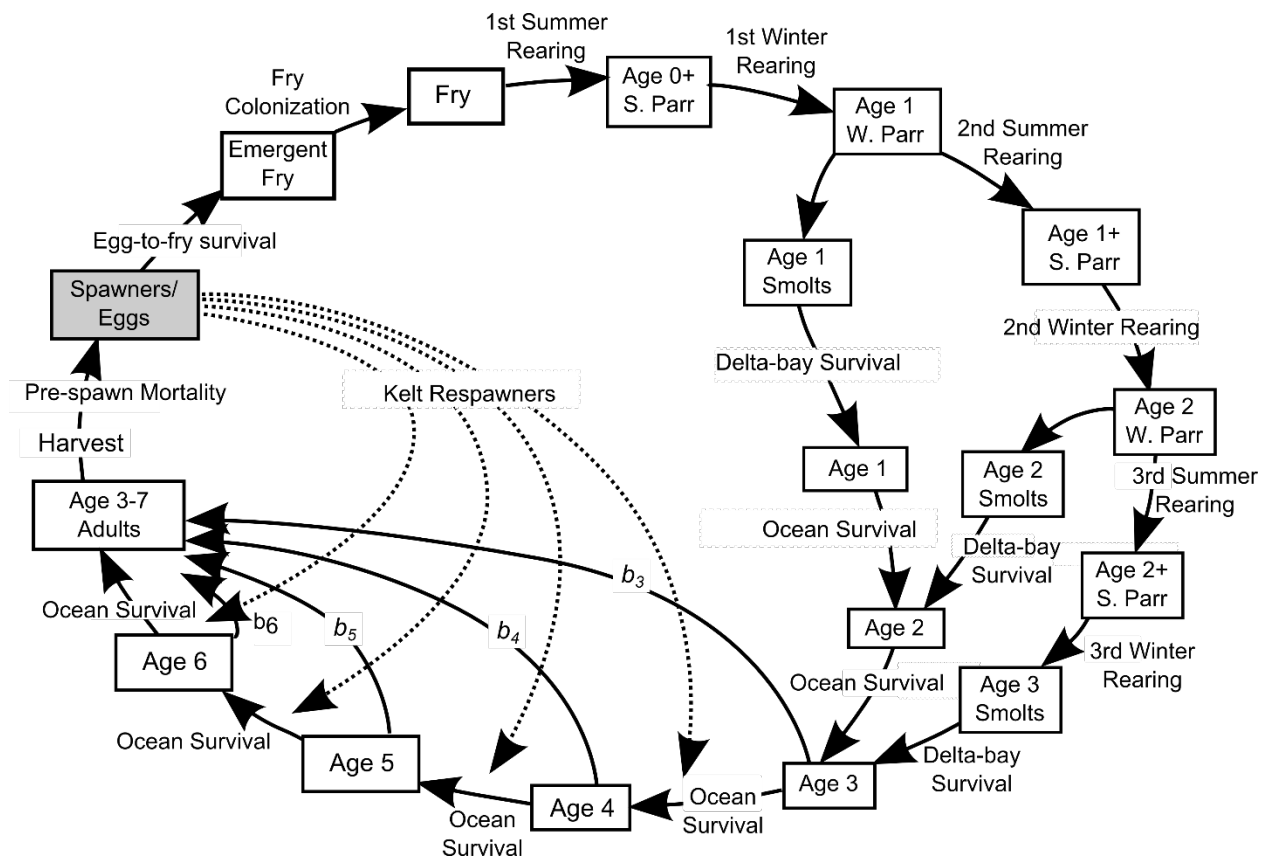
Figure 4.3.1. Schematic diagram of the life-cycle model for steelhead in the Chehalis River basin. Natal basin and mainstem splits not shown for simplicity. Gray box indicates that model outputs are expressed as number of spawners.

Table 4.3.1. Definitions of fish stage-location names in Figure 4.3.1. Migration from natal basin to mainstem not shown in Figure, but modeled natal basin and mainstem groups are included here for completeness.

Term	Definition
Spawners/eggs	Spawners are adults that have returned to spawn and survived upstream migration; number of eggs is fecundity x number of females (females = spawners x 0.5)
Emergent fry	Fry emerging from the gravel (prior to fry colonization stage)
Fry	Post-colonization fry (all stay in their natal subbasin)
Age-0+ summer parr	Juveniles at end of first summer rearing (all in natal subbasin)
Age-1 winter parr	Juveniles at end of first winter rearing that do not go the bay as smolts (all in natal subbasin)
Age-1 smolts	Age-1 juveniles entering bay at end of first year winter rearing (all from natal subbasin)
Age-1+ natal basin summer parr	Age-1+ juveniles in natal subbasin at end of summer rearing
Age-1+ mainstem summer parr	Age-1+ juveniles in mainstem at end of summer rearing
Age-2 natal basin winter parr	Age-2 juveniles in natal subbasin at end of winter rearing
Age-2 mainstem winter parr	Age-2 juveniles in mainstem at end of winter rearing
Age 2 natal basin smolts	Age-2 juveniles entering bay from natal subbasin at end of second year winter rearing (all from natal subbasin)
Age 2 mainstem smolts	Age-2 juveniles entering bay from mainstem at end of second year winter rearing (all from natal subbasin)
Age 2+ natal basin summer parr	Age-2+ juveniles in natal subbasin at end of summer rearing
Age 2+ mainstem summer parr	Age-2+ juveniles in mainstem at end of summer rearing
Age 3 natal basin smolts	Age-3 juveniles entering bay from natal subbasin at end of third year winter rearing (all from natal subbasin)
Age 3 mainstem smolts	Age-3 juveniles entering bay from mainstem at end of third year winter rearing (all from natal subbasin)
Age 3-7 adults	Adults returning to spawn (all age classes)

parr (or age-2 smolts for those that leave), end-of-summer age-2+ parr, and end of winter age-3 smolts. Because some age-1 parr move down to the mainstem at the end of the first winter (not shown in diagram), age-1+ and-2+ parr are split into natal and mainstem groups. Smolts then leave the basin, and experience delta-bay and annual marine productivity. A simple overview of the life stages and how capacities and productivities are calculated is shown in Table 4.3.2. Additional details of capacity and productivity calculations are in Appendix H and Appendix I.

The parameter estimates for current conditions are summarized in Tables 4.3.3 (capacity) and 4.3.4 (productivity). These parameter estimates define the baseline scenario (current habitat conditions) for the life-cycle model. In the next section (4.3.2 Diagnostic Scenarios), we describe how we modify these parameter estimates given a change to historical habitat conditions for any of the habitat factors that we model in our diagnostic scenarios.

For upstream migration and holding under current conditions, we model the stage as density-independent using an estimated productivity of 0.9 scaled by the passage rating and weighted by egg capacity, with no additional mortality due to temperature or development.

We model the spawning life stage with a hockey stick function using estimated egg capacity and fecundity. We use a density-independent productivity (F) of 5,400 eggs per female for first-time spawners (Stober et al. 1983, and unpublished Queets River data) and 8,000 eggs per female for repeat spawners (R2 Resource Consultants, Inc. 2008) (Table 4.3.4). Spawning capacity is expressed as egg capacity (c), which is the estimated maximum number of redds multiplied by the fecundity (Table 4.3.3). In large rivers (>20 m bankfull width), redd capacity is a function of spawning gravel area (digitized from aerial photography) and redd area (5.4 m², Orcutt et al. 1968). In small streams, we estimated the number of redds based on estimated spawning area divided by redd area (see Appendix H for details). When the number of returning spawners is below capacity, the number of eggs is the number of adults × percent females × fecundity. Spawning capacity is influenced by migration barriers and wood abundance in the diagnostic scenarios (Appendix I).

The incubation stage is modeled using density-independent incubation productivity. We assume that density dependence occurs in the spawning stage (i.e., the number of eggs in the gravel is limited by the egg capacity), and that once eggs are in the gravel there is no additional density-dependent mortality. Density-independent incubation productivity is 0.04 where the slope-width index is <0.05 due to very low sediment transport capacity (see Section 4.1.3 and Appendices C and I for more details). Where slope-width index is >0.05, we model incubation productivity as a function of percent fine sediment <0.85 mm, which is a function of current road density (productivity equation from Jensen et al. 2009):

$$p = \frac{1}{1+e^{-(1.989-0.185 \cdot sed)}},$$

where p is productivity and sed is percent fine sediment in spawning gravel.

The age-0+, age-1+, and age-2+ summer rearing stages are modeled as Beverton-Holt functions, using summer rearing capacity and density-independent summer rearing productivity as inputs. Habitat types and fish densities for age-0+ summer rearing are from Beamer and Henderson (1998), and Johnson et al. (1993) (Table 4.3.3). Fish densities are generally high in bank, bar, and backwater edge habitats of large rivers (>0.4 fish/m^2) (Beamer and Henderson 1998), and lower in the mid-channel (5% of the natural bank density, based on ratios in Beamer and Henderson 1998). In small streams, densities are high in both pools and riffles (we used the average of glides, riffles, rapids). We used the reported averages + one standard error from Johnson et al. (1993) (0.70 and 0.53 fish/m^2 for pools and riffles, respectively). We treat side channels as small streams, using the same pool and riffle densities. Floodplain ponds and sloughs and beaver ponds are not commonly used by age-0+ steelhead in summer, so they are assigned a density of 0. For summer rearing densities of age 1+ and 2+ steelhead (second and third summer), we did not have good field data in large rivers. However, we know that in the Newaukum River, densities for age-1+ steelhead in summer were 31% of those for age-0+ in August and 12% in September (Winkowski et al. 2018). Therefore, we chose to estimate large river bank, bar, and backwater densities at 31% of the age-0+ densities for those habitat types. Age-2+ densities are assumed to be the same as age-1+densities. In mid-channel for large rivers, age 1+ and older steelhead densities are 28% of the natural bank density (based on data in Beamer and Henderson, 1998). For the second and third summer in small streams, we used the reported average densities + one standard error from Johnson et al. (1993) for pools and riffles (0.18 and 0.07, respectively).

We estimated first-year summer productivity in ponds and floodplain habitats using the deep-pool survivals from Martens and Connolly (2014) (p = 0.74), and main-channel productivity from Grantham et al. (2012) using data near the high end of the range from the least modified stream reaches (p = 0.60) (Table 4.3.4). Second-year main channel survival is 0.85 in summer (~75th percentile of data in Harvey et al. 2005). Because we found no data for second or third year summer floodplain habitat survival we used the same value as first year floodplain productivity (p = 0.74). Differences in summer rearing habitat capacity and productivity among scenarios are mainly a function of changes in stream temperature, wood abundance, floodplain habitat areas, and beaver pond areas (Appendix I).

The age-0+, age-1+, and age-2+ winter rearing stages are modeled as Beverton-Holt functions, using winter rearing capacity and density-independent winter rearing productivity as inputs. Age-0+ winter fish densities are very low in all edge habitat types (0 to 0.31) (95th percentile of data from Beamer and Henderson 1998) (Table 4.3.3). In small streams, age-0+ winter densities are higher in pools and lower in riffles (0.16 and 0.11 fish/m^2) (average + one standard error from Johnson et al. 1993). We treat side channels as small streams, using the same densities as for pools and riffles. Floodplain ponds and sloughs and beaver ponds are not used at high densities by age-0+ steelhead in winter, and they are assigned a density of 0.03 fish/m^2 (J. Thompson, unpublished data). We did not have good age-1+ (second year) winter density data for steelhead in larger rivers, so we again assumed that age-1+ winter densities were 31% of age-0+ winter densities (the same percentage change as for summer, Winkowski et al. 2018). Age-2+ (third year) densities

54

were assumed to be the same as age-1+ densities. For small streams, pool and riffle densities were 0.09 and 0.04, respectively (mean + one standard error from Johnson et al. 1993).

We estimated first-year winter productivity at 0.52 in floodplain and pond habitats using the deep-pool survival values from Martens and Connolly (2014), and 0.35 in main channel habitats (2/3 of pond value based on McHugh et al. 2017). These estimates are consistent with recent freshwater survival estimates from the Cheakamus River in British Columbia (Korman and Schick 2019). Second- and third-year winter productivity in main channel habitats is 0.49 (1.4 x first-year winter survival, using the ratio of first-year summer to first-year winter survival). Because we found no data for second- or third-year floodplain habitat survival we used the same value as year 1 (p = 0.52).

The percentage of age-1 juveniles leaving the basin as smolts after their first winter is calibrated to produce 2% of returning adults as age-1 smolts, and 87% of returning adults as age-2 smolts (based on Quinault Indian Nation, unpublished data). The remaining juveniles leave the basin at age-3 and comprise 11% of the returning adults. Some steelhead parr move downstream from their natal basin to the mainstem at the end of the first summer, stopping in the first reach downstream of the tributary. Based on Bjornn (1978) and Hall et al. (2016), we estimated that 10% of juveniles leave subbasins <150 km², 2% of juveniles leave subbasins 150-450 km², and no fish leave subbasins >450 km². A percentage of steelhead parr also move downstream from their natal basin to rear in the mainstem at the end of the first winter, stopping in the first reach downstream of the tributary to spend their second and third year of rearing there. Based on Winter (1992) and Winkowski et al. (2018), we estimated that 50% of juveniles leave subbasins <150 km², 20% of juveniles leave subbasins 150-450 km², and no fish leave subbasins >450 km².

We modeled delta-bay productivity with a value of 0.14, which was back-calculated to achieve a total weighted average SAR of ~8% (M. Zimmerman, personal communication; N. Kendall, personal communication). Once in the ocean, all fish receive the same fixed annual productivity rates (0.8), followed by harvest (optional) (Table 4.3.4). We currently model all scenarios with harvest turned off. Each age class of fish in the ocean also has a propensity to spawn (b), so some proportion of each age class leaves the ocean population each year. A percentage of females for each age class also survive spawning and return to spawn again. We assume that 50% of spawners are females, and 80% of those females return to the ocean (i.e., the respawn kelt rate = 0.8 * 0.5, Howell et al. 1985). In the ocean, we apply a 0.6 reconditioning rate, and then a respawn return rate of 0.5. The cumulative respawner rate (product of the four numbers) is 0.12. In general, coastal populations have higher respawn rates, and the 12% respawn rate is within the range of values reported for coastal Oregon populations (Clemens 2015) and recent estimates for the Chehalis and Humptulips Rivers (Quinault Indian Nation, unpublished data).

Table 4.3.2. Overview of life stages, functions, and parameters used in the steelhead life-cycle model in the Chehalis River. See text for parameters and citations. Additional details are included in Appendices H (capacity changes) and I (productivity changes). DI = density independent, DD = density dependent. Gray highlight indicates freshwater life stages.

Life Stage	Function	Capacity	Productivity
Upstream migration and holding	DI	No capacity limit.	Constant among scenarios.
Spawning	DD (Hockey stick)	Varies with wood abundance and barriers.	Varies with barriers.
Incubation	DI	No capacity limit.	Varies with average percent fines and slope-width index.
Summer rearing –age 0+	DD (Beverton-Holt)	Varies with wood abundance, temperature, barriers.	Varies with wood abundance, temperature.
Winter rearing –age 1	DD (Beverton-Holt)	Varies with wood abundance, beaver ponds, floodplain habitat.	Varies with wood abundance, beaver ponds, floodplain habitat.
Summer rearing –age 1+	DD (Beverton-Holt)	Varies with wood abundance, temperature, barriers.	Varies with wood abundance, temperature.
Winter rearing –age 2	DD (Beverton-Holt)	Varies with wood abundance, beaver ponds, floodplain habitat.	Varies with wood abundance, beaver ponds, floodplain habitat.
Summer rearing –age 2+	DD (Beverton-Holt)	Varies with wood abundance, temperature, barriers.	Varies with wood abundance, temperature.
Winter rearing –age 3	DD (Beverton-Holt)	Varies with wood abundance, beaver ponds, floodplain habitat.	Varies with wood abundance, beaver ponds, floodplain habitat.
Delta-bay productivity	DI	No capacity limit.	Constant among scenarios.
Annual ocean productivity	DI	No capacity limit.	Constant among scenarios.

Table 4.3.3. Data used to estimate life-stage capacities in the steelhead life-cycle model for the Chehalis River. Habitat Data Source refers to the source of the habitat areas used to estimate capacity (i.e. the outputs of the NOAA spatial analysis, see Section 3.1). Additional details are in Appendix H. Historical values are estimated using the functions described in Appendix I. Gray highlight indicates freshwater life stages. Where second year rearing densities were unavailable, we set density at 20% of first year densities based on Winkowski et al. (2018).

Life Stage (Equation Form)	Habitat Data Source	Data Used to Estimate Life-stage Capacities (current condition)
Upstream migration and holding (density independent)	NA	NA (we found no data to estimate holding capacity)
Spawning (hockey stick)	Large river riffle area, attributed stream layer	Egg capacity = number of redds multiplied by fecundity (5400 eggs/female for maiden spawners; 8000 for respawners, Stober et al. 1983, R2 Resource Consultants, Inc. 2008) *Number of redds in large rivers (>20 m bankfull width):* Digitized riffle area divided by redd area (5.4 m^2) (Beechie et al. 2006a, redd area from Orcutt et al. 1968) *Number of redds in small streams (<20 m bankfull width):* Estimated riffle area divided by redd area (5.4 m^2) (redd area from Orcutt et al. 1968)
Incubation (density independent)	Attributed stream layer	NA (assumes that density dependence is in the spawning stage, and once eggs are in the gravel there is only density-independent productivity)
First year summer rearing -- age 0+ (Beverton-Holt)	Large river edge habitat, large river backwaters, floodplain habitat, attributed stream layer	*Density (fish/m^2):* Bank (natural) = 1.27 (Beamer and Henderson 1998) Bank (modified) = 0.64 (Beamer and Henderson 1998) Bar (boulder) = 1.59 (Beamer and Henderson 1998) Bar (gravel) = 1.59 (Beamer and Henderson 1998) Bar (sand) = 0 (Beamer and Henderson 1998) Backwater = 1.27 (Beamer and Henderson 1998) Mid-channel = 0.064 (Beamer and Henderson 1998) Pool (sm. stream) = 0.70 (Johnson et al. 1993) Riffle (sm. stream) = 0.53 (Johnson et al. 1993) Pond (<5 ha) = 0 (Johnson et al. 1993) Lake (>5 ha) = 0 (no data available) Marsh = 0 (no data available) Side-channel pool = 0.70 (Johnson et al. 1993) Side-channel riffle = 0.53 (Johnson et al. 1993) Floodplain pond (<5 ha) = 0 (Johnson et al. 1993) Slough = 0

Table 4.3.3 (cont.). Data used to estimate life-stage capacities in the steelhead life-cycle model.

Life Stage (Equation Form)	Habitat Data Source	Data Used to Estimate Life-stage Capacities (current condition)
First year winter rearing – age 1 (Beverton-Holt)	Large river edge habitat, large river backwaters, floodplain habitat, attributed stream layer	*Density (fish/m²):* Bank (natural) = 0.31 (Beamer and Henderson 1998) Bank (modified) = 0.31 Beamer and Henderson 1998) Bar (boulder) = 0.31 (Beamer and Henderson 1998) Bar (gravel) = 0.31 (Beamer and Henderson 1998)) Bar (sand) = 0 (Beamer and Henderson 1998) Backwater = 0 (Beamer and Henderson 1998) Mid-channel = 0.016 (Beamer and Henderson 1998) Pool (sm. stream) = 0.16 (Johnson et al. 1993) Riffle (sm. stream) = 0.11 (Johnson et al. 1993) Pond (<5 ha) = 0.03 (Johnson et al. 1993) Lake (>5 ha) = 0 (no data available) Marsh = 0 (no data available) Side-channel pool = 0.16 (Johnson et al. 1993) Side-channel riffle = 0.11 (Johnson et al. 1993) Floodplain pond (<5 ha) = 0.03 (Johnson et al. 1993) Slough = 0
Second and third year summer rearing -- age 1+ and 2+ (Beverton-Holt)	Large river edge habitat, large river backwaters, floodplain habitat, attributed stream layer	*Density (fish/m²)* Bank (natural) = 0.39 (31% of first summer density) Bank (modified) = 0.20 (31% of first summer density) Bar (boulder) = 0.49 (31% of first summer density) Bar (gravel) = 0.49 (31% of first summer density) Bar (sand) = 0 (31% of first summer density) Backwater = 0.39 (31% of first summer density) Mid-channel = 0.109 (Beamer and Henderson 1998) Pool (sm. stream) = 0.18 (Johnson et al. 1993) Riffle (sm. stream) = 0.07 (Johnson et al. 1993) Pond (<5 ha) = 0.07 (Johnson et al. 1993) Lake (>5 ha) = 0 (no data available) Marsh = 0 Side-channel pool = 0.18 (Johnson et al. 1993) Side-channel riffle = 0.07 (Johnson et al. 1993) Floodplain pond (<5 ha) = 0.07 (Johnson et al. 1993) Slough = 0

Table 4.3.3 (cont.). Data used to estimate life-stage capacities in the steelhead life-cycle model.

Life Stage (Equation Form)	Habitat Data Source	Data Used to Estimate Life-stage Capacities (current condition)
Second and third year winter rearing – age 2 and 3 (Beverton-Holt)	Large river edge habitat, large river backwaters, floodplain habitat, attributed stream layer	*Density (fish/m²)* Bank (natural) = 0.096 (31% of first winter density) Bank (modified) = 0.096 (31% of first winter density) Bar (boulder) = 0.096 (31% of first winter density) Bar (gravel) = 0.096 (31% of first winter density) Bar (sand) = 0 (31% of first winter density) Backwater = 0 (31% of first winter density) Mid-channel = 0.027 (Beamer and Henderson 1998) Pool (sm. stream) = 0.09 (Johnson et al. 1993) Riffle (sm. stream) = 0.04 (Johnson et al. 1993) Pond (<5 ha) = 0.01 (Johnson et al. 1993) Lake (>5 ha) = 0 (no data available) Marsh = 0 Side-channel pool = 0.09 (Johnson et al. 1993) Side-channel riffle = 0.04 (Johnson et al. 1993) Floodplain pond (<5 ha) = 0.01 (Johnson et al. 1993) Slough = 0
Delta-bay rearing	NA	NA (currently modeled as density independent)
Ocean	NA	NA (currently modeled as density independent)

Table 4.3.4. Data used to estimate life-stage productivities in the steelhead life-cycle model for the Chehalis River. Additional details are in Appendix I. Gray shading indicates freshwater life stages.

Life Stage (Equation Form)	Productivity or fecundity (current condition)
Upstream migration and holding (density independent)	Current and historical, p = 0.95.
Spawning (hockey stick)	Fecundity = 5400 eggs/female for maiden spawners; 8000 eggs/female for respawners (Stober et al. 1983, R2 Resource Consultants, Inc. 2008).
Incubation (density independent)	Slope-width index <0.05: p = 0.04 (based on data from Mobrand Biometrics Inc., 2003). Slope-width index >0.05: incubation productivity is a function of percent fine sediment <0.85 mm (Productivity equation from Jensen et al. 2009). See Appendix C for fine sediment estimates based on road density and slope area index. $$p = \frac{1}{1 + e^{-(1.989 - 0.185 \cdot sed)}}$$
First year summer rearing – age 0+ (Beverton-Holt)	Current condition in small stream and large river (low wood abundance, T < 18°C) p = 0.60 (Grantham et al. 2012), pond and floodplain habitats p = 0.74 (Martens and Connolly 2014). Varies with wood abundance and temperature (details in Section 4.3.2).
First year winter rearing – age 1 (Beverton-Holt)	Current condition: small stream with low wood abundance p = 0.35, ponds and sloughs p = 0. 52 (Martens and Connolly 2014, McHugh et al. 2017). Varies with wood abundance, beaver pond area, and floodplain habitat areas (details in Section 4.3.2).
Second and third year summer rearing – age 1+ and 2+ (Beverton-Holt)	Current condition in small stream and large river (low wood abundance, T < 18°C) p = 0.85 (Harvey et al. 2005), pond and floodplain habitats p = 0.74 (Martens and Connolly 2014). Varies with wood abundance and temperature (details in Section 4.3.2).
Second and third year winter rearing – age 2 and 3 (Beverton-Holt)	Current condition: small stream with low wood abundance p = 0.49 (1.4 x first-year p), ponds and sloughs p = 0.52 (Martens and Connolly 2014, McHugh et al. 2017). Varies with wood abundance, beaver pond area, and floodplain habitat areas (details in Section 4.3.2).
Delta-bay productivity	p = 0.14. Back-calculated from SAR of 0.08 and annual ocean productivities. Fixed in all scenarios. Recommended SAR from WDFW is 0.08.
Ocean productivity	p = 0.8 per year (Ricker 1976).
Maturation rate	b_3 = 0.01 (estimated to match age structure of adult returns). b_4 = 0.43 (estimated to match age structure of adult returns). b_5 = 0.76 (estimated to match age structure of adult returns). b_6 = 1 (estimated to match age structure of adult returns).
Respawn rate	Respawn kelt rate = 0.8 * 0.5 (Howell et al. 1985). Reconditioning of kelts in ocean = 0.6. Kelts from ocean to returning respawners = 0.5. Cumulative respawn rate = 0.12 (product of all rates above).
Harvest (optional)	No harvest in these model runs.

4.3.2 Diagnostic Scenarios: Steelhead

The diagnostic scenarios are used to model effects of habitat changes on steelhead populations, given specific assumptions of how each change in habitat quantity or quality affects life-stage capacities or productivities. Each scenario examines how a change in a single habitat factor independently affects steelhead abundance and productivity in each spatial unit. The nine habitat factors we model are:

1. Migration barriers
2. Fine sediment in spawning gravels
3. Wood abundance change in small streams and large rivers
4. Shade (temperature) changes in small streams and large rivers
5. Bank armor in large rivers
6. Large river channel straightening
7. Beaver pond changes in small streams
8. Floodplain habitat change (including side channels, ponds, marshes, and lakes)
9. Wood abundance and floodplain habitat change combined

Migration barriers: In the steelhead life-cycle model, migration barriers reduce spawning capacity and number of spawners above barriers according to the passage ratings assigned by WDFW (Table 4.3.3). For example, above a barrier with a passage rating of 0.33, spawning capacity and productivity are reduced by 2/3. As with coho and Chinook salmon, passage ratings are multiplicative when there are multiple barriers in succession. To evaluate the degree to which migration barriers influence steelhead abundance and productivity under these assumptions, we run a diagnostic scenario for "no barriers", in which we set all habitat conditions to current conditions with the exception that we remove all non-natural barriers.

Fine sediment in spawning gravels: Fine sediment affects density-independent incubation productivity in redds as a function of percent fine sediment in spawning gravels (Table 4.3.4). For the historical fine sediment scenario, the road density is set to zero, and incubation productivity in reaches with slope-width index <0.05 is 0.72 based on the empirical equation from Jensen et al. (2009) (see Appendix I for more detail). In reaches with slope-width index <0.05, mean percent fines is 27% for both current and historical conditions (based on data from Mobrand Biometrics, Inc. 2003), and density-independent incubation productivity is 0.04.

Wood abundance: The wood abundance scenario is intended to examine the effect of wood abundance alone, without a concomitant influence of wood on floodplain connection or of riparian shade on stream temperature. We model wood abundance influences on spawning capacity in small streams, summer rearing capacity and productivity for juvenile steelhead in small streams and large rivers, and winter rearing capacity and productivity for juvenile steelhead in small streams and large rivers (Table 4.3.2). For spawning capacity, wood abundance affects spawning capacity in small streams by increasing the number of pools and spawning areas.

For summer rearing in small streams, we model an effect of wood abundance on rearing capacity through changes in pool area as a function of land cover. We stratified habitat surveys conducted by WDFW by slope class and landcover, and extrapolated those values to the remaining reaches in each category (method from Beechie et al. 1994, 2001). In large rivers, we modified summer rearing capacity based on an estimated increase in wood cover in edge habitats, which have higher juvenile rearing densities (Beamer and Henderson 1998, Beechie et al. 2005a) (details in Appendix I). Juvenile salmonid data from Beamer and Henderson (1998) and Jamie Thompson (unpublished data) show that steelhead densities are 1.63 and 1.19 times higher in bar and bank edge units with high wood abundance than in those same units with low wood abundance. Based on aerial photograph observations in the nearby Queets River basin with high wood abundance, we estimated that under historical conditions approximately 5% of the habitat area would have wood cover. Using a weighted average of summer fish densities in areas with wood and without wood under natural conditions, we calculated a subbasin specific multiplier to increase rearing capacity under historical conditions, which ranged from 1.02 to 1.05. We also used this multiplier to estimate change in productivity due to wood for summer rearing in large rivers and small streams (McHugh et al. 2017).

For winter rearing, the large river and small stream capacity changes from an effect of wood were calculated in the same way as for summer rearing. For small streams, we estimated that winter pool areas were 43% of summer pool areas (based on habitat surveys in the same reaches at summer and winter base flows, Beechie 1998). For large river habitat capacity, the subbasin-specific wood multipliers were calculated as above for summer rearing habitat and were used to increase rearing capacity under historical conditions. Weighted average subbasin specific multipliers ranged from 1.07 to 1.10. For small streams, channels with low wood abundance (current condition) were assigned a density-independent winter rearing productivity of 0.35, and off-channel habitats (ponds, marshes) were assigned a value of 0.52 (Martens and Connolly 2014, McHugh et al. 2017). For density-independent winter first year rearing productivity in small channels with high wood abundance we used the same ratio of rearing productivities as for coho first winter (1.67) to modify rearing productivity in the high wood scenario. We did not have similar small stream productivity data for the second and third winters, so we used the same multipliers as for large rivers in those stages.

Shade and stream temperature: Decreased shade increases stream temperature (temperature model described in Appendix A), which decreases steelhead summer parr abundance and productivity via changes in summer rearing capacity and productivity. We first estimate a productivity multiplier based on stream temperature that decreases summer rearing productivity from its base value. We model the temperature effect on steelhead juvenile rearing using a functional relationship developed by Bear et al. (2007):

$$p = \frac{97.8846}{1 - e^{-((T-24.3522)/-0.5033)}}$$

Where T is the 7-DADM from the temperature models. Details of the analysis from Bear et al. (2007) are in Appendix I.

Bank armoring: Bank armoring affects the density of rearing salmonids, and therefore the rearing capacity of large rivers for all species. We digitized visible areas of rip-rap bank edge units (see Appendix E), and used steelhead summer and winter rearing densities for rip-rap banks (reanalyzed from data in Beamer and Henderson 1998). For the historical condition, we simply converted all rip-rap bank edge units to natural bank edge units, and used the higher summer and winter rearing density for natural banks to estimate rearing capacity for each unit (density data from Beamer and Henderson 1998). We did not estimate a productivity change for these unit type changes.

Main channel length (channel straightening): We assumed that large river channel straightening reduces both spawning and rearing habitat areas, and therefore spawning and rearing capacities of all species. We used reach-specific channel length template multipliers developed by Natural Systems Design (Tim Abbe, Susan Dickerson-Lange) and NOAA (Tim Beechie) to modify large river habitat areas for the historical condition. The large river length multipliers ranged from 1 to 1.5, with the majority being ≤1.2.

Beaver pond changes in small streams: Beaver ponds have a relatively small influence on summer rearing and overwintering capacity and productivity of steelhead. In our model, we assumed that summer rearing densities of steelhead in beaver ponds are similar between current and historical conditions, but that the area of beaver ponds was substantially greater historically (similar to calculations for coho salmon, Pollock et al. 2004).

Floodplain habitat change (side-channels, marshes, and ponds): Reductions in the array of floodplain habitats that were historically available (side-channels, marshes, and ponds) would reduce spawning, summer rearing, and winter rearing habitat capacity and productivities for juvenile steelhead. Loss of floodplain hyporheic connectivity also increases stream temperature (Appendix J). Our historical scenario includes increases in side-channel area based on side channel length multipliers developed by Natural Systems Design (Tim Abbe, Susan Dickerson-Lange) and NOAA (Tim Beechie), which ranged from 0 to 2.5 depending on the reach and channel type.

Delta-bay and marine productivities: Because the intent of the diagnostic scenarios is to evaluate the effect of changes in freshwater habitat conditions, we hold all of these values constant (see Table 4.3.4).

5. Diagnostic Scenario Results

In this chapter, we first describe the basin-scale diagnostic results by species (Section 5.1), and discuss how the importance of each habitat factor varies among species. In Section 5.2, we discuss each of the most important habitat factors separately, and how they vary among Ecological Diversity Regions. In Section 6, we highlight and describe the key restoration opportunities indicated by the analysis. Section 7 describes the restoration scenario results.

Each diagnostic scenario sets one habitat type or attribute to historical conditions, while holding all others to current conditions. For example, the historical shade scenario is modeled using historical shade levels (which reduces stream temperature), while fine sediment wood abundance, beaver ponds, floodplains, and other factors are held at their current conditions. To facilitate interpretation of the model results for these diagnostic scenarios, we use a single color scheme in which each diagnostic scenario is assigned a specific color (Figure 5.1). These same colors are used for all figures that portray results of the scenario analyses.
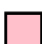
Color   **Scenario**

☐ Observed abundance

■ Modeled current and historical conditions

■ Migration barrier change (presence or removal of barriers)

■ Fine sediment change (forest road effects on egg-to-fry survival)

■ Wood abundance change (wood abundance, all rivers and streams)

■ Shade change (shade effect on temperature)

■ Large river bank condition change (rip-rap effects)

■ Large river length change (channel straightening effects)

■ Beaver pond change (small streams)

■ Floodplain habitat change (side channel, marsh and pond habitats)

■ Wood and floodplain change (wood, side channel, marsh and pond habitats)

Figure 5.1. Color scheme used in all life-cycle model results and maps in this report. To facilitate interpretation of the life-cycle model results, each color represents the same habitat change in all graphics and maps.

5.1 Diagnostic Results by Species

The diagnostic results indicate that restoration of shade, wood, beaver ponds and floodplain habitat provide the greatest opportunities to increase spawner abundances for the four species modeled in the Chehalis River basin (Table 5.1.1). While removal of migration barriers can provide only a modest increase in coho spawner abundance in the Chehalis River basin, barrier removals remain a cost effective restoration action that should be pursued where there is sufficient habitat gain by removal of a barrier. The largest modeled restoration potentials for coho salmon are in overwinter habitats such as beaver ponds and floodplain habitats, whereas the largest modeled restoration potentials for spring Chinook are restoring wood abundance, shade, and floodplain habitats. The largest modeled restoration potentials for fall Chinook and steelhead are restoring wood abundance, and to a lesser extent, floodplain habitats. Reduction of fine sediment may also be important, but uncertainty in fine sediment levels and sources of fine sediment preclude recommending specific sediment reduction actions at this time.

Table 5.1.1: Modeled number of spawners (N_{eq}, without harvest) in each diagnostic scenario for coho, spring Chinook, fall Chinook, and steelhead for the Chehalis basin (percent change in parentheses). Abundance cells (columns 2-5) with changes >25% are dark blue, and abundance cells with changes 10-25% are shaded light blue. Scenarios (column 1) with 3 or more species with abundance values >25% are dark blue, 2 species >25% are medium blue, and 1 species >25% are light blue. Gray cells are current and historical conditions.

Scenario	Coho	Spring Chinook	Fall Chinook	Steelhead
Current conditions	90,625	1,035	31,746	16,092
No barriers	98,645 (9%)	1,035 (0%)	32,388 (2%)	16,577 (3%)
Historical fine sediment	104,514 (15%)	1,618 (56%)	42,227 (33%)	18,166 (13%)
Historical wood	113,230 (25%)	1,363 (32%)	39,096 (23%)	20,949 (30%)
Historical shade	109,092 (20%)	1,454 (40%)	32,341 (2%)	17,399 (8%)
Historical bank conditions	90,712 (0%)	1,062 (3%)	32,346 (2%)	16,181 (1%)
Historical large river length	91,048 (0%)	1,108 (7%)	33,128 (4%)	16,795 (4%)
Historical beaver ponds	181,202 (100%)	1,042 (1%)	32,596 (3%)	16,064 (0%)
Historical floodplain habitat	145,702 (61%)	1,394 (35%)	36,439 (15%)	18,822 (17%)
Historical wood and floodplain	172,209 (90%)	1,797 (74%)	44,733 (41%)	24,285 (51%)
All historical conditions	396,226 (337%)	3,551 (243%)	67,570 (113%)	29,867 (86%)

5.1.1 Coho Salmon

Modeled coho salmon spawner abundance increased by 100% in the historical beaver pond scenario and 61% in the historical floodplain scenario (Figure 5.1.2, Table 5.1.2). The historical wood scenario increased modeled spawner abundance by only 25%, whereas the historical wood + floodplain scenario increased modeled spawner abundance by 90%. Historical shade, migration barriers, and fine sediment increased spawner abundance by only 9-20%, and all other scenarios produced less than 1% change. The diagnostic scenario with all historical conditions had a modeled spawner abundance more than 300% higher than the modeled current abundance (Table 5.1.2).

Figure 5.1.1. Modeled difference in spawner abundance (N_{eq}, without harvest) among diagnostic scenarios for coho salmon.

Changes in life-cycle productivity (P_n) and capacity (C_n) were of roughly similar magnitude to changes in spawner abundance, with the exception of the historical fine sediment and beaver pond scenarios (Table 5.1.2). The historical fine sediment scenario produced a large change in P_n but very little change in C_n and the historical beaver pond scenario produced a large change in C_n but little change in P_n. The ranking of scenarios with respect to changes P_n and C_n were also similar, again with the exception of historical fine sediment and beaver ponds.

These results suggest that increasing availability of winter rearing habitats is likely to provide the largest increase in coho salmon population abundance, and that increasing spawning and summer rearing habitats will have relatively smaller effects. Modeled coho salmon spawner abundance increased by ~50 to 100% in both the historical floodplain and historical beaver pond scenarios. Both types of changes substantially increase winter rearing capacity and productivity. By contrast, factors affecting summer rearing habitat such as changes in wood abundance or summer stream temperature produce much smaller changes in abundance. Moreover, the sensitivity analysis (Section 8.4.1) shows that coho salmon are particularly sensitive to changes in winter rearing productivity, which is higher in beaver pond and floodplain habitats than in main channels.

Table 5.1.2. Modeled coho spawner abundance (N_{eq}, without harvest) for all diagnostic scenarios, along with life-cycle productivity (P_n) and capacity (C_n) estimated from the life stage parameters (see Section 4 for details of the calculations). Shaded cells indicate changes >25%.

Scenario	Spawners (N_{eq})	P_n	C_n
Current conditions	90,625	4.1	120,062
Historical shade	109,092	4.3	142,228
Historical beaver ponds	181,202	4.5	232,742
Historical floodplain habitat	145,702	4.5	186,869
Historical wood	113,230	4.7	143,681
Historical wood + floodplain	172,209	5.1	214,434
No Barriers	98,645	4.2	129,123
Historical fine sediment	104,514	6.7	122,913
Historical large river bank conditions	90,712	4.1	120,245
Historical large river length	91,048	4.1	120,780
Historical conditions	396,226	9.3	443,840

5.1.2 Spring Chinook Salmon

Modeled spring Chinook spawner abundance increased by 41% in the historical shade scenario, by 35% in the historical floodplain scenario, by 57% in the fine sediment scenario, and by 32% in the historical wood abundance scenario (Figure 5.1.3, Table 5.1.3). The historical wood and floodplain combination scenario produced a 74% increase in spawner abundance. All other scenarios produced less than a 7% change in spawner abundance (no barriers, historical beaver ponds, historical large river bank conditions, and historical large river length). The diagnostic scenario with all historical conditions had a spawner abundance of 3,551 compared to modeled abundance under current conditions of 1,035 (an increase of 243%) (Table 5.1.3).
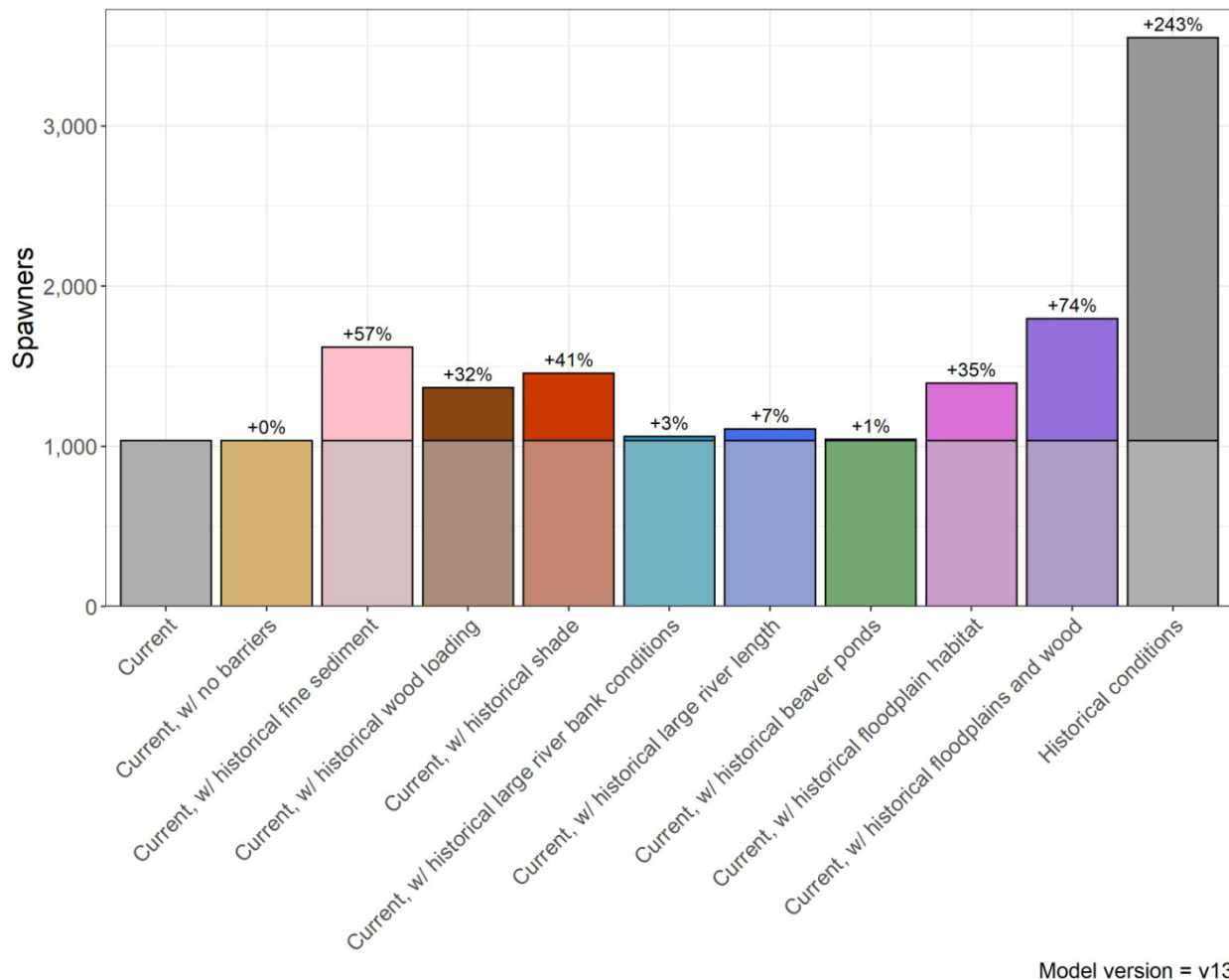
Figure 5.1.2. Modeled difference in spawner abundance (N_{eq}, without harvest) among diagnostic scenarios for spring Chinook salmon.

Changes in life-cycle productivity (P_n) and capacity (C_n) were of roughly similar magnitude to changes in spawner abundance, with the exception of the historical fine sediment scenario which produced a large change in P_n but very little change in C_n (Table 5.1.2).

These results suggest that increasing shade and floodplain connectivity will likely create the largest improvement in spring Chinook spawner abundance. Modeled spring Chinook spawner abundance increased by 35% or more in the historical shade and floodplain scenarios. Spring Chinook are sensitive to high temperatures during their prespawn period, and both the shade and floodplain scenarios reduce temperatures during that life-stage. Floodplain connectivity also increases spawning capacity by increasing the length of side channels, which are considered spawning areas. The historical wood abundance scenario produced an increase in modeled spawner abundance of 32%, suggesting that degradation of subyearling rearing habitats is also a large contributor to population decline. Finally, the historical fine sediment scenario also increased spawner abundance significantly (57%). Fine sediment has a large effect on spring Chinook incubation for two reasons: (1) survival is the dominant habitat factor influencing fry migrant abundance, and (2) modeled current fine sediment levels are higher in subbasins occupied by spring Chinook than in many other subbasins. However, field confirmation of fine sediment levels and sources is needed before identifying actions to reduce fine sediment.

Table 5.1.3. Modeled spring Chinook spawner abundance (N_{eq}, without harvest) for all diagnostic scenarios, along with life-cycle productivity (P_n) and capacity (C_n) estimated from the life stage parameters (see section 4 for details of the calculations). Shaded cells indicate changes >25%.

Scenario	Spawners (N_{eq})	P_n	C_n
Current conditions	1,035	2.0	2,021
Historical shade	1,454	2.4	2,459
Historical beaver ponds	1,042	2.0	2,035
Historical floodplain habitat	1,394	2.4	2,402
Historical wood	1,363	2.3	2,434
Historical wood + floodplain	1,797	2.6	2,894
No Barriers	1,035	2.0	2,021
Historical fine sediment	1,618	3.4	2,294
Historical large river bank conditions	1,062	2.1	2,072
Historical large river length	1,108	2.1	2,151
Historical conditions	3,551	4.8	4,488

5.1.3 Fall Chinook Salmon

Modeled fall Chinook spawner abundance increased by 41% in the historical wood and floodplain combination scenario, but most of that increase was apparently from wood abundance (23% in the wood abundance scenario alone) (Figure 5.1.4, Table 5.1.4). Modeled spawner abundance increased 33% in the historical fine sediment scenario, suggesting that fine sediment may be a significant issue, particularly for the fry migrant component of the population, which has little exposure to freshwater rearing conditions. All other scenarios produced a change in spawner abundance of 15% or less (no barriers, historical beaver ponds, historical large river bank conditions, historical large river length, historical shade, and historical floodplain habitat). The diagnostic scenario with all
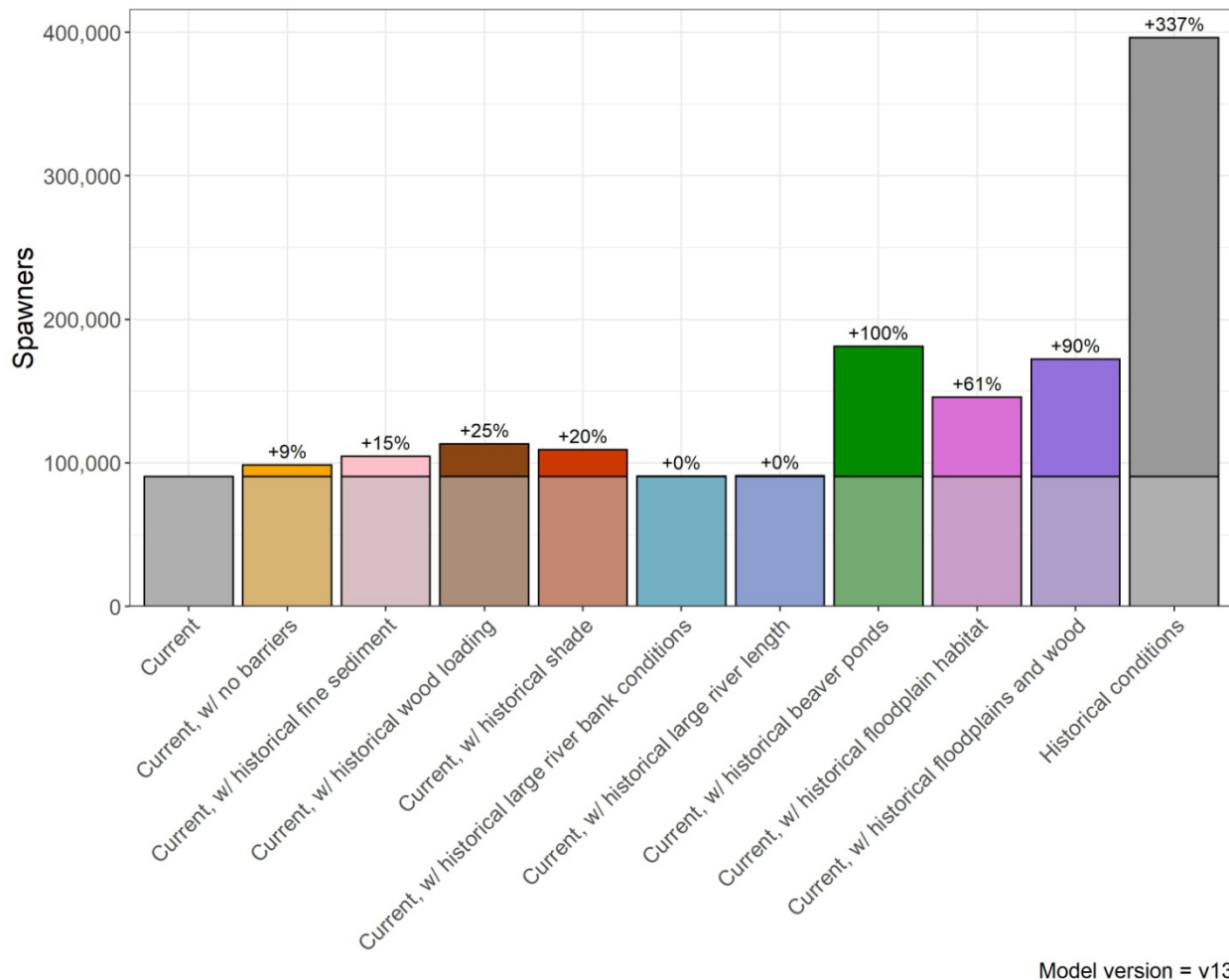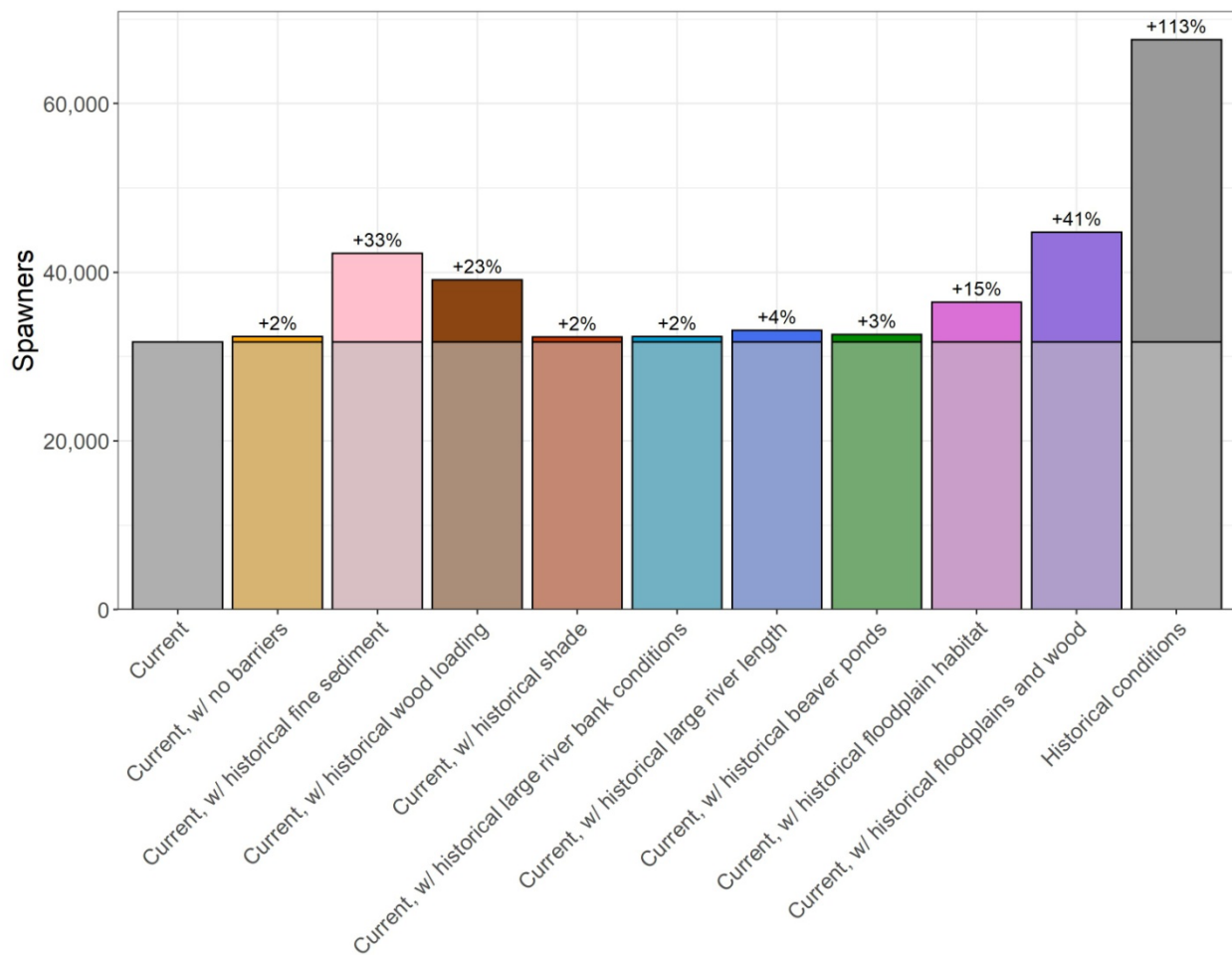

Figure 5.1.3. Modeled difference in spawner abundance (N_{eq}, without harvest) among diagnostic scenarios for fall Chinook salmon.

historical conditions had a spawner abundance of 67,570 compared to modeled abundance under current conditions of about 31,746 (an increase of 113%) (Table 5.1.4).

Changes in life-cycle productivity (P_n) and capacity (C_n) were of roughly similar magnitude to changes in spawner abundance, with the exception of the historical fine sediment scenario, which produced a large change in P_n but a smaller change in C_n (Table 5.1.4).

These results suggest that increasing wood abundance and floodplain connectivity may help increase fall Chinook spawner abundance, and that other factors, aside from fine sediment, will have relatively smaller influences on fall Chinook populations. Increased floodplain connectivity increases side channel spawning and rearing capacity through reconnection of side channels, whereas increased wood abundance can increase the number of pools and spawning riffles, which increases both spawning capacity and rearing capacity, as well as rearing productivity.

Table 5.1.4. Modeled fall Chinook spawner abundance (N_{eq}, without harvest) for all diagnostic scenarios, along with life-cycle productivity (P_n) and capacity (C_n) estimated from the life stage parameters (see section 4 for details of the calculations). Shaded cells indicate changes >25%.

Scenario	Spawners (N_{eq})	P_n	C_n
Current conditions	31,746	3.8	43,267
Historical shade	32,341	3.8	43,847
Historical beaver ponds	32,596	3.8	44,283
Historical floodplain habitat	36,439	3.8	49,284
Historical wood	39,096	4.1	51,639
Historical wood + floodplain	44,733	4.2	58,656
No Barriers	32,388	3.8	43,785
Historical fine sediment	42,227	5.6	51,441
Historical large river bank conditions	32,346	3.8	44,096
Historical large river length	33,128	3.8	45,116
Historical conditions	67,570	6.4	80,063

5.1.4 Steelhead

Modeled steelhead spawner abundance increased by 30% in the historical wood abundance scenario and 13 to 17% in the fine sediment and floodplain habitat scenarios (Figure 5.1.5, Table 5.1.5). The historical wood + floodplain scenario increased modeled spawner abundance by 51%. All other scenarios produced a change in abundance of 8% or less. The diagnostic scenario with all historical conditions had a modeled spawner abundance 86% higher than the modeled current abundance (Table 5.1.5).
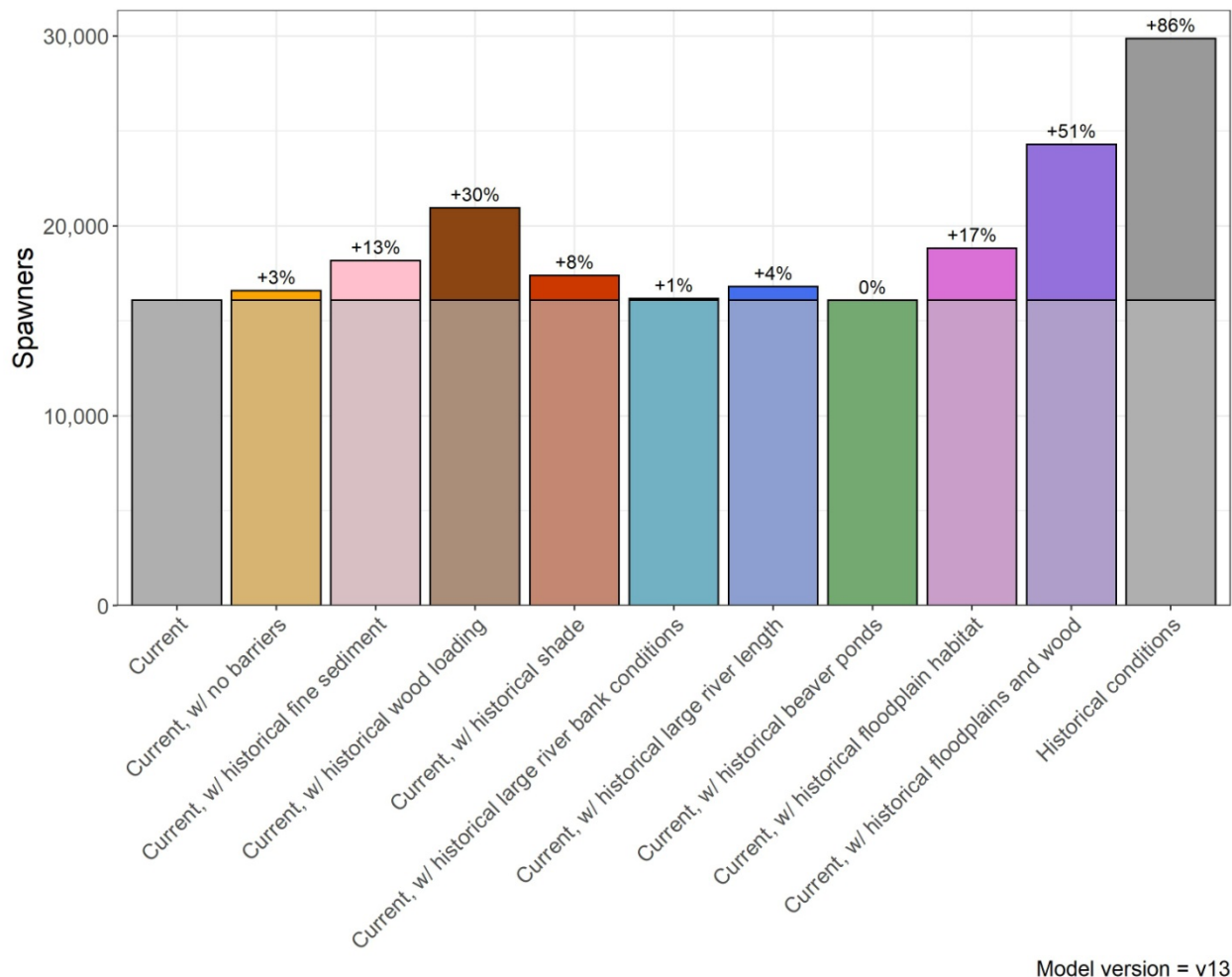
Figure 5.1.4. Modeled difference in spawner abundance (N_{eq}, without harvest) among diagnostic scenarios for steelhead.

Table 5.1.5. Modeled steelhead spawner abundance (N_{eq}, without harvest) for all diagnostic scenarios, along with life-cycle productivity (P_n) and capacity (C_n) estimated from the life stage parameters (see section 4 for details of the calculations). Shaded cells indicate changes >25%.

Scenario	Spawners (N_{eq})	P_n	C_n
Current conditions	16,092	4.0	21,437
Historical shade	17,399	4.1	22,947
Historical beaver ponds	16,064	4.1	21,328
Historical floodplain habitat	18,822	4.2	24,642
Historical wood	20,949	5.6	25,539
Historical wood + floodplain	24,285	5.9	29,271
No Barriers	16,577	4.1	21,925
Historical fine sediment	18,166	6.1	21,703
Historical large river bank conditions	16,181	4.0	21,550
Historical large river length	16,795	4.0	22,361
Historical conditions	29,867	9.4	33,435

Changes in life-cycle productivity (P_n) and capacity (C_n) were of roughly similar magnitude to changes in spawner abundance, with the exception of the historical fine sediment which produced a large change in P_n but very little change in C_n (Table 5.1.5). The ranking of scenarios with respect to changes P_n and C_n were also similar, again with the exception of historical fine sediment.

These results suggest that increasing wood is likely to provide the largest increase in steelhead spawner abundance, and that decreasing fine sediment or increasing floodplain habitat will have relatively smaller effects. Other habitat restoration actions, including increasing shade, are likely to provide less benefit to steelhead. This most likely is a result of the temperature-survival function for steelhead (Bear et al. 2007), in which increasing temperature has little effect on steelhead survival until the 7-DADM approaches 24°C (Appendix I.6).

5.2 Diagnostic Results by Scenario and EDR

The basin-level results indicate which types of habitat restoration have the greatest potential to increase salmon populations at the scale of the Chehalis basin, but the magnitude of restoration potential varies spatially, as do the distributions of species within the basin. Hence, the relative importance of each factor varies among species and EDRs. In this section, we describe the spatial variation in modeled effects of each diagnostic scenario

for each species (excluding diagnostic scenarios that produced little change for any species).

5.2.1 Historical Wood Abundance Scenario

The historical wood abundance scenario produced a moderate to large increase in modeled spawner abundance for all four species (Table 5.2.1). For coho salmon and fall Chinook, modeled percentage increases in spawner abundance relative to current conditions were similar across EDRs (generally 20-40%). For spring Chinook, the percent increase in spawner abundance was highest in the Mainstem Upper Chehalis EDR (56%), but the absolute abundance increase in that EDR was very low (9 spawners). Most of the modeled increase in spring Chinook spawner abundance in the historical wood scenario was in the Cascade Mountains EDR (Skookumchuck and Newaukum, 242 spawners). For steelhead, modeled spawner abundance increased between 27% and 70% in all EDRs except the mainstem EDRs.

The historical wood abundance scenario did not produce large changes in productivity except for steelhead, which showed increases >1.0 in all EDRs except the mainstem EDRs. The pattern of changes in capacity was similar to that of abundance, but the magnitudes of change were smaller across the basin and across species (Tables 5.2.2 and 5.2.3).

Table 5.2.1: Modeled increase in spawner abundance (N_{eq}, without harvest) in the historical wood scenario for coho, spring Chinook, fall Chinook, and steelhead by Ecological Diversity Region. Dark blue shade indicates changes >50%, medium blue indicates changes 25-50%, light blue indicates changes 10-25%, and no color indicates <10% change.

Ecological Region	Coho	Spring Chinook	Fall Chinook	Steelhead
Black Hills	2,438 (22%)	0	0 (0%)	277 (41%)
Black River	1,280 (22%)	0	329 (27%)	211 (31%)
Cascade Mountains	2,831 (34%)	242 (32%)	533 (27%)	516 (32%)
Central Lowlands	1,725 (46%)	0	0 (0%)	128 (70%)
Grays Harbor Tributaries	5,773 (23%)	0	1,275 (23%)	1,239
Mainstem: Lower Chehalis	0 (0%)	0	1,589 (23%)	313 (24%)
Mainstem: Middle Chehalis	0	10 (53%)	221 (37%)	0 (0%)
Mainstem: Upper Chehalis	0	9 (56%)	0 (0%)	0 (0%)
Olympic Mountains	6,208 (22%)	0	2,775 (21%)	1,630
Willapa Hills	2,261 (30%)	67 (28%)	395 (24%)	489 (35%)

Table 5.2.2: Modeled life-cycle productivity (P_n) in the historical wood scenario for coho, spring Chinook, fall Chinook, and steelhead by Ecological Diversity Region. Absolute increase from current in parentheses. Dark blue shade indicates changes >2.0, medium blue indicates changes 1.0-2.0, light blue indicates changes 0.5-1.0, and no color indicates <0.5 change.

Ecological Region	Coho	Spring	Fall Chinook	Steelhead
Black Hills	4.9 (0.8)	-	3.8 (0.4)	5.4 (2)
Black River	4.1 (0.4)	-	3.6 (0.3)	4.8 (1.3)
Cascade Mountains	3.5 (0.5)	2.4 (0.2)	3.8 (0.4)	4.5 (1.2)
Central Lowlands	4.5 (1.1)	-	2.1 (0.6)	3.1 (1.2)
Grays Harbor Tribs	5.1 (0.6)	-	4.1 (0.3)	6.1 (1.8)
Mainstem: Lower	1.6 (0.1)	-	4.1 (0.3)	4.1 (0.6)
Mainstem: Middle	-	1.4 (0.1)	2.1 (0.1)	4.2 (0.9)
Mainstem: Upper	-	1.4 (0.1)	2.1 (0.2)	2.7 (0.6)
Olympic Mountains	5.1 (0.7)	-	4.5 (0.4)	6.4 (1.8)
Willapa Hills	3.8 (0.6)	2 (0.2)	3.2 (0.3)	4.5 (1.4)

Table 5.2.3: Modeled life-cycle capacity (C_n) in the historical wood scenario for coho, spring Chinook, fall Chinook, and steelhead by Ecological Diversity Region. Dark blue shade indicates changes >50%, medium blue indicates changes 25-50%, light blue indicates changes 10-25%, and no color indicates <10% change.

Ecological Region	Coho	Spring	Fall Chinook	Steelhead
Black Hills	2,301 (16%)	-	0 (0%)	214 (22%)
Black River	1,427 (18%)	-	394 (23%)	168 (17%)
Cascade Mountains	3,031 (24%)	300 (21%)	614 (22%)	422 (18%)
Central Lowlands	1,753 (34%)	-	0 (0%)	0 (0%)
Grays Harbor Tribs	6,086 (19%)	-	1,466 (19%)	1,040 (20%)
Mainstem: Lower	0 (0%)	-	1,830 (20%)	319 (17%)
Mainstem: Middle	-	0 (0%)	339 (27%)	0 (0%)
Mainstem: Upper	-	23 (38%)	0 (0%)	0 (0%)
Olympic Mountains	6,336 (17%)	-	3,042 (18%)	1,383 (18%)
Willapa Hills	2,378 (21%)	81 (15%)	456 (18%)	375 (18%)

5.2.2 Historical Floodplain Habitat Scenario

Percent change in spawner abundance under the historical floodplain habitat scenario was high across all EDRs for coho salmon, except for the upper and middle mainstem EDRs (Table 5.2.4). In the upper and middle mainstem EDRs, abundance changes are zero because there are no spawners in those reaches. Increased survival of juveniles from improved mainstem habitat is included in the tributary EDR spawner abundance totals because all spawner abundance increases are reflected in the natal EDR regardless of where the increased productivity occurs. For coho, floodplain habitat is important for the overwinter life-stage, while for spring chinook, floodplains are most important for temperature reductions during the prespawn life-stage and for increasing spawning capacity through addition of side channel length. Because fall Chinook are less dependent on floodplain habitats, percent increases in spawner abundance are generally low, although modest increases may be gained in the Grays Harbor Tributaries and Olympic Mountains EDRs. For steelhead, the floodplain scenario suggests modest increases in spawner abundance, except in the lower mainstem Chehalis where increased side channel length increased spawner capacity significantly (>100% increase, but a small number of spawners).

In general productivity increases were low, although a moderate increase was produced for coho salmon in the Black River EDR (Table 5.2.5). As expected, the pattern of increases in life-cycle capacity across species and EDRs generally mirrors that of spawner abundance (Table 5.2.6).

Table 5.2.4: Modeled increase in spawner abundance (N_{eq}, without harvest) in the historical floodplain habitat scenario for coho, spring Chinook, fall Chinook, and steelhead by Ecological Diversity Region. Dark blue shade indicates changes >50%, medium blue indicates changes 25-50%, light blue indicates changes 10-25%, and no color indicates <10% change.

Ecological Region	Coho	Spring Chinook	Fall Chinook	Steelhead
Black Hills	2,776 (25%)	0	0	0
Black River	7,403 (124%)	0	0	193 (28%)
Cascade Mountains	11,178 (134%)	249 (33%)	0	405 (25%)
Central Lowlands	2,359 (63%)	0	0	0
Grays Harbor Tribs	10,758 (42%)	0	1,100 (20%)	246 (6%)
Mainstem: Lower	1,527 (403%)	0	258 (4%)	953 (73%)
Mainstem: Middle	0	14 (74%)	0	0
Mainstem: Upper	0	13 (81%)	0	0
Olympic Mountains	15,212 (54%)	0	2,930 (22%)	621 (10%)
Willapa Hills	3,673 (48%)	83 (34%)	0	105 (7%)

Table 5.2.5: Modeled life-cycle productivity (P_n) in the historical floodplain habitat scenario for coho, spring Chinook, fall Chinook, and steelhead by Ecological Diversity Region. Absolute increase from current in parentheses. Dark blue shade indicates changes >2.0, medium blue indicates changes 1.0-2.0, light blue indicates changes 0.5-1.0, and no color indicates <0.5 change.

Ecological Region	Coho	Spring	Fall Chinook	Steelhead
Black Hills	4.6 (0.5)	-	3.7 (0.3)	3.6 (0.2)
Black River	5 (1.3)	-	3.4 (0.1)	4.3 (0.9)
Cascade Mountains	3.9 (1)	2.5 (0.4)	3.6 (0.1)	3.6 (0.3)
Central Lowlands	3.8 (0.3)	-	1.6 (0.1)	2.1 (0.2)
Grays Harbor Tribs	4.7 (0.2)	-	3.8 (0)	4.3 (0)
Mainstem: Lower	2.2 (0.7)	-	3.9 (0.1)	4.4 (0.9)
Mainstem: Middle	1.6	1.5 (0.2)	1.9 (0)	3.5 (0.2)
Mainstem: Upper	-	1.4 (0.1)	1.9 (0)	2.3 (0.2)
Olympic Mountains	4.9 (0.4)	-	4.1 (0.1)	4.8 (0.2)
Willapa Hills	3.8 (0.6)	2.1 (0.3)	3 (0.1)	3.3 (0.2)

Table 5.2.6: Modeled life-cycle capacity (C_n) in the historical floodplain habitat scenario for coho, spring Chinook, fall Chinook, and steelhead by Ecological Diversity Region. Dark blue shade indicates changes >50%, medium blue indicates changes 25-50%, light blue indicates changes 10-25%, and no color indicates <10% change.

Ecological Region	Coho	Spring	Fall Chinook	Steelhead
Black Hills	3,031 (21%)	-	0 (0%)	0 (0%)
Black River	8,557 (106%)	-	0 (0%)	179 (19%)
Cascade Mountains	13,574	251 (18%)	0 (0%)	484 (21%)
Central Lowlands	3,057 (59%)	-	0 (0%)	0 (0%)
Grays Harbor Tribs	13,171 (40%)	-	1,505 (20%)	320 (6%)
Mainstem: Lower	2,355 (208%)	-	267 (3%)	1,104 (61%)
Mainstem: Middle	-	0 (0%)	0 (0%)	0 (0%)
Mainstem: Upper	-	38 (63%)	0 (0%)	0 (0%)
Olympic Mountains	18,173 (50%)	-	3,777 (22%)	711 (9%)
Willapa Hills	4,269 (38%)	83 (15%)	0 (0%)	0 (0%)

5.2.3 Historical Wood Abundance and Floodplain Habitat Scenario

The scenario that evaluates the combined effect of wood and floodplain habitat losses shows significant potential spawner abundance increases in all but the middle and upper mainstem EDRs (Table 5.2.7). Based on effects of the individual wood and floodplain scenarios on each species, we assume that most of the change in coho salmon and spring Chinook abundance is due to loss of floodplain habitat, whereas most of the change in fall Chinook abundance is due to loss of wood. For steelhead, the wood and floodplain scenario suggests significant increases in spawner abundance in all EDRs except the upper and middle mainstem EDRs.

Productivity increaseses were generally low except for coho and steelhead, which were moderate to high in most EDRs (Table 5.2.8). Life-cycle capacity increases were moderate to high across all EDRs for this scenario, especially for coho salmon (Table 5.2.9).

Table 5.2.7: Modeled increase in spawner abundance (N_{eq}, without harvest) in the historical wood abundance and floodplain habitat scenario for coho, spring Chinook, fall Chinook, and steelhead by Ecological Diversity Region. Dark blue shade indicates changes >50%, medium blue indicates changes 25-50%, light blue indicates changes 10-25%, and no color indicates <10% change.

Ecological Region	Coho	Spring Chinook	Fall Chinook	Steelhead
Black Hills	5,128 (47%)	0	0 (0%)	408 (60%)
Black River	8,856 (149%)	0	395 (33%)	438 (64%)
Cascade Mountains	15,222	544 (72%)	667 (33%)	1,035 (63%)
Central Lowlands	4,555 (123%)	0	0 (0%)	183 (99%)
Grays Harbor Tribs	17,267 (68%)	0	2,638 (47%)	1,557 (39%)
Mainstem: Lower	1,893 (499%)	0	1,878 (27%)	1,382
Mainstem: Middle	0	27 (142%)	324 (54%)	146 (99%)
Mainstem: Upper	0	27 (169%)	0 (0%)	0 (0%)
Olympic Mountains	22,312 (79%)	0	6,314 (48%)	2,389 (40%)
Willapa Hills	6,088 (80%)	164 (68%)	470 (28%)	611 (44%)

Table 5.2.8: Modeled life-cycle productivity (P_n) in the historical wood abundance and floodplain habitat scenario for coho, spring Chinook, fall Chinook, and steelhead by Ecological Diversity Region. Absolute increase from current in parentheses. Dark blue shade indicates changes >2.0, medium blue indicates changes 1.0-2.0, light blue indicates changes 0.5-1.0, and no color indicates <0.5 change.

Ecological Region	Coho	Spring	Fall Chinook	Steelhead
Black Hills	5.3 (1.2)	-	4 (0.6)	5.7 (2.3)
Black River	5.3 (1.5)	-	3.7 (0.4)	6 (2.5)
Cascade Mountains	4.4 (1.4)	2.8 (0.7)	4 (0.5)	5 (1.7)
Central Lowlands	4.9 (1.5)	-	2.3 (0.8)	3.4 (1.5)
Grays Harbor Tribs	5.3 (0.8)	-	4.1 (0.3)	6.1 (1.9)
Mainstem: Lower	2.4 (0.9)	-	4.2 (0.4)	5.3 (1.7)
Mainstem: Middle	1.8	1.6 (0.4)	2.1 (0.2)	4.4 (1)
Mainstem: Upper	-	1.5 (0.2)	2.1 (0.2)	2.9 (0.8)
Olympic Mountains	5.5 (1)	-	4.6 (0.5)	6.6 (2.1)
Willapa Hills	4.2 (1)	2.3 (0.5)	3.3 (0.4)	4.8 (1.6)

Table 5.2.9: Modeled life-cycle capacity (C_n) in the historical wood abundance and floodplain habitat scenario for coho, spring Chinook, fall Chinook, and steelhead by Ecological Diversity Region. Dark blue shade indicates changes >50%, medium blue indicates changes 25-50%, light blue indicates changes 10-25%, and no color indicates <10% change.

Ecological Region	Coho	Spring	Fall Chinook	Steelhead
Black Hills	5,316 (37%)	-	0 (0%)	359 (38%)
Black River	10,157	-	460 (26%)	384 (40%)
Cascade Mountains	17,954	607 (43%)	749 (27%)	998 (43%)
Central Lowlands	5,151 (99%)	-	0 (0%)	0 (0%)
Grays Harbor Tribs	19,921 (61%)	-	3,275 (43%)	1,416 (27%)
Mainstem: Lower	2,750 (243%)	-	2,117 (23%)	1,496 (82%)
Mainstem: Middle	-	21 (22%)	524 (42%)	170 (81%)
Mainstem: Upper	-	65 (108%)	0 (0%)	0 (0%)
Olympic Mountains	25,372 (70%)	-	7,472 (43%)	2,202 (29%)
Willapa Hills	6,923 (62%)	180 (33%)	523 (21%)	487 (24%)

5.2.4 Historical Beaver Pond Scenario

Not surprisingly, the historical beaver pond scenario produces very large spawner abundance increases for coho salmon (Table 5.2.10). Beaver ponds are a preferred winter rearing habitat for coho salmon, and estimated juvenile survival through the winter is considerably higher in beaver ponds than in stream channels. The model also produces small increases in spawner abundance for fall Chinook, but spring Chinook and steelhead show very little potential response to increased beaver pond habitat area.

Increases in productivity were relatively small across all EDRs and species, including coho salmon (Table 5.2.11). Increases in life-cycle capacity mirrored those of abundance (Table 5.2.12).

Table 5.2.10: Modeled increase in spawner abundance (N_{eq}, without harvest) in the historical beaver pond scenario for coho, spring Chinook, fall Chinook, and steelhead by Ecological Diversity Region. Dark blue shade indicates changes >50%, medium blue indicates changes 25-50%, light blue indicates changes 10-25%, and no color indicates <10% change.

Ecological Region	Coho	Spring	Fall Chinook	Steelhead
Black Hills	8,550 (78%)	0	0 (0%)	0 (0%)
Black River	4,706 (79%)	0	0 (0%)	0 (0%)
Cascade Mountains	9,170 (110%)	0 (0%)	0 (0%)	0 (0%)
Central Lowlands	4,828 (130%)	0	0 (0%)	0 (0%)
Grays Harbor Tribs	28,650	0	240 (4%)	0 (0%)
Mainstem: Lower	0 (0%)	0	0 (0%)	0 (0%)
Mainstem: Middle	0	0 (0%)	0 (0%)	0 (0%)
Mainstem: Upper	0	0 (0%)	0 (0%)	0 (0%)
Olympic Mountains	22,756 (81%)	0	384 (3%)	0 (0%)
Willapa Hills	11,957	0 (0%)	0 (0%)	0 (0%)

Table 5.2.11: Modeled life-cycle productivity (P_n) in the historical beaver pond scenario for coho, spring Chinook, fall Chinook, and steelhead by Ecological Diversity Region. Absolute increase from current in parentheses. Dark blue shade indicates changes >2.0, medium blue indicates changes 1.0-2.0, light blue indicates changes 0.5-1.0, and no color indicates <0.5 change.

Ecological Region	Coho	Spring	Fall Chinook	Steelhead
Black Hills	4.5 (0.5)	-	3.5 (0.1)	3.5 (0)
Black River	3.8 (0)	-	3.3 (0)	3.5 (0.1)
Cascade Mountains	3.7 (0.7)	2.2 (0)	3.5 (0)	3.3 (0)
Central Lowlands	3.2 (-0.2)	-	1.7 (0.1)	2 (0.1)
Grays Harbor Tribs	4.9 (0.4)	-	3.9 (0)	4.3 (0)
Mainstem: Lower	1.5 (0)	-	3.8 (0)	3.5 (0)
Mainstem: Middle	-	1.2 (0)	1.9 (0)	3.4 (0)
Mainstem: Upper	-	1.4 (0)	1.9 (0)	2.1 (0)
Olympic Mountains	5.1 (0.6)	-	4.1 (0.1)	4.6 (0.1)
Willapa Hills	3.8 (0.6)	1.8 (0)	2.9 (0)	3.2 (0)

Table 5.2.12: Modeled life-cycle capacity (C_n) in the historical beaver pond scenario for coho, spring Chinook, fall Chinook, and steelhead by Ecological Diversity Region. Dark blue shade indicates changes >50%, medium blue indicates changes 25-50%, light blue indicates changes 10-25%, and no color indicates <10% change.

Ecological Region	Coho	Spring	Fall Chinook	Steelhead
Black Hills	10,479 (72%)	-	0 (0%)	0 (0%)
Black River	6,362 (78%)	-	0 (0%)	0 (0%)
Cascade Mountains	11,448 (91%)	0 (0%)	0 (0%)	0 (0%)
Central Lowlands	7,156 (137%)	-	0 (0%)	0 (0%)
Grays Harbor Tribs	35,323	-	289 (4%)	0 (0%)
Mainstem: Lower	0 (0%)	-	0 (0%)	0 (0%)
Mainstem: Middle	-	0 (0%)	0 (0%)	0 (0%)
Mainstem: Upper	-	0 (0%)	0 (0%)	0 (0%)
Olympic Mountains	27,108 (74%)	-	433 (3%)	0 (0%)
Willapa Hills	15,503	0 (0%)	0 (0%)	0 (0%)

5.2.5 Historical Shade Scenario

The historical shade scenario produces a relatively small change in coho salmon spawner abundance (20%) despite high summer stream temperatures in the Chehalis basin (Figure 5.1.2). This is because the stream temperature *change* from current to historical shade is near 0°C in most EDRs, and less than 2°C in much of the remaining area (Figure 5.2.1). However, a few tributary EDRs have relatively large percentage changes in modeled coho spawner abundance because shade conditions are locally very poor, notably the Cascade Mountains, Black River, and Central Lowlands EDRs (all with increases of 45-75%) (Table 5.2.13).

Spring Chinook show large percent increases in modeled spawner abundance in the historical shade scenario in the Cascade Mountains, Willapa Hills, and Upper Mainstem Chehalis EDRs (Table 5.2.13). In these three EDRs, modeled stream temperatures have increased significantly over historical conditions within holding and spawning reaches for spring Chinook. Therefore, the historical shade scenario produced at least a 40% increase in each location. However, the Upper Mainstem Chehalis has very few spawners. Fall Chinook are less sensitive to temperature changes because they enter the river after the high summer temperatures, and the historical shade scenario produced modeled increases in abundance of less than 10% in all EDRs. Juvenile steelhead have a higher thermal tolerance than coho salmon, and the historical shade scenario shows only small increases in steelhead spawner abundance.

Table 5.2.13: Modeled increase in spawner abundance (N_{eq}, without harvest) in the historical shade scenario for coho, spring Chinook, fall Chinook, and steelhead by Ecological Diversity Region. Dark blue shade indicates changes >50%, medium blue shade indicates changes 25-50%, light blue shade indicates changes 10-25%, and no color indicates <10% change.

Ecological Region	Coho	Spring	Fall Chinook	Steelhead
Black Hills	1,485 (14%)	0	0 (0%)	0 (0%)
Black River	2,760 (46%)	0	0 (0%)	105 (15%)
Cascade Mountains	6,121 (74%)	305 (40%)	0 (0%)	324 (20%)
Central Lowlands	1,705 (46%)	0	0 (0%)	0 (0%)
Grays Harbor Tribs	1,394 (5%)	0	0 (0%)	0 (0%)
Mainstem: Lower	0 (0%)	0	233 (3%)	480 (37%)
Mainstem: Middle	0	14 (74%)	0 (0%)	0 (0%)
Mainstem: Upper	0	11 (69%)	0 (0%)	0 (0%)
Olympic Mountains	2,612 (9%)	0	0 (0%)	167 (3%)
Willapa Hills	1,925 (25%)	89 (37%)	0 (0%)	0 (0%)

Table 5.2.14: Modeled life-cycle productivity (P_n) in the historical shade scenario for coho, spring Chinook, fall Chinook, and steelhead by Ecological Diversity Region. Absolute increase from current in parentheses. Dark blue shade indicates changes >2.0, medium blue indicates changes 1.0-2.0, light blue indicates changes 0.5-1.0, and no color indicates <0.5 change.

Ecological Region	Coho	Spring Chinook	Fall Chinook	Steelhead
Black Hills	4.4 (0.4)	-	3.5 (0.1)	3.5 (0.1)
Black River	4.5 (0.7)	-	3.4 (0.1)	4 (0.6)
Cascade Mountains	3.6 (0.6)	2.6 (0.4)	3.6 (0.1)	3.7 (0.3)
Central Lowlands	3.6 (0.1)	-	1.6 (0)	2.2 (0.3)
Grays Harbor Tribs	4.7 (0.2)	-	3.8 (0)	4.3 (0)
Mainstem: Lower	1.9 (0.4)	-	3.9 (0.1)	3.7 (0.2)
Mainstem: Middle	-	1.5 (0.2)	1.9 (0)	3.6 (0.2)
Mainstem: Upper	-	1.4 (0)	1.9 (0)	2.2 (0.1)
Olympic Mountains	4.6 (0.2)	-	4.1 (0)	4.7 (0.1)
Willapa Hills	3.5 (0.3)	2.1 (0.3)	3 (0.1)	3.3 (0.2)

Table 5.2.15: Modeled life-cycle capacity (C_n) in the historical shade scenario for coho, spring Chinook, fall Chinook, and steelhead by Ecological Diversity Region. Dark blue shade indicates changes >50%, medium blue indicates changes 25-50%, light blue indicates changes 10-25%, and no color indicates <10% change.

Ecological Region	Coho	Spring	Fall Chinook	Steelhead
Black Hills	1,535 (11%)	-	0 (0%)	0 (0%)
Black River	3,129 (39%)	-	0 (0%)	0 (0%)
Cascade Mountains	7,481 (59%)	315 (22%)	0 (0%)	358 (15%)
Central Lowlands	2,290 (44%)	-	0 (0%)	0 (0%)
Grays Harbor Tribs	1,405 (4%)	-	0 (0%)	0 (0%)
Mainstem: Lower	0 (0%)	-	0 (0%)	614 (34%)
Mainstem: Middle	-	0 (0%)	0 (0%)	0 (0%)
Mainstem: Upper	-	36 (59%)	0 (0%)	0 (0%)
Olympic Mountains	2,933 (8%)	-	0 (0%)	151 (2%)
Willapa Hills	2,326 (21%)	86 (16%)	0 (0%)	0 (0%)

Increases in productivity were quite small across all EDRs and species, including coho salmon (Table 5.2.14). Increases in life-cycle capacity generally mirrored those of abundance (Table 5.2.15).

The comparison of current to historical shade levels in the Chehalis basin shows that more than 60% of the basin has riparian shade conditions that are currently near their historical potential, mostly inside the Olympic National Forest or state and private managed forests. Much of that stream length has a modeled temperature difference of <0.5°C, indicating very little potential for continued tree growth to improve temperature conditions in the future (Figure 5.2.1). Areas with temperature change >2°C are most concentrated in the Cascade Mountains EDR, and to a lesser extent in the Black River, Willapa Hills, and Lower and Middle Mainstem Chehalis EDRs. This pattern reflects two dominant riparian situations in the basin: (1) the current shade condition in many small streams is a closed canopy due to maturing riparian forests, and (2) historical shade conditions in large river channels are relatively open due to wide channels and limited shading even with tall trees adjacent to them. Areas with the largest modeled temperature changes are in small streams with little or no canopy currently and closed canopy under historical conditions (e.g., in the Skookumchuck basin).
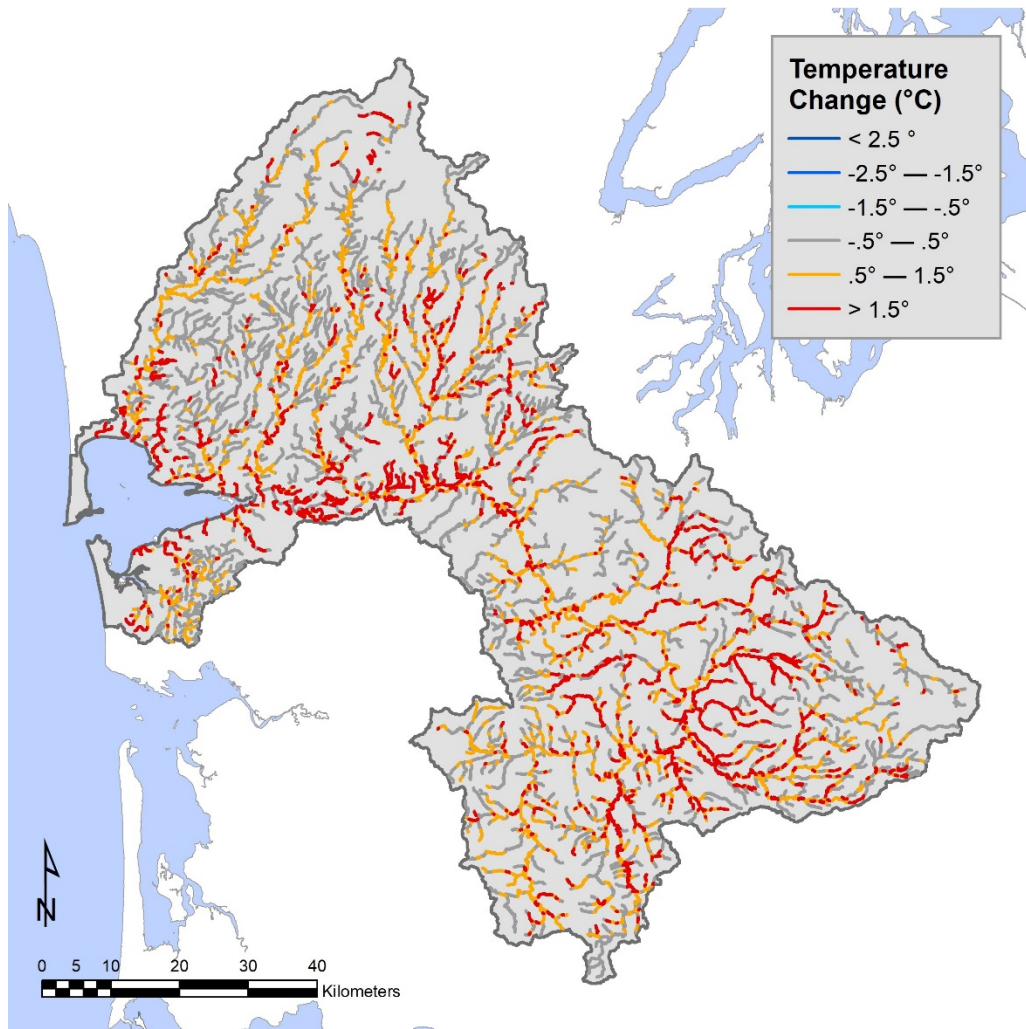
Figure 5.2.1. Modeled temperature change due to loss of riparian shade in the Chehalis basin.

5.2.6 No Barriers Scenario

The overall response of coho salmon was small for the diagnostic scenario with barriers removed (9% change), indicating that barriers have a relatively small impact on coho salmon at the scale of the entire Chehalis River basin. However, individual barriers have locally larger impacts when viewed at the EDR scale (Table 5.2.16). This indicates that barriers are an important restoration opportunity for coho salmon in some locations, but that overall a small proportion of coho habitat is blocked to adult migration. The primary uncertainty in this analysis is that we use the barrier passage rankings from WDFW as percent reductions in capacity and productivity.

There are no migration barriers in the range of spring Chinook spawning in the barrier database, so there is no response of spring Chinook in the diagnostic scenario with barriers removed. Fall Chinook and steelhead are exposed to a few barriers, but there are no significant impacts to basin-wide abundance.

Increases in productivity and life-cycle capacity were small across all EDRs and species (Tables 5.2.17 and 5.2.18). Slight negative productivity changes are due to opening up low productivity habitat, which can slightly reduce the average productivity for the EDR.

Table 5.2.16: Modeled increase in spawner abundance (N_{eq}, without harvest) in the no barriers scenario for coho, spring Chinook, fall Chinook, and steelhead by Ecological Diversity Region. Dark blue shade indicates changes >50%, medium blue shade indicates changes 25-50%, light blue shade indicates changes 10-25%, and no color indicates <10% change.

Ecological Region	Coho	Spring	Fall	Steelhead
Black Hills	900 (8%)	0	0 (0%)	0 (0%)
Black River	543 (9%)	0	0 (0%)	0 (0%)
Cascade Mountains	902 (11%)	0 (0%)	0 (0%)	0 (0%)
Central Lowlands	1,536 (41%)	0	0 (0%)	0 (0%)
Grays Harbor Tribs	1,468 (6%)	0	0 (0%)	110 (3%)
Mainstem: Lower	0 (0%)	0	0 (0%)	0 (0%)
Mainstem: Middle	0	0 (0%)	0 (0%)	0 (0%)
Mainstem: Upper	0	0 (0%)	0 (0%)	0 (0%)
Olympic Mountains	2,098 (7%)	0	588 (5%)	242 (4%)
Willapa Hills	583 (8%)	0 (0%)	0 (0%)	0 (0%)

Table 5.2.17: Modeled life-cycle productivity (P_n) in the no barriers scenario for coho, spring Chinook, Fall Chinook, and steelhead by Ecological Diversity Region. Absolute increase from current in parentheses. Dark blue shade indicates changes >2.0, medium blue indicates changes 1.0-2.0, light blue indicates changes 0.5-1.0, and no color indicates <0.5 change.

Ecological Region	Coho	Spring	Fall Chinook	Steelhead
Black Hills	4.2 (0.2)	-	3.4 (0)	3.4 (0)
Black River	3.7 (-0.1)	-	3.3 (0)	3.3 (-0.1)
Cascade Mountains	3.1 (0.1)	2.2 (0)	3.4 (0)	3.3 (0)
Central Lowlands	3.9 (0.4)	-	1.8 (0.3)	2 (0.1)
Grays Harbor Tribs	4.7 (0.2)	-	3.8 (0)	4.3 (0.1)
Mainstem: Lower	1.5 (0)	-	3.8 (0)	3.5 (0)
Mainstem: Middle	-	1.2 (0)	1.9 (0)	3.3 (0)
Mainstem: Upper	-	1.4 (0)	1.9 (0)	2.1 (0)
Olympic Mountains	4.7 (0.2)	-	4.3 (0.2)	4.8 (0.2)
Willapa Hills	3.3 (0.1)	1.8 (0)	2.9 (0)	3.1 (0)

Table 5.2.18: Modeled life-cycle capacity (C_n) in the no barriers scenario for coho, spring Chinook, fall Chinook, and steelhead by Ecological Diversity Region. Dark blue shade indicates changes >50%, medium blue indicates changes 25-50%, light blue indicates changes 10-25%, and no color indicates <10% change.

Ecological Region	Coho	Spring Chinook	Fall Chinook	Steelhead
Black Hills	998 (7%)	-	0 (0%)	0 (0%)
Black River	813 (10%)	-	0 (0%)	0 (0%)
Cascade Mountains	1,063 (8%)	0 (0%)	0 (0%)	0 (0%)
Central Lowlands	1,836 (35%)	-	0 (0%)	0 (0%)
Grays Harbor Tribs	1,505 (5%)	-	0 (0%)	124 (2%)
Mainstem: Lower	0 (0%)	-	0 (0%)	0 (0%)
Mainstem: Middle	-	0 (0%)	0 (0%)	0 (0%)
Mainstem: Upper	-	0 (0%)	0 (0%)	0 (0%)
Olympic Mountains	2,211 (6%)	-	505 (3%)	211 (3%)
Willapa Hills	709 (6%)	0 (0%)	0 (0%)	0 (0%)

5.2.7 Historical Fine Sediment Scenario

For fine sediment in spawning gravels, modeled changes in fine sediment are based on forest road density (Appendix C), resulting in relatively large potential increases in incubation productivity parameters for each species. Percent change in spawner abundance under the historical fine sediment scenario was most pronounced for spring and fall Chinook and steelhead, and somewhat lower for coho salmon (Table 5.2.19). There is little spatial variation in modeled abundance change for all species across the Chehalis basin. As stated earlier, there is high uncertainty in both the predicted fine sediment levels in the model as well as in identification of sediment sources.

Increases in productivity were moderate to high across all species and EDRs (Table 5.2.20). However, life-cycle capacity increases were generally low because fine sediment affects a density-independent life stage (5.2.21).

Table 5.2.19: Modeled increase in spawner abundance (N_{eq}, without harvest) in the historical fine sediment scenario for coho, spring Chinook, fall Chinook, and steelhead by Ecological Diversity Region. Dark blue shade indicates changes >50%, medium blue shade indicates changes 25-50%, light blue shade indicates changes 10-25%, and no color indicates <10% change.

Ecological Region	Coho	Spring Chinook	Fall Chinook	Steelhead
Black Hills	1,758 (16%)	0	0 (0%)	95 (14%)
Black River	623 (10%)	0	269 (22%)	0 (0%)
Cascade Mountains	2,131 (26%)	273 (36%)	506 (25%)	210 (13%)
Central Lowlands	989 (27%)	0	0 (0%)	0 (0%)
Grays Harbor Tribs	2,818 (11%)	0	1,330 (24%)	406 (10%)
Mainstem: Lower	0 (0%)	0	2,073 (30%)	302 (23%)
Mainstem: Middle	0	30 (158%)	549 (92%)	0 (0%)
Mainstem: Upper	0	43 (269%)	264 (80%)	0 (0%)
Olympic Mountains	3,373 (12%)	0	4,227 (32%)	570 (9%)
Willapa Hills	1,903 (25%)	237 (98%)	1,087 (65%)	252 (18%)

Table 5.2.20: Modeled life-cycle productivity (P_n) in the historical fine sediment for coho, spring Chinook, fall Chinook, and steelhead by Ecological Diversity Region. Absolute increase from current in parentheses. Dark blue shade indicates changes >2.0, medium blue indicates changes 1.0-2.0, light blue indicates changes 0.5-1.0, and no color indicates <0.5 change.

Ecological Region	Coho	Spring	Fall Chinook	Steelhead
Black Hills	6.9 (2.8)	-	5.2 (1.8)	5.6 (2.2)
Black River	5.2 (1.5)	-	5.2 (1.9)	5.1 (1.6)
Cascade Mountains	5.1 (2.1)	3.3 (1.1)	5 (1.5)	5.2 (1.9)
Central Lowlands	5.2 (1.7)	-	1.9 (0.4)	3 (1.1)
Grays Harbor Tribs	7.1 (2.5)	-	4.9 (1.1)	5.9 (1.7)
Mainstem: Lower	2.3 (0.8)	-	5.6 (1.8)	5 (1.5)
Mainstem: Middle	-	2.1 (0.9)	3.1 (1.2)	5.6 (2.3)
Mainstem: Upper	-	2 (0.6)	3.4 (1.5)	3.8 (1.7)
Olympic Mountains	7.5 (3.1)	-	6.2 (2.1)	7.1 (2.6)
Willapa Hills	6.3 (3.1)	3.9 (2.1)	5.9 (3)	6.3 (3.2)

Table 5.2.21: Modeled life-cycle capacity (C_n) in the historical fine sediment scenario for coho, spring Chinook, fall Chinook, and steelhead by Ecological Diversity Region. Dark blue shade indicates changes >50%, medium blue indicates changes 25-50%, light blue indicates changes 10-25%, and no color indicates <10% change.

Ecological Region	Coho	Spring	Fall Chinook	Steelhead
Black Hills	0 (0%)	-	0 (0%)	0 (0%)
Black River	0 (0%)	-	0 (0%)	0 (0%)
Cascade Mountains	0 (0%)	69 (5%)	329 (12%)	0 (0%)
Central Lowlands	0 (0%)	-	0 (0%)	0 (0%)
Grays Harbor Tribs	0 (0%)	-	1,104 (15%)	0 (0%)
Mainstem: Lower	0 (0%)	-	1,546 (16%)	186 (10%)
Mainstem: Middle	-	0 (0%)	442 (36%)	0 (0%)
Mainstem: Upper	-	59 (96%)	0 (0%)	0 (0%)
Olympic Mountains	0 (0%)	-	3,301 (19%)	0 (0%)
Willapa Hills	0 (0%)	97 (18%)	784 (31%)	0 (0%)

6. Potential Restoration Options

The process-based assessment approach first quantifies changes in key habitat-forming processes and habitat attributes, and then uses the life-cycle model to evaluate which degraded drivers (e.g., riparian change, floodplain change, etc.) represent the largest restoration opportunities for each species and spatial unit. Each diagnostic scenario evaluates one causal mechanism of habitat change, which equates to one potential restoration action type. The model evaluates the importance of each causal mechanism at the subbasin, EDR, and basin scales in order to help identify necessary restoration action types for the ASRP. The model does not evaluate the effect of individual actions at specific sites. Based on this approach, the diagnostic scenarios suggest that five types of habitat changes most constrain recovery of salmon populations: loss of floodplain habitat, loss of wood from streams and rivers, loss of beaver ponds, loss or reduction of riparian shade, and migration barriers. Therefore, restoration of these habitat attributes and removal of migration barriers have the most potential to significantly improve salmon populations (i.e., increase spawner abundance, life-cycle productivity and capacity).

Importantly, the process-based approach does not focus on construction of lost habitats, but on restoring the key mechanisms that create those habitats: floodplain connectivity, riparian functions (for wood recruitment and shade), beaver populations to create beaver pond habitat, and barrier removal. However, in the near term some habitat creation actions such as wood placement or constructing beaver dam analogs are important strategies for recovery of salmon because of the long lag time between riparian restoration and recovery of wood abundance or beaver populations. For the sixth potentially important constraint—increased fine sediment and reduced incubation survival—we do not know which locations currently have high fine sediment, nor do we know which sediment sources to address. Therefore, it is important to first determine where and why fine sediment is high so that sediment sources can be addressed.

6.1 Floodplain and Wood Restoration

The diagnostic scenarios indicate that the combination of restoring floodplain habitat and wood abundance is likely to significantly benefit all four species, with floodplain restoration most benefiting coho salmon and spring Chinook, and wood restoration most benefitting spring and fall Chinook and steelhead. Importantly, diagnostic runs that separately track the benefit of restoring mainstem habitats for each species indicate that floodplain habitat restoration in the lower mainstem (from the Skookumchuck to the Wynoochee) will increase multiple subpopulations of coho upstream of the Wynoochee River, and also improve spring and fall Chinook populations to a lesser degree. Among the tributary subbasins, the Skookumchuck, Black, Humptulips, and Satsop have large floodplain restoration potential, both when ranked by absolute abundance or by percent increase (Figure 6.1.1). Each of those areas had significant historical marsh habitat that has been lost or degraded (Appendix F). Only the Black River subbasin has an appreciable
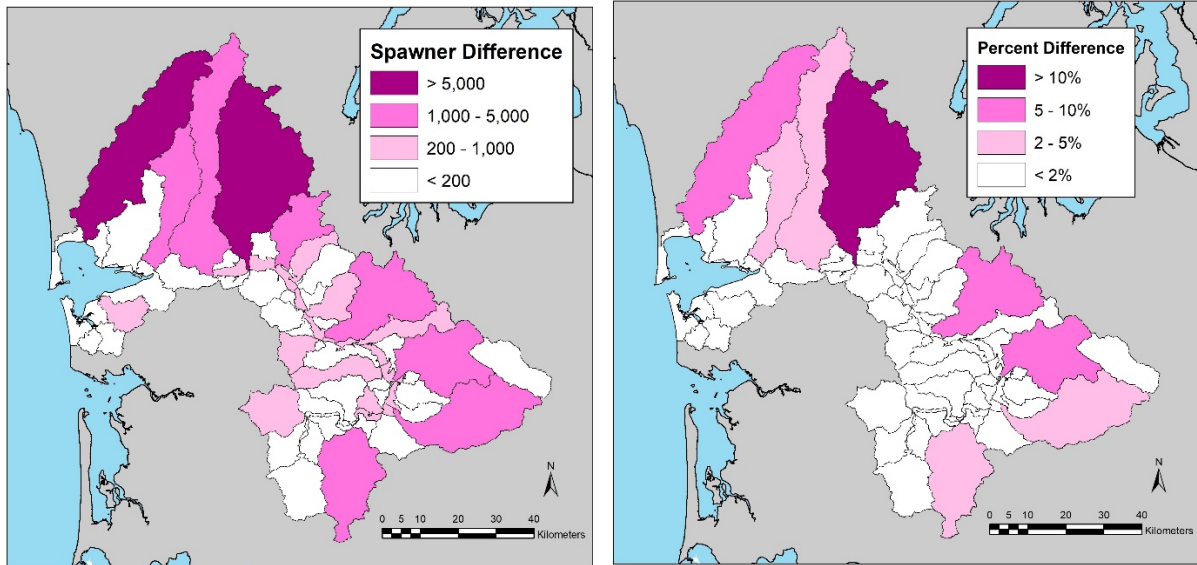
Figure 6.1.1. Map of potential coho spawner abundance increase through floodplain habitat restoration, by subbasin. Left panel is absolute change in subbasin abundance when floodplain habitat is set to historical condition in one subbasin at a time; right panel is percent increase in the *total Chehalis basin* abundance (increase in subbasin spawner abundance divided by total basin abundance) when floodplain habitat is set to historical condition in one subbasin at a time.

portion of its historical marsh remaining today. Other subbasins with relatively large potential absolute increases in coho spawner abundance include the Wishkah, Wynoochee, Newaukum, and South Fork Chehalis River subbasins. By contrast, the potential benefits of wood restoration are more evenly distributed across the subbasins (Section 5.2.1), and the analysis does not indicate strong spatial priorities for wood restoration. However, the scientific literature generally indicates that wood restoration in small, moderate-slope reaches has the greatest potential to increase pool area, which benefits multiple species that occupy those reach types (primarily coho salmon and steelhead).

6.2 Beaver Pond Restoration

Restoring beaver ponds to small streams is likely to significantly benefit coho salmon (more than doubling the population in the historical beaver pond scenario), with relatively small effects on the other three species. The potential for recovery of beaver ponds and beaver populations is greatest in small, low-slope channels with wide valleys (Dittbrenner et al. 2018). A scoring system to determine beaver intrinsic potential (BIP) ranks the suitability of reaches for supporting beaver dams based on channel slope, channel width and floodplain width. Using a modified version of the beaver intrinsic potential formula of Dittbrenner et al. (2108) (Table 6.2.1), we created a map of beaver restoration potential to help direct beaver restoration to the most suitable locations within the range of coho salmon in the Chehalis basin (Figure 6.2.1). In general, areas with lower potential are in the

91

upper Olympic Mountains, Black Hills, Cascade Foothills, and Willapa Hills, which are the four areas with predominantly volcanic lithology and steeper streams. Areas of alluvium, glacial deposits, and marine sedimentary rocks all contain significant low-slope stream length with high or medium beaver intrinsic potential.

Table 6.2.1. Scoring system for beaver intrinsic potential (BIP), modified from Dittbrenner (2018).

Stream slope and score		Stream width and score		Cumulative Score	BIP category
<1%	4	<7 m	4	7-8	High
1-2%	3	7-10 m	3	6	Medium
2-4%	2	10-18 m	2	4-5	Low
4-6%	1	18-24 m	1	<4	No BIP
6-10%	0.5				
>10%	0	>24 m	0		
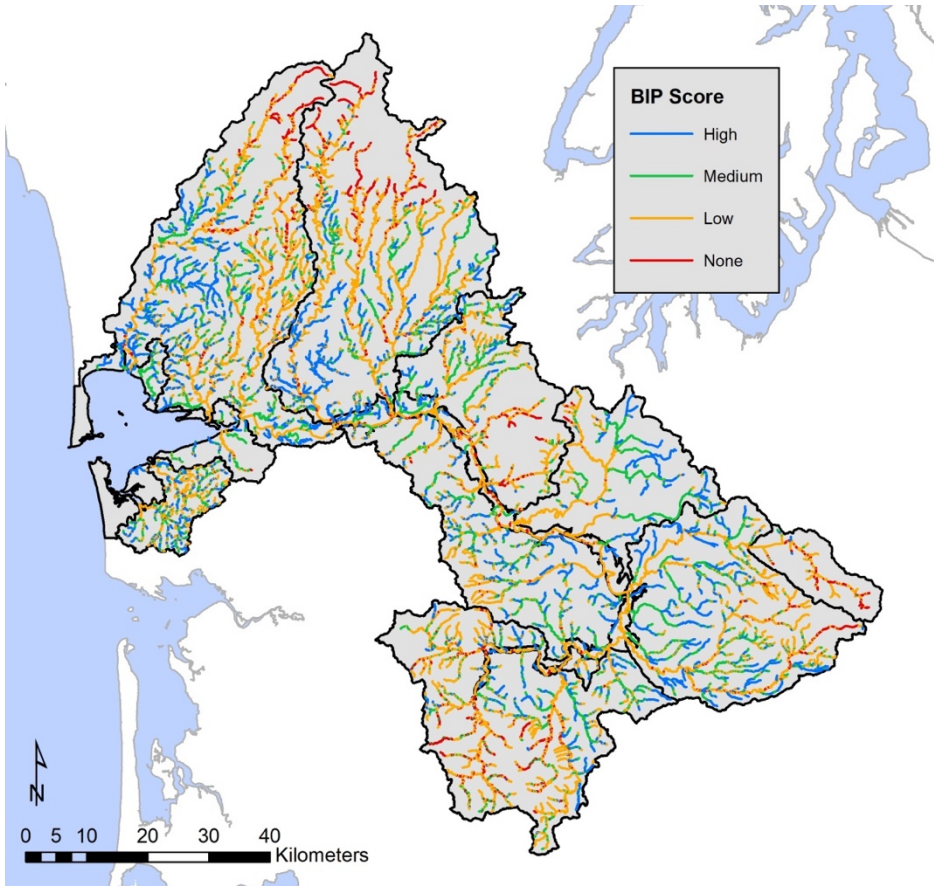
Figure 6.2.1. Map of beaver intrinsic potential in the Chehalis River basin, based on a modified version of the beaver intrinsic potential model of Dittbrenner et al. (2018).

6.3 Riparian Restoration

Riparian restoration is likely to significantly increase shade and reduce stream temperature in a few areas, and some of those areas are very important to spring Chinook. Modeling a historical shade scenario indicates that reduction of stream temperature in spring Chinook holding and rearing areas can potentially double the spring Chinook population under the current climate, and increase coho abundance by 20%. However, when we add projected temperature increases due to climate change the model indicates that stream warming due to climate change will likely exceed cooling due to increased shade, and net warming is likely to occur in most of the stream network by late-century. This is a result of the fact that much of the basin has shade levels at or near their historical potential, and continued tree growth does little to reduce stream temperature in the future. Figure 6.3.1 highlights areas that the riparian assessment indicates have the greatest potential for increasing shade and reducing stream temperature.

Riparian restoration may also increase wood recruitment in the future, although empirical studies and wood recruitment models both indicate that wood abundance in streams does not begin to increase until riparian forests are more than 60 years old (McHenry et al. 1998, Beechie et al. 2000). Currently, many riparian forests in the Olympic Mountains are functioning or only moderately impaired for wood recruitment (trees 75+ feet tall and riparian zone width >100 feet or trees 105+ feet tall and width >50 feet), but in most other areas of the basin riparian areas are impaired for the wood recruitment function (Figure A.15 in Appendix A). Significant increases in natural wood abundance are not expected until late-century, and wood placement is recommended as an interim restoration solution. However, riparian protection and restoration are important for assuring wood recruitment in the future.
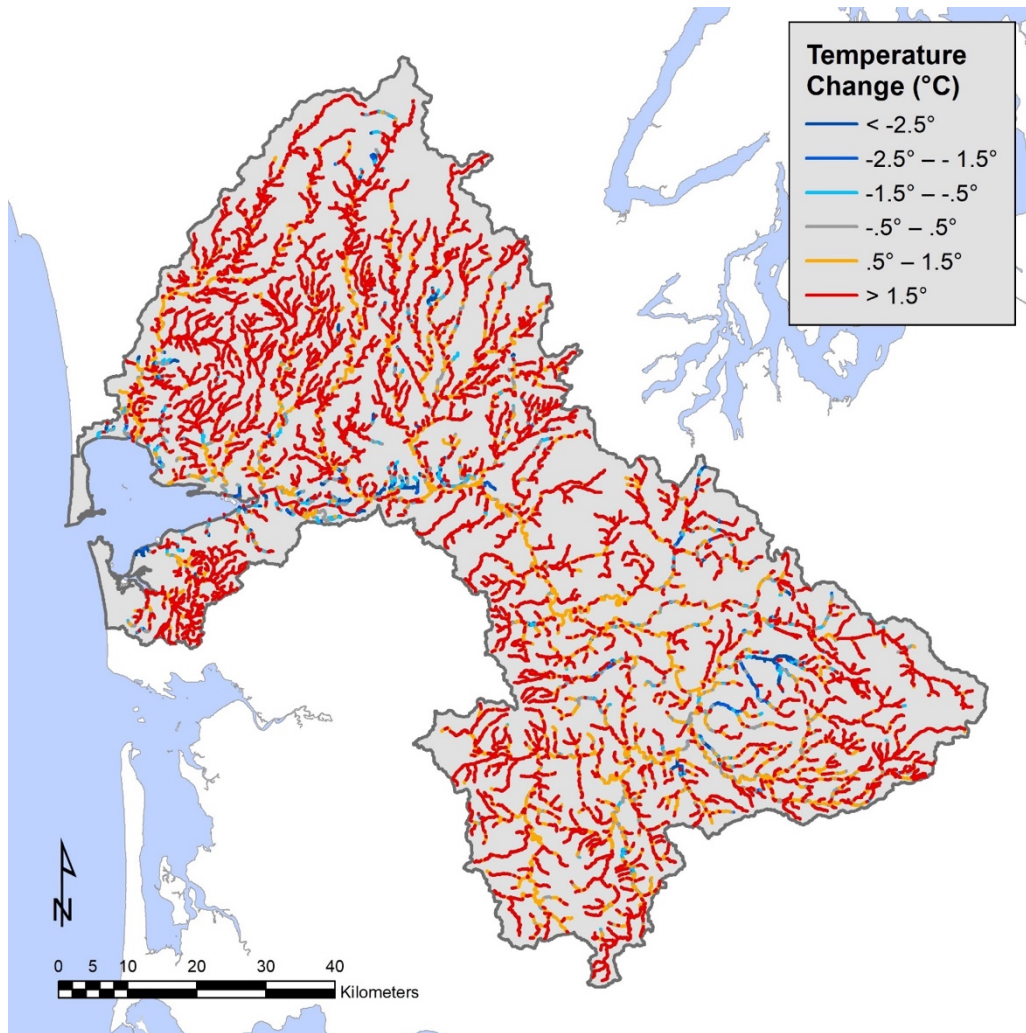
Figure 6.3.1. Areas of the Chehalis basin with high potential for increasing shade and reducing summer stream temperatures by late century (~2085). Blue colored reaches are reaches in which riparian restoration may produce a net decrease in stream temperature by late century despite projected 2°C warming due to climate change.

6.4 Barrier Removal

While the potential for barrier removals to benefit species is small overall (especially for spring Chinook, which have only one migration barriers within their range), there are specific subbasins in which barrier removals can significantly improve local subpopulations of coho salmon (Figure 6.4.1), and modestly improve fall Chinook and steelhead. The no-barrier diagnostic scenario indicates that barrier removals or passage improvements should provide the largest percentage increases in coho salmon abundance in the small tributaries to the mainstem from Wynoochee up to Crim Creek, but the largest potential absolute abundance increases are in the Satsop and Skookumchuck subbasins. A number of other large subbasins may also have significant benefit, including Cloquallum, Black River, Newaukum, and South Fork Chehalis. While barrier removals are not likely to

provide the largest abundance increases among scenarios for any species, the map of cumulative passage percentages (Figure 6.4.2) also indicates that local benefits can be large and potentially cost-effective to achieve.
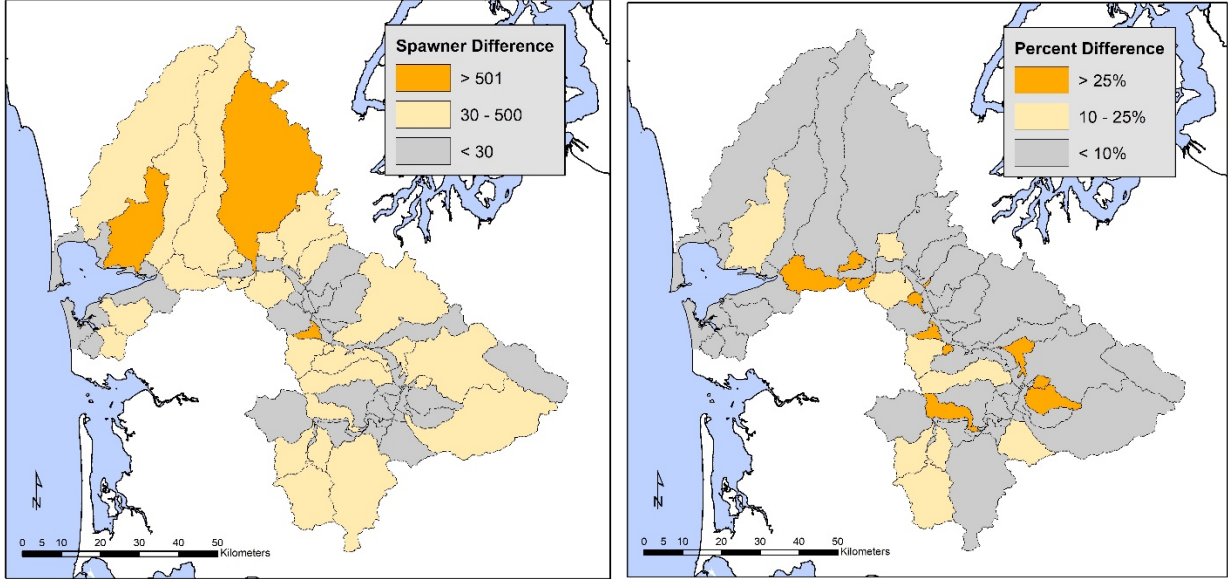
Figure 6.4.1. Map of subbasins highest potential coho salmon spawner abundance increase through barrier removals in the Chehalis River basin. Left panel is absolute abundance change in subbasins when all barriers are removed; right panel is percent increase in within-subbasin abundance when all barriers are removed (subbasin spawner abundance increase divided by current subbasin spawner abundance).
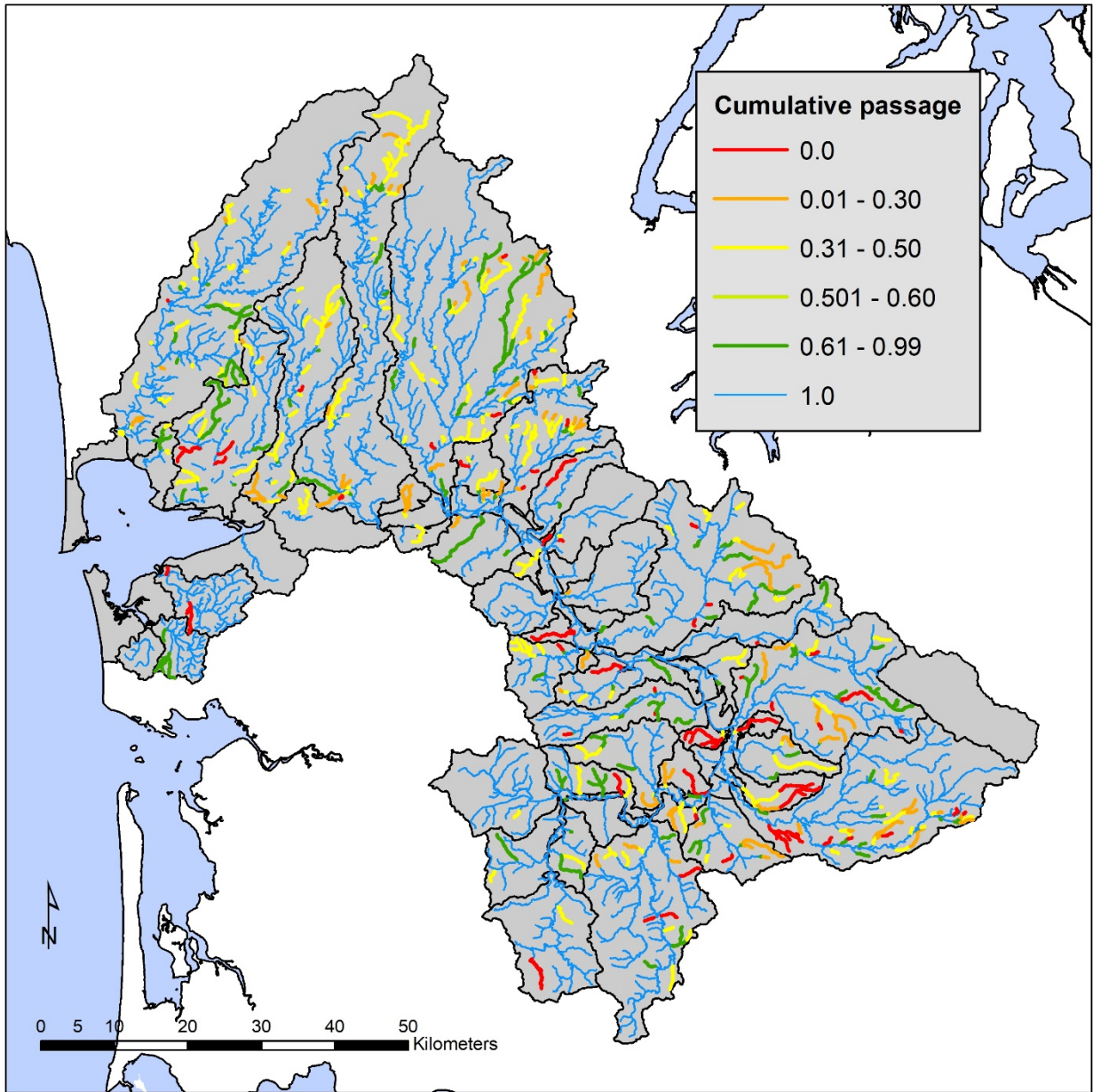
Figure 6.4.2. Map of cumulative passage percentage ratings above barriers in the Chehalis River basin.

6.5 Fine Sediment Reduction

The diagnostic scenario for historical fine sediment indicates that there is considerable potential to improve Chinook subpopulations (and to a lesser extent, steelhead) by reducing fine sediment levels in spawning gravels. However, the model of fine sediment is based on data relating forest roads to fine sediment levels, with no other land uses considered. Moreover, there are very few data on fine sediment in the Chehalis basin to confirm that fine sediment levels are in fact high relative to natural conditions. A reasonable conclusion from this analysis is that spring and fall Chinook subpopulations are very sensitive to fine sediment levels, but also that we are unsure where fine sediment levels are high within subbasins. This suggests that field assessments of fine sediment levels and sources of fine sediment should be conducted to confirm where reducing fine sediment should be a restoration priority, and to identify the most important sources of sediment to address through restoration actions.

7. Restoration Scenario Results

The ASRP restoration scenarios for each species include a No Action scenario and three restoration scenarios. Each future scenario includes the effects of climate change on stream temperature, modeled as a 1°C increase in the August ADA by mid-century, and a 2°C increase in the August ADA by late-century (Appendix J). Additionally, each future scenario includes the effects of future development on prespawn mortality in coho salmon, and effects of changing low flow (Appendix J). The No Action scenarios do not include restoration actions, whereas the restoration scenarios include the targeted restoration actions defined by the SRT. The model assumes immediate implementation of all restoration actions, and that all restoration effects except riparian functions are fully realized by mid-century and there is no decline in benefit through time. The model does not include factors such as permitting and landowner cooperation, budget limitations, or sequencing of restoration actions, except as those factors were considered in development of the ASRP restoration scenarios.

The restoration scenario results indicate that restoration actions increase abundance and productivity for all species, but also that impacts from climate change reduce those increases (Table 7.1). All three restoration scenarios increased spawner abundance for all species by mid-century even with climate change, as well as for fall Chinook in late-century. However, restoration actions hold spring Chinook to only a slight decrease by late-century with climate effects included. Coho and steelhead are projected to be near current abundance levels under Scenarios 2 and 3 in late century. That is, restoration actions can increase abundance of all species in the next few decades, and significantly limit projected declines in spawner abundance due to climate change by late century.

Table 7.1. Modeled number of spawners (N_{eq}, without harvest) in each restoration scenario for coho, spring Chinook, fall Chinook, and steelhead for the Chehalis basin (percent change in parentheses). Dark blue shaded cells indicate increases >25%, light blue shade cells indicate increases 10-25% (percentages in parentheses). Dark red shaded cells indicate decreases >25%, light red shade cells indicate decreases 10-25%.

Scenario	Coho		Spring Chinook		Fall Chinook		Steelhead	
Current	90,625		1,035		31,746		16,092	
	Mid-century	Late-century	Mid-century	Late-century	Mid-century	Late-century	Mid-century	Late-century
No Action	81,579 (-10%)	65,300 (-28%)	945 (-9%)	627 (-39%)	30,908 (-3%)	30,286 (-5%)	15,225 (-5%)	13,221 (-18%)
Scenario 1	99,561 (10%)	81,145 (-10%)	1,194 (15%)	846 (-18%)	34,387 (8%)	33,829 (7%)	17,416 (8%)	15,348 (-5%)
Scenario 2	105,330 (16%)	85,995 (-5%)	1,202 (16%)	853 (-18%)	34,998 (10%)	34,443 (8%)	17,846 (11%)	15,752 (-2%)
Scenario 3	113,846 (26%)	92,563 (2%)	1,251 (21%)	735 (-7%)	36,206 (14%)	35,634 (12%)	18,360 (14%)	16,343 (2%)

7.1 Coho Salmon

Modeled future coho salmon spawner abundance decreased in both of the No Action scenarios, by 10% in the mid-century scenario and 28% in the late century scenario (Figure 7.1, Table 7.2). Mid-century spawner abundance ranged from an increase of 10% in Scenario 1 to an increase of 26% in Scenario 3. Late-century spawner abundance ranged from a decrease of 10% in Scenario 1 to an increase of 2% in Scenario 3.

Mid-century changes in C_n were nearly identical in magnitude to changes in spawner abundance within each scenario, however changes in P_n differed substantially. Late century changes in spawner abundance and C_n were also similar in magnitude for Scenarios 1 and 2, however in Scenario 3, spawner abundance and C_n increased, while P_n decreased.

Figure 7.1. Projected coho spawner abundance (N_{eq}, without harvest) for the No Action alternative and three future restoration scenarios.

Table 7.2. Modeled number of coho salmon spawners (N_{eq}, without harvest) for the Chehalis basin for each restoration scenario compared to current conditions, along with life-cycle productivity (P_n) and capacity (C_n) estimated from the life stage parameters. Dark blue shaded cells indicate increases >25%, light blue shade cells indicate increases 10-25% (percentages in parentheses). Dark red shaded cells indicate decreases >25%, light red shade cells indicate decreases 10-25% (percentages in parentheses).

Scenario	Spawners (N_{eq})		P_n		C_n	
Current	90,625		4.1		120,062	
	Mid-century	Late-century	Mid-century	Late-century	Mid-century	Late-century
No Action	81,579 (-10%)	65,300 (-28%)	3.9 (-0.2)	3.6 (-0.5)	110,127 (-8%)	90,685 (-28%)
Scenario 1	99,561 (10%)	81,145 (-10%)	4.1 (0)	3.8 (-0.3)	131,689 (10%)	109,916 (-8%)
Scenario 2	105,330 (16%)	85,995 (-5%)	4.2 (+0.1)	3.9 (-0.2)	138,510 (15%)	115,835 (-4%)
Scenario 3	113,846 (26%)	92,563 (2%)	4.2 (+0.1)	3.9 (-0.2)	149,133 (24%)	124,014 (3%)

7.2 Spring Chinook Salmon

Spring Chinook are most sensitive to future temperature changes, and modeled future spring Chinook spawner abundance decreased in the No Action scenarios, by 9% in the mid-century scenario and 39% in the late century scenario (Figure 7.2, Table 7.3). Mid-century spawner abundance ranged from an increase of 15% in Scenario 1 to an increase of 21% in Scenario 3. Late-century spawner abundance decreased in all three scenarios, by 18% in Scenarios 1 and 2 and 7% in Scenario 3.

Mid-century changes in C_n were slightly lower than changes in spawner abundance within each scenario but showed the same pattern. The pattern of changes in P_n, however, differed substantially. Late-century changes in spawner abundance and C_n were also similar in magnitude for Scenarios 1, 2, and 3, but all decreasing in late century.

Figure 7.2. Projected spring Chinook spawner abundance (N_{eq}, without harvest) for the No Action alternative and three future restoration scenarios.

Table 7.3. Modeled number of spring Chinook salmon spawners (N_{eq}, without harvest) for the Chehalis basin for each restoration scenario compared to current conditions, along with life-cycle productivity (P_n) and capacity (C_n) estimated from the life stage parameters. Dark blue shaded cells indicate increases >25%, light blue shade cells indicate increases 10-25% (percentages in parentheses). Dark red shaded cells indicate decreases >25%, light red shade cells indicate decreases 10-25%.

Scenario	Spawners (N_{eq})		P_n		C_n	
Current	1,035		2.0		2,021	
	Mid-century	Late-century	Mid-century	Late-century	Mid-century	Late-century
No Action	945 (-9%)	627 (-39%)	2.0 (0)	1.7 (-0.4)	1,890 (-6%)	1,542 (-24%)
Scenario 1	1,194 (15%)	846 (-18%)	2.2 (+0.2)	1.9 (-0.1)	2,176 (8%)	1,793 (-11%)
Scenario 2	1,202 (16%)	853 (-18%)	2.2 (+0.2)	1.9 (-0.1)	2,188 (8%)	1,806 (-11%)
Scenario 3	1,251 (21%)	901 (-13%)	2.2 (+0.2)	1.9 (-0.1)	2,257 (12%)	1,885 (-7%)

7.3 Fall Chinook Salmon

Modeled future fall Chinook spawner abundance decreased by 3% in the mid-century No Action scenario, and by 5% in the late century No Action scenario, indicating that fall Chinook are much less sensitive to stream temperature change than coho salmon or spring Chinook. Modeled abundance increased in all future restoration scenarios (Figure 7.3, Table 7.4). Mid-century spawner abundance increased by 8% in Scenario 1, by 10% in Scenario 2, and by 14% in Scenario 3. Late-century spawner abundance increased by 7% in Scenario 1, 8% in Scenario 2, and 12% in Scenario 3.

Changes in C_n were similar in magnitude and pattern to changes in spawner abundance within each scenario. Changes in P_n, however, were very small in all scenarios in both mid- and late-century.
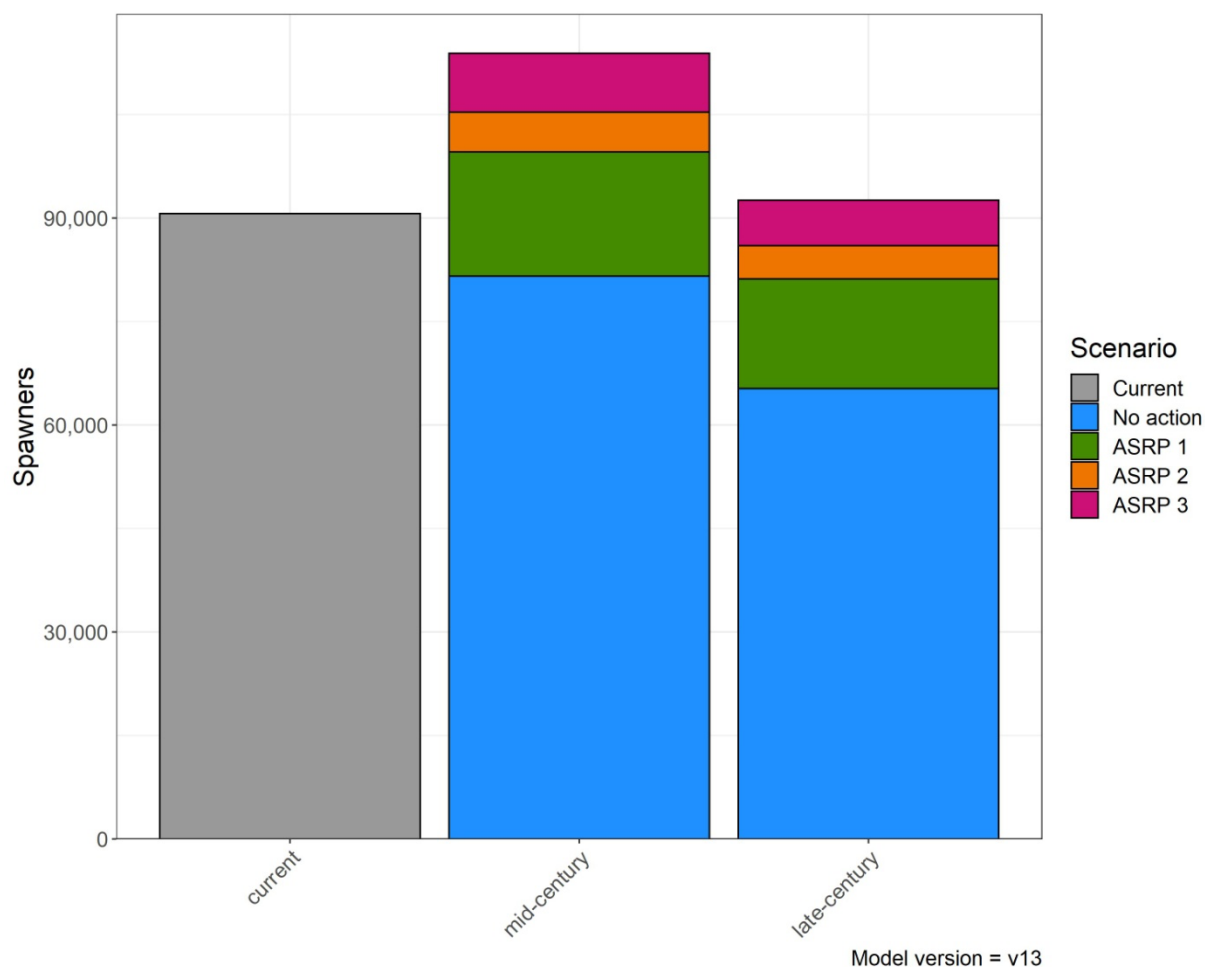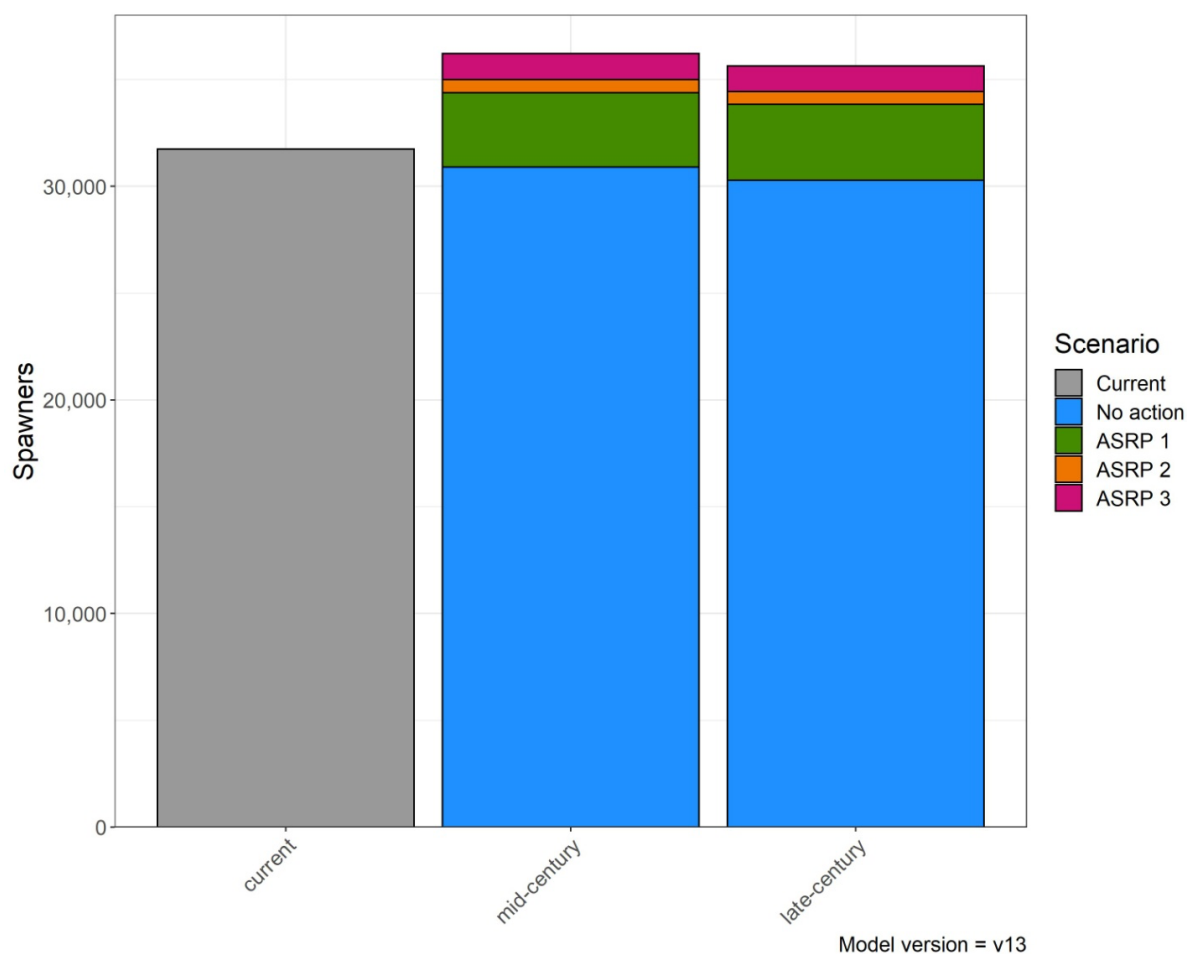

Figure 7.3. Projected fall Chinook spawner abundance (N_{eq}, without harvest) for the No Action alternative and three future restoration scenarios.

Table 7.4. Modeled number of fall Chinook salmon spawners (N_{eq}, without harvest) for the Chehalis basin for each restoration scenario compared to current conditions, along with life-cycle productivity (P_n) and capacity (C_n) estimated from the life stage parameters. Dark blue shaded cells indicate increases >25%, light blue shade cells indicate increases 10-25% (percentages in parentheses). Dark red shaded cells indicate decreases >25%, light red shade cells indicate decreases 10-25%.

Scenario	Spawners (N_{eq})		P_n		C_n	
Current	31,746		3.8		43,267	
	Mid-century	Late-century	Mid-century	Late-century	Mid-century	Late-century
No Action	30,908 (-3%)	30,286 (-5%)	3.7 (-0.1)	3.7 (-0.1)	42,167 (-3%)	41,542 (-4%)
Scenario 1	34,387 (8%)	33,829 (7%)	3.9 (+0.1)	3.8 (0)	46,366 (7%)	45,805 (6%)
Scenario 2	34,998 (10%)	34,443 (8%)	3.9 (+0.1)	3.9 (+0.1)	47,070 (9%)	46,512 (7%)
Scenario 3	36,206 (14%)	35,634 (12%)	4.0 (+0.2)	3.9 (+0.1)	48,315 (12%)	47,736 (10%)

7.4 Steelhead

Modeled future steelhead spawner abundance decreased by 5% in the mid-century No Action scenario, and by 18% in the late century No Action scenario, indicating that steelhead are somewhat less sensitive to stream temperature and low flow change than coho salmon or spring Chinook. Modeled abundance increased in all future restoration scenarios (Figure 7.4, Table 7.5). Mid-century spawner abundance increased by 8% in scenario 1, by 11% in scenario 2, and by 14% in scenario 3. Late-century spawner abundance changed by -5% in scenario 1, by -2% in scenario 2, and by +2% in scenario 3.

Changes in C_n were similar in magnitude and pattern to changes in spawner abundance within each scenario. Changes in P_n, however, were very small in all scenarios in both mid- and late-century.
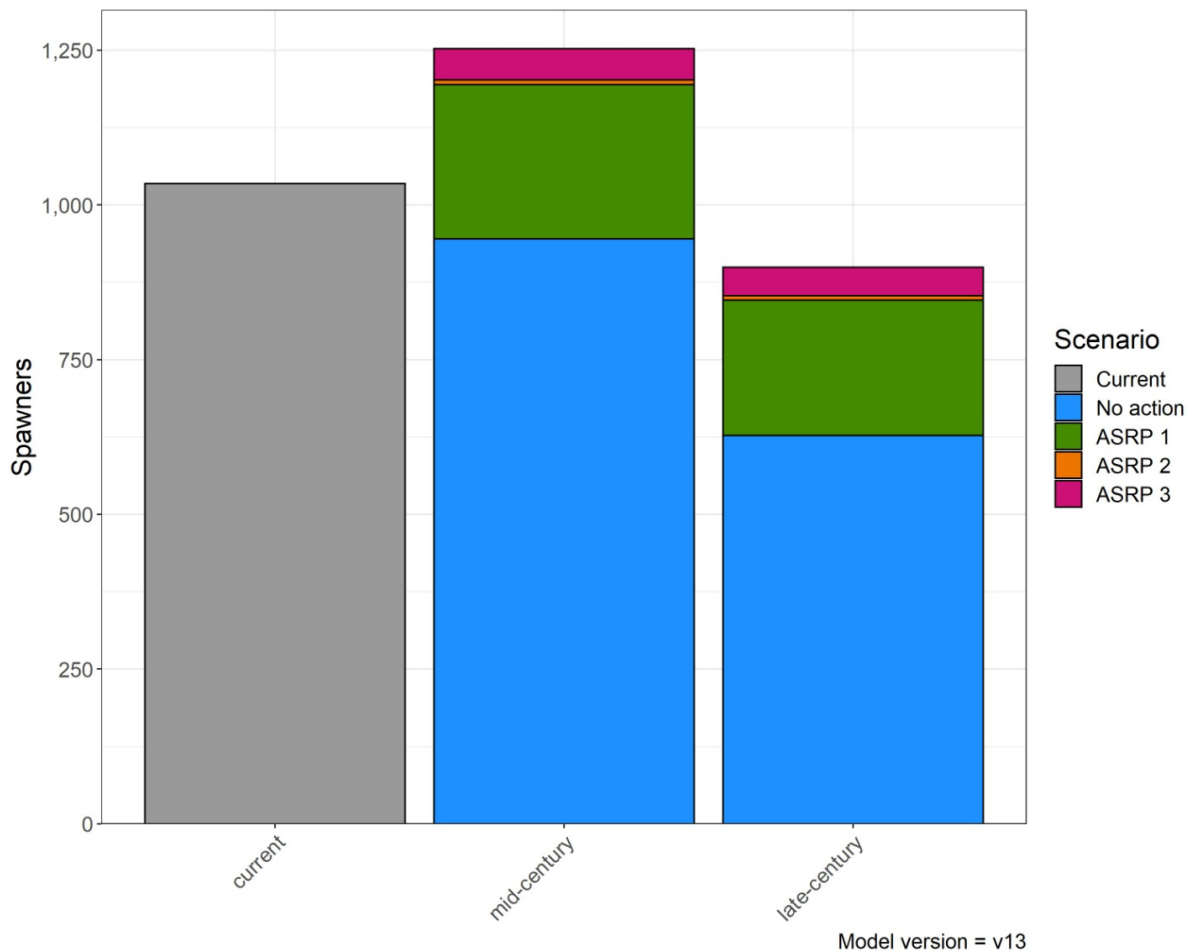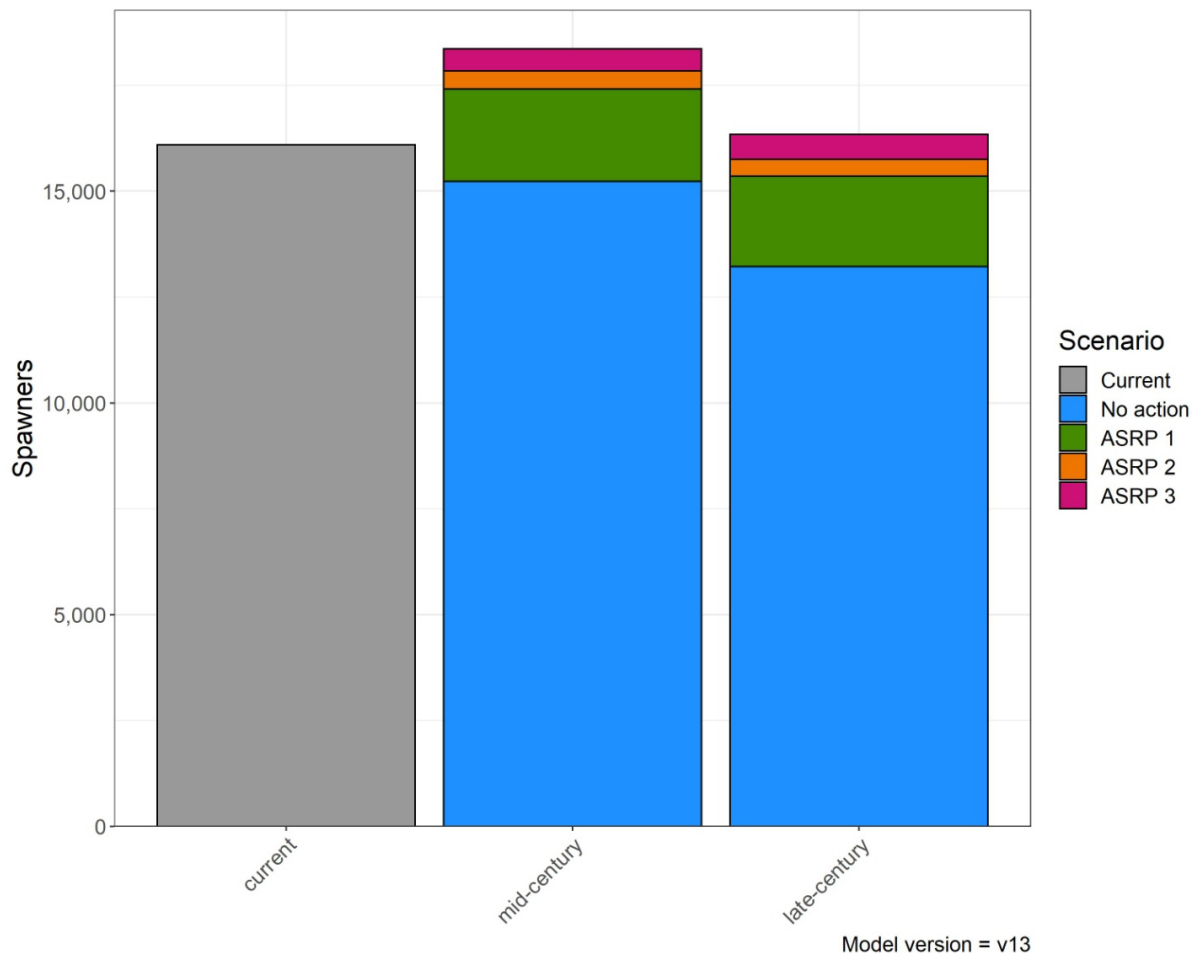

Figure 7.4. Projected steelhead spawner abundance (N_{eq}, without harvest) for the No Action alternative and three future restoration scenarios.

Table 7.5. Modeled number of steelhead spawners (N_{eq}, without harvest) for the Chehalis basin for each restoration scenario compared to current conditions, along with life-cycle productivity (P_n) and capacity (C_n) estimated from the life stage parameters. Dark blue shaded cells indicate increases >25%, light blue shade cells indicate increases 10-25% (percentages in parentheses). Dark red shaded cells indicate decreases >25%, light red shade cells indicate decreases 10-25%.

Scenario	Spawners (N_{eq})		P_n		C_n	
Current	16,092		4.0		21,437	
	Mid-century	Late-century	Mid-century	Late-century	Mid-century	Late-century
No Action	15,225 (-5%)	13,221 (-18%)	3.9 (-0.1)	3.7 (-0.3)	20,446 (-5%)	18,042 (-16%)
Scenario 1	17,416 (8%)	15,348 (-5%)	4.3 (+0.3)	4.1 (+0.1)	22,690 (6%)	20,286 (-5%)
Scenario 2	17,846 (11%)	15,752 (-2%)	4.4 (+0.4)	4.2 (+0.2)	23,048 (8%)	20,635 (-4%)
Scenario 3	18,360 (14%)	16,343 (2%)	4.6 (+0.6)	4.4 (+0.4)	23,493 (10%)	21176 (-1%)

8. Model Uncertainty and Sensitivity

Sources of uncertainty in the life-cycle model outputs include model uncertainty (accuracy of model form), parameter uncertainty (accuracy of parameter estimates, including measurement error and extrapolation error), scenario uncertainty (uncertainty in modeling future development or climate change effects), and natural variability (natural annual variation) (Rosenberg and Restrepo 1994; Francis and Shotton 1997; Steel et al. 2003). In this section, we describe model form uncertainty, parameter uncertainty, and scenario uncertainty. We do not include natural variation from year to year as part of parameter uncertainty because we consider it to be natural temporal variability. However, annual variation in a parameter can be incorporated into the model as stochastic variation to produce a time series of spawner abundance reflecting annual variation around the equilibrium population size (e.g., including the influence of annual variation in peak flows on incubation productivity).

In addition to our qualitative evaluation of uncertainty, we conducted a sensitivity analysis of the life-cycle model to quantify influences of each life-stage capacity or productivity on model outcomes, and to understand how the influence of a given parameter might differ under current or historical conditions (Helton et al. 2006; Storlie et al. 2009). It can help inform the focus of research and monitoring efforts, or suggest which life stages most limit a population. The approach we followed is similar to Zabel et al. (2006) and Jorgensen et al. (2017).

8.1 Model Form Uncertainty

As with all models, some of the uncertainty in the NOAA life-cycle model stems from how the model is structured. Sources of uncertainty in model structure include (1) which aspects of life histories are represented or omitted, (2) which habitat effects are represented or omitted, and (3) the accuracy of equations used to represent habitat effects on life stage parameters. It is important to note that the available basin-specific data limit our ability to parameterize and calibrate the life-cycle models. For example, some poorly quantified or rare life histories such as coho salmon age-0 nomads (Koski 2009; Bennett et al. 2015) or yearling Chinook salmon smolts that have been observed in estuary sampling (Sandell et al. 2014) are not modeled due to the paucity of density and productivity data for those life-history types.

We also do not know the extent to which model results are affected by inter- and intra-species interactions in the subbasins, delta, and bay, nor do we understand the exchange of individuals between reaches within or across tributaries (Rieman and Dunham 2000). These interactions, as well as predation by native and non-native species, may influence modeled current abundances were we able to include them, and they may also influence the potential success of restoration actions. For example, reconnection of a floodplain habitat that has abundant predators may not increase salmon populations as expected because the benefit of increased capacity is negated by decreased productivity. Finally, we do not know how natural fish production is affected by hatchery supplementation (e.g.,

Christie et al. 2014). While such interactions may be important, we do not have local data to incorporate such effects, nor were they within the scope of this study. Finally, we do not include potential adaptation to climate change in the model, which may ameliorate the modeled effect of climate change on populations.

While these limitations clearly constrained the development of the life-cycle models, it is not possible to quantify their associated uncertainties. Nonetheless, the fact that the models produce reasonable results without these added complexities suggests that this uncertainty may not appreciably affect the patterns of results from the NOAA models. That is, relative differences in model results among species or subbasins may not differ significantly were such effects to be included in the models. However, absolute abundances produced by the model could be increased or reduced.

8.2 Parameter Uncertainty

Uncertainty in the parameter estimates used in the life-cycle models can arise from natural spatial and temporal variation, extrapolation errors, and measurement errors, all of which influence the accuracy of parameters such as fish densities or productivity estimates. In most cases, there is substantial natural variation in the data underpinning the parameters and functions used in the models, and selection of any parameter value or function aims to capture a "typical" value or response function. For example, the functions relating incubation survival to fine sediment or rearing survival to stream temperature are single curves, while the original data show substantial variation around that curve. While some studies have used variation in parameter estimates to quantify this type of uncertainty using Monte Carlo simulations (e.g., Beechie et al. 2006a), using this method with the large number of parameters in the NOAA life-cycle models would produce such a wide range of outputs that it would be unusable. Therefore, we do not attempt to quantify this uncertainty, but acknowledge that uncertainty in the most sensitive parameters would have the largest influence on model outputs.

The reach-level habitat values used in the model also contain varying types and levels of uncertainty. For measured parameters such as large river bank habitat or riparian canopy opening angle, the main source of uncertainty is measurement error because these parameters are not extrapolated or modeled. By contrast, reach-level habitat values such as percent pool area in small streams are extrapolated from a sample of field surveys, and an important source of error is extrapolation error. We attempt to limit this type of error by stratifying the data by channel slope and adjacent land cover, and then extrapolate data to reaches in the same slope and land cover class. Finally, some habitat parameters are produced from other models, and prediction errors are an important source of uncertainty. For example, uncertainty in the modeled fine sediment values is likely high because those values are based only on density of unpaved roads, and do not account for other sediment sources such as bank erosion. Moreover, there are few data in the basin to validate the relationship, and the prudent management action is to first confirm where fine sediment levels are indeed high and which sources of fine sediment need to be addressed.

One specific uncertainty in the models is that we use data on current spawning and rearing densities or productivities to parameterize the current condition models. For capacities, we have used published densities for estimating capacity where possible (e.g., Nickelson 1998), assuming that those densities represent a high estimate of current observed densities. In other cases—such as with the large river densities—we reanalyzed density data and chose the 95th percentile of observed densities to calculate capacity, attempting to assure that capacity estimates were not biased low. By contrast, estimating density-independent productivity for each species and life stage based on observed data may be inherently biased low because the observations include density-dependent effects on survival. Therefore, we chose survival values from the high end of the observed ranges in all cases to limit the influence of this error as much as possible.

8.3 Scenario Uncertainty

In addition to the model and parameter sources of uncertainty, the restoration scenarios contain uncertainty embedded in projections of future land use and climate change. These are external to the NOAA model (i.e., these projections are provided to us from other sources). Because these are modeled futures, there is no way of reducing these uncertainties other than continued refinements of projections in population growth and climate change. Notably, the projected build-out from population growth produces very little response in modeled salmon abundance in the future scenarios, and by far the largest component of the future response is the projected change in stream temperature. This suggests that reducing uncertainty in the development estimates will likely have a small effect on the model results since the development effect is quite small. Sources of uncertainty in the stream temperature projections include uncertainty in projected green house gas emissions scenarios, as well as variation in the air temperature projections from the different climate models. One estimate of these combined future uncertainties is ±2°C by the 2080s (a term representing an average of the period from 2070-2099) (Beechie et al. 2013a). Additional uncertainty is introduced during the downscaling process to estimate air temperatures within the basin, and further in the process of estimating stream temperature from air temperature (Isaak et al. 2017). While we cannot meaningfully reduce this uncertainty in the NOAA Model, we acknowledge its potentially large effect on future habitat conditions and future salmon population performance. Higher temperatures than those modeled here will obviously be more detrimental to salmonids, whereas lower temperatures would be less detrimental.

8.4 Sensitivity Analysis

We used a global sensitivity analysis because of its strengths for understanding uncertainty in a life-cycle model that contains stochastic elements and multiple interactive factors (McCarthy et al. 1995; Coutts and Yokomizo 2014). In a local sensitivity analysis, one parameter at a time is manipulated—usually by some fixed percent—and model output is compared to average model output. While this approach can identify specific model sensitivities, it does not capture how model sensitivity to individual parameters varies among habitat scenarios in more complex models. That is, the sensitivity of each parameter depends on the values of other parameters. In the global sensitivity analysis all parameters

of interest are manipulated simultaneously and independently to capture this variation and evaluate their influences on model outputs relative to each other.

We used a regression-based, standardized regression coefficient (SRC) method because the results are easily interpretable (McCarthy et al. 1995; Cross and Beissinger 2001; Coutts and Yokomizo 2014). SRC has been used frequently to characterize parameter sensitivities of population viability analysis (PVA) models, including models for salmon (Zabel et al. 2006; Crozier et al. 2008; Lonsdorf et al. 2016; Mortensen and Reed 2016). In the SRC procedure (Zabel et al. 2006; 2015), the model was run 500 times with all parameters simultaneously and independently sampled from their identified ranges according to a random uniform distribution under current conditions and historical conditions. Parameter ranges from which we sampled were up to ±20% of the base value for each life-stage parameter in each scenario (current and historical), and any rearing productivity that exceeded 1.0 was set at 1.0. For example, a 20% increase in a rearing productivity value of 0.9 would produce a productivity of 1.08, which is not possible. Therefore, those rearing productivity values were capped at 1.0.

We generated the sensitivity dataset from the 500 model runs, and used the results to construct SRCs for comparisons. We focused on one output metric for the sensitivity analysis: the median number of spawners across each 100-year model run. We regressed the median number of spawners against the model parameters, which were the independent variables. Because the parameter values used in the sensitivity analysis were generated independently there were no collinearity concerns. We standardized the regression coefficients (divided by their standard error, and normalized by dividing by the largest absolute value) thereby making them more easily comparable. Coefficient values closest to or equal to +/-1 were relatively more influential than those closer to zero.

In interpreting these results, it is critical to distinguish between a model's sensitivity to a parameter based on a fixed percentage change, and the potential influence of a parameter on model results based on a realistic change in the parameter value. For example, changing the coho prespawn productivity value by 20% may have a large influence on modeled spawner abundance. However, a realistic change in prespawn productivity as a result of future changes in impervious area is <1.5% in most subbasins, and the potential difference in spawners between the current and future No Action scenarios is negligible.

8.4.1 Sensitivity Analysis: Coho Salmon

The global sensitivity analysis for the coho salmon model indicates that, under the current habitat scenario, adult equilibrium abundance is most sensitive to prespawn productivity (Figure 8.1). However, most subbasins have prespawn productivity above 0.85 and 80% of subbasins have little or no projected change in prespawn mortality due to future development. Therefore, even though coho spawner abundance is sensitive to this parameter, the parameter only changes significantly in 5 to 10 subbasins out of the 63 total subbasins.

The remaining parameters have more influence in the model because the parameter differences among scenarios are larger and more widespread across the subbasins. Of the remaining parameters, the model is most sensitive to overwinter productivity (~0.9), followed by summer rearing capacity (~0.4), incubation productivity,

Figure 8.1. Sensitivity analysis for the coho salmon life-cycle model under the current and historical habitat scenarios. All influence values are scaled relative to the most sensitive parameter (prespawn productivity), which has a value of 1.

summer rearing productivity, and winter rearing capacity (0.2-0.3). The rank order and magnitudes of sensitivities are nearly the same under the historical habitat scenario. These patterns suggest that restoration scenarios focusing on increasing winter rearing habitat quality and productivity will result in the largest increases in spawner abundance, but also that increasing summer and winter rearing capacity and summer rearing productivity may lead to significant increases in population size. As stated in Section 5, the fine sediment model has high uncertainty, so while incubation productivity is a sensitive parameter, it is unclear whether fine sediment is a widespread problem and whether restoration actions can be expected to produce a significant increase in the population. The model has virtually no sensitivity to egg capacity, indicating that increasing spawning capacity is a low priority.

8.4.2 Sensitivity Analysis: Spring Chinook Salmon

The sensitivity analysis for spring Chinook indicates that, under the current habitat scenario, adult equilibrium abundance is most sensitive to prespawn productivity. Prespawn productivities differ substantially among subbasins and scenarios due to changes in stream temperature (Figure 8.2). Following prespawn productivity, the model is most sensitive to subyearling rearing productivity, then incubation productivity, rearing capacity, and the June (late migrant) rearing productivity affected by stream temperature. The model is not sensitive to egg capacity. Under the historical habitat scenario, there are slight differences in the magnitudes of parameters but not in their rank order. These patterns support the diagnosis in Section 5, suggesting that restoration scenarios focusing on reducing stream temperature to increase prespawn productivity is an important restoration action. Increasing rearing habitat capacity and productivity may also result in relatively large increases in spawner abundance, and increasing incubation productivity may lead to significant increases in population size due to increased production of fry migrants.

8.4.3 Sensitivity Analysis: Fall Chinook Salmon

Under the current habitat scenario, the sensitivity analysis for fall Chinook shows that adult equilibrium abundance is most sensitive to subyearling rearing productivity. The model is also nearly equally sensitive to subyearling rearing capacity and prespawn productivity (Figure 8.3). However, prespawn productivity is a constant in the fall Chinook model, so it does not appreciably affect the diagnostic results. The model is also sensitive to incubation productivity, but less so for the June (late migrant) rearing productivity affected by stream temperature. The model is not sensitive to egg capacity. Under the historical habitat scenario, there are slight differences in the magnitudes of parameters and rank order, but the four most sensitive parameters remain highly sensitive. These patterns also support the diagnosis in Section 5, suggesting that restoration scenarios focusing on increasing rearing habitat capacity and productivity will result in the largest increases in spawner abundance, but also that increasing incubation productivity may lead to significant increases in population size due to increased production of fry migrants.

Figure 8.2. Sensitivity analysis for the spring Chinook salmon life-cycle model under the current and historical habitat scenarios. All influence values are scaled relative to the most sensitive parameter (prespawn productivity), which is assigned a value of 1.
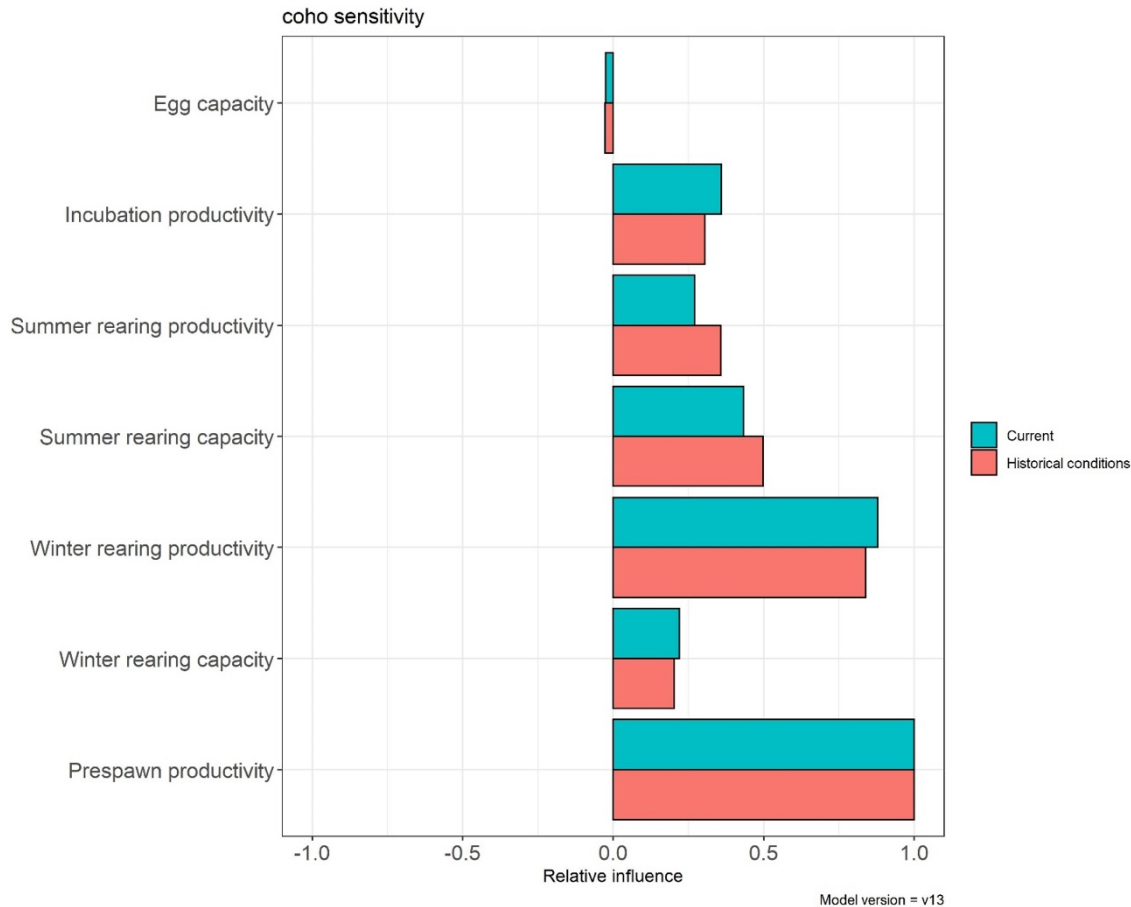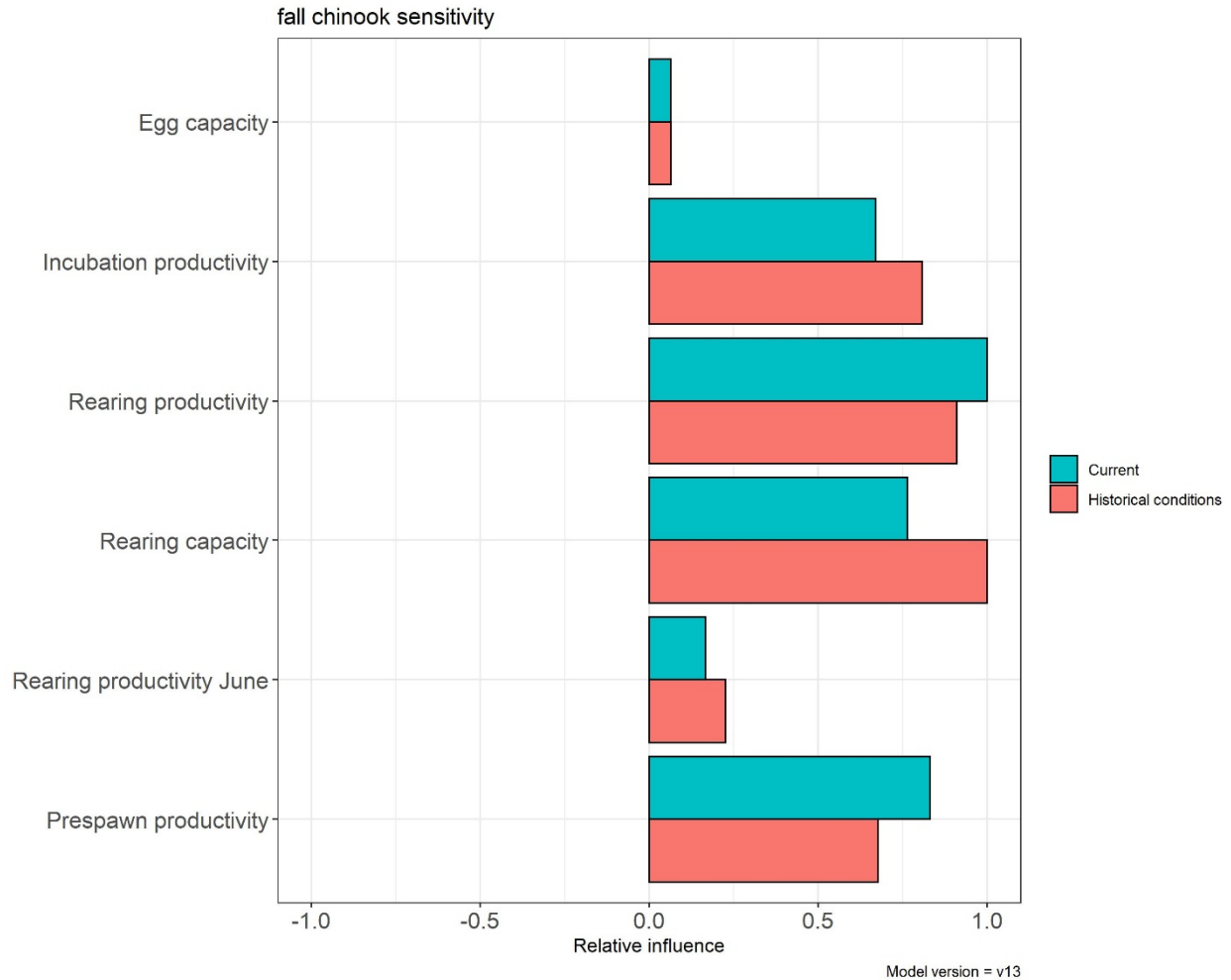
Figure 8.3. Sensitivity analysis for the fall Chinook salmon life-cycle model under the current and historical habitat scenarios. All influence values are scaled relative to the most sensitive parameter, which is assigned a value of 1.

8.4.4 Sensitivity Analysis: Steelhead

The global sensitivity analysis for the steelhead model indicates that, under the current habitat scenario, adult equilibrium abundance is most sensitive to second-year winter rearing productivity (Figure 8.4) (note that this value is also used in third-year winter rearing). The next most important sensitivities are second-summer rearing productivity, and prespawn productivity. The model is also moderately sensitive to first-winter rearing productivity, but relatively insensitive to the remaining capacity and productivity parameters. Model sensitivities under historical conditions are similar to those under current conditions.

These patterns suggest that restoration scenarios focusing on increasing summer and winter rearing habitat quality and productivity will result in the largest increases in

114

spawner abundance. As stated in Section 5, the fine sediment model has high uncertainty, so while incubation productivity is a sensitive parameter, it is unclear whether fine sediment is a widespread problem and whether restoration actions can be expected to produce a significant increase in the population. The model has virtually no sensitivity to egg capacity, indicating that increasing spawning capacity is a low priority.
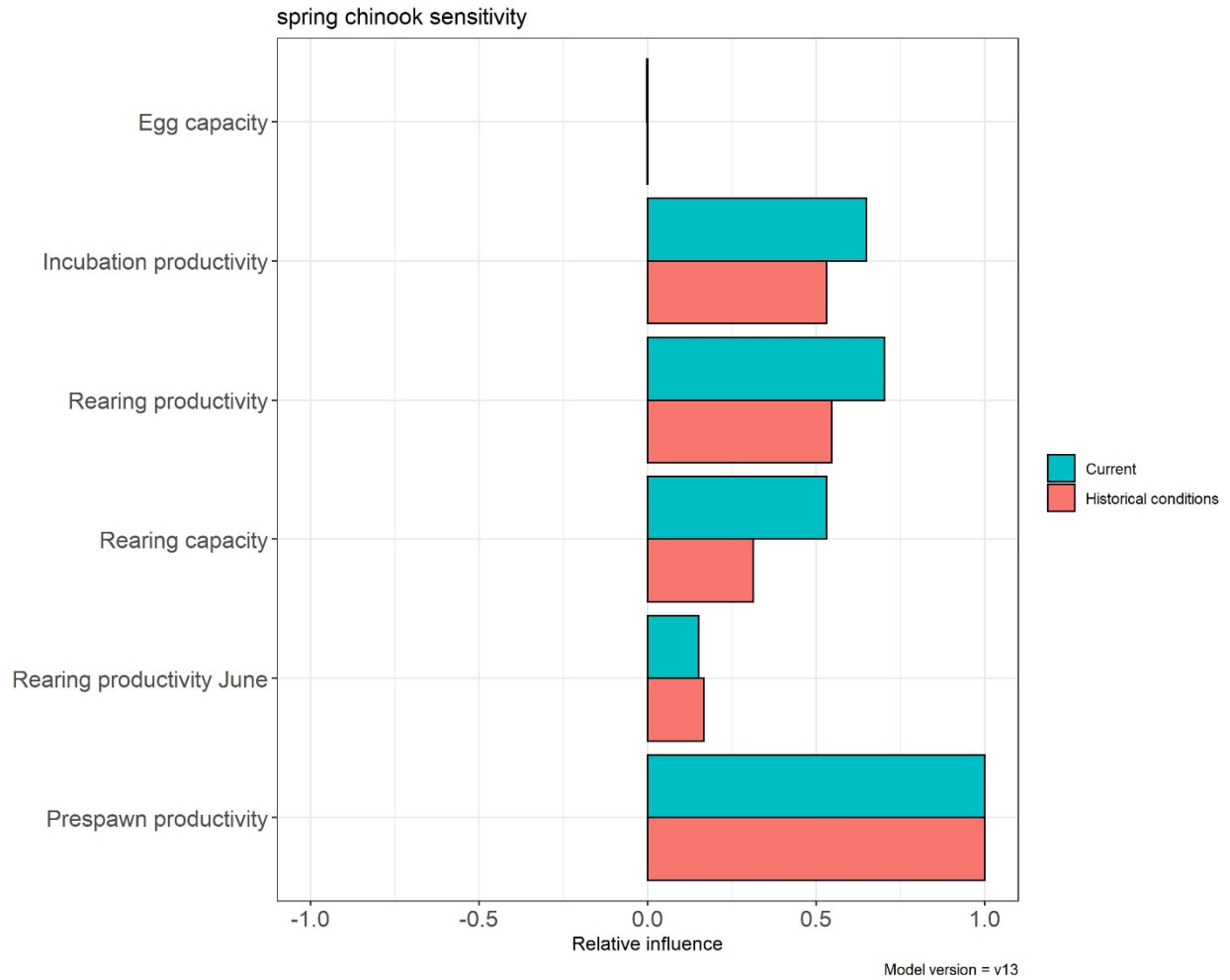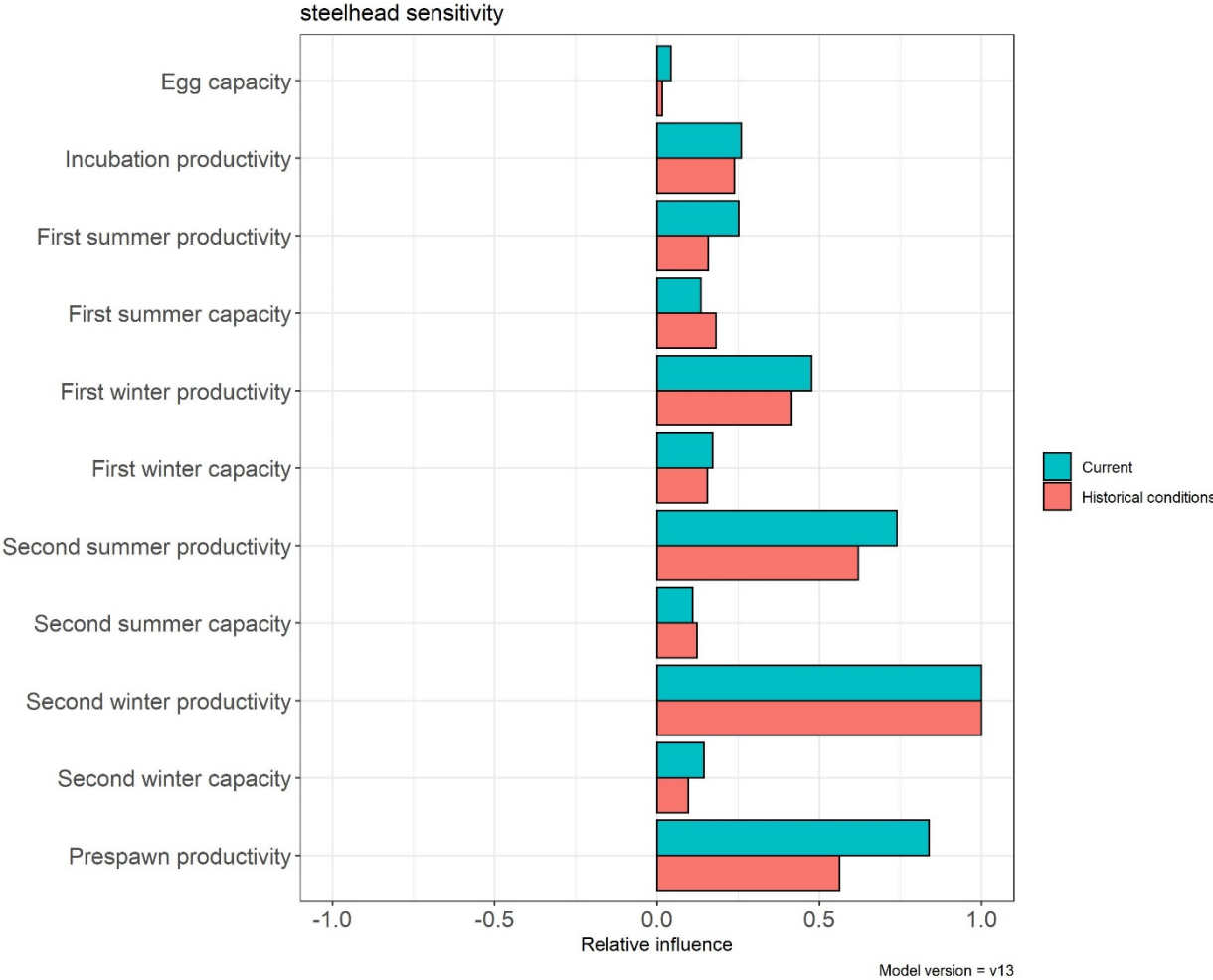

Figure 8.4. Sensitivity analysis for the steelhead life-cycle model under the current and historical habitat scenarios. All influence values are scaled relative to the most sensitive parameter (second winter rearing productivity), which has a value of 1.

References Cited

NOTE: This section includes references cited in the Appendices

Abbe, T. B., and D. R. Montgomery. 2003. Patterns and processes of wood debris accumulation in the Queets River basin, Washington. Geomorphology 51:81-107.

Agee, J. K. 1988. Successional dynamics in forest riparian zones. Pages 31-43 *in* K. J. Raedeke, editor. Streamside Management: Riparian Wildlife and Forestry Interactions. College of Forest Resources, University of Washington, Seattle, Washington, USA.

Agee, J. K. 1993. Fire Ecology of Pacific Northwest Forests. Island Press, Washington, D.C.

Arrigoni, A. S., G. C. Poole, L. A. K. Mertes, S. J. O'Daniel, W. W. Woessner, and S. A. Thomas. 2008. Buffered, lagged, or cooled? Disentangling hyporheic influences on temperature cycles in stream channels. Water Resources Research 44(9):W09418.

ASEP (Aquatic Species Enhancment Plan). 2014. Chehalis Basin Strategy: Reducing Flood Damage and Enhancing Aquatic Species.

Barton, K. 2015. MuMIn: Multi-Model Inference. R package version 1.14.0. http://CRAN.R-project.org/package=MuMIn

Bartz, K. L., K. Lagueux, M. D. Scheuerell, T. J. Beechie, A. Haas, M. H. Ruckelshaus. 2006. Translating restoration scenarios into habitat conditions: an initial step in evaluating recovery strategies for Chinook salmon (*Oncorhynchus tshawytscha*). Canadian Journal of Fisheries and Aquatic Sciences 63:1578-1595.

Bartz, K. K., M. J. Ford, T. J. Beechie, K. L. Fresh, G. R. Pess, R.E . Kennedy, M. L. Rowse, and M. Sheer. 2015. Trends in developed land cover adjacent to habitat for threatened salmon in Puget Sound, Washington, U.S.A. PLoS ONE 10(4): e0124415. DOI: 10.1371/journal.pone.0124415

Battin, J., M. W. Wiley, M. H. Ruckelshaus, R. N. Palmer, E. Korb, K. K. Bartz, and H. Imaki. 2007. Projected impacts of climate change on salmon habitat restoration. Proceedings of the National Academy of Sciences 104:6720–6725.

Beamer, E., A. McBride, C. Greene, R. Henderson, G. Hood, K. Wolf, K. Larsen, C. Rice, and K. Fresh. 2005. Delta and nearshore restoration for the recovery of wild Skagit River Chinook salmon: linking estuary restoration to wild Chinook salmon populations. Skagit Chinook Recovery Plan, Appendix D.

Beamer, E., and R. Henderson. 1998. Juvenile salmonid use of natural and hydromodified stream bank habitat in the mainstem Skagit River, northwest Washington. Skagit River System Cooperative, La Conner, Washington.

Beamer, E., G. Hood, and K. Wolf. 2014. Habitat and juvenile Chinook benefit predictions of candidate restoration projects within the Skagit tidal delta. Skagit Hydrodynamic Model Project Technical Report.

Bear, E.A., T.T. McMahon, and A.V. Zale. 2007. Comparative thermal requirements for westslope cutthroat trout and rainbow trout: Implications for species interactions and

development of thermal protection standards. Transactions of the American Fisheries Society 136:1113-1121. DOI: 10.1577/T06-072.1

Beechie, T. J. 1998. Rates and pathways of recovery for sediment supply and woody debris recruitment in northwestern Washington streams, and implications for salmonid habitat restoration. Ph.D. Dissertation. University of Washington, Seattle, Washington, USA.

Beechie, T., and S. Bolton. 1999. An approach to restoring salmonid habitat-forming processes in Pacific Northwest watersheds. Fisheries 24(4):6-15.

Beechie, T. J., and T. H. Sibley. 1997. Relationships between channel characteristics, woody debris, and fish habitat in northwestern Washington streams. Transactions of the American Fisheries Society 126(2):217-229.

Beechie, T., E. Beamer, and L. Wasserman. 1994. Estimating coho salmon rearing habitat and smolt production losses in a large river basin, and implications for habitat restoration. North American Journal of Fisheries Management 14(4):797-811.

Beechie, T. J., B. D. Collins, and G. R. Pess. 2001. Holocene and recent geomorphic processes, land use and salmonid habitat in two north Puget Sound river basins. Pages 37-54 *in* Dorava, J. B., D. R. Montgomery, F. Fitzpatrick, and B. Palcsak, editors. Geomorphic Processes and Riverine Habitat. Water Science and Application Volume 4, American Geophysical Union, Washington D.C.

Beechie, T. J., C. M. Greene, L. Holsinger, and E. Beamer. 2006a. Incorporating parameter uncertainty into evaluations of spawning habitat limitations on Chinook salmon populations. Canadian Journal of Fisheries and Aquatic Sciences 63(6): 1242-1250.

Beechie, T, H. Imaki, J. Greene, A. Wade, H. Wu, G. Pess, P. Roni, J. Kimball, J. Stanford, P. Kiffney, N. Mantua. 2013b. Restoring salmon habitat for a changing climate. River Research and Applications 29(8):939-960. DOI: 10.1002/rra.2590.

Beechie, T. J., D. Sear, J. Olden, G. R. Pess, J. Buffington, H. Moir, P. Roni, and M. M. Pollock. 2010. Process-based principles for restoring river ecosystems. BioScience 60:209-222.

Beechie, T. J., M. Liermann, E. M. Beamer, and R. Henderson. 2005a. A classification of habitat types in a large river and their use by juvenile salmonids. Transactions of the American Fisheries Society 134(3):717-729.

Beechie, T. J., M. Liermann, M. M. Pollock, S. Baker, and J. Davies. 2006b. Channel pattern and river-floodplain dynamics in forested mountain river systems. Geomorphology 78(1-2):124-141.

Beechie, T. J., G. R. Pess, E. M. Beamer, G. Lucchetti, R. E. Bilby. 2003. Role of watershed assessments in recovery planning for salmon. Pages 194-225 *in* Montgomery, D. R., S. Bolton, and D. B. Booth, editors. Restoration of Puget Sound Rivers. University of Washington Press, Seattle.

Beechie, T. J., G. R. Pess, H. Imaki, A. Martin, J. Alvarez, and D. H. Goodman. 2015. Comparison of potential increases in juvenile salmonid rearing habitat capacity among

alternative restoration scenarios, Trinity River, California. Restoration Ecology 23(1):75-84, DOI: 10.1111/rec.12131.

Beechie, T. J., G. Pess, P. Kennard, R. E. Bilby, and S. Bolton. 2000. Modeling recovery rates and pathways for woody debris recruitment in northwestern Washington streams. North American Journal of Fisheries Management 20:436–452.

Beechie, T., G. Pess, S. Morley, L. Butler, P. Downs, A. Maltby, P. Skidmore, S. Clayton, C. Muhlfeld, and K. Hanson. 2013a. Chapter 3: Watershed assessments and identification of restoration needs. Pages 50-113 *in* Roni, P. and T. Beechie, editors Stream and Watershed Restoration: A Guide to Restoring Riverine Processes and Habitats. Wiley-Blackwell, Chichester, UK.

Beechie, T., G. Pess, P. Roni, and G. Giannico. 2008. Setting river restoration priorities: a review of approaches and a general protocol for identifying and prioritizing actions. North American Journal of Fisheries Management 28:891–905.

Beechie, T., J. Richardson, A. Gurnell, and J. Negishi. 2013c. Chapter 2: Watershed processes, human impacts, and process-based restoration. Pages 11-49 In Roni, P. and Beechie, T. (eds.) Stream and watershed Restoration: A Guide to Restoring Riverine Processes and Habitats. Wiley-Blackwell, Chichester, UK.

Beechie, T. J., C. N. Veldhuisen, D. E. Schuett-Hames, P. DeVries, R. H. Conrad, and E. M. Beamer. 2005b. Monitoring treatments to reduce sediment and hydrologic effects from roads. Pages 35-65 *in* P. Roni, editor. Methods for Monitoring Stream and Watershed Restoration. American Fisheries Society, Bethesda, MD.

Bennett, T. R., P. Roni, K. Denton, M. McHenry, and R. Moses. 2015. Nomads no more: early juvenile coho salmon migrants contribute to the adult return. Ecology of Freshwater Fish 24:264-275.

Bisson, P. A., K. Sullivan, and J. L. Nielsen. 1988. Channel hydraulics, habitat use, and body form of juvenile coho salmon, Steelhead, and cutthroat trout in streams. Transactions of the American Fisheries Society 117:262–273.

Bjornn, T. C. 1978. Survival, Production, and Yield of Trout and Chinook Salmon in the Lemhi River, Idaho. Bulletin No. 27, College of Forestry, Wildlife and Range Sciences. University of Idaho, Moscow, ID.

Bowerman, T., A. Roumasset, M. L. Keefer, C. S. Sharpe, and C. C. Caudill. 2018. Prespawn mortality of female Chinook salmon increases with water temperature and percent hatchery origin. Transactions of the American Fisheries Society 147:31-42.

Bresenham, J. E. 1965. Algorithm for computer control of a digital plotter. IBM Systems journal 4:25-30.

Brett, J. R. 1952. Temperature tolerance in young Pacific salmon, genus Oncorhynchus. Journal of the Fisheries Board of Canada, 9(6), pp.265-323.

Brierley, G., and K. Fryirs. 2009. Don't fight the site: three geomorphic considerations in catchment-scale river rehabilitation planning. Environmental Management 43(6):1201-1218.

Brix, R. 1981. Data report of Grays Harbor juvenile salmon seining program, 1973-1980. Washington Department of Fish and Wildlife progress report #141.

Brown, G. 1972. An improved temperature model for small streams. Water Resources Research Institute Report 16.

Brown, T. G., and G. F. Hartman. 1988. Contribution of Seasonally Flooded Lands and Minor Tributaries to the Production of Coho Salmon in Carnation Creek, British Columbia. Transactions of the American Fisheries Society 117:546-551.

Buffington, J. M., and D. R. Montgomery. 1999. Effects of hydraulic roughness on surface texture of gravel-bed rivers. Water Resources Research 35:3507–3521.

Burnham, K. P., and D. R. Anderson. 2002. Model selection and inference: a practical information theoretical approach. Springer-Verlag, New York.

Burnham, K. P., D. R. Anderson, and K. P. Huyvaert. 2011. AIC model selection and multimodel inference in behavioral ecology: some background, observations, and comparisons. Behavioral Ecology and Sociobiology 65:23–35.

Busby, P. J., T. C. Wainwright, G. J. Bryant, L. J. Lierheimer, R. S. Waples, F. W. Waknitz, and I. V. Lagomarsino. 1996. Status Review of West Coast Steelhead from Washington, Oregon, Idaho, and California. NOAA Technical Memorandum NMFS-NWFSC-27.

Caissie, D., 2006. The thermal regime of rivers: a review. Freshwater Biology 51:1389-1406. https://doi.org/10.1111/j.1365-2427.2006.01597.x

Campbell, L., A. Claiborne, S. Ashcraft, M. Zimmerman, and C. Holt. 2017. Investigating juvenile life history and maternal run timing of Chehalis River spring and fall Chinook salmon using otolith chemistry. Report #FPT 17-15. Washington Department of Fish and Wildlife, Olympia, WA.

Cederholm, C. J., L. M. Reid, B. G. Edie, and E. O. Salo. 1982. Effects of forest road erosion on salmonid spawning gravel composition and populations of the Clearwater River, Washington. Pages 1-17 *in* K.A. Hashagen, editor. Habitat disturbance and recovery: proceedings of a symposium. California Trout, Inc., San Francisco.

Christie, M. R., M. J. Ford, and M. S Blouin. 2014. On the reproductive success of early-generation hatchery fish in the wild. Evolutionary Applications 7:883-896.

Clemens, B. J. 2015. A Survey of Steelhead Age and Iteroparity Rates from a Volunteer Angler Program in the Willamette River Basin, Oregon. North American Journal of Fisheries Management, 35(5):1046-1054, DOI: 10.1080/02755947.2015.1079572.

Collins, B. D., and D. R. Montgomery. 2011. The legacy of Pleistocene glaciation and the organization of lowland alluvial process domains in the Puget Sound region. Geomorphology 126:174-185.

Congleton, J. L., S. K. Davis, and S. R. Foley. 1981. Distribution, abundance and outmigration timing of chum and Chinook salmon fry in the Skagit salt marsh. Pages 153-163 *in* E. L. Brannon and E.O. Salo, editors. Proceedings of the Salmon and Trout Migratory Behavior Symposium. School of Fisheries, University of Washington, Seattle.

Coutts, S. R., and H. Yokomizo. 2014. Meta-models as a straightforward approach to the sensitivity analysis of complex models. Population Ecology 56:7-19.

Cramer Associates. 2007. Simulating fall redistribution and overwinter survival of Klamath River coho - review draft.

Crocker, R. L., and J. Major. 1955. Soil development in relation to vegetation and surface age at Glacier Bay, Alaska. Journal of Ecology 43:427-448.

Cross, P. C., and S. R. Beissinger. 2001. Using logistic regression to analyze the sensitivity of PVA models: a comparison of methods based on African wild dog models. Conservation Biology 15:1335-1346.

Crozier, L. G., R. W. Zabel, and A. F. Hamlet. 2008. Predicting differential effects of climate change at the population level with life-cycle models of spring Chinook salmon. Global Change Biology 14:2360249. doi: 10.1111/j.1365-2486.2007.01497.x

Dittbrenner, B. J., M. M. Pollock, J. W. Schilling, J. D. Olden, J. J. Lawler, and C. E. Torgersen. 2018. Modeling intrinsic potential for beaver (Castor canadensis) habitat to inform restoration and climate change adaptation. PLoS ONE 13(2):e0192538. ttps://doi.org/10.1371/journal.pone.0192538

Feist, B. E., E. R. Buhle, P. Arnold. J. W. Davis, and N. L. Scholz. 2011. Landscape ecotoxicology of coho salmon spawner mortality in urban streams. PLoS ONE 6(8):e23424, doi:10.1371/journal.pone.0023424

Feist, B. E., E. R. Buhle, D. H. Baldwin, J. A. Spromberg, S. E. Damm, J. W. Davis, and N. L. Scholz. 2017. Roads to ruin: conservation threats to a sentinel species across and urban gradient. Ecological Applications 27(8):2382-2396.

Fonda, R. W. 1974. Forest succession in relation to river terrace development in Olympic National Park, Washington. Ecology 55:927-942.

Francis, R.I.C.C., and R. Shotton. 1997. "Risk" in fisheries management: A review. Canadian Journal of Fisheries and Aquatic Sciences 54:1699-1715.

Franklin, J. F., and C.T. Dyrness. 1973. Natural Forest Vegetation of Oregon and Washington. USDA Forest Service General Technical Report PNW-8, Corvallis, Oregon, USA.

Fullerton, A. H., C. E. Torgersen, J. J. Lawler, R. N. Faux, E. A. Steel, T. J. Beechie, J. L. Ebersole, and S. G. Leibowitz. 2015. Rethinking the longitudinal stream temperature paradigm: region-wide comparison of thermal infrared imagery reveals unexpected complexity of river temperatures. Hydrological Processes 29:4719–4737. doi:10.1002/hyp.10506

Gallagher, S. P., and C. M. Gallagher. 2005. Discrimination of Chinook salmon, coho salmon, and steelhead redds and evaluation of the use of redd data for estimating escapement in several unregulated streams in Northern California. North American Journal of Fisheries Management 25:284–300, DOI: 10.1577/M04-016.1

Gannett, H. 1899. Nineteenth annual report of the United States Geological Survey, 1897-1898. Part V -- Forest Reserves. Government Printing Office. Washington, D.C.

Gendaszek, A. S. 2011. Hydrogeologic Framework and Groundwater/Surface-Water Interactions of the Chehalis River Basin, Southwestern Washington. U.S. Geological Survey Scientific Investigations Report 2011-5160, 42 p.

Godfrey, H. 1969. Chinook and Coho Salmon Hatchery Evaluation Studies: Eighth Progress Report. Fisheries Research Board of Canada, Manuscript Report Series No. 1053. Nanaimo, B.C.

Grantham, T. E., D. A. Newburn, M. A. McCarthy, and A. M. Merenlender. 2012. The role of streamflow and land use in limiting oversummer survival of juvenile steelhead in California streams. Transactions of the American Fisheries Society 141(3):585-598.

Greene, C. M., and T. J. Beechie. 2004. Habitat-specific population dynamics of ocean-type chinook salmon (*Oncorhynchus tshawytscha*) in Puget Sound. Canadian Journal of Fisheries and Aquatic Sciences 61:590-602.

Groot, C., and L. Margolis. 1991. Pacific Salmon Life Histories. UBC press.

Hall, J., P. Roni, T. Bennett, J. McMillan, K Hanson, R. Moses, M. McHenry, G. Pess, and W. Ehinger. 2016. Life history diversity of steelhead in two coast Washington watersheds. Transactions of the American Fisheries Society 145: 990-1005.

Hartig, F., J. M. Calabrese, B. Reineking, T. Wiegand, and A. Huth. 2011. Statistical inference for stochastic simulation models – theory and application. Ecology Letters 14:816-827. doi: 10.1111/j.1461-0248.2011.01640.x

Harvey, B. C., J. L. White, and R. J. Nakamoto. 2005. Habitat-specific biomass, survival, and growth of rainbow trout (*Oncorhynchus mykiss*) during summer in a small coastal stream. Canadian Journal of Fisheries and Aquatic Sciences 62:650-658.

Helton, J. C., J. D. Johnson, C. J. Sallaberry, and C. B. Storlie. 2006. Survey of sampling-based methods for uncertainty and sensitivity analysis. Reliability Engineering & System Safety 91:1175-1209.

Henderson, J. A., D. H. Peter, R. D. Lesher, and D. C. Shaw. 1989. Forested plant associations of the Olympic National Forest. R6 Ecology Technical Paper 001-88. U.S. Forest Service, Pacific Northwest Region, Portland, Oregon.

Hendrix, N., A. Criss, E. Danner, C. M. Greene, H. Imaki, A. Pike, and S. T. Lindley. 2014. Life Cycle Modeling Framework for Sacramento River Winter-run Chinook Salmon. U.S. Department of Commerce, NOAA Technical Memorandum NOAA-TM-NMFS-SFFSC-530.

Henning, J. A. 2004. An evaluation of fish and amphibian use of restored and natural floodplain wetlands. Washington Department of Fish and Wildlife. Prepared for Environmental Protection Agency, Region 10, EPA Grant number CD-97024901-1.

Honea, J. M., J. C. Jorgensen, M. M. McClure, T. D. Cooney, K. I. M. Engie, D. M. Holzer, and R. Hilborn. 2009. Evaluating habitat effects on population status: influence of habitat restoration on spring-run Chinook salmon. Freshwater Biology, 54(7):1576-1592.

Hood, W. G. 2007. Scaling tidal channel geometry with marsh island area: A tool for habitat restoration, linked to channel formation process. Water Resources Research 43:W03409, doi:10.1029/2006WR005083.

Howell, P., K. Jones, D. Scarnecchia, L. Lavoy, W. Kendra, and D. Ortmann. 1985. Stock Assessment of Columbia River Salmonids. Volume II: Steelhead Stock Summaries. Bonneville Power Administration, Project Number 83-335. Portland, OR.

IPCC (Intergovernmental Panel on Climate Change). 2013. Climate change: The physical science basis. Retrieved from http://www.ipcc.ch/

Isaak, D., S. Wenger, E. Peterson, J. Ver Hoef, S. Hostetler, C. Luce, J. Dunham, J. Kershner, B. Roper and D. Nagel. 2011. NorWeST: an interagency stream temperature database and model for the Northwest United States. US Fish and Wildlife Service, Great Northern Landscape Conservation Cooperative Grant. Project website: https://www.fs.fed.us/rm/boise/AWAE/projects/NorWeST.html.

Isaak, D. J., S. J. Wenger, E. E. Peterson, J. M. Ver Hoef, D. E. Nagel, C. H. Luce, S. W. Hostetler, J. B. Dunham, B. B. Roper, S. P. Wollrab, G. L. Chandler, D. L. Horan, and S. Parkes-Payne. 2017. The NorWeST summer stream temperature model and scenarios for the western U.S.: A crowd-sourced database and new geospatial tools foster a user community and predict broad climate warming of rivers and streams. Water Resources Research 53:9181-9205.

Jensen, D. W., E. A. Steel, A. H. Fullerton, and G. R. Pess. 2009. Impact of fine sediment on incubation survival of Pacific salmon: a meta-analysis of published studies. Reviews in Fisheries Science 17(3):348-359.

Johnson, S. L., M. F. Solazzi, and J. D. Rogers. 1993. Development and Evaluation of Techniques to Rehabilitate Oregon's Wild Salmonids. Annual Progress Report. Project Number F-125-R-5. Oregon Department of Fish and Wildlife, Portland, OR.

Jorgensen, J., and others. 2017. Chapter 9b: Wenatchee River spring-run Chinook salmon life-cycle model: hatchery effects, calibration, and sensitivity analyses. *In* Zabel, R., Cooney, T., and Jordan, C, editors. Interior Columbia Life Cycle Modeling. NWFSC draft report, Seattle, WA.

Kareiva, P., M. Marvier, and M. McClure. 2000. Recovery and management options for spring/summer Chinook salmon in the Columbia River Basin. Science 290:977-979.

Kinsel, C., G. Volkhardt, L. Kishimoto, and P. Topping. 2007. 2006 Skagit River Wild Salmon Production Evaluation. Washington Department of Fish and Wildlife, FPA 07-05, Olympia, WA.

Kondolf, G. M., M. W. Smeltzer, and S. F. Railsback. 2001. Design and performance of a channel reconstruction project in a coastal California gravel-bed stream. Environmental Management 28:761–776.

Kondolf, G. M., A. J. Boulton, S. O'Daniel, G. C. Poole, F. J. Rahel, E. H. Stanley, E. Wohl, A. Bang, J. Carlstrom, C. Cristoni, H. Huber, S. Koljonen, P. Louhi, and K. Nakamura. 2006. Process-based ecological river restoration: Visualizing three-dimensional connectivity

and dynamic vectors to recover lost linkages. Ecology and Society 11: 5. (31 December 2009; www.ecologyandsociety.org/vol11/iss2/art5).

Korman, J., and J. Schick. 2019. Cheakamus River steelhead juvenile and adult abundance monitoring – data report: Implementation Year 11. Reference: CMSMON-03. Ecometric Research, Vancouver, B.C.

Koski, K. V. 2009. The fate of coho salmon nomads: the story of an estuarine-rearing strategy promoting resilience. Ecology and Society 14(1): 4. [online] URL: http://www.ecologyandsociety.org/vol14/iss1/art4/

Lanier, A., T. Haddad, L. Mattison, and L. Brophy. 2014. Core CMECS GIS processing methods, Oregon estuary project of special merit. Oregon Coastal Management Program. Salem, OR.

Latterell, J. J., and R. J. Naiman. 2007. Sources and dynamics of large logs in a temperate floodplain river. Ecological Applications 17:1127-1141.

Latterell, J. J., J. S. Bechtold, R. J. Naiman, T. C. O'Keefe, and R. Van Pelt. 2006. Dynamic patch mosaics and channel movement in an unconfined river valley of the Olympic Mountains. Freshwater Biology 51:523-544.

Lestelle, L. C. 2007. Coho Salmon (*Oncorhynchus kisutch*) Life History Patterns in the Pacific Northwest and California. Report to U.S. Bureau of Reclamation, Biostream Environmental, Poulsbo, WA.

Liedtke, T. L., M. S. Zimmerman, R. G. Tomka, C. Holt, and L. Jennings. 2016. Behavior and Movements of Adult Spring Chinook Salmon (*Oncorhynchus tshawytscha)* in the Chehalis River Basin, Southwestern Washington, 2015. U.S. Geological Survey Open-File Report 2016-1158, 57 p., http://dx.doi.org/10.3133/ofr20161158.

Lisle, T. E. 1982. Effects of aggradation and degradation on riffle-pool morphology in natural gravel channels, northwestern California. Water Resources Research 18:1643-1651.

Lonsdorf, E. V., W. E. Thogmartin, S. Jacobi, K. Aagaard, J. Coppen, E. Davis, T. Fox, P. Heglund, R. Johnson, M. T. Jones, K. Kenow, J. E. Lyons, K. Luke, S. Still, B. Tavernia. 2016. A generalizable energetics-based model of avian migration to facilitate continental-scale waterbird conservation. Ecological Applications 26:1136-1153.

Madej, M. A. 2001. Erosion and sediment delivery following removal of forest roads. Earth Surface Processes and Landforms 26:175-190.

Madej, M. A., and V. Ozaki. 1996. Channel response to sediment wave propagation and movement, Redwood Creek, California, USA. Earth Surface Processes and Landforms 21:911-927.

Martens, K. D., and P. J. Connolly. 2014. Juvenile anadromous salmonids production in upper Columbia River side channels with different levels of hydrological connection. Transactions of the American Fisheries Society 143(3):757-767.

Mauger, G., S. Lee, C. Bandaragoda, Y. Serra, and J. Won. 2016. Effect of Climate Change on the Hydrology of the Chehalis Basin. Climate Impacts Group, University of Washington, Seattle, WA. 53 pp.

McCarthy, S. G., J. P. Incardona, and N. L. Scholz. 2008. Coastal storms, toxic runoff, and the sustainable conversation of fish and fisheries. American Fisheries Society Symposium 64, Bethesda, MD.

McCarthy, M. A., M. A. Burgman, and S. Ferson. 1995. Sensitivity analysis for models of population viability. Biological Conservation 73:93-100.

McCullough, D. A. 1999. A review and synthesis of effects of alterations to the water temperature regime on freshwater life stages of salmonids, with special reference to Chinook salmon. Report number EPA 910-R-99-010, U.S. Environmental Protection Agency, Seattle, Washington.

McCullough, D., S. Spalding, D. Sturdevant, and M. Hicks. 2001. Summary of technical literature examining the physiological effects of temperature on salmonids. *US* Environmental Protection Agency Report USEPA-910-D-01-005 Issue paper 5.

McDade, M. H., F. J. Swanson, W. A. McKee, J. F. Franklin, and J. Van Sickle. 1990. Source distances for coarse woody debris entering small streams in western Oregon and Washington. Canadian Journal of Forest Research 20:326-330.

McHenry, M. L., E. Schott, R. H. Conrad, and G. B. Grette. 1998. Changes in the quantity and characteristics of large woody debris in streams of the Olympic Peninsula, Washington, U.S.A. (1982–1993). Canadian Journal of Fisheries and Aquatic Sciences 55:1395–1407.

McHugh, P. A., W. C. Saunders, N. Bouwes, C. E. Wall, S. Bangen, J. M. Wheaton, M. Nahorniak, J. R. Ruzycki, I. A. Tattam, and C. E. Jordan. 2017. Linking models across scales to assess the viability and restoration potential of threatened population of steelhead (*Oncorhynchus mykiss*) in the Middle Fork John Day River, Oregon, USA. Ecological Modelling 355:24-38.

Mobrand Biometrics, Inc. 2003. Assessment of Salmon and Steelhead Performance in the Chehalis River Basin in Relation to Habitat Conditions and Strategic Priorities for Conservation and Recovery Actions. Mobrand Biometrics, Inc. Vashon, WA.

Montgomery, D. R., T. B. Abbe, J. M. Buffington, N. P. Peterson, K. M. Schmidt, and J. D. Stock, 1996. Distribution of bedrock and alluvial channels in forested mountain drainage basins. Nature 381:587-589.

Montgomery, D. R., E. M. Beamer, G. R. Pess, and T. P. Quinn. 1999. Channel type and salmonid spawning distribution and abundance. Canadian Journal of Fisheries and Aquatic Sciences 56:377-387.

Montgomery, D. R., J. M. Buffington, R. D. Smith, K. M. Schmidt, and G. Pess. 1995. Pool spacing in forest channels. Water Resources Research 31:1097-1105.

Moore, R., D. Spittlehouse and A. Story. 2005. Riparian microclimate and stream temperature response to forest harvesting: a review. Journal of the American Water

Resources Association 41:813-834. https://doi.org/10.1111/j.1752-1688.2005.tb03772.x

Moore, M. E., F. A. Goetz, D. M. Van Doornik, E. P. Tezak, T. P. Quinn, Reyes-Tomassini, J. J., and B. A. Berejikian. 2010. Correction: Early Marine Migration Patterns of Wild Coastal Cutthroat Trout (*Oncorhynchus clarki clarki*), Steelhead Trout (*Oncorhynchus mykiss*), and Their Hybrids. PLOS ONE 5(10). doi: 10.1371/annotation/89faa149-4569-4b03-a073-9ac3aeed86cd

Mortensen, J., and J. M. Reed. 2016. Population viability and vital rate sensitivity of an endangered avian cooperative breeder, the White-Breasted Thrasher (*Ramphocinclus brachyurus*). PLoS ONE 11(2): e0148928. doi:10.1371/journal.pone.0148928

Moussalli, E., and R. Hilborn. 1986. Optimal stock size and harvest rate in multistage life history models. Canadian Journal of Fisheries and Aquatic Sciences 43:135-141.

Munger, T. T. 1940. The cycle from Douglas fir to hemlock. Ecology 21:451-459.

Myers, J. M., R. G. Kope, G. J. Bryant, D. Teel, L. J. Lierheimer, T. C. Wainwright, W. S. Grant, F. W. Waknitz, K. Neely, S. T. Lindley, and R. S. Waples. 1998. Status Review of Chinook Salmon (*Oncorhynchus tshawytscha*) from Washington, Oregon, California, and Idaho. NOAA Technical Memorandum NMFS-NWFSC-35. NOAA-NMFS, Seattle, WA.

Naiman, R. J., H. Decamps, and M. E. McClain. 2010a. Riparia: Ecology, Conservation, and Management of Streamside Communities. Academic Press.

Naiman, R. J., J. S. Bechtold, T. Beechie, J. J. Latterell, and R. Van Pelt. 2010b. A process-based view of floodplain forest dynamics in coastal river valleys of the Pacific Northwest. Ecosystems 13:1-31.

Nelson, A., and K. Dube. 2015. Channel response to an extreme flood and sediment pulse in a mixed bedrock and gravel bed river. Earth Surface Processes and Landforms 1-18. DOI: 10.1002/esp.3843

Nickelson, T. E. 1998. A Habitat-based Assessment of Coho Salmon Production Potential and Spawner Escapement Needs for Oregon Coastal Streams. Oregon Department of Fish and Wildlife, Information Reports Number 98-4, Portland, OR.

Ogston, L., S. Gidora, M. Foy, and J. Rosenfeld. 2014. Watershed-scale effectiveness of floodplain habitat restoration for juvenile coho salmon in the Chilliwack River, British Columbia. Canadian Journal of Fisheries and Aquatic Sciences 72: 479–490. dx.doi.org/10.1139/cjfas-2014-0189.

Orcutt , D. R., B. R. Pulliam, and A. Arp. 1968. Characteristics of Steelhead Trout Redds in Idaho Streams, Transactions of the American Fisheries Society, 97(1): 42-45, DOI: 10.1577/1548-8659(1968)97[42:COSTRI]2.0.CO;2.

Perry, L., L. Reynolds, T. J. Beechie, M. Collins, and P. Shafroth. 2015. Incorporating climate change predictions into riparian restoration and design. Ecohydrology 8:863-879.

Pollock, M. M., G. R. Pess, T. J. Beechie, and D. R. Montgomery. 2004. The importance of beaver ponds to coho salmon production in the Stillaguamish River basin, Washington, USA. North American Journal of Fisheries Management 24:749-760.

Pollock, M. M., M. Heim, and D. Werner. 2003. Hydrologic and geomorphic effects of beaver dams and their influence on fishes. American Fisheries Society Symposium 37:213-233

Poole G. C., S. J. O'Daniel, K. L. Jones, W. W. Woessner, E. S. Bernhardt, A. M. Helton, J. A. Stanford, B. R. Boer, and T. J. Beechie. 2008. Hydrologic spiraling: the role of multiple interactive flow paths in stream ecosystems. River Research and Applications 24:1018-1031.

Quinn, T. P. 2005. The Behavior and Ecology of Pacific Salmon and Trout. American Fisheries Society, Bethesda, Maryland.

Quinn, T. P., and N. P. Peterson. 1996. The influence of habitat complexity and fish size on over-winter survival and growth of individually marked juvenile coho salmon (*Oncorhynchus kisutch*) in Big Beef Creek, Washington. Canadian Journal of Fisheries and Aquatic Sciences 53:1555-1564.

R Core Team. 2015. R: A Language and Environment for Statistical Computing. R Foundation for Statistical Computing. Vienna, Austria. https://www.R-project.org

R2 Resource Consultants, Inc. 2008. Snohomish Basin steelhead Trout (*Oncorhynchus mykiss*) "State of the Knowledge", Technical Memorandum. Redmond, WA.

Reeves, G., F. Everest, and T. Nickelson. 1989. Identification of physical habitats limiting the production of coho salmon in western Oregon and Washington. U.S. Forest Service General Technical Report PNW-GTR-245, Portland, Oregon.

Reid, L. M., and T. Dunne. 1984. Sediment production from forest road surfaces. Water Resources Research 20:1753-1761.

Rice, C., J. Chamberlin, J. Hall, T. Zackey, J. Schilling, J. Kubo, .M. Rustay, F. Leonetti, and G. Guntenspergen. 2014. Monitoring ecosystem response to restoration and climate change in the Snohomish River estuary. Report to the Tulalip Tribes.

Richter, B. D., J. V. Baumgartner, D. P. Braun, and J. Powell. 1998. A spatial assessment of hydrologic alteration within a river network. Regulated Rivers: Research and Management 14:329-340.

Richter, B. D., J. V. Baumgartner, R. Wigington, and D. P. Braun. 1997. How much water does a river need? Freshwater Biology 37:231-249.

Ricker, W.E. 1976. Review of the rate of growth and mortality of Pacific salmon in salt water, and noncatch mortality caused by fishing. Journal of the Fisheries Board of Canada 33:1483-1524.

Rieman, B. E., and J. B. Dunham. 2000. Metapopulations and salmonids: a synthesis of life history patterns and empirical observations. Ecology of Freshwater Fish 9:51-64.

Roni, P., P. J. Anders, T. J. Beechie, and D. J. Kaplowe. 2017. Review of tools for identifying, planning, and implementing habitat restoration for Pacific salmon and steelhead. North American Journal of Fisheries Management. DOI: 10.1002/nafm.10035

Rosenberg, A. A., and V. R. Restrepo. 1994. Uncertainty and risk evaluation in stock assessment advice for U.S. marine fisheries. Canadian Journal of Fisheries and Aquatic Sciences 51:2715-2720

Rot, B. W., R. J. Naiman, and R. E. Bilby. 2000. Stream channel configuration, landform, and riparian forest structure in the Cascade Mountains, Washington. Canadian Journal of Fisheries and Aquatic Sciences 57:699-707. DOI: 10.1139/f00-002.

Rutherford, J. C., S. Blackett, C. Blackett, L. Saito and R. J. Davies-Colley. 1997. Predicting the effects of shade on water temperature in small streams. New Zealand Journal of Marine and Freshwater Research 31:707-721. https://doi.org/10.1080/00288330.1997.9516801

Salo, E. O., and W. H. Bayliff. 1958. Artificial and natural production of silver salmon (*Oncorhynchus kisutch*) at Minter Creek, Washington. Research Bulletin of the Washington Department of Fisheries 4:76 p.

Sandell, T., Fletcher, A. McAninch, and M. Wait. 2014. Grays Harbor juvenile fish use assessment: 2013 Annual Report. Wild Fish Conservancy,

Sarikhan, I., K. Stanton, T. Contreras, M. Polenz, J. Powell, T. Walsh, and R. Logan. 2008. Landslide Reconnaissance Following the Storm Event of December 1-3, 2007, in Western Washington. Washington Division of Geology and Earth Resources Open File Report 2008-5. Olympia, Washington.

Scheuerell, M. D., R. Hilborn, M. H. Ruckelshaus, K. K. Bartz, K. M. Lagueux, A. D. Hass, and K. Rawson. 2006. The Shiraz model: a tool for incorporating anthropogenic effects and fish-habitat relationships in conservation planning. Canadian Journal of Fisheries and Aquatic Sciences 63:1596–1607.

Seedang, S., A. G. Fernald, R. M. Adams, and D. H. Landers. 2008. Economic analysis of water temperature reduction practices in a larger river floodplain: and exploratory study of the Willamette River, Oregon. River Research and Applications 24:941-959.

Seixas, G. B., T. J. Beechie, C. Fogel, and P. M. Kiffney. 2018. Historical and Future Stream Temperature Change Predicted by a Lidar-Based Assessment of Riparian Condition and Channel Width. Journal of the American Water Resources Association 1–18. https://doi.org/10.1111/1752-1688.12655.

Simenstad, C., and D. Eggers 1981. Juvenile salmonid and baitfish distribution, abundance, and prey resources in selected areas of Grays Harbor, Washington. Grays Harbor and Chehalis River improvements to navigation environmental studies. U.S. Army Corps of Engineers, Seattle, WA.

Steel, E. A., M. C. Liermann, P. McElhaney, N. L. Scholtz, and A. C. Cullen. 2003. Managing uncertainty in habitat recovery planning. Pages 137-156 *in* T. J. Beechie, E. A. Steel, P. R. Roni, and E. Quimby, editors. Ecosystem Recovery Planning for Listed Salmon: an Integrated Assessment Approach for Salmon Habitat. U.S. Dept. Commer. NOAA Tech. Memo. NMFS-NWFSC-58.

Stober, Q. J., C. R. Steward, and F. Winchell. 1983. Tolt River Fisheries and Instream Flow Analysis. University of Washington, School of Fisheries, Fisheries Research Institute. Seattle, WA.

Storlie, C. B., L. P. Swiler, J. C. Helton, and C. J. Sallaberry. 2009. Implementation and evaluation of nonparametric regression procedures for sensitivity analysis of

computationally demanding models. Reliability Engineering & System Safety 94:1735-1763.

Story, A., R. Moore, and J. Macdonald. 2003. Stream Temperatures in Two Shaded Reaches Below Cutblocks and Logging Roads: Downstream Cooling Linked to Subsurface Hydrology. Canadian Journal of Forest Research 33: 1383–96. https://doi.org/10.1139/x03-087.

Sullivan, K., J. Tooley, K. Doughty, J. E. Caldwell and P. Knudsen, 1990. Evaluation of prediction models and characterization of stream temperature regimes, Washington Department of Natural Resources Timber/Fish/Wildlife Report TFW-WQ3-90-006, Olympia, WA.

The Nature Conservancy. 2009. Indicators of Hydrologic Alteration Version 7.1 User's Manual, Arlington, Virginia, USA.

Turner, T. R., S. D. Duke, B. R. Fransen, M. L. Reiter, A. J. Kroll, J. W. Ward, J. L. Bach, T. E. Justice, and R. E. Bilby. 2010. Landslide densities associated with rainfall, stand age, and topography on forested landscapes, southwestern Washington, USA. Forest Ecology and Management 259:2233–2247. DOI:10.1016/j.foreco.2010.01.051.

Van Glubt, S. 2017. Hydrodynamic and Water Quality Modeling of the Chehalis River Using CE-QUAL-W2. Dissertations and Theses. Paper 3486. Portland State University, Portland, OR.

Van Pelt, R., T. C. O'Keefe, J. J. Latterell, and R. J. Naiman. 2006. Structural development and stand evolution of riparian forests along the Queets River, Washington. Ecological Monographs 76:277-298.

Van Sickle, J., and S. V. Gregory. 1990. Modeling inputs of large woody debris to streams from falling trees. Canadian Journal of Forest Research 20:1593-1601.

Wampler, P. L., E. E. Knudson, M. Hudson, and T. A. Young. 1993. Chehalis River Basin Fishery Resources: Salmon and steelhead stream habitat degradations. U.S. Fish and Wildlife Service, Olympia, WA.

Weitkamp, L. A., T. C. Wainwright, G. J. Bryant, G. B. Milner, D. J. Teel, R. G. Kope, and R. S. Waples. 1995. Status review of coho salmon from Washington, Oregon, and California. U.S. Department of Commerce, NOAA Technical Memorandum NMFS-NWFSC-24.

Winkowski, J., E. Walther, and M. Zimmerman. 2018. Summer Riverscape Patterns of Fish, Habitat, and Temperature in Sub Basins of the Chehalis River, 2013-2016, FPT 18-01. Washington Department of Fish and Wildlife, Olympia, Washington. https://wdfw.wa.gov/publications/01999/.

Winkowski, J., and M. S. Zimmerman. 2019. Chehalis River Smolt Production, 2018, FPA 19-01. Washington Department of Fish and Wildlife, Olympia, WA.

Winter, B. D. 1992. Determinate Migratory Behavior of Steelhead (Oncorhynchus mykiss) Parr. Ph.D. Dissertation, University of Washington, Seattle, WA.

Zabel, R. W., M. D. Scheuerell, M. M. McClure, and J. G. Williams. 2006. The interplay between climate variability and density dependence in the population viability of Chinook salmon. Conservation Biology 20:190-200.

Zabel, R. and numerous co-authors. 2015. Life-Cycle models of salmonid populations in the interior Columbia River Basin. Northwest Fisheries Science Center draft report.

Zimmerman, M. S. 2018. 2018 Wild Coho Forecasts for Puget Sound, Washington Coast, and Lower Columbia., Washington Department of Fish and Wildlife, Olympia, Washington, https://wdfw.wa.gov/publications/ 01962.

Zwieniecki, M. A., and M. Newton, 1999. Influence of streamside cover and stream features on temperature trends in forested streams of western Oregon. Western Journal of Applied Forestry 14:106-113. https://doi.org/10.1093/wjaf/14.2.106.

Appendix A. Riparian Assessment

Two important influences of riparian forests on stream habitat are (1) shading to regulate water temperature and (2) wood recruitment to structure physical habitat (Naiman et al. 2010a). The riparian analysis evaluates changes in these functions by comparing current riparian conditions (tree height, canopy opening angle, buffer width, etc.) to a historical or reference condition. We assess current conditions using lidar tree height data where available, and using aerial photography where lidar data were unavailable. We estimate historical conditions using separate reference conditions for confined channels and floodplain channels.

A.1 Riparian Reference Condition

For reference conditions (e.g., the natural potential tree height), we stratified the basin into floodplain channels with varying rates of lateral channel migration and floodplain turnover, and non-floodplain channels with stable riparian landforms (terraces or hill slopes) (Figure A.1). Channels without floodplains are typically dominated by upland forest types in western Washington (Beechie et al. 2000, Rot et al. 2000), and most riparian areas in the Chehalis River basin are in the western hemlock zone or Sitka spruce zone (Franklin and Dyrness 1973). In the western hemlock zone, the main successional pathway is Douglas-fir colonization after fire, Douglas-fir dominance during the first 200 to 300 years, and succession to western hemlock as the stand ages beyond 300 years (Munger 1940, Franklin and Dyrness 1973). The Sitka spruce zone can be considered a sub-zone of the western hemlock zone (Franklin and Dyrness 1973), and successional pathways are similar with the exception that some disturbed areas may be recolonized by red alder and only very slowly succeed to Sitka spruce or dense shrub communities (Franklin and Dyrness 1973). Because the average time between forest fires (referred to as the fire return interval) in these forests is between 180 and 230 years (Agee 1993), much of the study area was dominated by Douglas-fir since stands often burned before western hemlock or Sitka spruce became the dominant species. Regional forest inventories in Western Washington prior to widespread logging indicate that forests consisted of 64% fir, 16% cedar, 14% hemlock and 6% spruce (Gannett 1899).

Floodplain channels have floodplains >4 times the width of the main channel (main channels are usually >15 m wide and floodplains are typically hundreds of meters wide), and multiple side channels may flow across the floodplain (Beechie et al. 2006b, Latterell et al. 2006). Because these channels constantly erode floodplain surfaces at one location and create new ones at other locations, the riparian forest consists of many small stands of varying ages and species compositions (Figure A.1). The common successional pathway begins with red alder or black cottonwood establishment and gradually succeeds to western red cedar, Sitka spruce, and western hemlock (Agee 1988, Van Pelt et al. 2006). The average length of time a floodplain surface persists before being eroded again by the river (termed the erosion return interval) ranges from 8 to 89 years, depending on channel pattern and rate of lateral channel migration (Beechie et al. 2006b). These erosion return intervals are considerably shorter than fire return intervals on the uplands, and the relative
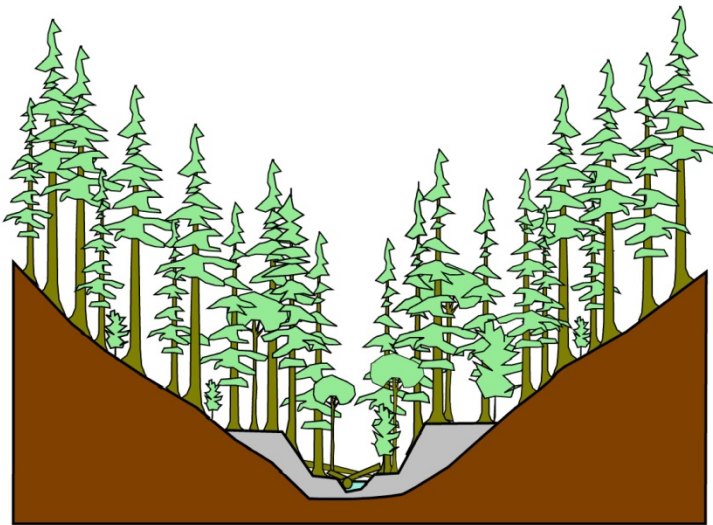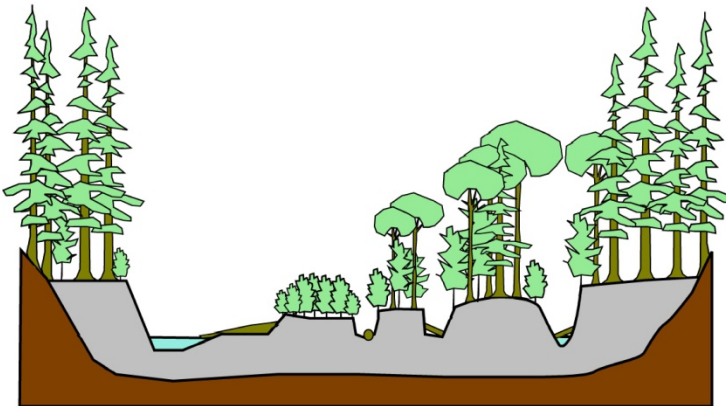
Figure A.1. Illustration of the two main physical settings for riparian forests in the study area, and their typical riparian forest structures. Primary disturbance processes and return intervals are indicated adjacent to each illustration.

constancy of erosion rates through time produces distinct, stable patch age structures that persist for decades (Latterell et al. 2006, Naiman et al. 2010b). Large trees recruited from the floodplain into the channel contribute to the formation of stable log jams and islands, which often persist long enough to allow old growth forests to develop on a portion of the valley floor (Abbe and Montgomery 2003, Latterell and Naiman 2007).

In both floodplain and non-floodplain riparian forests, the fire and erosion disturbance regimes would have created a wide range of riparian forest ages (Beechie et al. 2000, 2006b). We reviewed the literature on riparian disturbance regimes and estimated the proportion of the landscape that would have been in various age classes, as well as the tree species composition expected in each environment (Figure A.2). Based on the review, we assumed mature dense conifer with a site potential tree height of 170 feet (52 m) for the historical condition along streams <20 m wide. For comparison, in a prior study we found that average tree height in unlogged forests was approximately 50 m based on descriptions

in Gannett (1899), and average tree height at six present-day old-growth sites in the Stillaguamish River basin was 48 m (M. Pollock, unpublished data). For mixed forests along larger channels (streams > 20 m wide), we used a typical tree height for mature hardwoods (30 m). For comparison, the weighted average height of species found on Stillaguamish River floodplains were 29 m and 34 m for the mainstem and the North Fork, respectively (B. Collins, unpublished data).
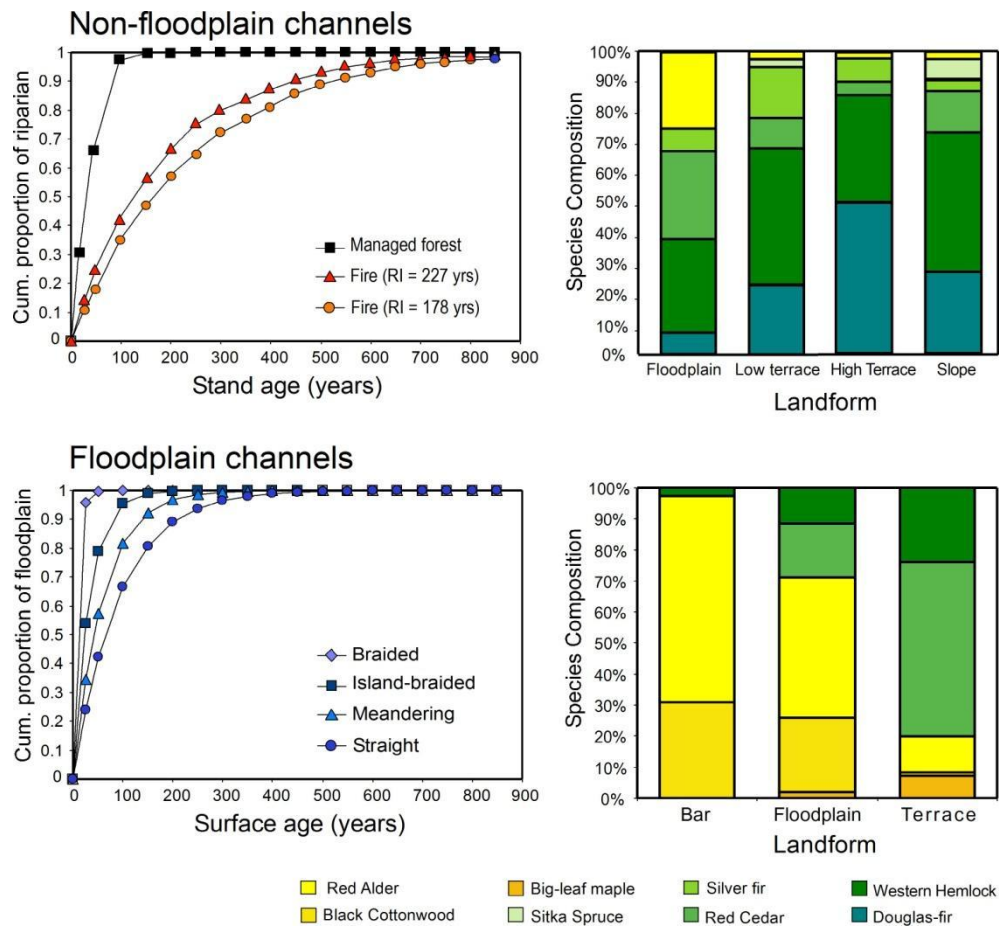
Figure A.2. Summary of reference conditions for non-floodplain and floodplain channels (upper and lower panels, respectively). For non-floodplain channels, the left panel shows cumulative stand age distribution under modeled fire return intervals of 178 and 227 years compared that of current managed forests (fire return intervals from Beechie 1998, and current managed forest ages are from the Continuous Vegetation Survey (CVS) database for western Washington). The upper right panel shows species composition by landform (Rot et al. 2000). For floodplain channels, the lower left panel shows modeled cumulative floodplain surface age distributions by channel type (based on erosion return intervals in Beechie et al. 2006b). The lower right panel shows species composition by landform (data from Van Pelt et al. 2006 and Beechie unpublished data).

A.2 Methods

We mapped current riparian tree heights and buffer widths in the Chehalis River basin using lidar and aerial photography, and used those data to estimate current riparian shade and wood recruitment potential. We then used the reference conditions described above to estimate historical conditions for riparian shade and wood recruitment potential. In the following sections, we describe the riparian measurements and calculation of canopy opening angle, stream temperature change, and wood recruitment potential.

A.2.1 Stream Shade Assessment

To estimate stream temperature changes due to past riparian logging, we identified and mapped canopy opening angle changes between the mid-1800s (prior to widespread logging, agriculture, and development) and the present. We calculated the canopy opening angle (θ) based on channel width (W) and average riparian tree height (z) (Figure A.3):

$$\theta = \left(90 - \left(\frac{z_L}{\frac{W}{2}} \right) \right) + \left(90 - \left(\frac{z_R}{\frac{W}{2}} \right) \right)$$

where z_L and z_R are tree height plus bank height on each side of the channel, and $W/2$ is the horizontal distance from the channel center to the first tree. The inverse tangent functions are subtracted from 90°, so a channel with complete canopy closure will have $\theta = 0°$ and a channel with no vegetation on either bank will have $\theta = 180°$.
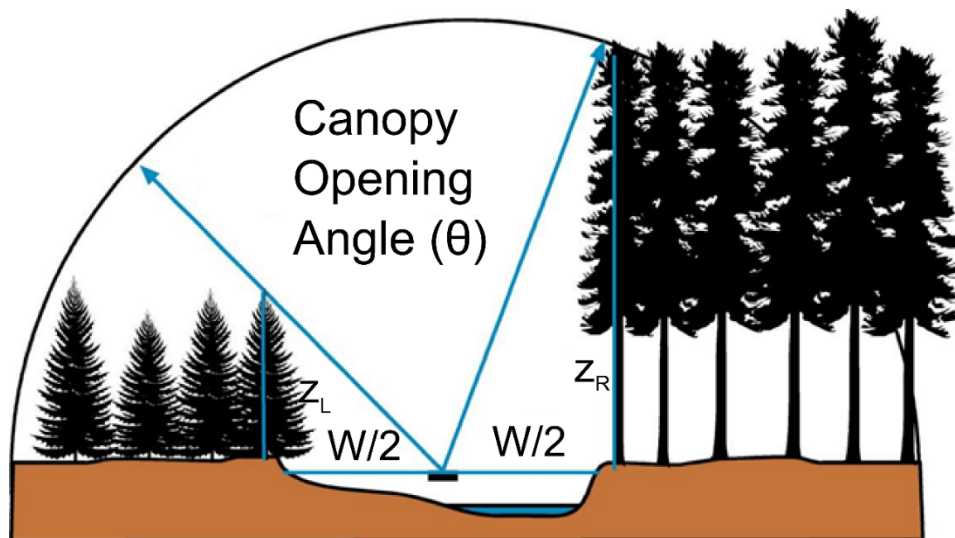
Figure A.3. Illustration of canopy opening angle and the parameters used to calculate it. Left bank tree height and right bank tree height are z_L and z_R, respectively, and W is bankfull channel width. See text for details of the calculation.

Lidar-based riparian assessment

We downloaded all available lidar digital elevation model data in the Chehalis river basin from the Puget Sound Lidar Consortium (pugetsoundLIDAR.ess.washington.edu). The datasets included Lewis County acquisitions from 2003, 2005, and 2006, Chehalis River (Lewis and Grays Harbor Counties) from 2012, Southwest Washington (Pacific and Grays Harbor Counties) from 2009, a portion of the Puget Sound Lowlands supermosaic covering Mason County (2002), and the Thurston County acquisition from 2011. With the exception of the Thurston County dataset, the lidar point clouds for these regions have been preprocessed into ESRI file geodatabase format by the Consortium for convenient download and use. We downloaded the Thurston County point clouds in the native LAS format and processed the data for first returns and bare earth gridded rasters using the ArcGIS module in Python (Arcpy).

We automated the workflow for processing DEMs using Arcpy as follows. We first projected each raster into the Universal Transverse Mercator projection (zone 10N), and then clipped each dataset into tiles for more efficient processing. Next, we processed each bare earth tile using the ArcGIS Fill algorithm, and calculated the flow direction (FD) grid using the filled bare earth DEM and a D8 flow routing scheme. Finally, we exported ASCII text files of the top surface DEM, the original bare earth DEM, the filled bare earth DEM, and the FD grid. We read the text files into Matlab using the function ReadArcGrid.m (T. Perron, http://web.mit.edu/perron/www/downloads.html) and created difference maps by subtracting the un-filled bare earth DEM from the top surface DEM for each tile.

We selected channel head locations manually in ArcMap by digitizing points at the farthest upstream ends of the salmon or steelhead distributions. Next, we used an algorithm developed in Matlab to measure riparian condition at 10 m intervals along the channels flowing from each channel head. The algorithm iterates through each channel head within each tile within each lidar dataset and proceeds in the following manner:

1. Search down the FD grid and extract each pixel that lies at the lowest point in the channel.
2. From these, extract transect location pixels at the transect spacing interval (300 m).
3. Find the angle perpendicular to the channel at each transect location. The algorithm accomplishes this by bisecting the angle formed between the current transect location pixel and 100 pixels upstream and downstream from the current transect location point. We decided to use ±100 pixels by visual inspection of a series of different values.
4. Using this angle, project the transect line 100 m to either side of the channel using the Bresenham line algorithm (Bresenham 1965).
5. Extract values of the difference map along the transect line for one side of the channel.
6. Find the left bank tree height (z_L) and distance from the channel point (W/2 in the equation for θ above) by searching for the first peak in the data that exceeds the threshold for shade (2 m). Repeat for the opposite bank (z_R).

7. Calculate the current canopy opening angle (θ_{curr}) using these heights and distances in the equation for θ above.
8. Calculate buffer width for shade and wood recruitment by finding the first and last peaks that exceed 20 and 120 ft, respectively. The buffer width is the distance between these points.

These data were exported into ArcGIS and cleaned to remove spurious points. Data cleaning was necessary because the flow routing search algorithm used to find the channel bottom locations (step 1 of the algorithm above) was in places diverted by roads, earthworks, or other unnatural aspects of the modern landscape. To ensure these erroneous points did not affect the final data, we manually removed points that clearly did not lie in channel bottoms. This process removed fewer than 4% of the data. These sites were later evaluated manually using the aerial photograph procedure described below.

Once we completed processing the lidar data, we then repeated the calculations with a "historical" or natural potential riparian condition (θ_{hist}). As described earlier, we assumed mature dense conifer with a site potential tree height of 170 feet (52 m) along streams <20 m wide (non-floodplain channels), and mixed hardwood-conifer forests with a typical tree height of 30 m along streams >20 m wide (floodplain channels).

Finally, the difference in canopy opening angle was calculated as:

$$\Delta\theta = \theta_{hist} - \theta_{curr}$$

We produced maps of both the historical and current canopy opening angles, as well as a map of changes in the canopy opening angle between the historical and current condition as an index of shade losses. Where the calculated change was negative—that is, at sites where current tree height is taller than the reference tree height—we considered the change to be zero (3.5% of sites).

Where there are no trees present, the total current canopy opening width is 200 m (the maximum allowed by the algorithm), the tree heights are 0 m, and thus the canopy opening angle is equal to 180°. However, the canopy opening width for the historical condition is undefined because W is undefined. Therefore, for transects in which no vegetation is found for the current condition we used the modeled bankfull width for the historical canopy opening width.

Aerial-photograph-based riparian assessment

Where lidar data were unavailable, we used aerial photographs to measure riparian vegetation similarly to the lidar-based method. We used the National Elevation Dataset 10 m DEM and an algorithm based on steps 1 and 2 above to draw transect locations at 300 m intervals throughout the Chehalis basin. At each location, we measured the channel width (defined as the distance between the first and last instance of a shade-providing tree) and width of forested buffers on each side of the channel that extended out to the margins of the buffer or to 100 m, whichever came first.

To estimate tree height from aerial photography, two observers first visually classified tree size (tall, medium, short, and no vegetation) from aerial photography at 232 sites where lidar tree heights were available. The lidar tree height was then assigned to each classified point, and the distribution of tree heights were plotted to examine both observer variation and the range of tree heights contained in each classified size class (Figure A.4). Because there was generally good agreement between observers, we pooled the data for each size class and calculated the median tree height for each size class. These median tree heights were then used for estimating current canopy opening angles and wood recruitment potential.

We visually classified the left bank (z_1) and right bank (z_2) tree height class at each transect location, then used a python spatial model to calculate the current canopy opening angle (θ_{curr}) as described above for the lidar data. We also calculated the historical canopy opening angle using the assumed mature tree heights of floodplain and non-floodplain channels, and then calculated the change in canopy opening angle. Finally, we produced maps of current and historical canopy opening angle as well as changes in canopy opening from historical to current conditions across the entire basin.
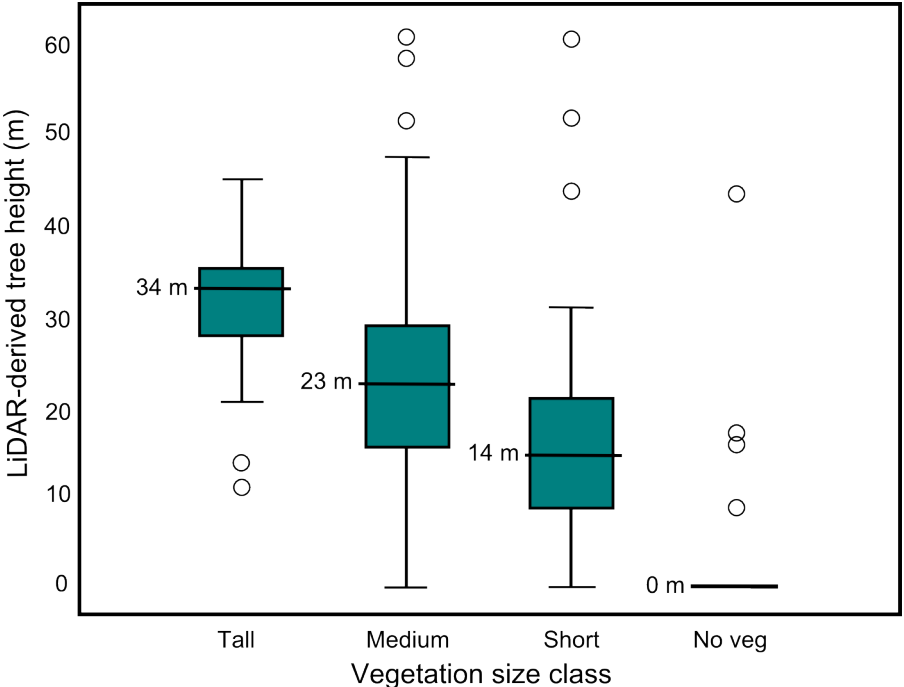
Figure A.4. Box and whiskers plots of lidar tree heights in each size class identified on aerial photography (bar is the median, box represents the 25th to 75th percentiles, whiskers represent the 10th and 90th percentiles, and circles are "outliers"). Each point represents one point at which an observer classified a tree size class on aerial photography and tree height in the lidar data set. There were two observers, and for each observer there were a total of 232 point measurements at 116 sites (one point on each side of the stream at each site), so there were a total of 464 points. Sample sizes for each size class are: Tall = 29, Medium = 307, Short = 104, and No veg = 24.

136

A.2.2 Stream Temperature Modeling

For current temperatures, we used the WDFW Chehalis Thermalscape data for tributaries to the mainstem Chehalis (J. Winkowski, unpublished data), and the Portland State University Temperature data for the mainstem Chehalis from Crim Creek to Porter Creek (Van Glubt 2017). We then used empirical tree height measurements and reference tree heights to calculate the change in canopy opening angle between historical and current conditions, and a tree growth model to calculate future canopy opening angles. Finally, we used our shade and temperature model (Seixas et al. 2018) to calculate changes in stream temperature between historical, current, and future mid-century and late-century riparian conditions.

Current Temperature

For current conditions, we use the WDFW Chehalis Thermalscape modeled estimates of current mean August temperature for tributaries to the mainstem Chehalis (J. Winkowski, unpublished data), and the Portland State University (PSU) Temperature data for the mainstem Chehalis from Crim Creek to Porter Creek (Van Glubt 2017). However, the Thermalscape model did not estimate the effect of shade on stream temperature. Therefore, we only use the Thremalscape and PSU data for current temperature, and we built an empirical temperature model to estimate the change in temperature with a change in riparian shade (Seixas et al. 2018).

The Chehalis Thermalscape and PSU data (Winkowski, unpublished data) provide the August average of daily averages (ADA) for each reach. For the NOAA model, we needed the seven-day average daily maximum (7-DADM) for coho and steelhead summer rearing and spring Chinook prespawning, and the June 1-21 average daily maximum (ADM) for spring and fall Chinook outmigration. We used measured riverscape temperatures (from WDFW) at all available sites to calculate the August ADA, the 7-DADM (n = 80), and the June 1-21 ADM (n = 43). We then regressed each metric against the August ADA so we could convert the reach-level August ADAs to each of the other three temperature metrics. The two equations are:

7-DADM = 1.02(AugADA) + 3.81, and

Jun1-21 ADM = 0.96 (AugADA) + 0.61.

We used these equations to convert the AugADA in each reach to the current temperature metrics needed for the life-cycle models.

Shade-Temperature Model

Stream water temperature is controlled by complex physical interactions between the air, water, and channel bed, as well as turbulence, tributary confluence effects, and longitudinal effects such as increasing flow volume with distance from the source (Brown 1972, Moore et al. 2005, Fullerton et al. 2015). Nonetheless, it has been well-documented that reduction or removal of riparian shade results in significant warming. Among 18 studies that employed a rigorous before-after effect size study design, Moore et al. (2005) found a

median after-treatment warming of 2.5°C, while the maximum warming was 11.6°C. Other studies show that the rate at which the temperature of a package of flowing water equilibrates with its surroundings is proportional to stream size (due to thermal inertia), and may also vary due to the riparian condition of the reaches through which it flows (Sullivan et al. 1990, Moore et al. 2005, Caissie 2006). The length of stream over which temperature equilibrates is in the range of 150 to 200 m for small streams (Zwieniecki and Newton 1999, Story et al. 2003). However, Rutherford et al. (1997) presented modeling results suggesting that first order streams could equilibrate to a 50% reduction in riparian cover ~85% faster than third order streams. Given this uncertainty, we chose to append the mean value of canopy opening angle within 300 m upstream of each NorWeST data point. This 300 m length encompasses the commonly published values but also reflects the longer recovery distance in larger channels.

Seixas et al. (2018) developed an empirical temperature model relating stream temperature to drainage area and canopy opening angle. The final temperature model from Seixas et al. 2018 is:

$$T = -9.15 + 0.035\theta + 3.00 log\ (A)$$

where T is water temperature (August 7-DADM), θ is canopy opening angle, and A is drainage area. We use this model for estimating change in temperature from current to historical or future conditions.

Historical Temperature

We modeled the historical canopy opening angle using the reference tree height, and then calculated the change in the 7-DADM from current to historical conditions for each reach using the temperature model above. Because the tree growth component modifies the 7-DADM, we empirically related the Jun1-21ADM to the 7-DADM so we could relate the change in 7-DADM to a change in Jun1-21ADM. The regression equation is:

Jun1-21 ADM = 0.98 (7-DADM) – 3.90.

Note that when calculating a *change* in any given temperature we only need the slope of the equation. Therefore, we convert the change in 7-DADM to the change in Jun1-21ADM for each reach using:

ΔJun1-21 ADM = 0.98 (Δ7-DADM).

A.2.3 Wood Recruitment Assessment

For the wood recruitment assessment, we used the tree height data from lidar and aerial photograph estimates as above, but employed different thresholds that represent the potential for trees to provide functional wood in the near term. Wood recruitment to streams is a function of tree species, tree height, and distance from stream, as well as the propensity of trees to fall toward the stream rather than away from it (e.g., Van Sickle and Gregory 1990, McDade et al. 1990). Modeled wood recruitment from our reference stands yields an estimate of the cumulative wood recruitment from the riparian forest (Figure A.5)

(Beechie et al. 2000). However, as shown by McDade et al. (1990), this simple model tends to over-estimate recruitment distances compared to field measurements. The two main factors influencing the over-estimate are that (1) many trees in the stand are smaller than the mean height, and (2) trees on hillslopes or near stream banks tend to fall toward the stream more often than away from it. Therefore, actual wood recruitment distances tend to be shorter than those predicted by the model.

Based primarily on the field data, we selected threshold buffer widths to determine whether wood recruitment was likely currently impaired, moderately impaired, or functioning. For non-floodplain, conifer riparian forests, more than 85% of total wood from mature or old-growth conifers originates from within 30 m (~100 feet) of the stream (Figure A.5). Therefore, where trees are classified as tall (>30 m), buffer widths of >30 m are considered "functioning" (Table A.1). By contrast, less than ~65% of total wood originates from within 15 m (~50 feet) of the stream, and we consider these narrower buffers "impaired". Buffers between 15 and 30 m wide are considered moderately impaired. Where trees are small or where there are no trees, wood
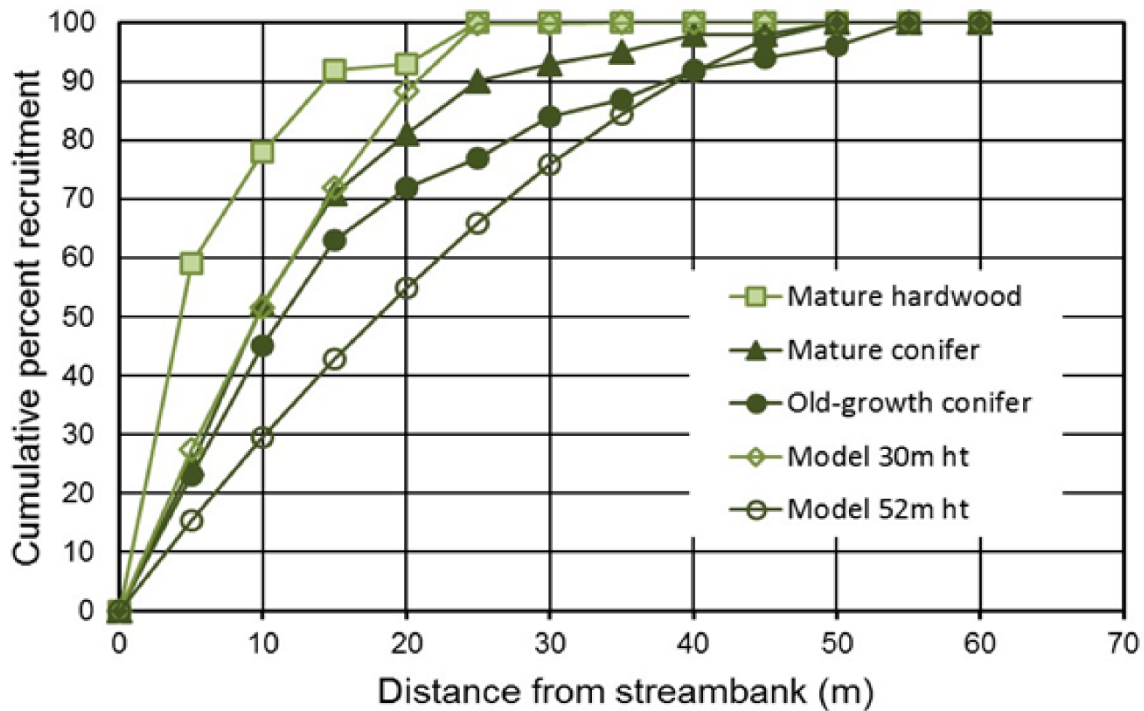
Figure A.5. Cumulative percent recruitment by stand type for field data (McDade et al. 1990) and a probability model (Van Sickle and Gregory 1990). The model 30 m height is approximately the height of mature alder (Beechie 1998) and the model 52 m height is the site potential tree height for Douglas-fir. Field data are from McDade et al. (1990).

Table A.1. Classification of wood recruitment functioning for non-floodplain channels based on tree height and buffer width. All function classes based on tree height and Figure A.5.

Tree height class	Buffer width (m)		
	<15 m	15–30 m	>30 m
Tall (33 m)	Impaired	Mod. Impaired	Functioning
Medium (23 m)	Impaired	Impaired	Mod. Impaired
Short (15 m)	Impaired	Impaired	Impaired
No vegetation (0 m)	Impaired	Impaired	Impaired

recruitment condition is rated as "impaired" regardless of buffer width. Medium height trees were rated "moderately impaired" where the buffer width was >30 m, and "impaired" where buffer width was <30 m.

For hardwood riparian forests or mixed species forests in floodplains with mean height >30 m, 70 to 90% of total wood originates from within 15 m (~50 feet) of the stream. Therefore, where trees are classified as tall ($\geq$34 m), buffer widths of >15 m are considered functioning and buffer widths < 15 m are moderately impaired (Table A.2). All riparian areas with short trees or no vegetation are considered impaired. For buffers with medium tree heights, widths <15 m are rated impaired, 15-30 m are moderately impaired, and buffers >30 m are functioning.

For mapping these functional groups, we use the average tree height and buffer width from both sides of each reach, and map the averaged wood recruitment rating. For data summaries (e.g., number of reaches in each functional group), we tally each side of the stream separately. We use the term 'riparian segment' when referring to one side of one reach.

Table A.2. Classification of wood recruitment functioning for floodplain channels based on tree height and buffer width. All function classes based on tree height and Figure A.5.

Tree height class	Buffer width (m)		
	<15 m	15–30 m	>30 m
Tall (33 m)	Mod. Impaired	Functioning	Functioning
Medium (23 m)	Impaired	Mod. Impaired	Functioning
Short (15 m)	Impaired	Impaired	Impaired
No vegetation (0 m)	Impaired	Impaired	Impaired

A.3 Results

We first present changes in stream shade, then stream temperature, and then the wood recruitment function ratings. Note that for all analyses the reference condition varies with stream size. Figure A.6 shows the distribution of stream size classes in the Chehalis River basin.
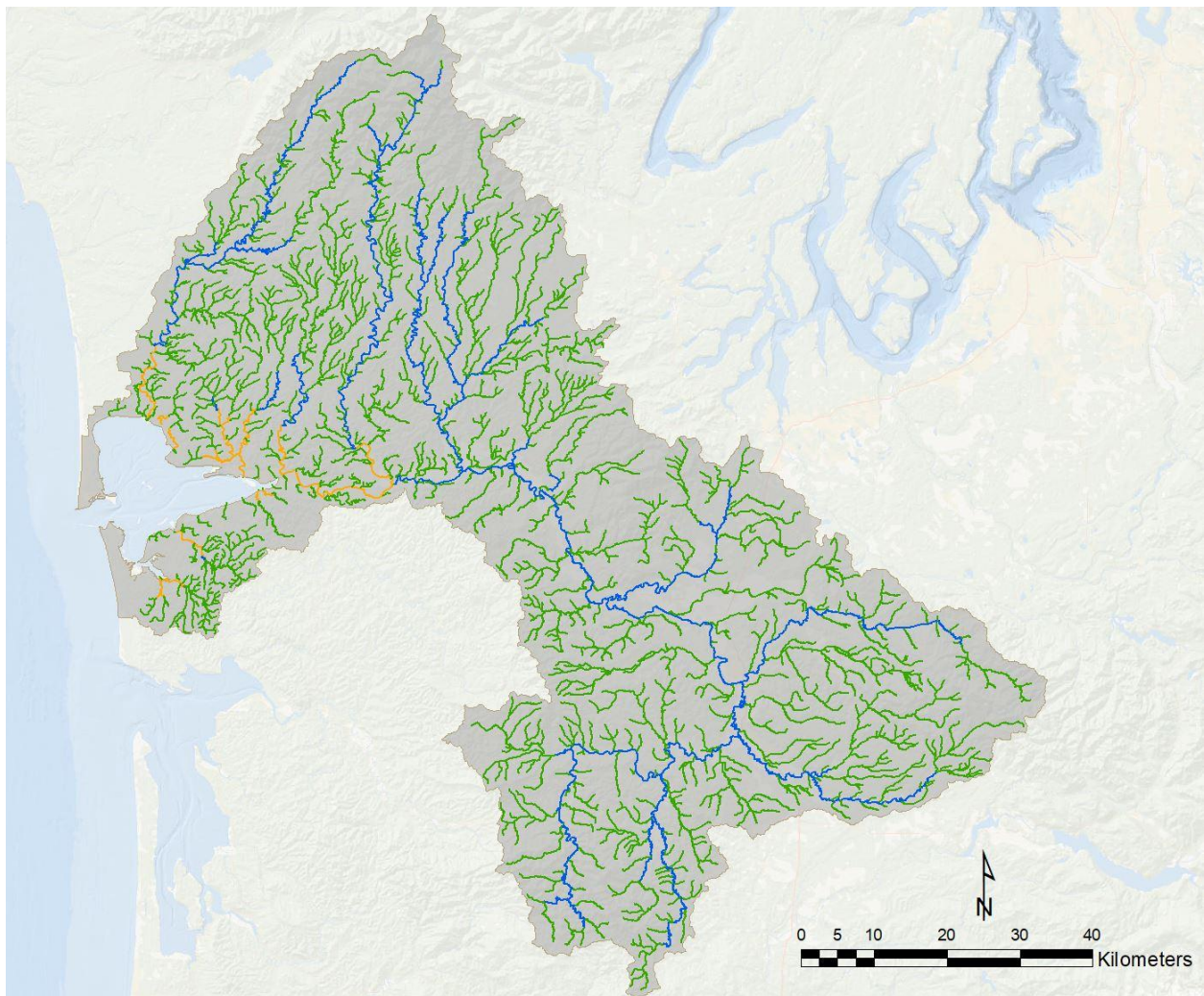
Figure A.6. Distribution of large rivers and small streams in the Chehalis River basin. The riparian reference condition for large rivers (bankfull width > 20 m) is hardwood-dominated forests typical of Pacific Northwest floodplain environments, and the reference condition for small streams (< 20 m bankfull width) is mature conifer typical of non-floodplain environments.

A.3.1 Stream Shade Change

The number of reaches in the lowest canopy opening angle class (<10°) decreased from 50% of reaches historically to 44% currently (Figure A.7). The number of reaches in the highest canopy opening angle class is four times higher than it was historically, increasing from 4% of reaches to 16%. These reaches were concentrated in the southern portion of the basin where there is more agricultural and urban land. Overall, the percentage of reaches with canopy opening angles <50° decreased, while the percentage of reaches with canopy opening angle >50° increased.
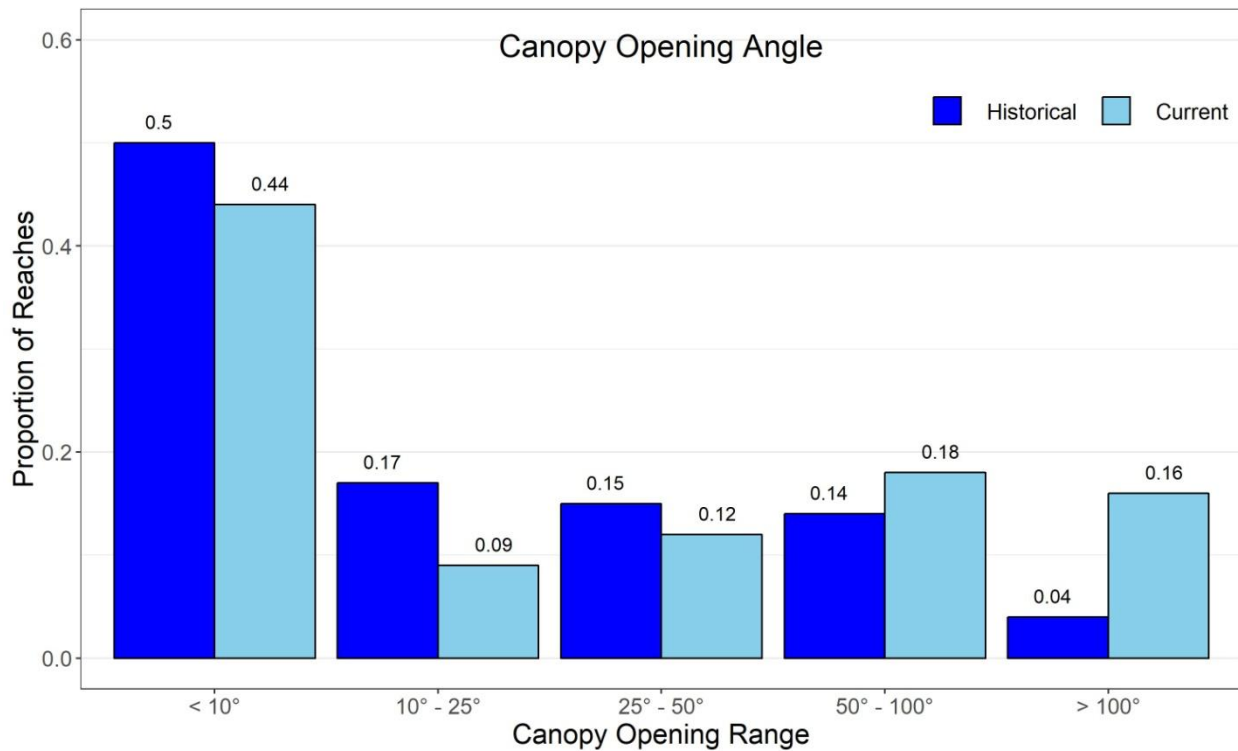
Figure A.7. Frequency distributions (proportion of total reaches) of historical and current canopy opening angles in The Chehalis River basin. Note the large increase in very wide canopy opening angles (>100°).

A.3.2 Stream Temperature Change

The upper incipient lethal temperature for most salmonids (the temperature at which 50% of fish die during a 7-day period following exposure) is ~24-26° (Brett 1952; McCullough 1999, McCullough et al. 2001). The current temperature data from WDFW and PSU indicate that many of the larger fish-bearing streams (including tributaries) of the Chehalis River basin are at or near this threshold at least during the hottest month of the year (Figure A.8). Historically, fewer reaches exceeded the critical value. It is also notable that the change in temperature from historical to current conditions is <0.5°C in much of the basin (Figure A.9).

(A) Current   **(B) Historical**
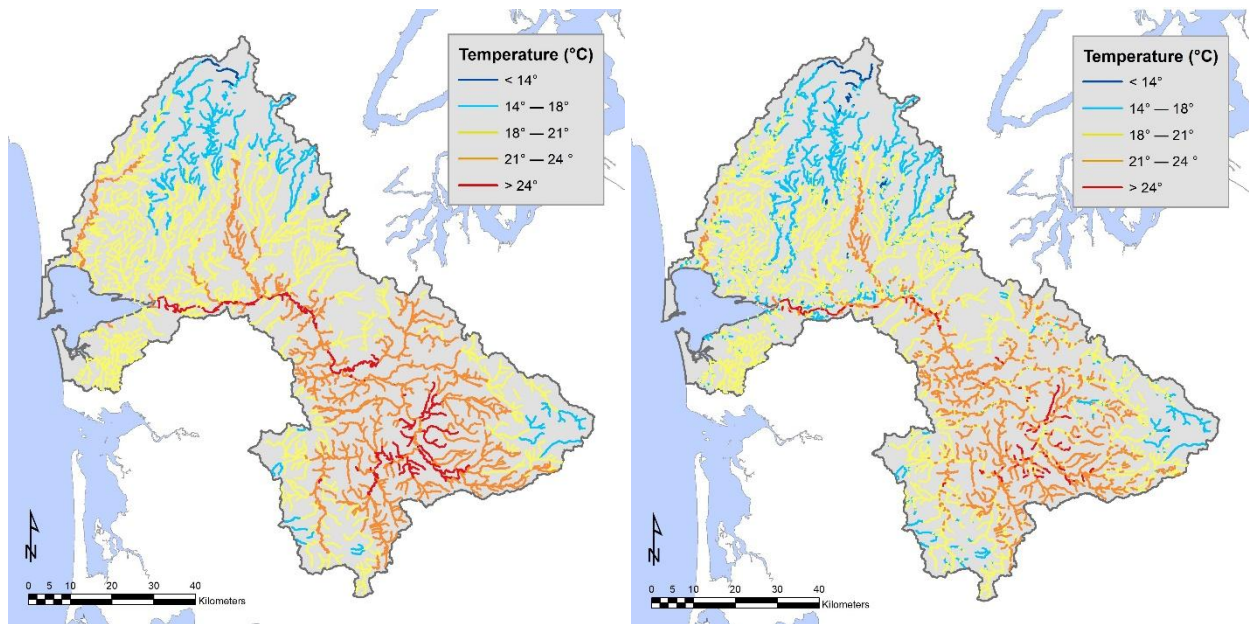
Figure A.8. Maps of modeled 7-DADM stream temperature under (A) current and (B) historical riparian conditions. Current condition is from the Chehalis Thermalscape and PSU data; historical condition is based on modeled temperature reduction from current condition using the NOAA shade model (Seixas et al. 2018).
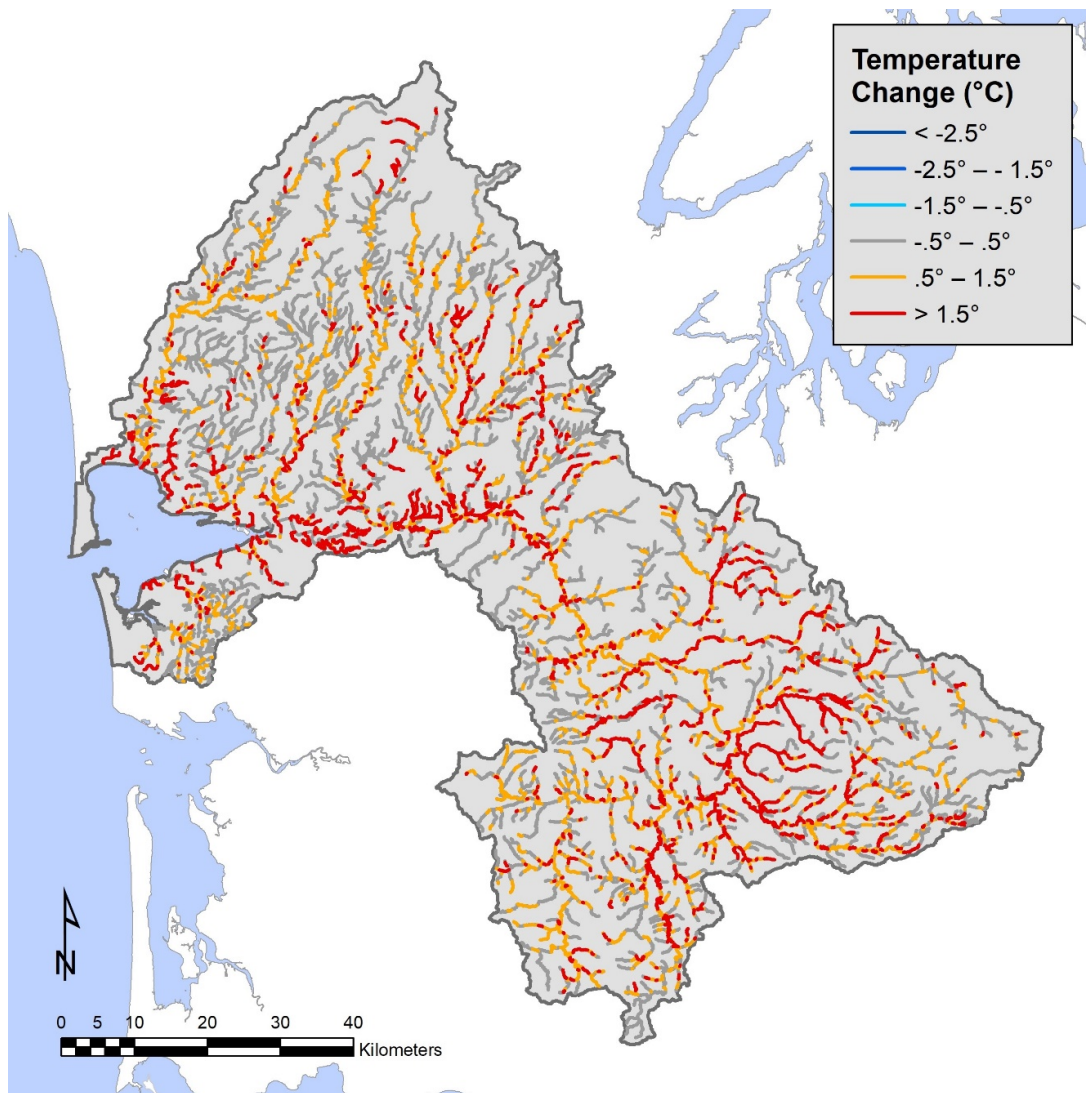
Figure A.9. Change in 7-DADM from historical to current conditions.

In the year 2045, a tree growth scenario without climate change shows areas where riparian restoration may have the largest effect on stream temperature (Figures A.10(A), A.11(A)). Notably, Figure A.11(A) shows that temperatures can be most dramatically reduced in relatively small streams where even small amounts of tree growth can dramatically reduce the canopy opening angle. When climate change is added to the model (temperature increase of 1°C by 2045), temperatures increase in much of the basin because riparian trees in much of the forested area are currently relatively tall, canopy opening angles are narrow, and additional tree growth does not significantly reduce the canopy opening angle or modeled temperature. By contrast, in areas of high restoration potential, tree growth can still reduce temperature by 2045 even with a temperature increase due to climate change. The patterns for 2085 (Figures A.12, A.13) are similar that of the 2040s, but with fewer areas achieving temperature reduction sufficient to overcome the warming due to climate change. Nonetheless, tree growth is sufficient to limit warming to less than 1.5°C in many areas.

144

(A) 2045 w/ tree growth, no climate change change

(B) 2045 w/tree growth, w/climate change
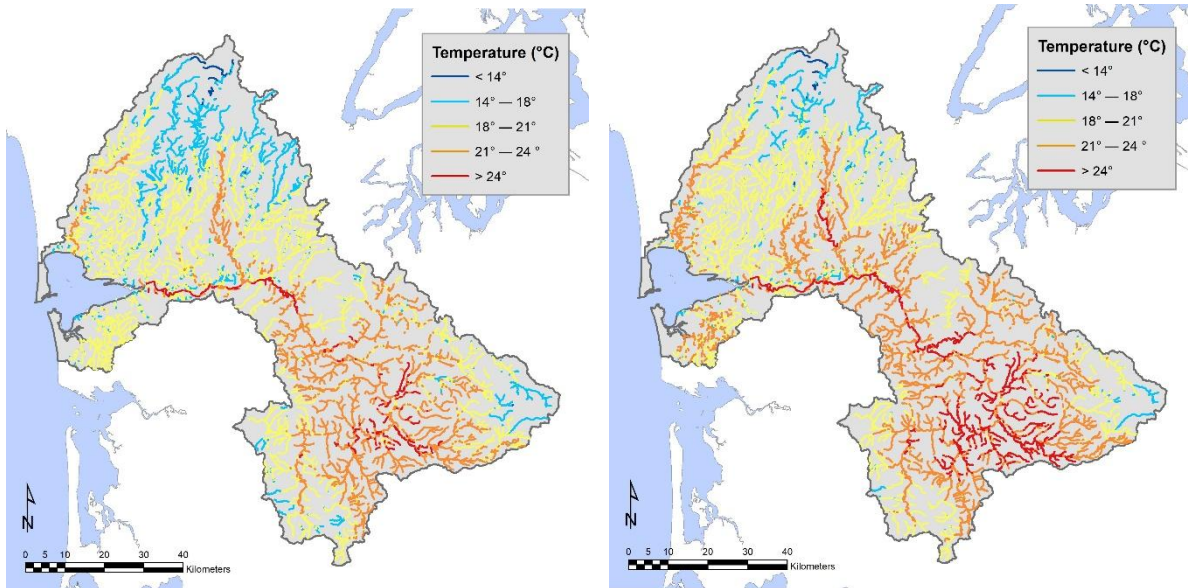
Figure A.10. Modeled 7-DADM stream temperature at 2045 (A) with tree growth from current condition but no climate change, and (B) with tree growth from current condition and with climate change.

(A) ΔT 2045, w/tree growth, no clim. chg.

(B) ΔT 2045, w/tree growth, w/clim. chg
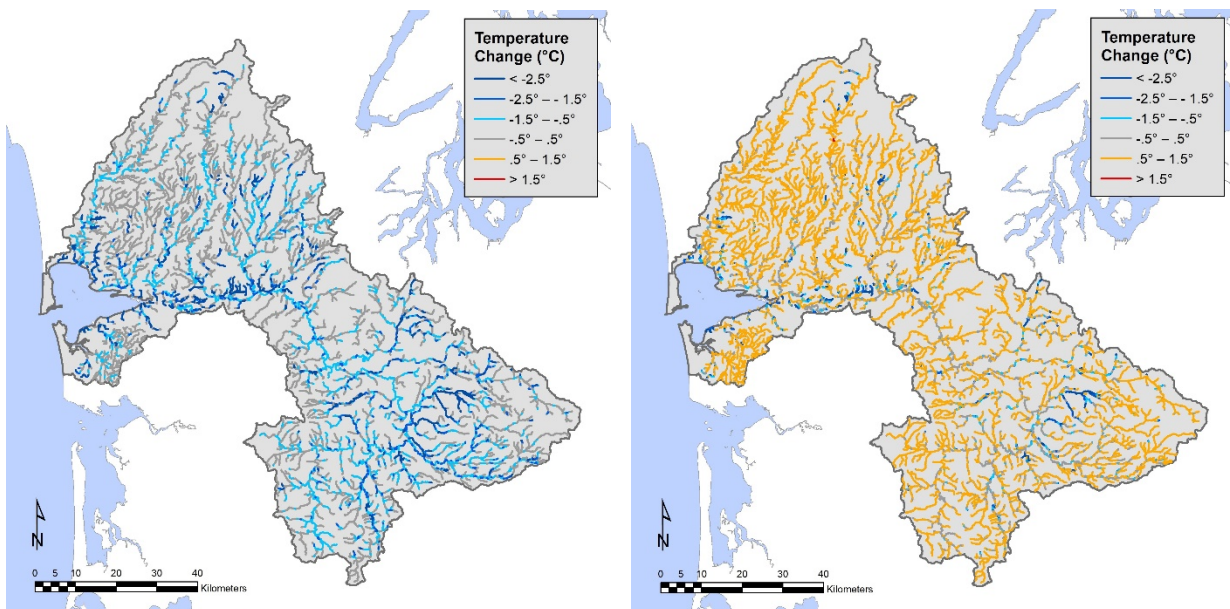
Figure A.11. Modeled change in 7-DADM stream temperature at 2045 (A) with tree growth from current condition but no climate change, (B) with tree growth from current condition and with climate change, and (C) without tree growth and with climate change. The maximum modeled increase in any reach by 2045 is +1°C.

145
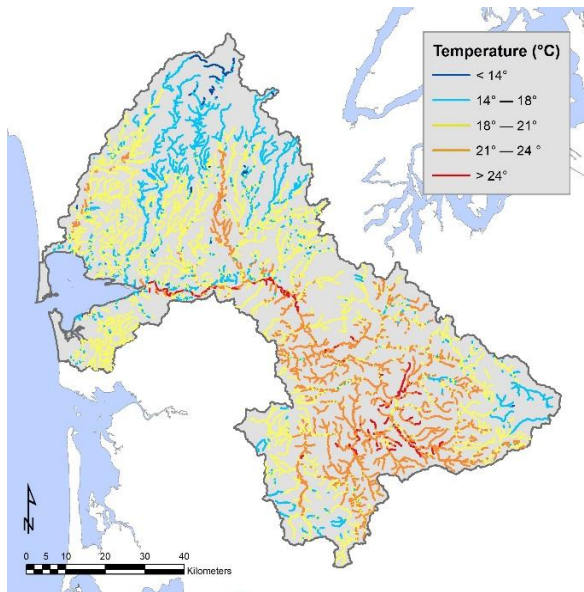
(A) 2085, w/ tree growth, no clim. chg.   **(B) 2085, w/ tree growth, w/ clim. chg.**
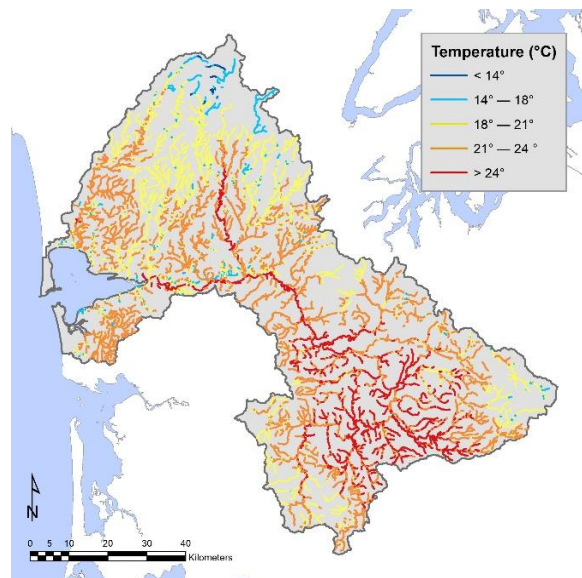
Figure A.12. Modeled 7-DADM stream temperature at 2085 (A) with tree growth from current condition but no climate change, and (B) with tree growth from current condition and with climate change.
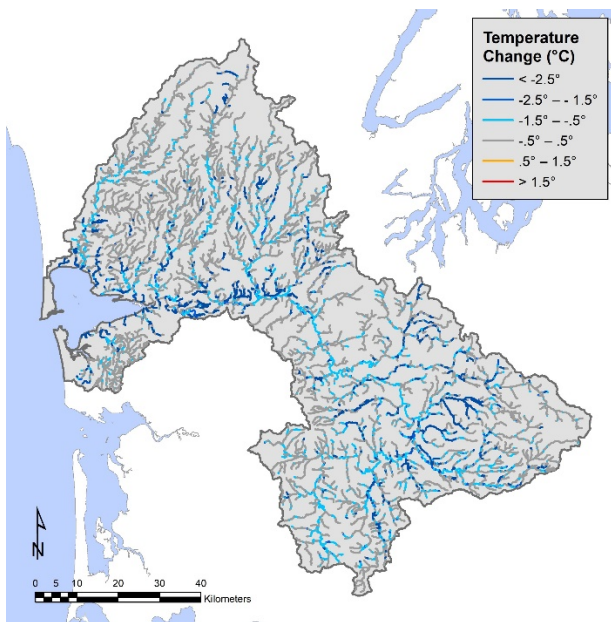
(A) ΔT 2085, w/tree growth, no clim. chg.   **(B) ΔT 2085, w/tree growth, w/clim. chg**
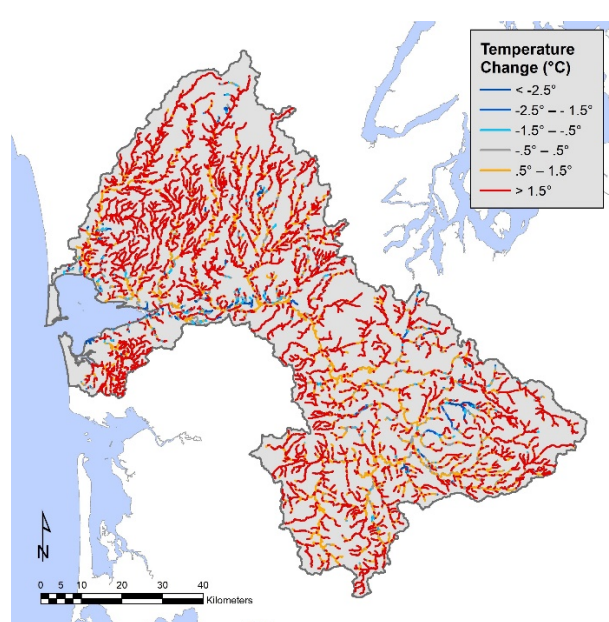
Figure A.13. Modeled change in 7-DADM stream temperature at 2085 (A) with tree growth from current condition but no climate change, and (B) with tree growth from current condition and with climate change. The maximum modeled increase in any reach by 2085 is +2°C.

146

To help guide restoration actions toward areas with the greatest potential for increased shade and decreased temperature, we created a plot of potential change in canopy opening angle as a function of tree height and canopy opening width (Figure A.14). This plot shows that tree growth can have the largest effects on shade at channel widths between about 5 and 40 m wide and when trees are small. As channel width increases, a change in tree height has less effect on shade. Similarly, when trees are greater than about 15 m (~50 feet) tall, further increases in tree height have relatively small effects on canopy opening angle even in small streams.
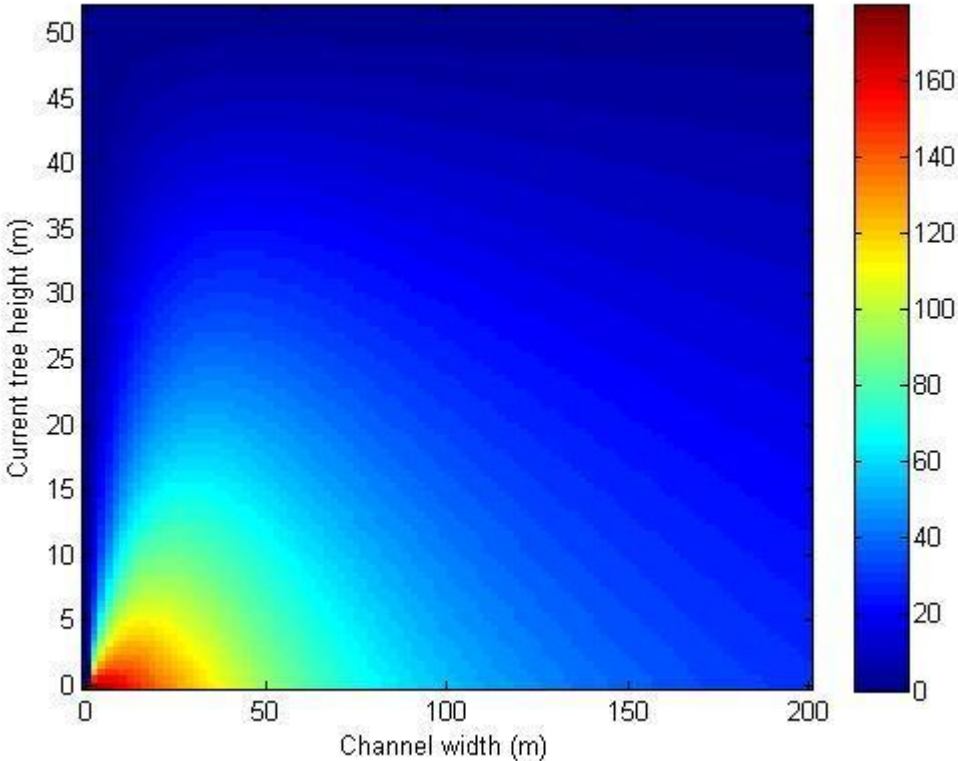
Figure A.14. Illustration of change in canopy opening angle from a reference tree height of 52 m as a function of channel width and riparian tree height. For example, at a channel width of 10 m and a tree height of 5 m, the canopy opening angle is about 110 degrees wider than if the channel was bordered by trees 52 m tall. Growing the trees to 10 m would reduce the canopy opening angle by about 40 degrees.

A.3.3 Wood Recruitment Potential

Wood recruitment ratings were mostly impaired across the Chehalis River basin. Wood recruitment was impaired for 72% of riparian segments, moderately impaired for 20% of reaches, and functioning for 8% of segments. Wood recruitment was impaired for much of the southern portion of the basin where there is a higher amount of urban, agricultural, and commercial forest lands (Figure A.15). The highest concentration of reaches

147

with functioning wood recruitment were located in the northern portion of the basin within the Olympic National Park and National Forest (Humptulips, Wynoochee, and Satsop Rivers) (Table A.3). Six subbasins have more than 70% of reaches impaired: Black River, Scatter Creek, Skookumchuck River, Skookumchuck to South Fork, Newaukum River, and South Fork Chehalis.
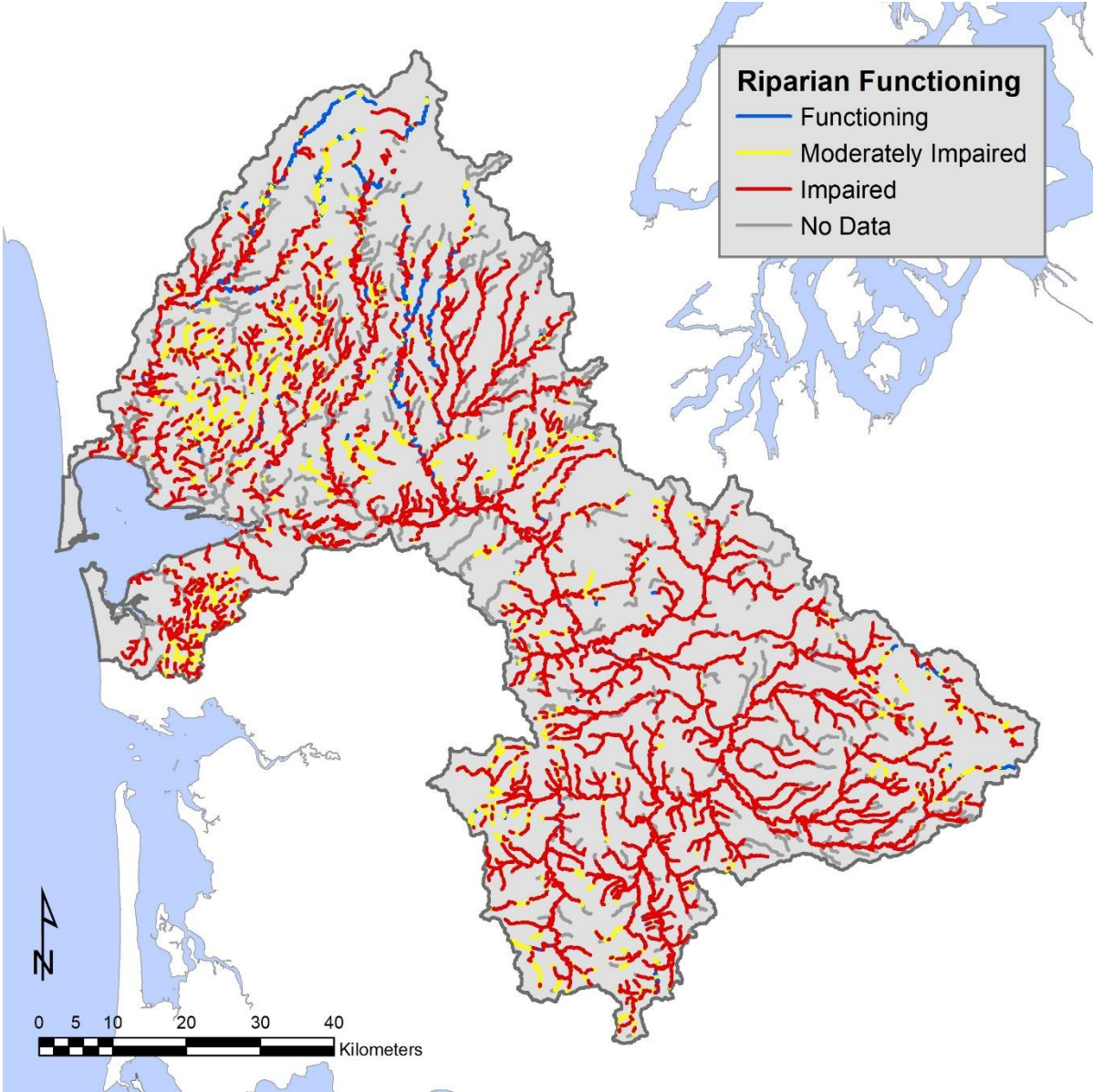
Figure A.15. Average wood recruitment ratings for reaches in the Chehalis River basin. Impaired reaches have small trees and/or buffer width <15 m, functioning reaches have tall trees and wide buffers (>30 m on small streams and >15 m wide on large rivers). Condition ratings are defined in Tables A.1 and A.2.

Table A.3. Number and percent of riparian segments in each subbasin that were rated functioning, moderately impaired, and impaired for wood recruitment potential. Note that a riparian segment is one side of one 200-m reach.

EDR	Wood Recruitment Rating (# of riparian segments)			Wood Recruitment Rating (% of riparian segments)		
	Functioning	Mod. Impaired	Impaired	Functioning	Mod. Impaired	Impaired
Black Hills	56	652	1,844	2%	26%	72%
Black River	21	160	1,873	1%	8%	91%
Cascade Mountains	108	500	4,176	2%	10%	87%
Central Lowlands	35	389	2,874	1%	12%	87%
Grays Harbor Tributaries	1,069	3,227	5,202	11%	34%	55%
Lower Chehalis Estuary	0	46	634	0%	7%	93%
Mainstem: Lower Chehalis	75	25	784	8%	3%	89%
Mainstem: Middle Chehalis	43	5	472	8%	1%	91%
Mainstem: Upper Chehalis	38	8	154	19%	4%	77%
Olympic Mountains	1,091	1,129	4,362	17%	17%	66%
Upper Skookumchuck	91	189	296	16%	33%	51%
Total Basin	2,627	6,330	22,671	8%	20%	72%

Appendix B. Hydrologic Assessment

The hydrologic assessment examines historical discharge records to evaluate (1) long-term trends in key discharge parameters such as peak and low flows and (2) effects of existing dams on stream flows. Because we do not have long term records of land cover change, we cannot directly determine whether flow change is correlated with land use change. Therefore, we also evaluate whether temporal trends in flows are correlated with weather data (e.g., precipitation) to rule out weather trends as a potential cause of stream flow trends.

B.1 Methods

We used the software package Indicators of Hydrologic Alteration (IHA, The Nature Conservancy 2009) to derive five types of flow statistics with a total of 32 parameters (Table B.1) from daily mean flow data for 11 USGS river gaging stations within the Chehalis River basin (Table B.2, Figure B.1). The IHA software analyzes and identifies two types of flow changes. First, the full period of record can be analyzed to derive flow statistics for each station and look for temporal trends (one-period analysis). Second, where a dam has been constructed upstream of a gaging station the software looks for abrupt changes in flow parameters before and after construction and operation of the dam (two-period analysis). For the gages downstream of dams in the Wynoochee and Skookumchuck basins, the gage records were analyzed using the two-period analysis, and differences in IHA flow parameters were evaluated using distributions from simulated median and coefficients of dispersion for each period to generate significance values similar to p-values (The Nature Conservancy 2009). For the remaining gages not influenced by dams, we used the single period analysis to look for temporal trends in each of the flow metrics throughout the period of record.

For gages without dams we also developed regressions between the IHA flow metrics and local and regional climate metrics to assess the relationship between trends in flow metrics and regional climate patterns. We selected annual 1-day maximum, 1-day minimum, base flow index, rise rate, fall rate, June low flow, extreme low flow duration, extreme low flow frequency, high flow duration, and high flow frequency as metrics that could be indicators of river conditions that could influence Viable Salmon Population (VSP) parameters (i.e., growth, survival, abundance, and productivity). Regional climate metrics were derived from a variety of sources (Table B.3). Local weather data were derived from daily precipitation and snowfall at two weather stations located in the two main geographic regions of the Chehalis basin gages considered in this analysis (Figure B.1). These weather stations are located near the cities of Aberdeen (Station GHCND:USC00450008) and Centralia (Station GHCND:USC00451276) at elevations of approximately 3 m and 56 m above sea level, respectively (NOAA National Centers for Environmental Information available at: http://gis.ncdc.noaa.gov/map/viewer/#app=cdo). Daily precipitation and snowfall totals at both stations were available from 1925 to present, which covers the period of record for all river gage stations used in this analysis. Other available weather stations within the basin were located at similar low elevations, but had much shorter periods of record and did not cover time periods equivalent to those of the river gages used
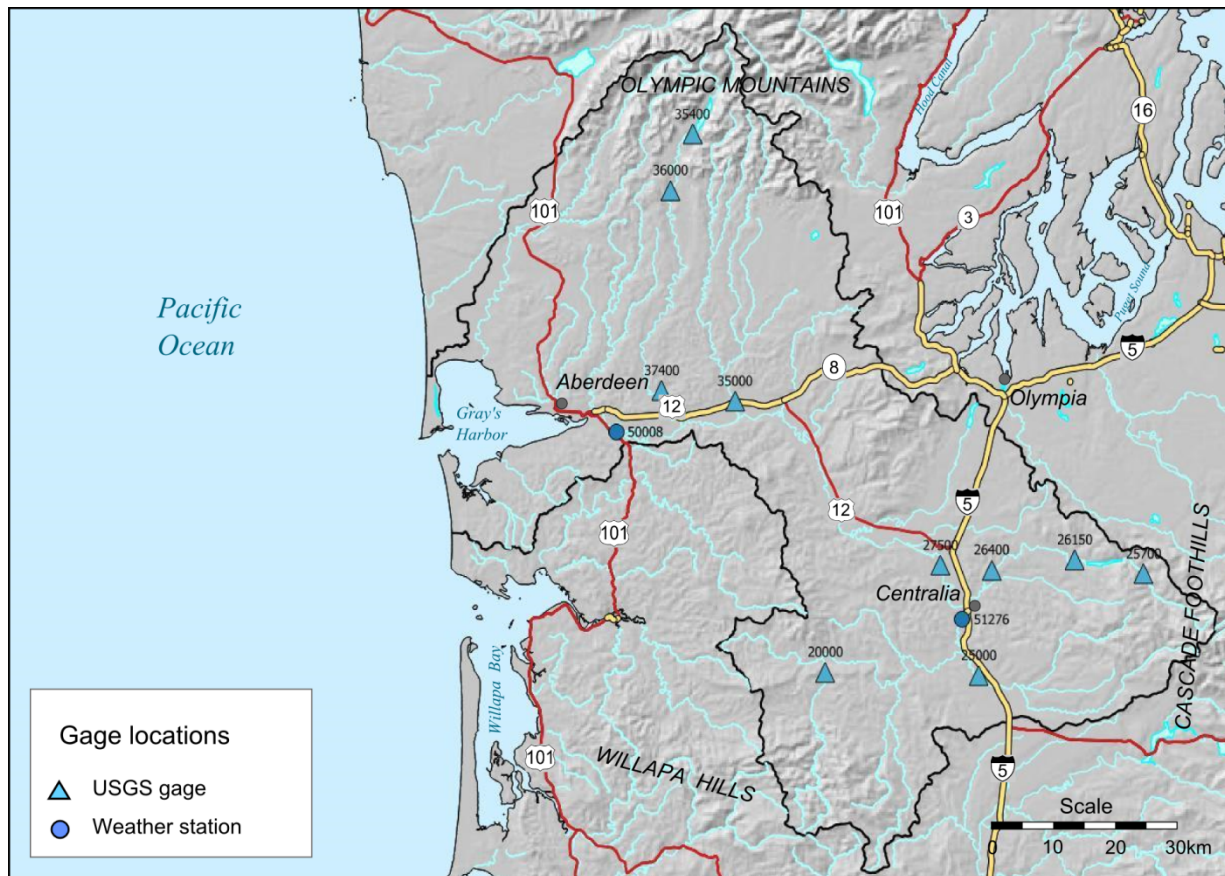
Figure B.1. Locations of USGS stream flow gages and NOAA weather stations in the Chehalis River basin that were used in the hydrologic analysis.

in this analysis. With over 98% of the daily record being complete, missing precipitation data were assumed to be a value of zero for this analysis. Cumulative precipitation and snowfall summaries were derived by water year for all local climate stations, and antecedent precipitation accumulations were derived from daily precipitation totals for the four days prior to annual 1-day maximum flows for each water year. Antecedent precipitation was only used for regressions of 1-day maximum flows.

We used the Multi-Model Inference package (Barton 2015) in R statistical software (R Core Team 2015) to develop all subsets modeling on standardized predictor variables, and to select models using Akaike's Information Criterion adjusted for small sample sizes (AICc) (Burnham and Anderson 2002; Burnham et al. 2011). Models were selected with a ΔAICc of less than seven based on the premise that models within this range have some support and should rarely be dismissed (Burnham et al. 2011). Selected models were averaged based on calculated model weights, and standardized coefficient plots were produced from the averaged model to compare effects of each parameter. Standardized coefficients with larger positive or negative values were considered to have a stronger relationship with the response, while those with smaller values were considered to have a weaker relationship. Standardized coefficients with 95% confidence intervals that spanned both negative and positive values were interpreted as factors for which we have low confidence in the estimated direction of the effect.

151

Table B.1: Indicators of Hydrologic Alteration (IHA) and Environmental Flow Components (EFC) hydrological parameter groups and parameters.

IHA Group	Parameters
Monthly conditions	Median value for each calendar month
Magnitude and duration of annual extreme water conditions	Annual minima 1-day median
	Annual maxima 1-day median
	Annual minima 3-day median
	Annual maxima 3-day median
	Annual minima 7-day median
	Annual maxima 7-day median
	Annual minima 30-day median
	Annual maxima 30-day median
	Annual minima 90-day median
	Annual maxima 90-day median
	Number of zero-flow days
	Base flow index (7-day minimum flow/mean flow for year)
Timing of annual extreme water conditions	Julian date of each annual 1-day maximum
	Julian date of each annual 1-day minimum
Frequency and duration of high and low pulses	Number of high pulses each year
	Number of low pulses each year
	Median duration of high pulses within each year in days
	Median duration of low pulses within each year in days
Rate and frequency of water condition changes	Rise rate (median of positive differences between consecutive daily means)
	Fall rate (median of negative differences between consecutive daily values)
	Number of reversals
EFC Group	**Parameters**
Low flows	Median values of low flows during each calendar month
Extreme low flows	Median of extreme low flow peaks within each year
	Median duration in days of extreme low flow peaks within each year
	Median Julian date of extreme low flow
	Median number of extreme low flows
High flow pulses	Median flow of high flow pulse event
	Median high flow pulse event duration (days)
	Median flow peak during maximum flow event
	Median Julian date of peak flow events
	Median rise rate of high flow pulse
	Median fall rate of high flow pulse
Small floods	Median flow of small flood event
	Median small flood event duration (days)
	Median flow peak during small flood event
	Median Julian date of small flood events
	Median rise rate of small flood
	Median fall rate of small flood
Large floods	Median flow of large flood event
	Median large flood event duration (days)
	Median flow peak during large flood event
	Median Julian date of large flood events
	Median rise rate of large flood
	Median fall rate of large flood

Table B.2. USGS river gages in study area.

Station ID	Water year start	Latitude	Longitude	Location
12037400	1956	47.01	-123.65	45.9 miles downstream of Wynoochee Dam
12036000	1925	47.29	-123.65	11.0 miles downstream of Wynoochee Dam
12035400	1965	47.38	-123.60	0.5 miles downstream of Wynoochee Dam
12035000	1930	47.00	-123.49	Satsop River near Satsop, WA
12026400	1969	46.77	-122.92	Skookumchuck River near Bucoda, WA
12026150	1970	46.79	-122.74	Skookumchuck River below Bloody Run Creek near Centralia, WA
12025700	1968	46.77	-122.59	Skookumchuck River near Vail, WA
12025000	1943	46.62	-122.94	Newaukum River near Chehalis, WA
12027500	1929	46.77	-123.03	Chehalis River near Chehalis, WA
12020000	1939	46.62	-123.27	Chehalis River near Doty, WA

Table B.3. Data sources for regional climate metrics.

Data	Source	Data location
Monthly indices of Pacific Decadal Oscillation (PDO)	University of Washington	http://jisao.washington.edu/pdo/PDO.latest
North Pacific Gyre Oscillation (NPGO)	California Current Ecosystem Long Term Ecological Research	http://www.o3d.org/npgo/
Southern Oscillation Index (SOI)	National Atmospheric and Oceanic Administration	https://www.ncdc.noaa.gov/teleconnections/enso/indicators/soi/
Coastal Upwelling Index (UWI) (48°North and 125°West, 45°North and 125°West)	National Atmospheric and Oceanic Administration	https://www.pfeg.noaa.gov/products/PFELData/upwell/monthly/upindex.mon
Sea Surface Temperature (SST)	Amphitrite Point 48.550°North and 125.320°West from British Columbia Lighthouse monitoring program	http://www.pac.dfo-mpo.gc.ca/science/oceans/data-donnees/lighthouses-phares/data/amphitrt.txt)
Sea Level at one long-term coastal monitoring station	Neah Bay, WA from University of Hawaii Sea Level Center	ftp://ftp.soest.hawaii.edu/uhslc/woce/m558.dat

B.2 Results

B.2.1 Temporal Trends in Hydrological Parameters

Upper Chehalis, Newaukum, and Skookumchuck Rivers

The two long-term flow gaging stations analyzed for the mainstem Chehalis River were located in the upper and middle Chehalis River basin. One station is located upriver of the Newaukum and Skookumchuck River confluences near Doty, WA (USGS 12020000, Figure B.2) and one is located downstream of the Skookumchuck River confluence near Chehalis, WA (USGS 12027500). We detected significant trends in both IHA flow parameters (Table B.4) and EFC flow parameters (Table B.5). At the farthest upriver station on the Chehalis River mainstem, we detected significant increasing trends in annual 1-day maximum flows and significant decreasing trends in 1-day to 7-day minimum flows (Table B.4, Figure B.2). However, increasing trends in annual low flow metrics were detected at the mainstem station located below the confluence of the Skookumchuck River (Table B.4). This apparent difference in low flow trends could be the result of a hydroelectric dam and reservoir constructed on the Skookumchuck River in 1970. A two-period analysis of flow metrics at the mainstem Chehalis River station located below the Skookumchuck River confluence indicates that a number of annual and monthly low flow metrics increased significantly following dam construction in the Skookumchuck River (Table B.6, Figure B.3). Further analysis of the post-dam period for this station indicated that minimum flow metrics did not have statistically significant trends during the post-dam period (Table B.4). This finding supports the conclusion that increasing trends in annual minimum flows observed in the full time series for the mainstem Chehalis River station located below the Skookumchuck River confluence was due to a shift in base flow following dam construction on the Skookumchuck River (Figure B.3).

Within the Skookumchuck River, three long-term river flow gages were available with two located downstream of the reservoir (USGS 12026400 and 12026150) and one above the reservoir (USGS 12025700). Both gages downstream of the reservoir could not be used in a two-period analysis given that time series for these gages begin around the time of dam construction. We detected significant trends in both IHA flow parameters (Table B.7) and EFC flow parameters (Table B.8) for the Skookumchuck River. At the gage located just 1.2 miles downstream of the Skookumchuck dam (USGS 12026150), we detected statistically significant increasing trends in annual and monthly low flow metrics (Table B.7 and Table B.8). These increasing trends included 1-day through 7-day, and 90-day annual minimum flows and increasing low flows for the months of April and June through August. In addition, we detected significant increasing trends in median monthly flows in the months of June through August downstream of the Skookumchuck dam (Table B.7). These increasing trends in annual minimum flow, monthly low flow, and monthly median flows detected just downstream of the dam could be related to releases of stored water from the reservoir during these periods. This conclusion is supported by the observation that annual low flows and base flow index show significant decreasing trends over time at the Skookumchuck River gage located above the reservoir (Table B.7, Figure B.4).

Aside from a significant increase in June low flows, the Skookumchuck River gage located near Bucoda, WA (approximately 14 miles downstream of the dam) did not show similar increasing trends in annual low flows, monthly low flows, and monthly median flows (Table B.7 and Table B.8). This suggests that flow impacts from the dam operation attenuate or are mitigated or masked by other unknown factors farther downstream within the Skookumchuck River, even though the impact of dam construction was detected in the mainstem Chehalis River downstream of the Skookumchuck River confluence (Figure B.3). However, we did detect significant decreasing trends in rise rates at both gages located below the Skookumchuck dam (Table B.7), which provides evidence for downstream impacts given that dams can attenuate high flow pulse events.

Within the Newaukum River, one long-term river gage time series was available for a station located near Chehalis, WA in the lower reaches of the Newaukum River (USGS 12025000). At this station, we detected statistically significant positive trends in annual 1-day and 3-day maximum flows (Figure B.5 and Table B.4). These increases in annual maximum flows were coupled with a significant increasing trend in large flood frequency (Table B.5). We also detected a significant increasing trend in low flow and median flow for the month of June, and a significant decreasing trend in median February flows in the Newaukum River (Table B.4 and Table B.5).

Satsop and Wynoochee Rivers

Long-term time series for river flow were only available for the Satsop and Wynoochee Rivers in the lower Chehalis River basin, with no stations located on the mainstem Chehalis River (Figure B.2). Within the Satsop River (USGS 12035000), we only detected significant decreasing trends in low flow pulse count and rise rate, and a significant positive trend in fall rates (Table B.9). We did not detected significant trends in any EFC flow parameters for the Satsop River (Table B.10).

All three Wynoochee River gages are located below the Wynoochee Dam, which was built in 1972 (Figure B.2). All gages have pre-dam and post-dam hydrographic records, which allowed us to use two-period analyses to examine dam impacts and trends in post-dam time series. However, fewer than 20 years of pre-impact flow data were available for two of the gages on the Wynoochee River (USGS 12035400 and 12037400) and variation in estimates may be inflated as a result of increased inter-annual variation with fewer than 20 years of pre-impact flow data (Richter et al. 1997; Richter et al. 1998). From the two-period analyses for all Wynoochee River gages, we detected significant increasing trends for all annual minimum flow parameters and the base flow index following dam construction (Table B.11, B.12, and B.13). The shift in annual low flow metrics is apparent in the station with the longest pre-impact time series, where annual low flows like the 1-day minimum flows show a clear increase following dam construction (Figure B.7). Although sufficiently long pre-impact time series were only available for one station downstream of the Wynoochee River dam, the consistency of patterns among stations supports the finding that annual low flows increased following dam construction.

Table B.4. Non-parametric regression statistics for all IHA hydrological parameter groups for the Chehalis River mainstem and Newaukum River. Statistically significant regressions are highlighted in green and bold. Values less than 0.01 are indicated by a value of 0.00. IHA parameter names are abbreviated from the list provided in the methods section.

| | | Chehalis River Mainstem | | | | | | | | | Newaukum River | | |
| | | 12027500 (1929-2015) | | | 12027500 (1971-2015, post-dam) | | | 12020000 (1940-2015) | | | 12025000 (1943-2015) | | |
IHA Group	Parameter	Slope	P	R²	Slope	P	R²	Slope	P	R²	Slope	P	R²
Magnitude and monthly conditions	OCT	1.68	0.50	0.01	6.90	0.25	0.05	-0.67	0.50	0.01	-0.27	0.50	0.00
	NOV	2.55	0.50	0.00	5.63	0.50	0.00	1.60	0.50	0.01	0.28	0.50	0.00
	DEC	-2.30	0.50	0.00	-27.62	0.50	0.02	-0.46	0.50	0.00	-0.84	0.50	0.00
	JAN	-2.83	0.50	0.00	-16.35	0.50	0.01	0.13	0.50	0.00	-0.17	0.50	0.00
	FEB	-9.78	0.50	0.01	-22.96	0.50	0.02	-4.35	**0.05**	0.06	-4.08	**0.03**	0.08
	MAR	3.60	0.50	0.00	1.44	0.50	0.00	1.28	0.50	0.01	1.39	0.50	0.01
	APR	4.10	0.50	0.01	13.68	0.25	0.04	0.24	0.50	0.00	1.33	0.25	0.03
	MAY	5.66	**0.01**	0.07	11.47	0.10	0.07	0.19	0.50	0.00	1.17	0.10	0.05
	JUN	3.76	**0.01**	0.08	6.70	0.25	0.05	0.41	0.25	0.02	1.32	**0.03**	0.08
	JUL	1.16	**0.05**	0.05	-0.12	0.50	0.00	0.01	0.50	0.00	0.25	0.25	0.02
	AUG	0.65	**0.01**	0.07	-0.09	0.50	0.00	-0.10	0.10	0.04	0.07	0.50	0.01
	SEP	0.96	0.25	0.02	-2.83	0.25	0.05	-0.33	0.25	0.02	0.07	0.50	0.00
Magnitude and duration of annual extreme water conditions	1-day min	0.59	**0.00**	0.12	-0.31	0.50	0.01	-0.08	**0.01**	0.10	0.06	0.25	0.02
	3-day min	0.64	**0.00**	0.13	-0.17	0.50	0.00	-0.09	**0.01**	0.11	0.05	0.50	0.02
	7-day min	0.67	**0.00**	0.13	-0.22	0.50	0.00	-0.10	**0.01**	0.10	0.05	0.50	0.01
	30-day min	0.75	**0.01**	0.11	-0.41	0.50	0.01	-0.09	0.10	0.05	0.06	0.50	0.01
	90-day min	0.94	**0.03**	0.07	-0.90	0.50	0.02	-0.12	0.50	0.02	0.12	0.50	0.01
	1-day max	60.01	0.25	0.02	19.96	0.50	0.00	46.54	**0.05**	0.05	33.44	**0.01**	0.12
	3-day max	29.33	0.50	0.01	-17.16	0.50	0.00	19.15	0.10	0.04	17.68	**0.03**	0.07
	7-day max	8.98	0.50	0.00	-43.27	0.50	0.01	8.83	0.25	0.03	6.87	0.25	0.03
	30-day max	-1.38	0.50	0.00	-14.48	0.50	0.00	2.44	0.50	0.01	1.51	0.50	0.00
	90-day max	-2.31	0.50	0.00	-7.44	0.50	0.00	0.31	0.50	0.00	-0.02	0.50	0.00
	# of zero days	0.00	0.50	0.00	0.00	0.50	0.00	0.00	0.50	0.00	0.00	0.50	0.00
	Base flow index	0.00	0.10	0.04	0.00	0.50	0.00	0.00	0.10	0.04	0.00	0.50	0.00
Timing of annual extreme water conditions	Date of min	0.02	0.50	0.00	0.37	0.25	0.05	0.07	0.50	0.01	0.17	0.25	0.03
	Date of max	0.34	0.50	0.00	-0.35	0.50	0.00	-0.17	0.50	0.00	0.44	0.50	0.00
Frequency and duration of high and low pulses	Low pulse #	-0.01	0.25	0.02	-0.01	0.50	0.01	-0.01	0.50	0.01	-0.01	0.50	0.02
	Low pulse dur.	0.10	0.50	0.01	0.09	0.50	0.00	0.02	0.50	0.00	0.09	0.50	0.01
	High pulse #	0.01	0.50	0.01	0.04	0.25	0.06	0.01	0.50	0.00	0.01	0.50	0.00
	High pulse dur.	0.01	0.50	0.00	-0.03	0.50	0.00	0.00	0.50	0.00	0.00	0.50	0.00
Rate and frequency of water condition changes	Rise rate	-0.71	0.25	0.02	-1.21	0.50	0.02	-0.38	**0.03**	0.07	-0.18	0.25	0.03
	Fall rate	0.19	0.25	0.02	0.14	0.50	0.00	0.02	0.50	0.00	0.03	0.50	0.00
	# of reversals	-0.05	0.25	0.02	-0.03	0.50	0.00	0.10	**0.05**	0.06	0.07	0.25	0.02

Table B.5. Non-parametric regression statistics for all EFC hydrological parameter groups for the Chehalis River mainstem and Newaukum River. Statistically significant regressions are highlighted in green and bold. Values less than 0.01 are indicated by a value of 0.00. EFC parameter names are abbreviated from the list provided in the methods section.

| | | Chehalis River Mainstem | | | | | | | | | Newaukum River | | |
| | | 12027500 (1929-2015) | | | 12027500 (1971-2015, post-dam) | | | 12020000 (1940-2015) | | | 12025000 (1943-2015) | | |
EFC Grp	EFC Parameter	Slope	P	R²	Slope	P	R²	Slope	P	R²	Slope	P	R²
Monthly low flows	OCT Low Flow	0.06	0.50	0.00	5.00	0.25	0.04	-0.25	0.50	0.00	-0.25	0.50	0.01
	NOV Low Flow	1.63	0.50	0.00	0.07	0.50	0.00	-0.06	0.50	0.00	-0.13	0.50	0.00
	DEC Low Flow	4.33	0.25	0.02	-0.64	0.50	0.00	-0.55	0.50	0.01	-0.88	0.25	0.03
	JAN Low Flow	3.96	0.25	0.03	2.17	0.50	0.00	0.48	0.50	0.01	0.48	0.50	0.01
	FEB Low Flow	1.68	0.50	0.00	1.92	0.50	0.00	-0.49	0.50	0.01	-0.59	0.50	0.01
	MAR Low Flow	0.83	0.50	0.00	2.05	0.50	0.00	0.16	0.50	0.00	-0.14	0.50	0.00
	APR Low Flow	3.81	0.25	0.03	11.59	0.10	0.07	-0.16	0.50	0.00	0.44	0.50	0.01
	MAY Low Flow	5.11	**0.01**	0.08	8.04	0.25	0.04	0.28	0.50	0.01	0.97	0.10	0.04
	JUN Low Flow	3.42	**0.01**	0.08	5.69	0.25	0.05	0.38	0.25	0.02	1.01	**0.03**	0.09
	JUL Low Flow	0.93	0.10	0.04	0.55	0.50	0.00	0.03	0.50	0.00	0.20	0.25	0.02
	AUG Low Flow	0.46	0.25	0.02	0.63	0.50	0.01	0.09	0.25	0.02	0.06	0.50	0.01
	SEP Low Flow	-0.02	0.50	0.00	-1.84	0.50	0.02	-0.03	0.50	0.00	-0.18	0.50	0.01
Extreme low flows	Extreme low peak	-0.01	0.50	0.00	0.00	0.50	0.00	-0.01	0.50	0.00	0.06	**0.05**	0.06
	Extreme low dur.	0.07	0.50	0.02	0.14	0.50	0.01	0.08	0.25	0.03	-0.03	0.50	0.01
	Extreme low timing	-0.02	0.50	0.00	0.29	0.25	0.04	-0.05	0.50	0.00	0.19	0.10	0.04
	Extreme low freq.	-0.03	**0.00**	0.14	0.01	0.50	0.01	0.01	0.50	0.01	0.00	0.50	0.00
High flow pulses	High flow peak	-17.08	0.10	0.03	-6.48	0.50	0.00	-2.81	0.50	0.01	-0.20	0.50	0.00
	High flow dur.	0.01	0.50	0.00	0.00	0.50	0.00	-0.01	0.50	0.00	-0.01	0.50	0.00
	High flow timing	0.31	0.50	0.00	0.57	0.50	0.00	-1.57	**0.05**	0.06	0.08	0.50	0.00
	High flow freq.	0.00	0.50	0.00	0.05	0.10	0.07	0.00	0.50	0.00	0.00	0.50	0.00
	High flow rise rate	-6.56	0.10	0.04	3.39	0.50	0.00	0.27	0.50	0.00	0.47	0.50	0.01
	High flow fall rate	2.87	**0.03**	0.07	0.99	0.50	0.00	0.56	0.50	0.02	0.01	0.50	0.00
Small floods	Small Flood peak	3.44	0.50	0.00	-50.10	0.50	0.02	27.18	**0.05**	0.13	12.81	0.10	0.09
	Small Flood dur.	0.03	0.50	0.00	-0.07	0.50	0.01	0.08	0.50	0.01	-0.15	0.50	0.04
	Small Flood timing	0.55	0.50	0.01	0.94	0.50	0.01	-0.66	0.50	0.01	-0.38	0.50	0.00
	Small Flood freq.	0.00	0.50	0.01	-0.01	0.50	0.02	0.00	0.50	0.01	0.01	0.25	0.02
	Small Flood riserate	16.99	0.50	0.01	39.77	0.50	0.03	10.89	0.50	0.02	22.04	0.10	0.09
	Small Flood fallrate	1.49	0.50	0.00	-11.55	0.50	0.03	-1.49	0.50	0.01	-5.36	**0.01**	0.22
Large floods	Large flood peak	139.70	0.50	0.19	582.60	0.50	0.44	186.50	0.50	0.23	70.35	0.10	0.50
	Large flood dur.	-0.29	0.25	0.30	-0.13	0.50	0.06	-0.13	0.50	0.22	-0.11	0.50	0.02
	Large flood timing	-3.00	0.25	0.25	6.10	0.50	0.10	2.48	0.50	0.11	-4.04	0.50	0.10
	Large flood freq.	0.00	0.50	0.01	0.00	0.50	0.00	0.00	0.25	0.02	0.00	**0.03**	0.08
	Large flood riserate	81.87	0.50	0.14	626.30	**0.01**	0.94	137.90	0.25	0.24	65.88	0.25	0.26
	Large flood fallrate	-35.76	0.25	0.31	-38.71	0.50	0.04	-27.25	0.50	0.20	-9.00	0.50	0.08
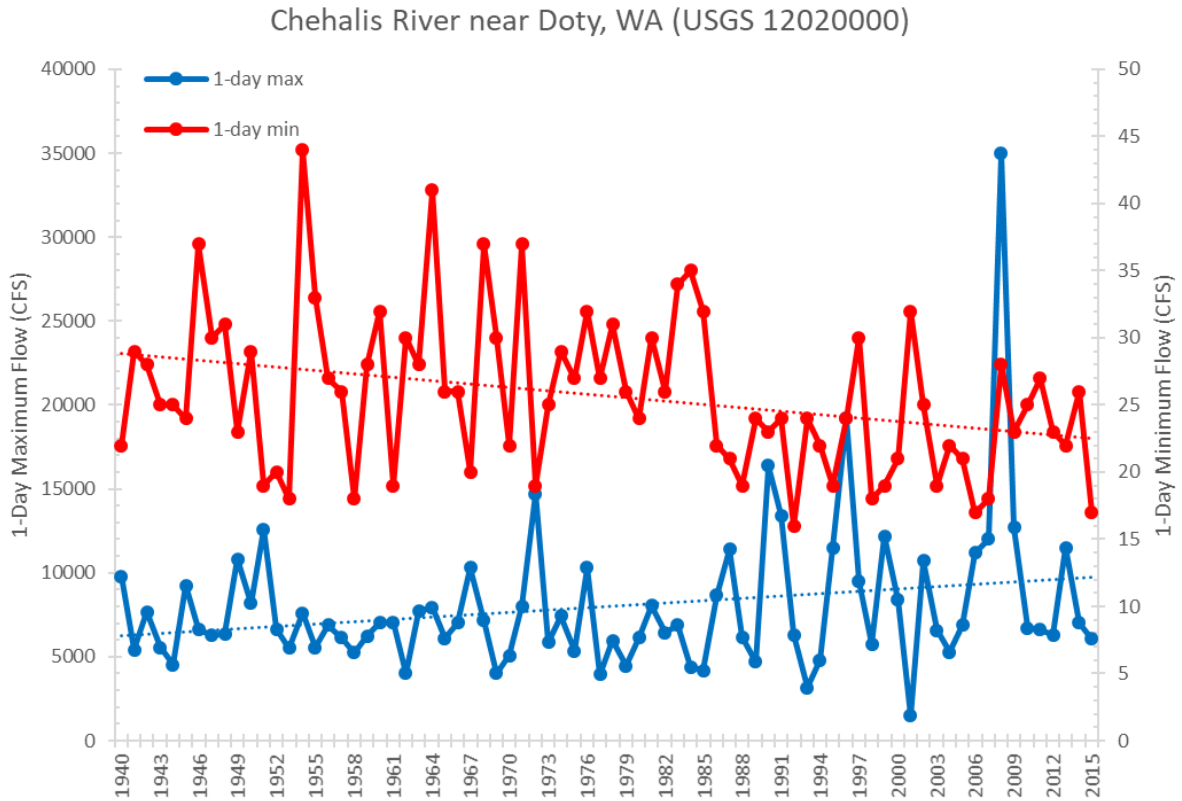
Figure B.2. Increasing trend in 1-day maximum flow and decreasing trend in 1-day minimum flows in the upper Chehalis River mainstem station. Regression lines are shown as dotted lines and are statistically significant (p < 0.05). Regression statistics for both trends are in Table B.4.

Table B.6. Non-Parametric IHA Scorecard for pre-impact (1929-1970) and post-impact (1971-2015) at USGS 12027500 on the mainstem Chehalis River below the confluence of Skookumchuck River. Medians are in CFS, bold values are significant at p < 0.05.

IHA Parameter	MEDIANS		COEFF. of DISP.		Deviation Factor		Significance Count	
	Pre	Post	Pre	Post	Medians	C.D.	Medians	C.D.
October	434.5	404	1.288	0.9332	0.0702	0.2756	0.7508	0.2933
November	1773	2320	1.836	1.068	0.3089	0.4183	0.2983	0.1421
December	4765	4150	0.8122	1.311	0.1291	0.614	0.5275	0.02302
January	4835	4490	0.8257	0.7094	0.07135	0.141	0.3403	0.5415
February	4358	4000	0.6925	0.4525	0.08204	0.3466	0.2342	0.2422
March	3350	3580	0.7396	0.743	0.06866	0.004685	0.5656	0.993
April	2293	2365	0.5098	0.7326	0.03162	0.4369	0.8068	0.2222
May	1035	1180	0.6519	0.7127	0.1401	0.09323	0.0831	0.7217
June	571.8	768.5	0.5582	0.5065	0.3441	0.09253	**0.0030**	0.7187
July	313.5	381	0.492	0.3819	0.2153	0.2238	**0.0050**	0.4324
August	200.5	250	0.4526	0.31	0.2469	0.3151	**0.0060**	0.2192
September	206	280	0.4964	0.3241	0.3592	0.347	**0.0000**	0.1271
1-day minimum	140	191	0.3768	0.2853	0.3643	0.2427	**<0.0001**	0.2172
3-day minimum	142.7	192	0.368	0.2847	0.3458	0.2263	**<0.0001**	0.2933
7-day minimum	148.3	193.4	0.3545	0.2917	0.3044	0.1771	**<0.0001**	0.3974
30-day minimum	175.2	231	0.4108	0.2989	0.3191	0.2725	**<0.0001**	0.2623
90-day minimum	259.8	320.3	0.5607	0.4071	0.2328	0.2739	**0.0050**	0.2793
1-day maximum	22450	25700	0.4131	0.6206	0.1448	0.5022	0.0681	0.04204
3-day maximum	19870	22670	0.3523	0.5324	0.1409	0.5109	0.0521	0.08809
7-day maximum	15800	17670	0.2866	0.4532	0.1188	0.5809	0.0871	0.02002
30-day maximum	9301	9705	0.3771	0.4484	0.04343	0.1893	0.6126	0.4084
90-day maximum	6924	6831	0.2975	0.496	0.01346	0.6674	0.6897	0.04805
Number of zero days	0	0	0	0				
Base flow index	0.05905	0.07261	0.4611	0.3678	0.2295	0.2023	**0.0060**	0.4204
Date of minimum	250	241	0.08607	0.1011	0.04918	0.1746	**0.0461**	0.6587
Date of maximum	24	13	0.1277	0.1462	0.06011	0.1444	0.2583	0.4865
Low pulse count	4	3	0.375	0.3333	0.25	0.1111	0.2743	0.7878
Low pulse duration	16.5	16	1.242	1.063	0.0303	0.1448	0.8749	0.6436
High pulse count	8	8	0.5	0.375	0	0.25	0.0811	0.3283
High pulse duration	7	8	0.6429	0.5938	0.1429	0.07639	0.1231	0.7808
Low Pulse Threshold	354.3							
High Pulse Threshold	3428							
Rise rate	201.5	173	0.8368	0.8353	0.1414	0.001898	0.4124	0.993
Fall rate	-100	-90	-0.4	-0.6111	0.1	0.5278	0.2793	0.03704
Number of reversals	86	85	0.1657	0.1588	0.01163	0.04149	0.5656	0.9079
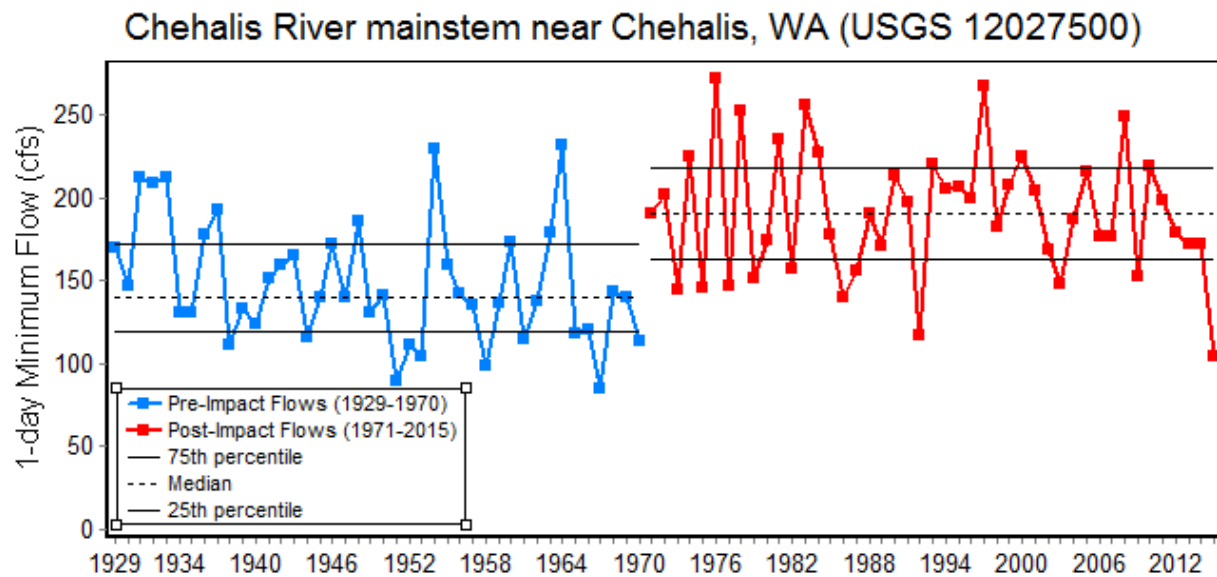
Figure B.3. Two-period comparison of 1-day minimum flows on the mainstem Chehalis River downstream of the Skookumchuck River confluence at USGS Station 12027500 before (Pre-Impact Flows) and after (Post-Impact Flows) construction of the dam on the Skookumchuck River in 1970. Median 1-day minimum flows, and the 25th and 75th percentile 1-day minimum flows, are also shown for the pre and post-impact periods.

Table B.7. Non-parametric regression statistics for all IHA hydrological parameter groups for the Skookumchuck River, above and below the reservoir. Statistically significant regressions are highlighted in green and bold. Values less than 0.01 are indicated by a value of 0.00. IHA parameter names are abbreviated from the list provided in the methods section.

| IHA Group | IHA Parameter | Below Skookumchuck Reservoir | | | | | | Above Reservoir | | |
| | | 12026400 (1969-2015) | | | 12026150 (1970-2015) | | | 12025700 (1968-2015) | | |
		Slope	P	R²	Slope	P	R²	Slope	P	R²
Magnitude and monthly conditions	OCT	-1.00	**0.05**	0.10	0.03	0.50	0.00	-0.05	0.50	0.00
	NOV	-1.02	0.50	0.01	0.79	0.50	0.01	1.22	0.50	0.02
	DEC	-1.82	0.50	0.01	0.55	0.50	0.00	-1.43	0.50	0.02
	JAN	-3.51	0.50	0.03	-2.30	0.50	0.03	-0.62	0.50	0.00
	FEB	-1.91	0.50	0.01	-0.78	0.50	0.00	-1.79	0.25	0.05
	MAR	-0.41	0.50	0.00	0.81	0.50	0.00	0.62	0.50	0.01
	APR	1.71	0.25	0.03	1.79	0.10	0.07	0.76	0.50	0.03
	MAY	1.25	0.25	0.04	0.89	0.25	0.05	0.40	0.50	0.01
	JUN	1.25	0.10	0.07	1.41	**0.01**	0.16	0.23	0.50	0.01
	JUL	0.16	0.50	0.01	0.77	**0.00**	0.22	-0.17	0.25	0.03
	AUG	-0.03	0.50	0.00	0.50	**0.03**	0.12	-0.10	0.10	0.06
	SEP	-0.47	0.25	0.06	-0.07	0.50	0.00	-0.30	0.10	0.06
Magnitude and duration of annual extreme water conditions	1-day min	-0.09	0.50	0.00	0.54	**0.01**	0.17	-0.11	**0.00**	0.24
	3-day min	-0.06	0.50	0.00	0.51	**0.01**	0.15	-0.12	**0.00**	0.26
	7-day min	-0.07	0.50	0.00	0.50	**0.03**	0.14	-0.12	**0.00**	0.25
	30-day min	-0.18	0.50	0.01	0.34	0.10	0.08	-0.13	**0.03**	0.12
	90-day min	-0.02	0.50	0.00	0.54	**0.01**	0.17	-0.26	**0.03**	0.11
	1-day max	8.93	0.50	0.00	-3.06	0.50	0.00	11.89	0.50	0.02
	3-day max	5.68	0.50	0.00	-5.15	0.50	0.01	4.43	0.50	0.01
	7-day max	1.73	0.50	0.00	-2.97	0.50	0.01	0.48	0.50	0.00
	30-day max	0.19	0.50	0.00	-0.75	0.50	0.00	-0.23	0.50	0.00
	90-day max	-0.68	0.50	0.00	-0.35	0.50	0.00	0.20	0.50	0.00
	# of zero days	0.00	0.50	0.00	0.00	0.50	0.00	0.00	0.50	0.00
	Base flow index	0.00	0.50	0.00	0.00	0.50	0.02	0.00	**0.05**	0.09
Timing of annual extreme water conditions	Date of min	0.60	0.50	0.02	0.85	0.50	0.03	0.34	0.10	0.06
	Date of max	0.14	0.50	0.00	-0.77	0.50	0.01	-0.80	0.50	0.01
Frequency and duration of high and low pulses	Low pulse #	-0.02	0.50	0.01	-0.02	0.50	0.01	-0.05	**0.01**	0.16
	Low pulse dur.	0.25	0.50	0.02	0.08	0.50	0.00	0.70	**0.01**	0.20
	High pulse #	-0.01	0.50	0.00	0.00	0.50	0.00	0.03	0.50	0.02
	High pulse dur.	-0.22	0.50	0.02	0.06	0.50	0.01	0.01	0.50	0.00
Rate and frequency of water condition changes	Rise rate	-0.25	**0.00**	0.21	-0.21	**0.00**	0.24	0.04	0.50	0.00
	Fall rate	0.13	**0.03**	0.12	0.07	0.25	0.06	0.03	0.50	0.02
	# of reversals	-0.14	0.50	0.02	0.17	0.25	0.04	-0.01	0.50	0.00

Table B.8. Non-parametric regression statistics for all EFC hydrological parameter groups for the Skookumchuck River, above and below the reservoir. Statistically significant regressions are highlighted in green and bold. Values less than 0.01 are indicated by a value of 0.00. EFC parameter names are abbreviated from the list provided in the methods section.

| EFC Group | EFC Parameter | Below Skookumchuck Reservoir | | | | | | Above Reservoir | | |
| | | 12026400 (1969-2015) | | | 12026150 (1970-2015) | | | 12025700 (1968-2015) | | |
		Slope	P	R²	Slope	P	R²	Slope	P	R²
Monthly low flows	OCT Low Flow	-0.94	**0.01**	0.16	-0.40	0.25	0.05	0.02	0.50	0.00
	NOV Low Flow	-0.65	0.50	0.01	0.18	0.50	0.00	-0.22	0.50	0.00
	DEC Low Flow	-0.76	0.50	0.01	0.01	0.50	0.00	-0.05	0.50	0.00
	JAN Low Flow	0.43	0.50	0.00	1.05	0.50	0.04	0.18	0.50	0.00
	FEB Low Flow	0.37	0.50	0.00	0.69	0.50	0.02	-0.03	0.50	0.00
	MAR Low Flow	-0.01	0.50	0.00	0.54	0.50	0.01	-0.04	0.50	0.00
	APR Low Flow	1.47	0.10	0.07	1.25	**0.03**	0.12	0.40	0.50	0.02
	MAY Low Flow	0.61	0.50	0.01	0.43	0.50	0.02	0.14	0.50	0.00
	JUN Low Flow	0.96	**0.05**	0.08	0.88	**0.01**	0.18	0.14	0.50	0.00
	JUL Low Flow	0.22	0.50	0.02	0.54	**0.03**	0.16	-0.12	0.50	0.01
	AUG Low Flow	0.11	0.50	0.01	0.43	**0.01**	0.19	0.00	0.50	0.00
	SEP Low Flow	-0.67	**0.00**	0.23	-0.30	0.10	0.08	-0.35	**0.03**	0.12
Extreme low flows	Extreme low peak	-0.18	0.25	0.04	-0.06	0.50	0.02	-0.06	**0.01**	0.14
	Extreme low dur.	0.34	0.10	0.08	0.34	0.25	0.04	0.16	0.25	0.05
	Extreme low timing	0.02	0.50	0.00	0.83	0.50	0.03	0.05	0.50	0.00
	Extreme low freq.	-0.01	0.50	0.01	-0.06	**0.00**	0.25	0.02	0.50	0.03
High flow pulses	High flow peak	3.79	0.50	0.02	6.87	0.10	0.08	2.39	0.50	0.03
	High flow dur.	0.12	0.10	0.06	0.11	0.25	0.03	0.03	0.50	0.00
	High flow timing	0.18	0.50	0.00	1.00	0.25	0.04	-0.50	0.50	0.00
	High flow freq.	-0.02	0.50	0.01	0.00	0.50	0.00	0.03	0.50	0.01
	High flow rise rate	0.87	0.50	0.01	0.31	0.50	0.00	0.67	0.50	0.03
	High flow fall rate	-0.46	0.50	0.02	-0.11	0.50	0.00	-0.30	0.25	0.05
Small floods	Small Flood peak	-38.41	**0.01**	0.29	-17.58	0.10	0.15	-3.03	0.50	0.01
	Small Flood dur.	-0.65	0.25	0.08	-0.40	0.50	0.02	-0.10	0.50	0.01
	Small Flood timing	1.22	0.50	0.01	-0.83	0.50	0.00	0.40	0.50	0.00
	Small Flood freq.	0.00	0.50	0.01	0.00	0.50	0.00	0.00	0.50	0.01
	Small Flood riserate	16.23	0.50	0.06	2.16	0.50	0.00	2.84	0.50	0.01
	Small Flood fallrate	0.65	0.50	0.00	0.32	0.50	0.00	-1.68	0.50	0.05
Large floods	Large flood peak	38.47	0.50	0.22	34.42	0.50	0.31	19.01	0.50	0.08
	Large flood dur.	-0.92	0.50	0.02	-2.96	**0.05**	0.80	-0.11	0.50	0.06
	Large flood timing	-16.31	0.50	0.44	-0.26	0.50	0.06	4.01	0.50	0.19
	Large flood freq.	0.00	0.50	0.02	0.00	0.50	0.00	0.00	0.50	0.01
	Large flood riserate	-59.86	0.50	0.27	47.88	0.10	0.73	21.45	0.50	0.29
	Large flood fallrate	-16.03	0.50	0.42	-8.37	0.50	0.15	-1.35	0.50	0.04
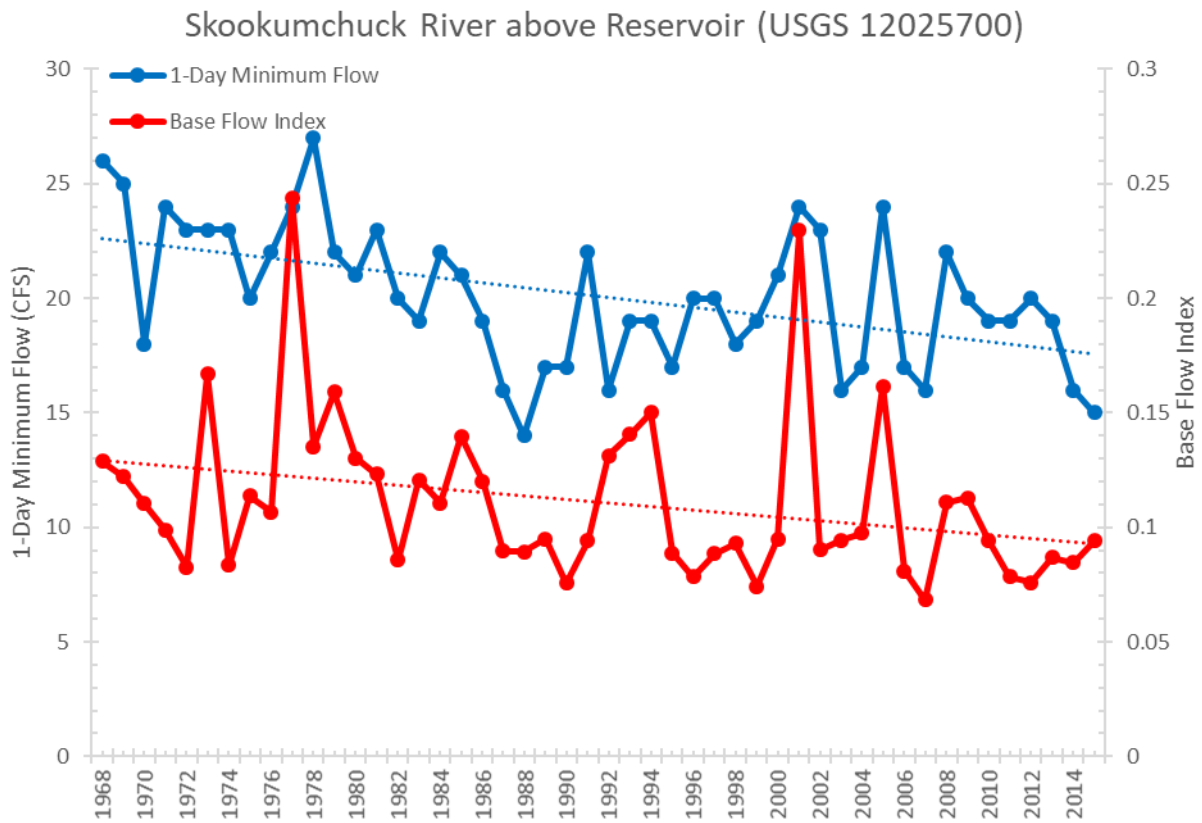
Figure B.4. Decreasing trends in 1-day minimum flow and base flow index (7-day minimum flow/annual mean flow) for the Skookumchuck River above the Skookumchuck dam and reservoir (USGS 12025700). Regression lines are shown as dotted lines and are statistically significant (p < 0.05). Regression statistics for both trends are in Table B.7.
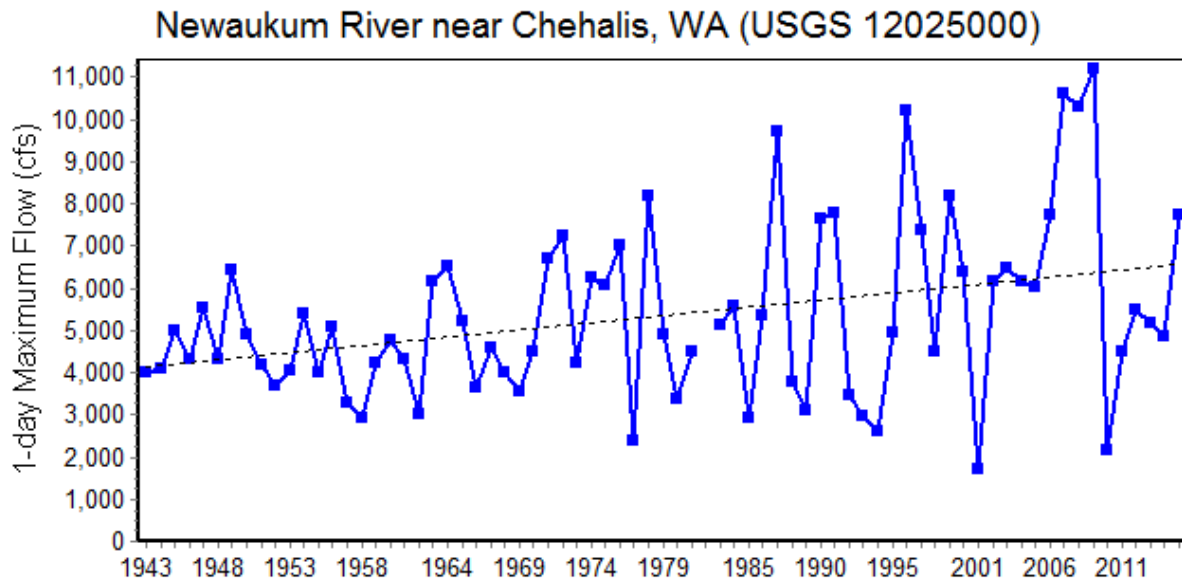
Figure B.5. Increasing trend in 1-day maximum flow on the Newaukum River at USGS Station 12025000 near Chehalis, WA. Regression line is shown as a dotted line and is statistically significant (p < 0.05). Regression statistics are in Table B.4.

Table B.9. Non-parametric regression statistics for all IHA hydrological parameter groups for the Wynoochee and Satsop Rivers. Statistically significant regressions are highlighted in green and bold. Values less than 0.01 are indicated by a value of 0.00. IHA parameter names are abbreviated from the list provided in the methods section.

| | Wynoochee - Post Dam, Below Reservoir | | | | | | | | | Satsop River | | |
| | 12035400 (1973-2015) | | | 12036000 (1972-2015) | | | 12037400 (1972-2015) | | | 12035000 (1930-2015) | | |
IHA Parameter	Slope	P	R^2	Slope	P	R^2	Slope	P	R^2	Slope	P	R^2
OCT	0.18	0.50	0.00	5.82	0.25	0.05	8.70	0.25	0.05	0.98	0.50	0.00
NOV	5.86	0.50	0.03	7.03	0.50	0.02	7.45	0.50	0.01	9.29	0.25	0.03
DEC	2.29	0.50	0.01	0.50	0.50	0.00	-9.05	0.50	0.02	-2.43	0.50	0.00
JAN	8.62	**0.05**	0.10	11.25	0.10	0.08	10.78	0.50	0.02	3.04	0.50	0.00
FEB	0.12	0.50	0.00	-3.53	0.50	0.01	-9.67	0.50	0.02	-2.96	0.50	0.00
MAR	8.59	**0.01**	0.20	5.53	0.25	0.04	11.08	0.25	0.06	2.33	0.50	0.00
APR	-0.48	0.50	0.01	0.05	0.50	0.00	6.08	0.25	0.05	1.25	0.50	0.00
MAY	-0.33	0.50	0.00	-0.41	0.50	0.00	2.33	0.50	0.01	1.36	0.50	0.01
JUN	-1.29	0.50	0.02	-1.41	0.50	0.02	-2.05	0.50	0.02	0.81	0.50	0.01
JUL	-0.40	0.50	0.01	-0.37	0.50	0.00	-0.31	0.50	0.00	0.39	0.50	0.01
AUG	0.19	0.50	0.01	0.14	0.50	0.00	0.78	0.25	0.05	0.24	0.50	0.01
SEP	-0.07	0.50	0.00	-0.47	0.50	0.00	-1.25	0.50	0.01	0.01	0.50	0.00
1-day min	0.61	**0.03**	0.13	0.40	0.50	0.02	0.80	0.10	0.09	-0.07	0.50	0.00
3-day min	0.55	**0.03**	0.12	0.49	0.50	0.02	0.80	0.10	0.09	-0.06	0.50	0.00
7-day min	0.45	**0.05**	0.10	0.31	0.50	0.01	0.78	0.10	0.08	-0.05	0.50	0.00
30-day min	0.24	0.25	0.03	0.43	0.50	0.02	0.89	0.10	0.07	0.12	0.50	0.00
90-day min	-0.09	0.50	0.00	-0.32	0.50	0.01	-0.06	0.50	0.00	0.32	0.50	0.01
1-day max	-33.53	0.10	0.07	-26.26	0.50	0.02	-4.57	0.50	0.00	58.02	0.10	0.03
3-day max	-31.48	**0.05**	0.09	-27.58	0.25	0.03	-10.44	0.50	0.00	33.09	0.25	0.02
7-day max	-21.15	**0.05**	0.10	-23.62	0.25	0.05	-25.36	0.50	0.02	22.63	0.25	0.03
30-day max	-3.21	0.50	0.01	-4.95	0.50	0.01	-3.90	0.50	0.00	5.41	0.50	0.01
90-day max	-0.48	0.50	0.00	-0.66	0.50	0.00	1.31	0.50	0.00	5.87	0.50	0.02
# of zero days	0.00	0.50	0.00	0.00	0.50	0.00	0.00	0.50	0.00	0.00	0.50	0.00
Base flow index	0.00	0.50	0.00	0.00	0.50	0.00	0.00	0.50	0.01	0.00	0.25	0.02
Date of min	0.77	0.50	0.01	-0.31	0.50	0.03	0.16	0.50	0.01	0.10	0.25	0.02
Date of max	1.09	0.50	0.01	0.76	0.50	0.00	-1.10	0.50	0.01	1.05	0.25	0.03
Low pulse #	-0.20	**0.00**	0.49	-0.05	**0.05**	0.09	-0.05	**0.05**	0.10	-0.01	**0.05**	0.04
Low pulse dur.	0.18	0.50	0.02	0.14	0.50	0.01	0.26	0.25	0.05	0.05	0.50	0.00
High pulse #	-0.06	0.25	0.06	-0.05	0.25	0.04	-0.05	0.25	0.05	0.00	0.50	0.00
High pulse dur.	0.08	0.25	0.06	0.06	0.25	0.05	0.15	**0.03**	0.13	0.03	0.25	0.03
Rise rate	-1.06	**0.01**	0.16	-0.95	**0.03**	0.14	-0.92	0.25	0.04	-1.57	**0.01**	0.11
Fall rate	0.72	0.10	0.09	0.34	**0.05**	0.09	0.17	0.50	0.01	0.41	**0.01**	0.11
# of reversals	-0.01	0.50	0.00	0.03	0.50	0.00	0.01	0.50	0.00	0.01	0.50	0.00

Table B.10. Non-parametric regression statistics for all EFC hydrological parameter groups for the Wynoochee and Satsop Rivers. Statistically significant regressions are highlighted in green and bold. Values less than 0.01 are indicated by a value of 0.00. EFC parameter names are abbreviated from the list provided in the methods section.

| | Wynoochee - Post Dam, Below Reservoir | | | | | | | | | Satsop River | | |
| | 12035400 (1973-2015) | | | 12036000 (1972-2015) | | | 12037400 (1972-2015) | | | 12035000 (1930-2015) | | |
EFC Parameter	Slope	P	R²	Slope	P	R²	Slope	P	R²	Slope	P	R²
OCT Low Flow	-1.03	0.50	0.03	0.73	0.50	0.01	2.51	0.50	0.02	1.01	0.50	0.00
NOV Low Flow	0.04	0.50	0.00	-1.17	0.50	0.01	1.95	0.50	0.01	1.17	0.50	0.00
DEC Low Flow	0.23	0.50	0.00	-1.00	0.50	0.01	1.16	0.50	0.00	1.42	0.50	0.01
JAN Low Flow	1.67	0.25	0.06	2.76	0.25	0.05	6.81	**0.03**	0.13	2.48	0.25	0.02
FEB Low Flow	1.56	0.25	0.04	1.18	0.50	0.01	3.28	0.50	0.03	0.08	0.50	0.00
MAR Low Flow	1.57	0.25	0.06	2.48	0.25	0.05	5.62	0.10	0.07	-1.12	0.50	0.00
APR Low Flow	-0.19	0.50	0.00	0.43	0.50	0.00	4.84	**0.05**	0.10	1.21	0.50	0.01
MAY Low Flow	-1.01	0.50	0.02	-1.04	0.50	0.01	1.03	0.50	0.00	1.33	0.50	0.01
JUN Low Flow	0.20	0.50	0.00	-1.13	0.50	0.02	-1.89	0.50	0.02	0.85	0.50	0.01
JUL Low Flow	-0.18	0.50	0.00	-0.05	0.50	0.00	0.04	0.50	0.00	0.38	0.50	0.01
AUG Low Flow	0.15	0.50	0.00	-0.21	0.50	0.01	0.00	0.50	0.00	0.43	0.25	0.03
SEP Low Flow	0.62	0.50	0.01	-1.03	0.50	0.01	-1.39	0.50	0.01	-1.05	0.50	0.01
Extreme low peak	-0.28	**0.05**	0.13	-0.23	0.50	0.02	-0.03	0.50	0.00	0.05	0.50	0.00
Extreme low dur.	0.52	**0.01**	0.23	0.33	**0.05**	0.12	0.45	**0.03**	0.14	-0.01	0.50	0.00
Extreme low timing	1.42	0.25	0.04	0.05	0.50	0.00	0.02	0.50	0.00	0.00	0.50	0.00
Extreme low freq.	-0.19	**0.00**	0.55	-0.05	**0.03**	0.11	-0.07	**0.01**	0.21	-0.01	0.50	0.01
High flow peak	-5.09	0.50	0.03	6.07	0.50	0.02	34.10	0.10	0.09	9.19	0.25	0.02
High flow dur.	0.11	0.25	0.06	0.07	0.10	0.07	0.15	**0.05**	0.10	0.01	0.50	0.01
High flow timing	-1.72	0.50	0.03	0.27	0.50	0.00	-0.06	0.50	0.00	-0.03	0.50	0.00
High flow freq.	-0.05	0.25	0.04	-0.04	0.50	0.02	-0.04	0.25	0.04	-0.01	0.50	0.00
High flow rise rate	-0.59	0.50	0.00	1.76	0.50	0.02	-0.51	0.50	0.00	-0.38	0.50	0.00
High flow fall rate	1.78	0.10	0.09	2.30	0.10	0.08	1.53	0.50	0.02	-0.38	0.50	0.00
Small Flood peak	-4.70	0.50	0.01	-6.96	0.50	0.02	-30.46	0.25	0.11	10.17	0.50	0.01
Small Flood dur.	0.40	0.25	0.09	0.50	0.10	0.18	0.20	0.50	0.03	-0.11	0.50	0.03
Small Flood timing	3.07	0.50	0.06	0.65	0.50	0.00	-0.30	0.50	0.00	0.12	0.50	0.00
Small Flood freq.	-0.01	0.25	0.06	-0.01	0.50	0.03	-0.01	0.50	0.01	0.01	0.10	0.04
Small Flood riserate	-23.20	0.10	0.20	-7.95	0.50	0.01	-5.03	0.50	0.00	43.93	0.25	0.04
Small Flood fallrate	9.68	0.10	0.16	9.08	0.10	0.17	9.69	0.50	0.07	-9.61	0.25	0.06
Large flood peak	49.50	0.50	0.19	102.90	0.10	0.72	-115.60	0.50	0.07	-14.35	0.50	0.00
Large flood dur.	-0.07	0.50	0.00	1.48	**0.00**	0.97	-1.23	**0.01**	0.93	0.12	0.50	0.04
Large flood timing	-2.04	0.50	0.35	-1.10	0.50	0.21	-18.72	0.10	0.68	2.28	0.50	0.13
Large flood freq.	0.00	0.25	0.04	0.00	0.50	0.02	0.00	0.50	0.01	0.00	0.50	0.01
Large flood riserate	231.60	0.10	0.72	30.52	0.50	0.03	241.30	**0.01**	0.91	-130.20	0.25	0.22
Large flood fallrate	-18.88	0.50	0.06	16.00	0.50	0.46	-25.04	0.50	0.09	9.41	0.50	0.06

Median July, August, and September flows were significantly higher at all three gages following dam construction (Table B.11, B.12, and B.13). The greatest increases were observed at the gage farthest downstream from the dam while increases were similar at the two gages closest to the dam (Table B.11, B.12, and B.13). We also detected significant decreases in median monthly flows in April at both gages closest to the dam, and in May at the gage closest to the dam (Table B.12 and B.13). High pulse count and the number of reversals were also significantly reduced closest to the dam following dam construction (Table B.13). Farther downstream, low pulse counts, low pulse duration, rise rate, and fall rates were significantly reduced while the number of reversals increased significantly following dam construction (Table B.12). At the station farthest from the dam, we also detected significantly lower fall rates following dam construction (Table B.11).

In the period after dam construction on the Wynoochee River, we detected significant positive trends in minimum annual flows and significant negative trends in maximum annual flows only at the station closest to the dam (Table B.9). Median flows in the months of January and March also had significant positive trends over time at the station closest to the dam (Table B.9). We also detected a consistent decreasing trend for low pulse counts and extreme low frequencies at all three stations below the Wynoochee River dam in the period after dam construction (Table B.9 and Table B.10). The decreasing trend in the frequency of extreme low flow events was coupled with a consistent increasing trend in the duration of extreme low flow events at all three stations below the Wynoochee River dam (Table B.10).

B.2.2 Relationships among Climate and Flow Metrics

High flow metrics

Annual maximum 1-day flows had strong positive correlations with both total annual cumulative precipitation and cumulative precipitation in the 4-days prior to the peak annual flow event, with statistically significant correlations being observed at all stations (Table B.14). Correlations between 1-day maximum flow and cumulative winter Pacific Decadal Oscillation (PDO) were consistently negative throughout the Chehalis basin stations, although the correlations were only statistically significant for the three Skookumchuck stations. Correlations between 1-day maximum flows and all other climate metrics varied in both direction and strength throughout the basin.

Table B.11. Non-Parametric IHA Scorecard for pre-impact (1957-1972) and post-impact (1973-2016) at USGS 12037400 below the Wynoochee River Dam. Bold values indicate statistical significance at p < 0.05.

IHA Parameter	MEDIANS		COEFF. of DISP.		Deviation Factor		Significance Count	
	Pre	Post	Pre	Post	Medians	C.D.	Medians	C.D.
October (CFS)	500	440	1.118	1.514	0.12	0.3539	0.7187	0.3173
November (CFS)	1488	1490	0.7997	1.227	0.001681	0.5345	0.9930	0.1291
December (CFS)	2295	1710	0.4096	1.07	0.2549	1.613	0.3383	0.0040
January (CFS)	2065	1820	0.6816	0.7308	0.1186	0.07214	0.5816	0.8098
February (CFS)	1793	1630	0.7476	0.638	0.09066	0.1465	0.6136	0.5646
March (CFS)	1580	1230	0.6158	0.748	0.2215	0.2146	0.1972	0.4434
April (CFS)	966.5	767.5	0.6176	0.6182	0.2059	0.001097	0.1241	0.999
May (CFS)	658	566	0.5756	0.7049	0.1398	0.2247	0.3974	0.4535
June (CFS)	357	415.5	0.791	0.6113	0.1639	0.2271	0.3944	0.3944
July (CFS)	159	299	0.4843	0.4415	0.8805	0.08839	**<0.0001**	0.7678
August (CFS)	73.5	217	1.786	0.318	1.952	0.8219	**<0.0001**	0.06406
September (CFS)	86.5	237.5	1.428	0.7347	1.746	0.4854	**<0.0001**	0.3654
1-day minimum (CFS)	25.5	163	1.861	0.2454	5.392	0.8681	**<0.0001**	0.1762
3-day minimum (CFS)	27.67	163.3	1.757	0.2449	4.904	0.8606	**<0.0001**	0.1852
7-day minimum (CFS)	35.43	167.6	1.514	0.2575	3.73	0.8299	**<0.0001**	0.1812
30-day minimum (CFS)	67.62	197.5	1.15	0.2766	1.921	0.7594	**<0.0001**	0.1101
90-day minimum (CFS)	136.2	263.3	1.121	0.3639	0.9332	0.6755	**<0.0001**	0.04905
1-day maximum (CFS)	12650	11900	0.6364	0.4008	0.05929	0.3701	0.4595	0.2703
3-day maximum (CFS)	10250	10180	0.426	0.3906	0.006345	0.08297	0.8849	0.8478
7-day maximum (CFS)	6289	7324	0.4898	0.4763	0.1646	0.02752	0.1662	0.9129
30-day maximum (CFS)	3610	3718	0.3337	0.4581	0.03006	0.3729	0.7528	0.1331
90-day maximum (CFS)	2873	2719	0.3296	0.3851	0.05369	0.1684	0.5686	0.5726
Number of zero days (n)	0	0	0	0				
Base flow index	0.03005	0.138	1.121	0.2711	3.594	0.7582	**<0.0001**	0.2122
Date of minimum (Julian)	248	261	0.0888	0.1202	0.07104	0.3538	0.2292	0.1471
Date of maximum (Julian)	354	350	0.1086	0.1557	0.02186	0.434	0.9079	0.1291
Low pulse count (n)	3	3	0.6667	1	0	0.5	0.4975	0.09309
Low pulse duration (days)	23.5	13.25	1.968	1.642	0.4362	0.1659	0.1141	0.7568
High pulse count (n)	11	9	0.4318	0.3333	0.1818	0.2281	0.0581	0.5215
High pulse duration (days)	5	5.5	0.675	0.7273	0.1	0.07744	0.4655	0.8398
Rise rate (CFS)	125	90	0.696	0.6611	0.28	0.05013	0.1151	0.9139
Fall rate (CFS)	-56	-40	-0.6317	-0.625	0.2857	0.0106	**0.0230**	0.993
Number of reversals (n)	99.5	96	0.08291	0.125	0.03518	0.5076	0.2623	0.1081

Table B.12. Non-Parametric IHA Scorecard for pre-impact (1925-1972) and post-impact (1973-2016) at USGS 12036000 below the Wynoochee River Dam. Bold values indicate statistical significance at p < 0.05.

IHA Parameter	MEDIANS		COEFF. of DISP.		Deviation Factor		Significance Count	
	Pre	Post	Pre	Post	Medians	C.D.	Medians	C.D.
October (CFS)	407	385.5	0.844	0.963	0.05283	0.1411	0.7958	0.5295
November (CFS)	874	939.8	0.7223	1.206	0.07523	0.6704	0.8008	0.006006
December (CFS)	1145	1215	0.5002	0.7385	0.06114	0.4763	0.6667	0.05105
January (CFS)	970	1085	0.6649	0.9025	0.1186	0.3573	0.1301	0.1301
February (CFS)	931	946.5	0.7876	0.6046	0.01665	0.2324	0.8498	0.3233
March (CFS)	786	718.5	0.5709	0.6343	0.08588	0.111	0.5566	0.6717
April (CFS)	697.5	519.8	0.4373	0.3733	0.2548	0.1464	**<0.0001**	0.5646
May (CFS)	554	455.5	0.5487	0.5324	0.1778	0.0298	0.06507	0.8799
June (CFS)	396.3	389.3	0.6009	0.4313	0.01767	0.2823	0.7928	0.1451
July (CFS)	228.5	340.5	0.5591	0.2746	0.4902	0.5088	**<0.0001**	0.03303
August (CFS)	155	286.5	0.4065	0.1667	0.8484	0.5899	**<0.0001**	0.02002
September (CFS)	144.5	309.5	0.519	0.4786	1.142	0.07791	**<0.0001**	0.7598
1-day minimum (CFS)	106	250	0.25	0.143	1.358	0.428	**<0.0001**	0.2332
3-day minimum (CFS)	106.8	251.5	0.2574	0.1435	1.354	0.4426	**<0.0001**	0.2262
7-day minimum (CFS)	109.9	254.5	0.2715	0.1374	1.317	0.4939	**<0.0001**	0.1291
30-day minimum (CFS)	132	269.8	0.3652	0.1506	1.044	0.5875	**<0.0001**	0.03504
90-day minimum (CFS)	206.3	321.3	0.4968	0.2027	0.5578	0.5919	**<0.0001**	0.02603
1-day maximum (CFS)	7090	7245	0.6358	0.4079	0.02186	0.3585	0.7307	0.1762
3-day maximum (CFS)	5440	5862	0.5933	0.4774	0.07751	0.1953	0.3664	0.3684
7-day maximum (CFS)	3765	4300	0.487	0.5199	0.1421	0.06745	0.1121	0.7417
30-day maximum (CFS)	2089	2321	0.3409	0.4302	0.1111	0.2622	0.1291	0.2713
90-day maximum (CFS)	1564	1761	0.2942	0.3738	0.1261	0.2706	0.1211	0.3123
Number of zero days (n)	0	0	0	0				
Base flow index	0.1448	0.2923	0.2466	0.2909	1.019	0.1798	**<0.0001**	0.5365
Date of minimum (Julian)	258	265	0.07719	0.1066	0.03825	0.3805	0.4705	0.1001
Date of maximum (Julian)	358	352.5	0.1516	0.1612	0.03005	0.06306	0.5826	0.7788
Low pulse count (n)	3	1	1	2	0.6667	1	**<0.0001**	0.01602
Low pulse duration (days)	14.5	7	1.431	1.357	0.5172	0.05164	**0.01802**	0.8599
High pulse count (n)	13	11	0.2885	0.4545	0.1538	0.5758	0.1451	0.05205
High pulse duration (days)	4.5	5	0.4444	0.7	0.1111	0.575	0.2042	0.07107
Rise rate (CFS)	117	61.5	0.531	0.7134	0.4744	0.3436	**0.004004**	0.1061
Fall rate (CFS)	-36	-20	-0.5556	-0.7	0.4444	0.26	**<0.0001**	0.3984
Number of reversals (n)	91	98	0.1676	0.1199	0.07692	0.2845	**0.003003**	0.3854

Table B.13. Non-Parametric IHA Scorecard for pre-impact (1966-1972) and post-impact (1973-2016) at USGS 12035400 below the Wynoochee River Dam. Bold values indicate statistical significance at p < 0.05.

| IHA Parameter	MEDIANS		COEFF. of DISP.		Deviation Factor		Significance Count	
	Pre	Post	Pre	Post	Medians	C.D.	Medians	C.D.
October (CFS)	276	283	1.877	0.4885	0.02536	0.7397	0.9169	0.0951
November (CFS)	695.5	530.8	0.3019	1.326	0.2369	3.393	0.5375	0.001001
December (CFS)	730	665.5	0.411	0.9467	0.08836	1.304	0.7397	0.02703
January (CFS)	662	628	0.6012	0.8225	0.05136	0.368	0.7207	0.3363
February (CFS)	568	513.5	0.5396	0.6322	0.09595	0.1715	0.5886	0.7147
March (CFS)	510	343	0.5902	0.8717	0.3275	0.477	0.1762	0.1752
April (CFS)	525	222	0.4352	0.1622	0.5771	0.6274	**<0.0001**	0.5546
May (CFS)	398	240	0.9171	0.5563	0.397	0.3935	**0.02202**	0.2442
June (CFS)	309	247	0.4078	0.5233	0.2006	0.2833	0.3013	0.5115
July (CFS)	161	238	0.1553	0.3162	0.4783	1.036	**<0.0001**	0.06707
August (CFS)	96	222.5	0.9375	0.1629	1.318	0.8262	**<0.0001**	0.06206
September (CFS)	120	243.3	1.125	0.3895	1.027	0.6538	**<0.0001**	0.2442
1-day minimum (CFS)	60	196	0.4333	0.07015	2.267	0.8381	**<0.0001**	0.2022
3-day minimum (CFS)	60	196.2	0.4278	0.07901	2.269	0.8153	**<0.0001**	0.3373
7-day minimum (CFS)	67.14	197.4	0.4021	0.06711	1.94	0.8331	**<0.0001**	0.3644
30-day minimum (CFS)	92.43	205.5	0.4623	0.07234	1.223	0.8435	**<0.0001**	0.2002
90-day minimum (CFS)	136.2	236.4	0.6081	0.201	0.7361	0.6695	**<0.0001**	0.1101
1-day maximum (CFS)	4260	4755	0.8498	0.4485	0.1162	0.4722	0.3003	0.2372
3-day maximum (CFS)	3137	3660	0.9458	0.4235	0.1668	0.5522	0.2683	0.1461
7-day maximum (CFS)	2083	2581	1.015	0.4583	0.2394	0.5485	0.1181	0.1311
30-day maximum (CFS)	1142	1401	0.7951	0.3993	0.2267	0.4978	0.1572	0.1011
90-day maximum (CFS)	906.6	1038	0.5405	0.4169	0.145	0.2286	0.2633	0.5225
Number of zero days (n)	0	0	0	0				
Base flow index	0.1336	0.3678	0.3702	0.2705	1.753	0.2693	**<0.0001**	0.8338
Date of minimum (Julian)	258	144.5	0.09016	0.4638	0.6202	4.144	0.1652	0.01201
Date of maximum (Julian)	342	342.5	0.1913	0.1687	0.002732	0.1179	0.974	0.7467
Low pulse count (n)	3	2	1.667	1.5	0.3333	0.1	0.3243	0.8498
Low pulse duration (days)	12	6	3.083	1.688	0.5	0.4527	0.3574	0.6667
High pulse count (n)	16	9	0.5	0.5278	0.4375	0.05556	**0.01001**	0.9309
High pulse duration (days)	4	5.5	0.75	0.8182	0.375	0.09091	0.2993	0.8448
Rise rate (CFS)	96.5	12	0.5751	2.531	0.8756	3.401	0.1071	0.009009
Fall rate (CFS)	-30	-33.5	-0.5833	-1.321	0.1167	1.264	0.7347	0.03303
Number of reversals (n)	99	68.5	0.1111	0.2445	0.3081	1.201	**<0.0001**	0.008008
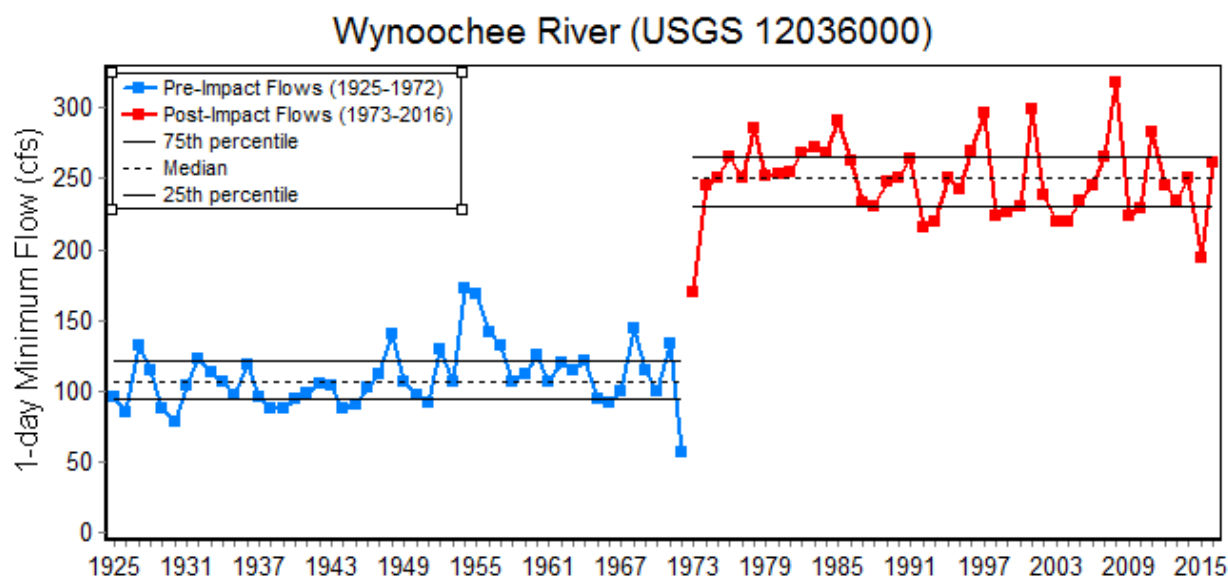
Figure B.6. Two-period comparison of 1-day minimum flows on the Wynoochee River downstream of the Wynoochee dam (USGS 12036000) before (Pre-Impact Flows) and after (Post-Impact Flows) dam construction in 1972. Median 1-day minimum flows, and the 25th and 75th percentile 1-day minimum flows, are also shown for the pre and post-impact periods.

High flow duration had a consistent positive correlation with cumulative annual precipitation throughout the basin, although the correlations were only statistically significant in the Newaukum, farthest downstream Skookumchuck, and middle Wynoochee stations (Table B.14). Correlations between high flow duration and all other climate metrics varied in both the direction and strength throughout the basin, although several correlations were statistically significant. These included a significant positive correlation between cumulative winter NPGO and high flow duration at Satsop and the farthest upriver Wynoochee stations, and cumulative summer UWI and the farthest downstream Wynoochee station. Strong negative correlations between cumulative winter UWI and high flow duration was observed at all three Wynoochee stations, although the correlation was statistically significant at only the farthest upriver station.

Correlations between high flow frequency and climate metrics were generally mixed in direction and strength across the basin, although a few patterns and statistically significant correlations were observed (Table B.14). Correlations between average summer SL and high flow frequency were consistently positive throughout the basin, with statistically significant correlations being observed at the farthest upriver and downstream stations on the Wynoochee River. Cumulative winter UWI was negatively correlated with high flow frequency at all but one station, with a statistically significant correlation for the farthest downstream station on the Skookumchuck River. Correlations between cumulative summer UWI and high flow frequency were negatively correlated with all but one station,

171

with a statistically significant correlation being observed at the farthest downstream station on the Wynoochee River.

Table B.14. Correlations of high flow metrics from IHA analysis with local and regional climate metrics for all USGS stations. Climate metrics are four-day antecedent precipitation for date of 1-day maximum flow (4-day Sum PRCP – for 1-day maximum flows only); total cumulative annual precipitation at Aberdeen, WA (Total PRCP); total cumulative annual snowfall at Aberdeen, WA (Total SNOW); cumulative summer southern oscillation index (Summer SOI); cumulative summer upwelling index (Summer UWI); average summer sea level (Summer SL); cumulative winter north pacific gyre oscillation index (Winter NPGO); cumulative winter pacific decadal oscillation index (Winter PDO); and cumulative winter upwelling index (Winter UWI). Pearson's correlation values are provided in each cell, with statistically significant (α = 0.05) correlations being bold. Shading indicates both the strength and direction of the correlation, with blue for positive correlations to red for negative correlations and the intensity increasing with increasing deviation from zero.

IHA Metric	River	USGS Site	4-day Total Prcp	Total Prcp	Total Snow	Sum. SOI	Sum. UWI	Sum. SL	Win. NPGO	Win. PDO	Win. UWI
1-day max	Chehalis	12020000	**0.36**	**0.30**	-0.15	0.02	-0.02	-0.24	0.05	-0.25	0.17
	Chehalis	12027500	**0.48**	**0.50**	-0.03	-0.05	0.11	-0.12	-0.09	-0.18	0.06
	Newaukum	12025000	**0.63**	**0.40**	-0.15	-0.10	-0.04	**-0.28**	0.10	-0.11	0.15
	Satsop	12035000	**0.36**	**0.39**	-0.19	-0.20	-0.22	-0.04	-0.21	-0.11	0.03
	Skookumchuck	12025700	**0.37**	**0.39**	-0.08	-0.04	0.00	-0.12	0.05	**-0.41**	0.20
	Skookumchuck	12026150	**0.58**	**0.53**	0.25	-0.16	-0.13	0.24	-0.04	**-0.51**	0.15
	Skookumchuck	12026400	**0.68**	**0.57**	0.01	-0.05	0.20	-0.17	-0.05	**-0.31**	0.05
	Wynoochee	12035400	**0.39**	**0.53**	0.16	-0.05	-0.06	0.18	-0.20	-0.10	-0.15
	Wynoochee	12036000	**0.39**	**0.48**	0.13	0.01	0.08	0.04	-0.20	-0.10	-0.26
	Wynoochee	12037400	**0.33**	**0.35**	0.08	-0.15	0.04	-0.09	-0.28	-0.25	-0.09
High flow duration	Chehalis	12020000		0.26	0.03	0.12	-0.04	0.09	0.11	-0.05	-0.17
	Chehalis	12027500		0.25	-0.10	0.08	-0.07	-0.24	-0.01	0.12	-0.03
	Newaukum	12025000		**0.36**	0.11	0.09	-0.08	-0.12	-0.03	0.02	0.01
	Satsop	12035000		0.25	-0.07	-0.05	0.11	-0.02	**0.34**	0.20	-0.09
	Skookumchuck	12025700		0.22	-0.04	0.17	-0.08	-0.16	0.03	-0.17	0.11
	Skookumchuck	12026150		0.18	-0.10	0.04	-0.17	0.00	-0.23	-0.01	0.01
	Skookumchuck	12026400		**0.33**	0.05	0.10	-0.13	-0.21	-0.02	-0.17	0.08
	Wynoochee	12035400		0.05	-0.08	-0.02	0.12	-0.22	**0.33**	0.22	**-0.41**
	Wynoochee	12036000		**0.46**	-0.11	-0.07	0.03	-0.31	0.16	0.19	-0.26
	Wynoochee	12037400		0.25	0.09	-0.07	**0.34**	-0.25	0.24	0.21	-0.31
High flow frequency	Chehalis	12020000		0.07	0.15	0.03	-0.18	0.13	-0.12	-0.02	-0.02
	Chehalis	12027500		-0.08	0.04	0.15	-0.15	0.24	-0.26	0.03	-0.03
	Newaukum	12025000		-0.08	-0.06	0.19	-0.15	0.14	-0.19	0.05	-0.06
	Satsop	12035000		0.08	0.23	0.10	0.02	0.02	-0.19	0.01	-0.03
	Skookumchuck	12025700		0.08	0.22	0.04	-0.18	0.20	-0.06	0.09	-0.10
	Skookumchuck	12026150		0.21	0.09	0.28	-0.24	0.11	0.04	0.09	-0.26
	Skookumchuck	12026400		0.24	0.33	0.18	-0.21	0.33	-0.18	0.02	**-0.39**
	Wynoochee	12035400		**0.33**	0.00	-0.14	-0.25	**0.42**	-0.14	-0.12	0.10
	Wynoochee	12036000		0.04	0.07	0.21	-0.12	0.31	-0.05	0.01	-0.06
	Wynoochee	12037400		0.00	-0.17	0.21	**-0.41**	**0.46**	-0.01	0.02	-0.07

Low flow metrics

Annual 1-day minimum flows had consistently positive correlations with cumulative annual precipitation, with statistically significant correlations being observed at the Newaukum, Satsop, and farthest downstream station on the Wynoochee River (Table B.15). Annual 1-day minimum flows were also consistently correlated with cumulative summer UWI, with all stations being negatively correlated with summer UWI. However, the correlations between 1-day minimum and summer UWI were statistically significant at only the farthest downstream Wynoochee and Chehalis River stations. Average summer SL was also strongly related to annual 1-day minimum flows in the Chehalis, Newaukum, Satsop, and farthest upriver Skookumchuck River stations, although the correlations differed in direction among these stations (Table B.15). Cumulative winter PDO had strong statistically significant negative correlations with 1-day minimum flows at the Satsop, farthest upriver Skookumchuck, and farthest downstream Wynoochee River Stations.

Total cumulative annual snowfall was also strongly correlated with 1-day minimum flows for a subset of stations, with a significant positive correlation being observed at the farthest upriver station above the reservoir on the Skookumchuck and statistically significant negative correlations at the two stations downstream of the reservoir (Table B.15). Annual minimum flows for the middle station on the Wynoochee River also had a statistically significant correlation with total annual snowfall. The base flow index had a consistently negative and statistically significant correlation with total annual precipitation throughout the basin. Correlations with base flow index also had consistent positive correlations with winter PDO and UWI, with a subset of these correlations being statistically significant. Base flow was also negatively correlated with summer UWI at all but one station.

The duration of extreme low flows was consistently negatively correlated with total annual precipitation, but was only statistically significant at the middle Wynoochee River station (Table B.15). Extreme low flow duration had consistent positive correlations with winter PDO, with the correlation being statistically significant at the farthest downstream station on the Wynoochee River. Summer UWI was positively correlated with extreme low flow duration for all but one station, with statistically significant correlations observed at the farthest upriver Skookumchuck and farthest downstream Wynoochee stations. Correlations between extreme low flow frequency and climate metrics were mixed in strength and direction throughout the basin. While some correlations were statistically significant, no strong patterns were apparent.

June low flows had consistently positive correlations with total annual precipitation, summer SOI, and winter NPGO, although correlations were only statistically significant among a subset of stations with total precipitation and summer SOI correlations (Table B.15). Winter PDO was also consistently negatively correlated with June low flows at all three Wynoochee stations, with non-significant negative correlations being observed at all other stations except one. Summer UWI was also consistently negatively correlated with June low flows, with statistically significant correlations observed at the farthest upriver Chehalis and Skookumchuck stations.

Table B.15. Correlations of low flow metrics from IHA analysis with local and regional climate metrics for all USGS stations.

IHA Metric	River	USGS Site	Total Prcp	Total Snow	Sum. SOI	Sum. UWI	Sum. SL	Win. NPGO	Win. PDO	Win. UWI
1-day min	Chehalis	12020000	0.07	0.18	0.16	-0.25		0.15	-0.12	
	Chehalis	12027500	0.15	-0.21		**-0.28**	**-0.47**	0.08		0.13
	Newaukum	12025000	**0.31**	-0.17	0.18	-0.20	**-0.26**	**0.36**	-0.21	
	Satsop	12035000	**0.27**	0.18	0.07	-0.16	**0.36**	0.05	**-0.30**	0.19
	Skookumchuck	12025700	0.08	**0.42**	0.05	-0.09	0.26	0.07	**-0.44**	0.16
	Skookumchuck	12026150	0.14	**-0.52**	-0.01	-0.01	-0.11	-0.05	0.05	-0.15
	Skookumchuck	12026400	0.24	**-0.32**	-0.12	-0.04	-0.08		-0.05	-0.06
	Wynoochee	12035400	0.25	-0.04	-0.19	-0.13		0.08	-0.08	
	Wynoochee	12036000	0.11	**-0.43**	0.16	-0.11		-0.02	0.17	
	Wynoochee	12037400	**0.37**	0.00	0.21		0.07		**-0.36**	0.11
base flow index	Chehalis	12020000	**-0.54**	-0.03	0.00	-0.14	0.11	0.15	0.15	
	Chehalis	12027500	**-0.62**	**-0.28**	-0.08	-0.21	-0.26	0.14		**0.31**
	Newaukum	12025000	**-0.47**	-0.22	-0.05	-0.17	-0.10		0.13	
	Satsop	12035000	**-0.65**		0.04	-0.10	0.24		0.12	
	Skookumchuck	12025700	**-0.63**	0.02	-0.08	-0.03	0.13	0.04	0.21	0.18
	Skookumchuck	12026150	**-0.72**	**-0.42**	-0.07	0.10	-0.26	0.12	**0.35**	0.11
	Skookumchuck	12026400	**-0.56**	-0.31	-0.20	-0.14	0.09	0.03	0.21	0.20
	Wynoochee	12035400	**-0.75**		-0.03	-0.14	0.00		0.23	**0.42**
	Wynoochee	12036000	**-0.71**	**-0.36**	0.02	-0.25	0.16		0.29	**0.36**
	Wynoochee	12037400	**-0.62**	-0.04		**-0.37**	0.12	0.13		**0.45**
extreme low flow duration	Chehalis	12020000	-0.20	-0.02	-0.17	**0.36**	-0.18	-0.06	0.15	
	Chehalis	12027500	-0.16	0.12		0.18	-0.10		0.26	-0.15
	Newaukum	12025000	-0.10		-0.24		0.03	0.09	0.10	-0.04
	Satsop	12035000	-0.28	-0.15	0.05	0.20	-0.10	0.02	0.20	-0.26
	Skookumchuck	12025700	-0.14	-0.18	0.01	**0.48**	-0.15	-0.01	0.33	-0.11
	Skookumchuck	12026150	-0.18	-0.07	0.31	0.13	-0.37	0.09	0.10	-0.13
	Skookumchuck	12026400	-0.07	-0.12	-0.04	0.26	-0.22	0.09	0.38	-0.26
	Wynoochee	12035400	-0.12	-0.17	-0.26	0.23	-0.14	-0.16	0.10	0.21
	Wynoochee	12036000	**-0.34**	-0.13	0.13	0.09	-0.28	0.15	0.14	0.05
	Wynoochee	12037400	-0.23	-0.12	-0.28	**0.44**	-0.15	-0.19	**0.39**	0.14
extreme low flow frequency	Chehalis	12020000	0.04	-0.03	0.00	0.07	-0.16	-0.11	0.03	-0.10
	Chehalis	12027500	0.24	0.23	-0.11	-0.02	**0.29**	-0.12	-0.23	-0.03
	Newaukum	12025000	**-0.31**	0.12	-0.07	**0.32**	-0.03	**-0.46**	0.12	0.04
	Satsop	12035000	-0.06	0.00	0.00	0.13	-0.14	-0.11	0.24	-0.06
	Skookumchuck	12025700	-0.25	-0.15	0.08	-0.09	**-0.29**	-0.03	0.18	-0.08
	Skookumchuck	12026150	-0.25	0.26	**-0.36**	0.07	0.21	0.09	-0.04	0.17
	Skookumchuck	12026400	**-0.32**	-0.02	0.01	-0.14	0.06	-0.04	-0.08	0.11
	Wynoochee	12035400	-0.20	0.26	**0.38**	-0.04	0.10	-0.10	0.13	-0.02
	Wynoochee	12036000	0.01			0.02	0.18	-0.26	-0.06	-0.18
	Wynoochee	12037400	-0.15	0.29	0.09	-0.09	0.12	-0.29	-0.04	-0.11
June low flow	Chehalis	12020000	0.14	-0.08	**0.26**	**-0.30**	-0.04	0.18	0.02	0.04
	Chehalis	12027500	0.25	-0.12	**0.33**	-0.22	-0.21	0.22	0.00	-0.06
	Newaukum	12025000	**0.27**	-0.19	0.23	-0.25	-0.14	0.20	-0.02	-0.08
	Satsop	12035000	0.23	-0.09	0.14	-0.36	-0.06	0.24	-0.06	0.09
	Skookumchuck	12025700	0.25	0.02	0.26	**-0.31**	0.03	0.17	-0.14	-0.09
	Skookumchuck	12026150	0.26	-0.11	**0.48**	-0.01	-0.31	0.28	-0.16	-0.13
	Skookumchuck	12026400	**0.34**	-0.06	**0.36**	-0.18	-0.18	0.20	-0.21	-0.11
	Wynoochee	12035400	**0.35**	-0.05	0.03	-0.21	0.00	0.35	**-0.35**	0.00
	Wynoochee	12036000	**0.40**	0.04	0.18	-0.14	0.08	0.26	**-0.37**	-0.05
	Wynoochee	12037400	**0.38**	-0.08	0.28	-0.27	0.07	0.24	**-0.33**	0.00

Appendix C. Fine Sediment Supply Assessment

Sediment supply to streams is an essential natural process for maintaining channel morphology and sustaining fish habitat (Beechie et al. 2010, 2013c). However, increased sediment supply due to land uses can overwhelm river channels, resulting in increased fines in the bed, pool filling, channel aggradation, and channel widening (Beechie et al. 2005b, 2013c). On the other hand, loss of sediment storage mechanisms such as large wood jams can result in sediment poor bedrock channels (Montgomery et al. 1996). The fine sediment fraction (sand and smaller) is typically produced by surface erosion (especially from forest roads or agricultural lands), and tends to increase fine sediment in spawning gravels or partially fill pools (Reid and Dunne 1984, Cederholm et al. 1982, Lisle 1982). The coarse sediment fraction (larger than sand) is typically produced by mass wasting (especially from forest roads and clearcutting) and tends to result in channel aggradation and widening, as well as pool shallowing and reduced frequency of pools (Madej and Ozaki 1996, Madej 2001, Beechie et al. 2005b).

In the Chehalis basin there is little indication of increased coarse sediment supply with the exception of a high concentration of landslides in the Upper Chehalis and Stillman Creek area during the intense rain storms of 2007. This landslide cluster and its effects on channel morphology has been analyzed in prior studies (Sarikhan et al. 2008, Turner et al. 2010, Nelson and Dube 2015). In this assessment we do not expand on previous landslide studies, and focus instead on changes in surface erosion from forest roads and potential changes in fine sediment spawning gravels.

We first examined fine sediment data from the Chehalis (Mobrand Biometrics, Inc. 2003) to establish a correlation between percent fines and road density in the drainage basin upstream of the sample location. The fine sediment data used in this analysis was collected between 1996 and 1999, and included 134 bulk samples in 13 sample reaches (Figure C.1, Figure C.2). Between 2 and 15 bulk samples were collected in each reach, which ranged in stream length from 0.3 to 1.5 miles (480 – 2100 m). Percent fines (< 0.85 mm) for each sample were calculated, and samples from the same reach were averaged to give a single estimate of percent fines per reach. Because we expect very little sediment to be generated from paved roads, we used only unpaved roads in forest lands to calculate a road density (Figure C.1). The basin was largely categorized as forested lands, with the majority of other land use being developed land and agriculture (Figure C.1). For each NHD segment in the Chehalis we used the ArcPy library to sequentially generate the midpoint of the stream segment, delineate a watershed upstream of that point using a flow accumulation raster, clip the roads layer to that watershed, and calculate the length of road within the watershed and the area of the watershed (see section 4.5.1 for methods on generating the flow accumulation raster). To calculate road area, we assumed a uniform 10 meter width for all roads used in the analysis, and calculated road density using the equation:

$$road\ density = \frac{road\ length\ [m]*10[m]}{area\ [m^2])}$$
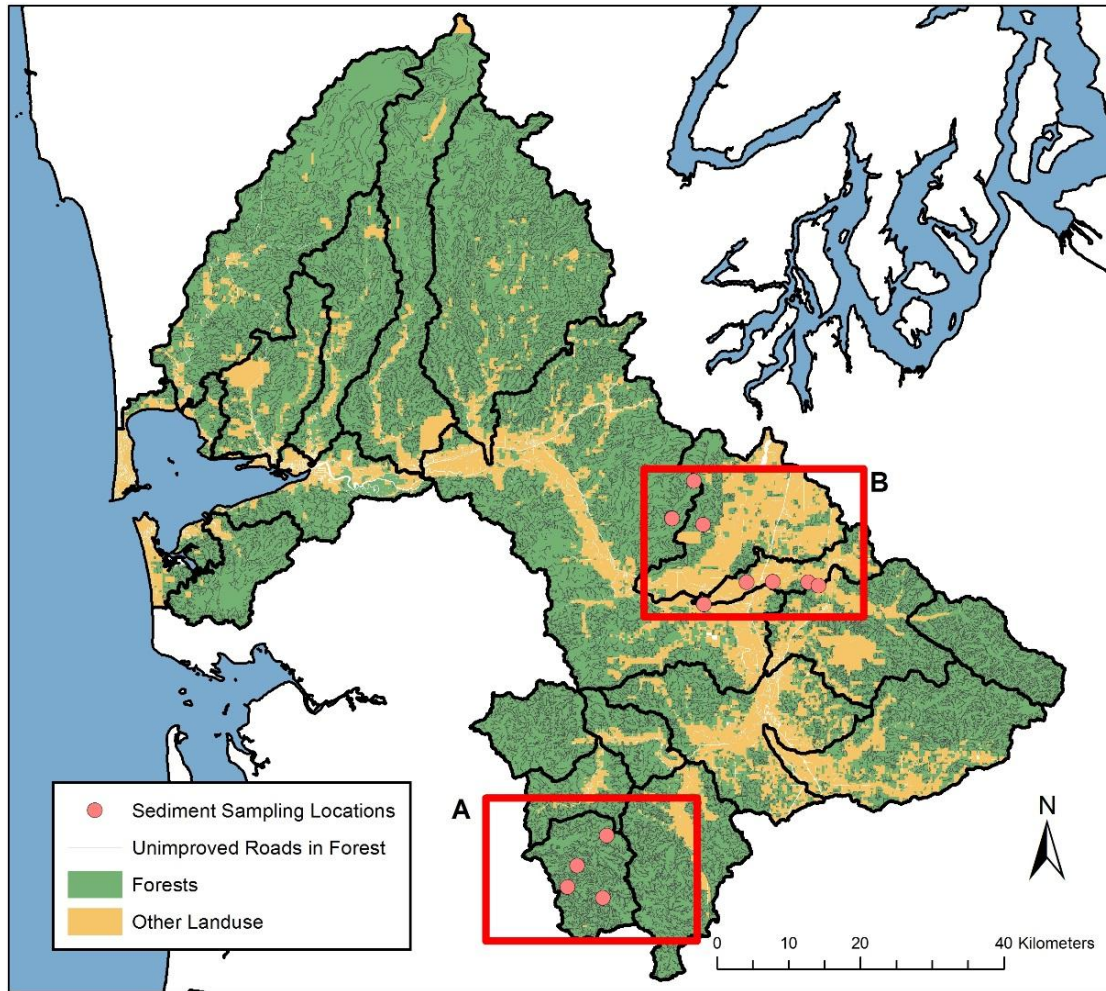
Figure C.1. Map of unpaved roads and land cover in the Chehalis River basin. For the road density analysis the roads layer was filtered to Unimproved Roads (gray lines) and clipped to forested lands (green area). Fine sediment sample sites also shown (Mobrand Biometrics, Inc. 2003). See Figure C.3 for larger view of areas A and B, including site names.

After one complete run in 2017, we modified our method to save computation time on subsequent model runs. The modified method uses the Flow Accumulation tool, which counts all cells upstream of any given cell. Flow Accumulation can use a 'weight raster' as an input. We created a weight raster using the unimproved roads in forest lands layer converted into a binary raster, snapped to our DEM (same cell size and location). In this way we could count the number of road pixels upstream of any given point. Comparing the results of all 61,383 points from our original watershed tool analysis and the new flow accumulation method, revealed a linear relationship between the road area results from the two methods. As the flow accumulation method is coarser, we converted count of road pixels into road area using the following equation:

$$Road\ Area = road\ pixel\ count * pixel\ size^2 * correction\ factor$$

176
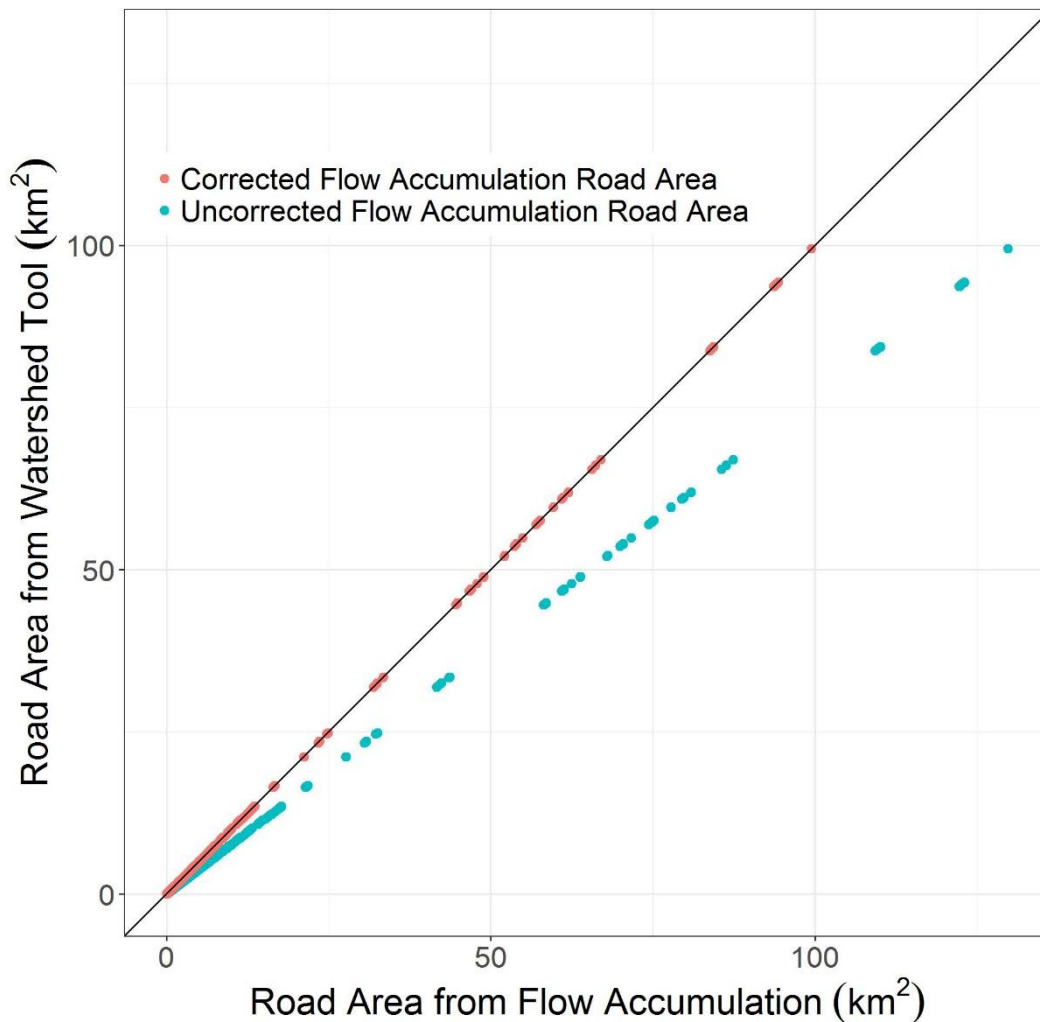
Figure C.2. Corrected and uncorrected road areas using the flow accumulation algorithm. The correction factor is 0.767.

where *road pixel count* is the output of the flow accumulation tool at the center point of a particular stream segment, *pixel size* is the length of one side of a pixel of the DEM in meters, and the *correction factor* is the slope of a linear model relating road area from the watershed tool to the road area from the flow accumulation tool. For our analysis the correction factor is 0.767 (Figure C.2).

The beginning and end of each sample reach were located using GIS, and NHD streamline segments were clipped within the sample reaches to assign a slope and bankfull width to each fine sediment sample reach. Where sample reaches spanned several NHD stream segments, we calculated a weighted average slope, bankfull width, and road density (see 4.5.1 for methods on estimating slope and bankfull width).

We found no correlation between percent fine sediment and road density in the Chehalis fine sediment data, so we then compared the Chehalis fine sediment data to those of an earlier study in the Queets River basin in which fine sediment was correlated with road density (Cederholm et al. 1982). We found that most observations fell within the range of (Cederholm et al. 1982), but there was a group of observations which did not (Figure C.3A). The sediment samples which did not follow the road density-fine sediment relationship were taken in Scatter Creek and
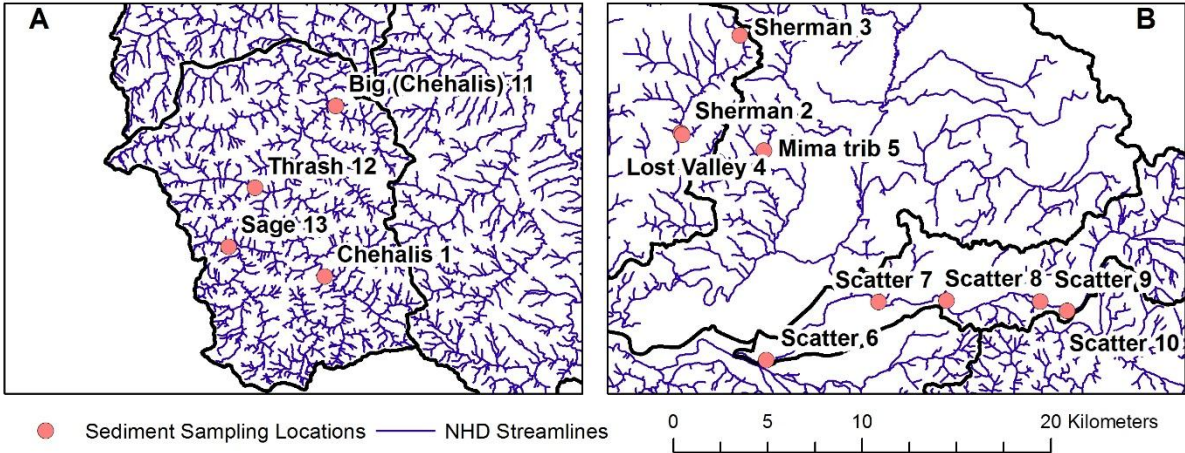
Figure C.3. Location of fine sediment sample sites in (A) the upper Chehalis River basin, and (B) the middle Chehalis River basin. Inset locations shown in Figure C.1.

Table C.1. Data sources and filters used to create the roads layer used for the road density analysis.

GIS Layer	Filter	Source
Roads	Unimproved roads	https://fortress.wa.gov/dnr/adminsa/gisdata/metadata/road.html
Landuse	Designated forest land under chapter 84.33 RCW, Non-commercial forest, Public Timberland/non-designated forest, Timberland Classified under Chapter 84.34 RCW	http://www.ecy.wa.gov/services/gis/data/planningCadastre/landuse.htm

a tributary to Mima Creek, which are reaches with very low stream power. These reaches have relatively low road density but high percentages of fine sediment. We therefore assumed for this analysis that low stream power reaches do not follow the road density-fine sediment relationship, and have high amounts of fine sediment due to other geomorphic processes. To account for this we calculated a shear stress index ($Slope * Bankfull\ Width$) for each reach and set a threshold of 0.05. Below this 0.05 threshold we fixed the percent fines at 27.6%, which is an average of the field samples under the threshold (Figure C.4).

Above this threshold we modeled fine sediment throughout the basin using a regression relationship between the fraction of fine sediment in a stream segment and the road density within the drainage area above that segment (Cederholm et al. 1982):

$$sed = 5.74 + 2.05x$$

where sed is the percent fine sediment < 0.85 mm, and x is the road density, or percent of the basin covered in road area.
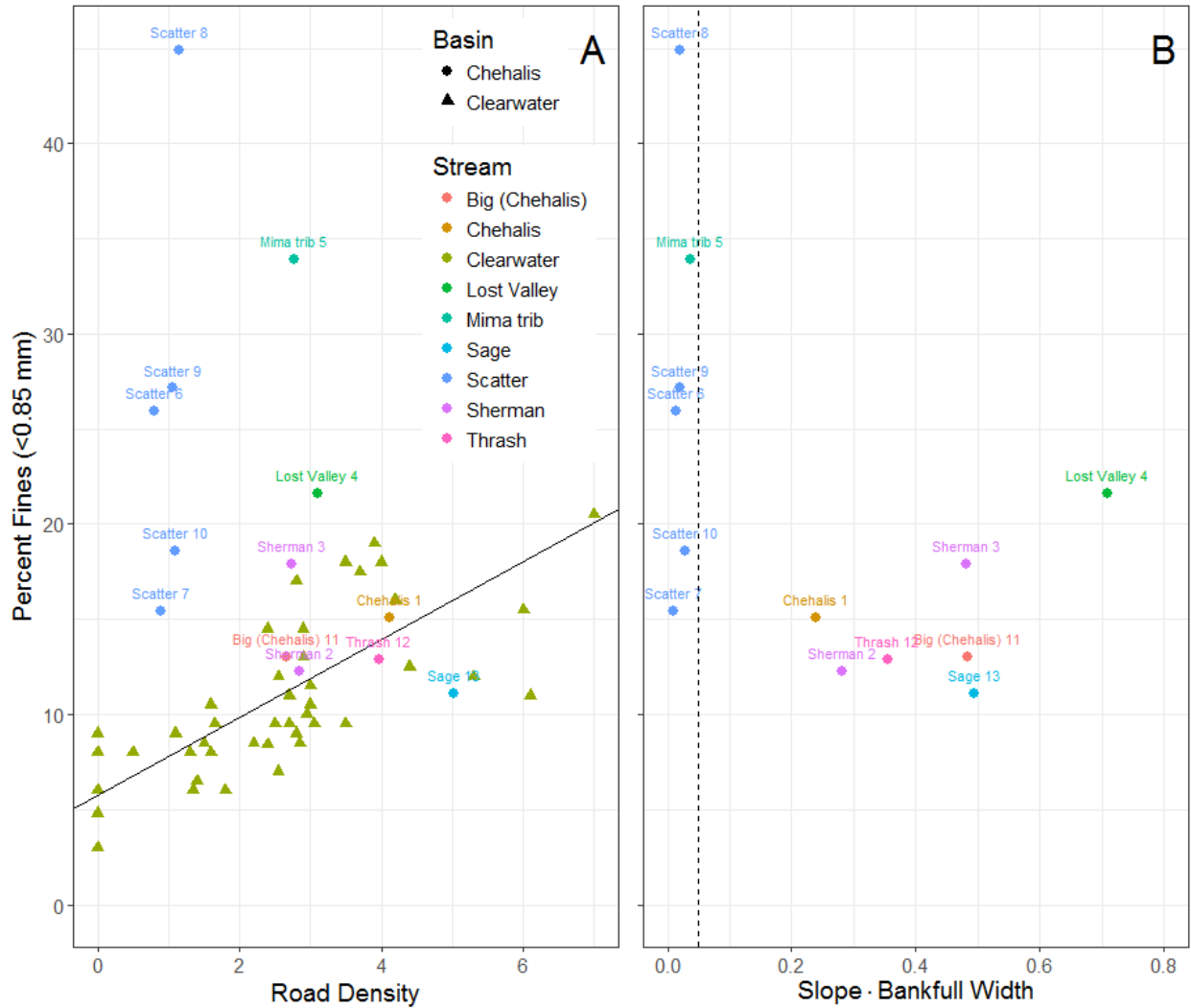
Figure C.4. (A) Comparison of fine sediment values and road density from the Chehalis (circles, Mobrand Biometrics, Inc. 2003) to published values of fine sediment plotted against road density for the Queets and Clearwater Rivers on the Olympic Peninsula (triangles, Cederholm et al. 1982). The line represents the linear model from Cederholm et al. (1982). Note samples from Scatter Creek and Mima trib have particularly high percent fines at relatively low road density. (B) Percent fines plotted against the shear stress index ($Slope * Bankfull\ Width$) showing the grouping of very low-power reaches. We used a threshold of 0.05 (dotted line) as a threshold above which we applied the road density-fine sediment model, and below which we assigned the averaged value of the below-threshold points (27.6% fines).

Appendix D. Migration Barrier Assessment

The migration barrier assessment is intended to evaluate reductions in spawning or rearing capacity or productivity based on the existing barrier inventory assembled by WDFW. The barrier database includes 1790 structures, each of which has a passability rating assigned by a surveyor in the field. These data were jointly evaluated by ICF, International and NOAA to identify errors, and errors were corrected (e.g., some barriers were erroneously assigned to a mainstem reach when they should have been assigned to tributary). Some barriers were not located within the salmon bearing portion of the stream network, so the passage ratings do not affect spawning capacity. For those within the salmon bearing network, each barrier data record contained a passage value (usually 0, 0.33, 0.67 or 1), indicating the degree of passability of that structure.

Of the 1790 potential barriers in the database, 10 were removed in the error checking process. Potential barriers were classified as culverts, dams, waterfalls, or not specified. The vast majority of those were on small streams. Therefore, barriers primarily affected spawner abundances of coho salmon and steelhead, which have the greatest extent of small stream spawning habitat in the Chehalis River basin. A map of the cumulative passability ratings above potential barriers is shown in Figure D.1.

We use the passage ratings to reduce spawning or rearing capacity and productivity above barriers, which is then processed through the life-cycle models to determine barrier effects on abundance or productivity of each species. To account for the barrier effect on salmon productive capacity of upstream reaches, we chose to reduce the number of spawners accessing habitat upstream of barriers by multiplying the upstream spawning capacity (potential number of adults and eggs for each species) by the passage value. Where there were multiple barriers, we multiplied successive passability ratings to represent the cumulative reduction in number of spawners accessing upstream spawning habitat. Rearing habitat areas were not reduced unless the passage rating was zero. Where the rating was zero, we assumed that no juveniles could occupy upstream habitat, and we eliminated that rearing capacity above those barriers. Where the cumulative passage rating is >0, the model estimates that fewer adults spawn in areas upstream of barriers, but all of the rearing habitat is available to their offspring.
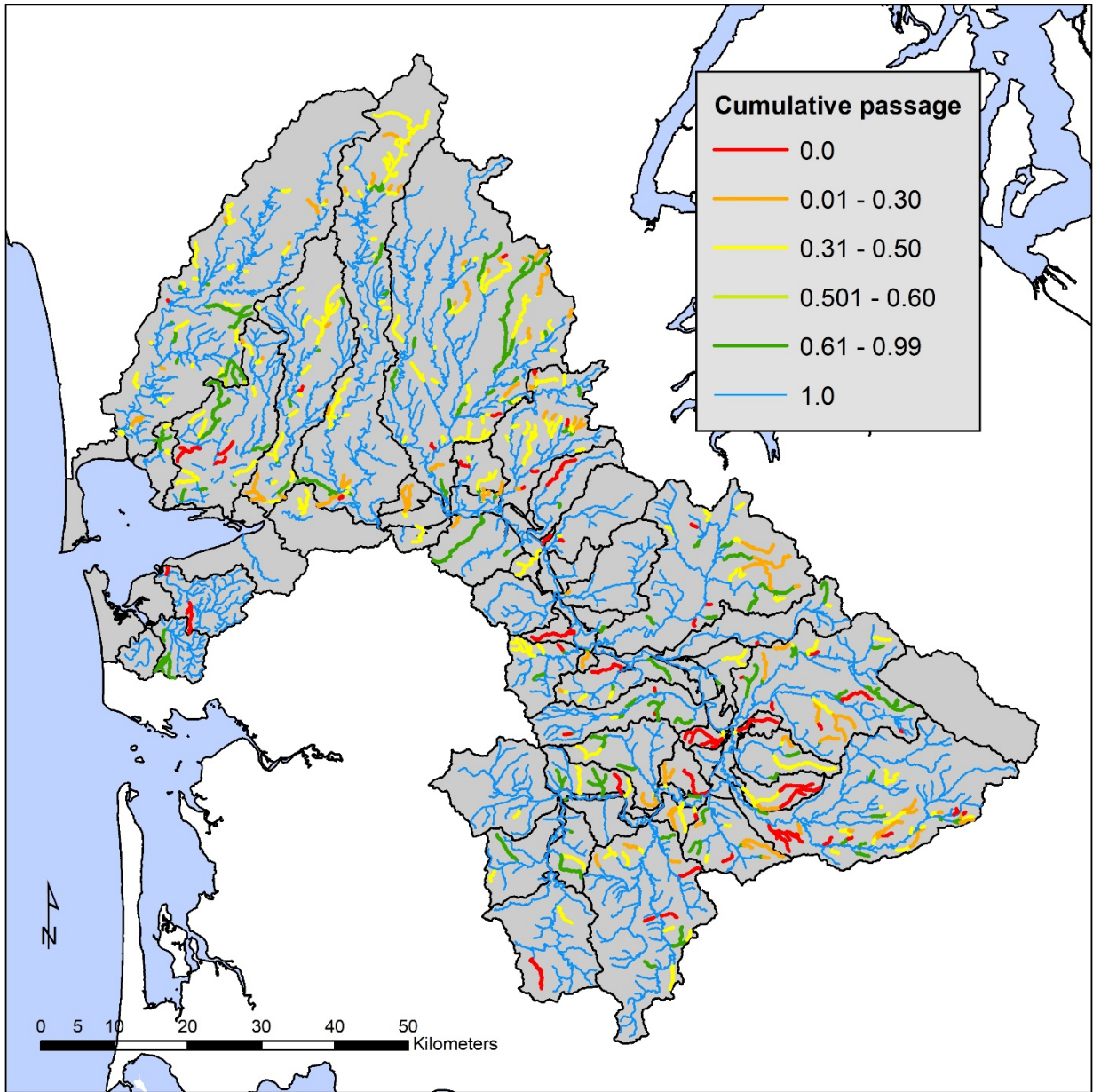
Figure D.1. Map of final passability ratings for reaches within the salmon and steelhead ranges used in this study.

Appendix E. Small Stream and Large River Habitat Assessment

To estimate riverine rearing habitat capacity for juvenile salmonids, we used two different habitat typing systems, one for small streams (<20 m bankfull width) and one for large rivers (>20 m bankfull width). In small streams, suitable depths and velocities for rearing salmonids are typically found in pools, with the exception that steelhead may occupy faster riffles when other species occupy pools (Bisson et al. 1988). In large rivers, suitable rearing depths and velocities are typically in edge habitat units because mid-channel pools and riffles are typically too deep and fast for most rearing juveniles (Beechie et al. 2005a). For small streams, we simplified the suite of habitat types to pool and riffle because these two unit types sufficiently explain small-stream habitat capacity at the river basin scale (Table E.1) (Beechie et al. 1994). For large rivers, we used bank edge, bar edge, backwater, and rip-rap edge habitat types, as well as the mid-channel habitat (Beamer and Henderson 1998, Beechie et al. 2005a).

E.1 Attributing Stream Segments in GIS

We first used spatial join to classify each segment by Ecological Diversity Region (EDR), subbasin, and Geospatial Unit (GSU). Some manual reclassification was done where the habitat unit intersected a spatial unit boundary and had been assigned to the wrong unit. Species distributions were assigned using the SWIFD species distributions. The most critical attributes for our analysis of all stream habitats were channel slope, drainage area, mean annual precipitation, bankfull width, wetted width, and for small streams, adjacent land use.

Table E.1. Description of habitat unit types used in small streams (< 20 m bankfull width) and large rivers (>20 m bankfull width) in the Chehalis River basin.

Stream size	Habitat unit type	Description
Small stream	Riffle	Shallow, fast water (typically >0.45 m/sec)
	Pool	Deep, slow water (typically < 0.45 m/sec)
Large river	Bank edge	Vertical or steeply sloping shore, velocity <0.45 m/sec, depth <1.0 m, no bank modification
	Bar edge	Gently sloping shore, velocity <0.45 m/sec, depth <1.0 m
	Backwater	Partially enclosed areas separated from the main river channel, velocity <0.45 m/sec
	Modified bank edge	Vertical or steeply sloping shore, velocity <0.45 m/sec, depth <1.0 m, banks are rip-rapped or armored
	Mid-channel	All habitat area not included in bank and backwater habitats

We used the 1:24,000 scale Statewide Integrated Fish Distribution line work (SWIFD) (modified from the National Hydrography Dataset, NHD), and recreated stream attributes so that we would have the most spatially accurate stream segments currently available. In this dataset, most of the large, low-elevation stream reaches match recent aerial photography, so locations of important salmon streams are reasonably accurate.

To generate the stream attributes, we first divided the SWIFD river network into 200-m segments using the 'split by equal lengths' tool in ET GeoWizards, and burned the network into the 10-m digital elevation model to assure that the segment outlet elevation was lower than all points upstream, and that the correct drainage area was assigned to the segment. We imported bankfull width and wetted width from EDT data files. We calculated segment slope (percent) by subtracting the elevation of the downstream end of the segment from that of the upstream end, and dividing by the segment length:

$$Slope = \frac{Elevation_{up} - Elevation_{down}}{Reach\ length}.$$

We then classified each SWIFD stream segment as estuary, large river, or small stream and exported new shapefiles for each of these habitat categories. All main channel Chehalis River segments upstream of the Wynoochee River confluence were classified as freshwater. Downstream of the Wynoochee confluence, all segments that intersected with a tidal maximum shapefile were classified as estuary. We used bankfull width values to distinguish small streams from large rivers, with bankfull width < 20 m classified as small streams, and those > 20 m classified as large rivers. To improve accuracy of classifications, small streams with wetted widths between 10 and 20 m were manually examined using aerial photography and lidar, and reclassified as needed based on measurement of bankfull width. Some large river segments with seemingly erroneous estimated wetted widths were also further verified or reclassified based on aerial photography and lidar.

E.2 Estimating Large River Edge Habitat Change

For large rivers we digitized current edge habitat unit lengths from aerial photography and used field data on edge unit widths to estimate areas for historical and current edge habitat. We highlighted the extent of large river stream segments in the NHD, then created a new data layer of edge habitats. We digitized sand, gravel, and boulder bars (lines), natural and modified banks (lines), and backwater pools (polygons) along each side of the wetted channel using high resolution (30 cm) aerial photography (Source: Microsoft July 8, 2010) at 1:3,000 scale or closer. To delineate modified versus natural banks, we used aerial photography, lidar, and bank stabilization and levee spatial data as a guide. The length of a bank unit paralleling stabilization and levee structures and bridge abutments was typically classified as modified using the spatial data, and then verified using aerial photography and lidar. Finally, every modified bank unit was copied, and the copy was reclassified as a natural bank for the historical condition.

We measured edge unit widths and wetted widths in the field at summer low flow and built a regression to estimate average widths for each edge unit type (Figure E.1). We measured these widths at 119 transects in 8 reaches of differing wetted width, encompassing natural

bank edge units, modified bank edge units, and bar edge units. The regression equations are:

Bar edge width = 0.087(WW) + 2.11, R^2 = 0.12

Natural bank edge width = 0.084(WW) + 0.33, R^2 = 0.33

Modified bank edge width = 0.089(WW) + 0.17, R^2 = 0.43

As expected, bar edge units were wider and more variable in width than natural or modified bank edge units (Figure E.1). Natural and modified bank edge units were similar in width on average. To extrapolate edge unit widths across the Chehalis River basin, we used the regression equations to calculate edge unit widths for all edge habitats based on the mean estimated wetted width of segments joined within the 300 m radius of each edge unit

We calculated edge unit areas (ha) in a new field in the edge unit shapefile by multiplying unit length by the estimated unit width from the regression. For bar units and bank units without corresponding hydromodified banks, the historical unit area was considered the same as the current unit area. For modified bank units, area of modified banks represented the current bank habitat, and area of corresponding natural bank (the copy) represented the historical bank habitat. Hence, the unit areas changed little between the historical and current states.
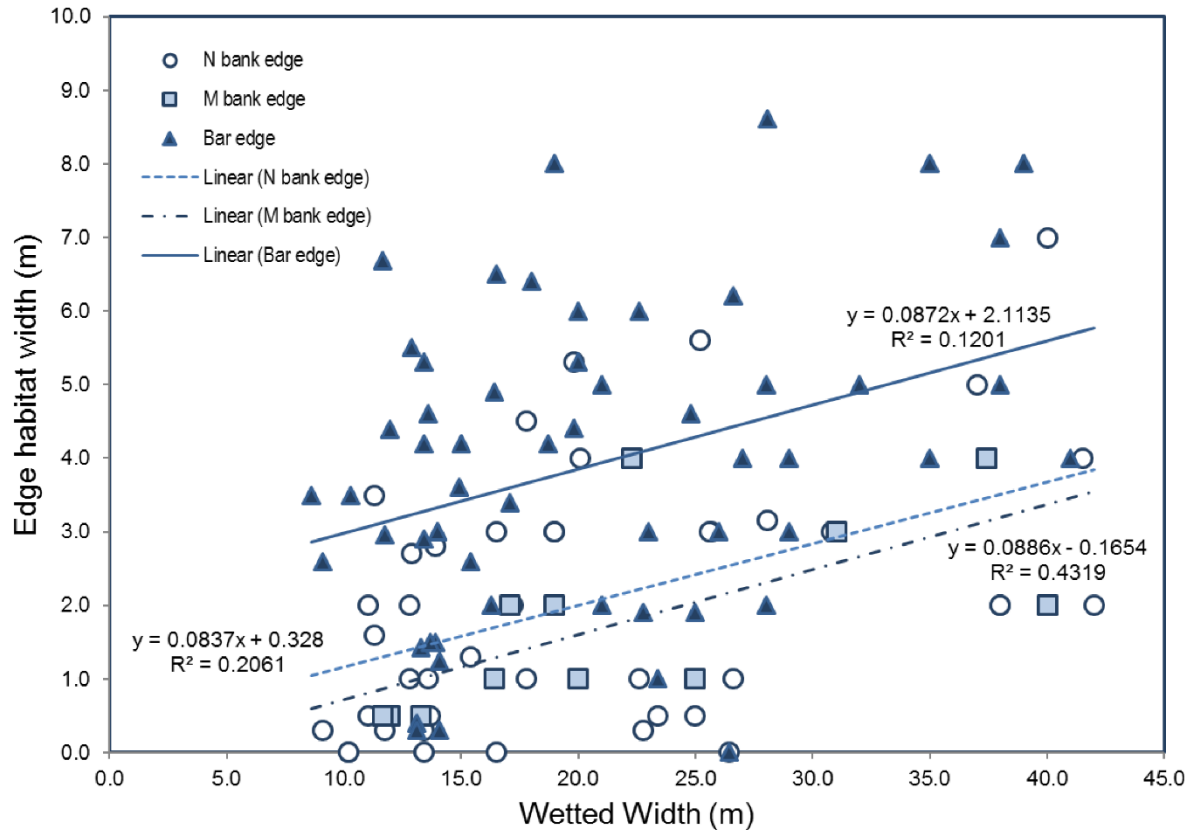
Figure E.1. Relationship of bar edge, natural bank edge (Bank edge) and modified bank edge (M bank) unit widths to wetted widths in large rivers of the Chehalis River basin at summer low flow.

E.3 Estimating Small Stream Habitat Change

To estimate the area of historical and current pools and riffles in small streams, we extrapolated percent pool area from surveys of small streams in the Chehalis River basin (current condition) and reference streams from Puget Sound (representing historical condition) to small streams in the SWIFD, based on slope and landcover classes (Beechie et al. 1994, 2001). Historical mean percent pool areas were summarized by slope class based on reference site data (Beechie et al. 1994, Beechie and Sibley 1997, Beechie et al. 2001), assuming predominantly mature forest cover across the landscape and natural wood abundance in channels (Table E.2). For current mean percent pool areas, we used 339 recent habitat surveys conducted by WDFW in small streams of the Chehalis River basin from 1999 to 2014. Survey reaches were between 50 and 100 m long. We used mean reach slopes and located each reach in GIS to assign the dominant land cover class to each reach (NOAA's C-CAP 30-m resolution land cover data) (Figure E.2). We then calculated mean percent pool by area for each slope and land cover class for each reach (Beechie et al. 2001), resulting in a percent pool matrix for historical (reference) and current (land cover classes) periods in small streams Table E.2). For those small stream segments with landcover classified as "water" we used the percent pool for "wetland" segments. Several

segments with landcover classified as "water" overlapped with pond or lake floodplain habitat polygons. For these segments we set both pool and riffle area to 0 to avoid double counting the area in both small stream and lake or pond habitat. The capacities for these segments are reflected in the rearing capacities of the overlapping floodplain polygons. We then extrapolated the percent pool matrix to all small stream NHD segments in the Chehalis River basin. Finally, we applied the appropriate pool matrix percentages to the area estimates to generate area of pool for each segment. All remaining area in each segment was classified as riffle habitat. This procedure resulted in area estimates for pools and riffles in each small stream segment for historical and current scenarios.

Table E.2. Mean percent pool area by slope class and landcover class from field surveys in the Chehalis River basin (WDFW, unpublished data), and reference sites in Puget Sound (Beechie et al. 1994, Beechie and Sibley 1997, Beechie et al. 2001). The 'Reference' column shows percent pool for historical periods, whereas landcover classes show current percent pool.

Slope class	Percent pool by landcover class					
	Reference	Forest	Wetland	Agriculture	Developed	Bare
0-0.02	79%[a]	75%	89%	92%	74%	83%
0.02-0.04	66%[b]	48%	53%	60%	51%	50%
>0.04	35%[c]	34%	32%[d]	31%	35%[d]	35%

a. Updated based on higher proportion of very low slope streams in the Chehalis basin
b. Based on reference sites from Beechie et al. (1994) and Beechie and Sibley (1997)
c. Based on reference sites from Beechie et al. (2001)
d. Value from the Bare category used as surrogate
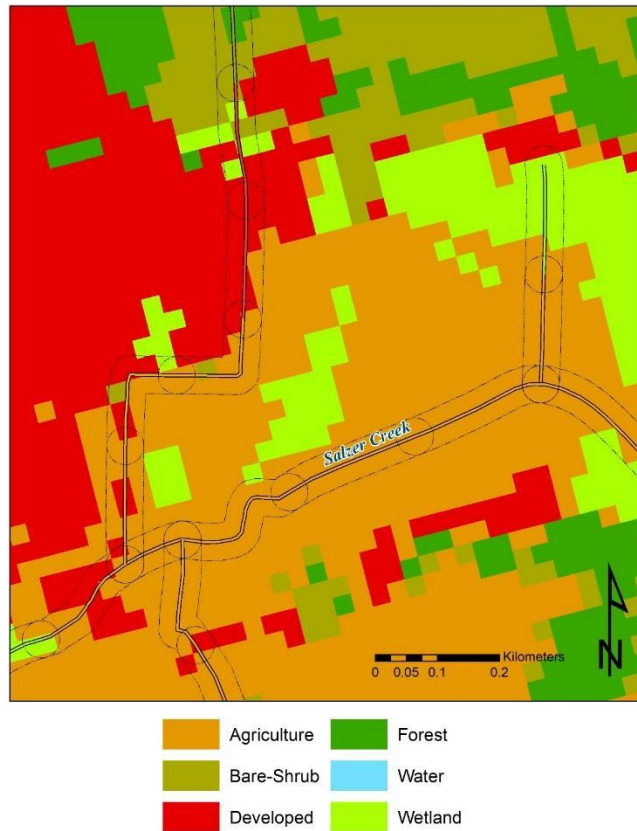
Figure E.2. Illustration of classification procedure for small stream adjacent land cover, showing 30 m buffers (hashed lines) on each side of NHD stream segments. Each stream segment was attributed with the dominant land cover class contained within the 30 m buffer using C-CAP 30-meter resolution data. Percent pool ratios from Table E.2 were applied to each segment based on landcover and slope classifications.

Numerous small stream segments also overlapped floodplain marsh polygons. We considered removing the stream area from the marsh habitat area, but found that the total area of overlap was very small compared to the total area of marsh (98 ha of small stream-marsh overlap compared to 4108 ha of total marsh and 2988 ha of total small stream habitat; or 2% and 3% of the total areas, respectively). Moreover, streams often run through marshes, so marshes are partially composed of habitats that function similarly to pool-riffle habitat (Henning 2004). We therefore opted not to remove overlapping small stream and marsh habitat given the small magnitude of the potential error relative to differences between historical and current habitat areas.

E.4 Beaver Pond Habitat Change

A 1993 USFWS report included maps of beaver dams for portions of the Chehalis basin (Wampler et al. 1993), which we used to estimate current beaver pond densities in small streams. We used the data from eight subbasins in which they only surveyed streams in the small stream class (<20 m bankfull width), because that is the only area in which we applied the beaver dam estimates. We assumed that in large rivers the floodplain habitat data should capture most ponds and marshes. Beaver dam densities ranged from 0.1 to 1.1 ponds/km among subbasins, with a length-weighted average of 0.6 ponds/km (Table E.3). We ultimately reduced the density to 0.55 to avoid double counting of modeled beaver ponds with ponds already in the floodplain habitat data set. To account for inundation of pools and riffles by ponds in the historical condition, we used a typical pond length of 25 m which inundates 1.5% of the stream length. Therefore, we reduced pool and riffle areas by 1.5% for the current condition to account for inundation by ponds.

We estimated historical pond area in small streams within the range of all salmon species using a pond frequency of 6 ponds/km (10 times the current number) and a median pond area of 500 m^2 (Pollock et al. 2004), which is equivalent to 3,000 m^2 of pond area per km of stream. The assumption of 6 ponds/km is conservative, as it is lower than most frequencies observed where there are relatively undisturbed beaver populations (Pollock et al. 2003). To account for inundation of pools and riffles by ponds in the historical condition, we used a typical pond length of 25 m which inundates 15% of the stream length. Therefore, we reduced pool and riffle areas by 15% for the historical condition to account for inundation by ponds.

Table E.3. Estimated pond densities from maps and data in Wampler et al. (1993). Number of ponds is the manually-counted number of dam symbols in each subbasin from the published maps. Stream length in miles is from Table 2 in Wampler et al. (1993).

Subbasin (as delineated in Wampler et al. 1993)	# Ponds	Sm Str Length (mi)	Sm Str Length (km)	Density (ponds/km)
Newman	76	94	151	0.5
Porter	4	27	43	0.1
Gibson	19	38	61	0.3
Scatter	30	31	50	0.6
China	35	37	60	0.6
Stearns	35	20	32	1.1
Elk	39	43	69	0.6
Lincoln	111	63	101	1.1
Weighted average				**0.6**

E.5 Large River Length and Side Channel Change

We estimated the difference in large river edge habitat areas between current and historical conditions using reach-specific main channel length multipliers, which increase habitat unit areas by the specified multiplier in each reach (Table E.4). In addition, we estimated the amount of side channel length lost using similar multipliers for side channel length. Both sets of multipliers were developed by NOAA and Natural Systems Design (NSD) from several sources including:

(1) the results of the Ecological Corridor analysis in the Skookumchuck River watershed and ad hoc analyses to test the framework (see Methods memo, NSD 2018);
(2) reach-scale assessments of geomorphic setting, current conditions, and reference values of sinuosity and side-channel length from Beechie et al. (2006b) and Collins and Montgomery (2011); and
(3) measurements of current sinuosity, valley slope and channel slope by Tim Beechie and—where available—the lidar bare-earth hillshade and aerial photography.

Table E.4. Large river main channel and side channel length multiplier values for the mainstem Chehalis and Chehalis tributaries by river reach.

River	Reach	Large River Multiplier	Side-Channel Multiplier
WF Satsop (1-5)	Middle Satsop Rd to D3000 Rd	1.3	1.2
WF Satsop (6,7)	D3000 Rd to Muller Rd	1	0.1
WF Satsop (8A)	Muller Rd to Cougar Smith Rd	1	1.5
WF Satsop (8B, 9)	Cougar Smith Rd up to lidar boundary	1	0.1
WF Satsop (11, 12, 13)	From beginning of lidar in Olympic foothills to FS Road 2153	1	0.6
EF Satsop (5-9)	South end Meadowlark Rd to forks	1.3	1.2
EF Satsop (10A, 10B, 11, 12A, 12B, 13, 14A)	South end Meadowlark Rd to forks	1.3	1.2
EF Satsop (14B, 14C, 14D, 14E, 15)	W Plug Mill Rd to hatchery	1.1	1.1
Wishkah (5-7)	South end Riverside Rd to W Wishkah Rd	1.2	1.3
Wynoochee (2-15)	Olympic Hwy to N. End Matzen Rd	1.2	1.5
Humptulips (6A-15)	Robinson Rd to Big Creek	1.2	1.5
Humptulips (16-23B)	Big Creek to W Fork	1.2	1.5
Chehalis (54-62)	South Fork to Newaukum	1.1	0.7
Chehalis (49-53)	Newaukum to Skookumchuck	1.1	0.1
Chehalis (40-48)	Skookumchuck to Black	1.3	1
Chehalis (18-39)	Black to Satsop	1.1	1
Skookumchuck (1-9)	Mainstem	1.3	1.2

The values for each category were then refined and spatially explicit estimates for the reaches of main stem Chehalis and were developed collaboratively between NOAA and NSD. Main channel length multipliers ranged from 1.0 to 1.3, and side channel length multipliers ranged from 0.1 to 1.5.

For spawning capacity, we treat side channels as small streams, and assume that side channels had high wood abundance and high spawning capacity for all species (See also Appendix H). For summer and winter rearing habitat capacity, we treat side channels as small streams with a wetted width of 1 m. Because we did not have data on wetted widths of historical side channels, we arbitrarily chose a wetted width of 1 m, based on the observation that many side channels are dry most of the year and other side channels have wetted widths larger than 1 m.

Appendix F. Floodplain Habitat Assessment

F.1 Methods

Historical and current floodplain aquatic habitat areas in the Chehalis River basin were estimated from the General Land Office (GLO) cadastral survey maps dating from 1853 to 1901 (http://www.blm.gov/or/landrecords/survey/ySrvy1.php), as well as from the following contemporary aquatic habitat inventory data sets: National Hydrography Dataset NHDWaterbody1710 1:24,000 (NHD), Washington Department of Natural Resources (WDNR) water body hydrography 1:24,000 (WBHYDRO), unpublished data from Washington Department of Fish and Wildlife (Hayes WDFW), and a new floodplain habitat polygon shapefile we created based on aerial photography (Photo) and Light Detection and Ranging data (lidar, http://pugetsoundLIDAR.ess.washington.edu/) (hereafter, these combined contemporary data are referred to as HYDRO). We first digitized historical features from the GLO survey maps (Figure F.1), but recognized that many features that exist today were missing from those maps, either because GLO surveyors did not consistently record them, or because these features were not noted in un-surveyed areas between section lines. Therefore, we also classified features in HYDRO as historical habitats if they appeared to be in a relatively natural state, under the assumption that contemporarily mapped features (except man-made), likely existed historically in some form. We then estimated current habitat areas based on the five contemporary data sets included in HYDRO. In the following paragraphs we detail our methods for GLO mapping, and combining and classifying habitats in the contemporary data sets.

F.1.1 Historical Habitat Mapping from General Land Office Surveys

The GLO surveys, conducted between 1853 and 1901 in the Chehalis River basin, recorded geographic and natural resource information along township and section lines as they established the township and range system for defining property and ownership boundaries in the United States. Land surveys of each 36 square-mile township were conducted as straight line transects along the North, South, East, and West boundaries of each township, as well as along the boundaries of each square-mile subdivision (section). Surveys included a map showing major geographic features (e.g., rivers and streams, mountainous areas, and homesteads), an index map indicating where survey notes were located, and survey notebooks.
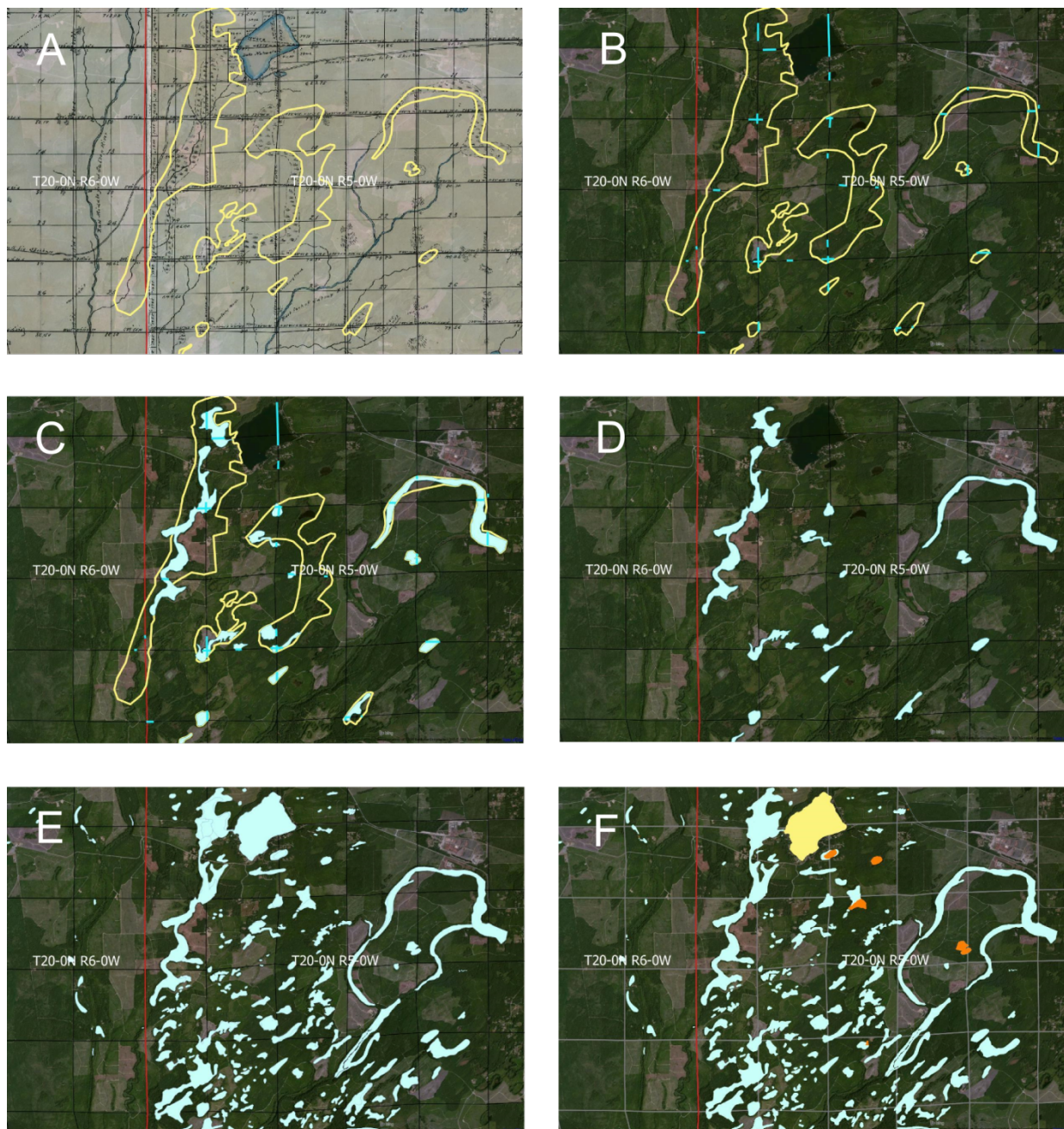
Figure F.1. Sequence of generating historical floodplain polygons: (A) draft marsh polygons (yellow lines) from GLO maps using lidar for boundary location, (B) draft marsh polygons with QA/QC lines (blue lines) from GLO notes, (C) corrected polygons (blue polygons) based on QA/QC lines and aerial photography, (D) final GLO floodplain habitat polygons, (E) GLO data combined with contemporary data sets to form final floodplain habitat polygons, and (F) final floodplain habitat polygons color coded by type (blue = marsh, yellow = lake, orange = pond). Red line is township boundary, gray lines in (F) are section boundaries; each section is one square mile for scale.

The GLO survey records are currently maintained by the US Bureau of Land Management (BLM) in a searchable database of the Land Status and Cadastral Survey Records (http://www.blm.gov/or/landrecords/survey/ySrvy1.php). Each township web page includes (1) digital copies of the hand-drawn cadastral survey maps, (2) a digital copy of the section index denoting the page and volume location of survey notes for each boundary of each section, and (3) digital copies of the detailed, hand-written field notes describing land features. In many cases there were multiple surveys, and we used the earliest, original survey when it covered the full township. Where the original survey covered only a portion of a township, we used the earliest additional re-surveys as needed to complete the mapping of habitat features in that township. We georeferenced each historical GLO survey map and digitized all floodplain habitats drawn on those maps using lidar to help determine the location and shape of each polygon (Collins and Montgomery 2001). Lentic features mapped with a solid outline and no marsh symbology were classified as ponds, and those mapped with a dashed outline and/or marsh symbology were classified as marshes. Narrow, linear, lotic features with a solid outline were classified as sloughs. Each GLO polygon was then classified by period as historical (Hist), and status as natural (Nat) under the presumption that the habitat had not been degraded or modified by European settlers at the time of survey.

For Quality Assurance/Quality Control (QA/QC), we located the field notes for each digitized habitat feature on the draft floodplain habitats map, and used survey distances and feature descriptions to correct polygon shapes and sizes, and to correct habitat types where necessary (Figure F.1). We created QA/QC lines along township or section survey transects to guide corrections to polygon shapes and locations. Each line in the file represented the surveyed width of an aquatic habitat (marsh, pond, slough, lake). That is, each line started where the surveyor first encountered an aquatic habitat, and continued to the point that the surveyor exited that habitat. For each line segment we recorded whether the map-based draft polygon shape should be edited (Yes, No), whether the polygon type should be changed (Yes, No, NA), and the new polygon type if applicable (marsh, slough, pond, lake, NA). The habitat nomenclature we followed is shown in Table F.1. In general, terms that referred to marsh or swamp were classified as marsh, ponds and beaver ponds were classified as ponds, and sloughs and bayous were classified as sloughs. References to river bottom, creek bottom, swale, and the like were not mapped as floodplain habitats because they were rarely mapped as marshes and appeared to refer to the valley bottom or floodplain rather than aquatic habitat features. We also created an MS Excel file containing additional data for each line segment. Additional data included location details, year of survey, surveyor name, filename of the scanned survey notes, start and end distances of habitat features, and direct quotes of the survey notes for that survey segment (Table F.2).

Once we completed transcribing field notes and creating the QA/QC lines, we used the QA/QC lines and recent aerial photography to make corrections to pond, lake, marsh, and slough boundaries (Figure F.1). In most cases, locations of aquatic features noted in the surveys matched well with current topography and/or current aquatic features in aerial photography. Therefore, we had relatively high confidence in the polygon type and area for most features. In a few cases, the lines and polygons did not match the topography well, nor did they match the current aerial photography well. Most often these were in heavily

modified agricultural or urban areas, and we had lower confidence in those polygon boundaries and areas. In general, we were conservative on the size and number of features, as we tended to delete or reduce the size of polygons when we were uncertain of the boundaries of a habitat feature.

F.1.2 Combining the GLO and Contemporary Habitat Data Sets

We combined the five contemporary data sets (NHD, WBHYDRO, WDNR, Hayes WDFW, Photo) into a single file of contemporary data sets (HYDRO), and then merged the GLO and HYDRO shapefiles to create a final dataset that included both historical and current habitats (Figure F.1). Each polygon was classified as being present during historical (Hist), current (Curr), or both historical and current (Both) periods, and assigned a current functional status (Nat: natural, Nat mod: natural modified, or Man-made). If there was no GLO habitat unit where there was a HYDRO polygon and it appeared relatively undisturbed, it was classified as being present during 'Both' periods and condition was considered to be 'Natural'. Where GLO and HYDRO polygons co-occurred, those derived from HYDRO were generally smaller in area than GLO polygons, indicating a reduction in area of habitat over time. Those units from HYDRO that overlapped a GLO polygon and were similar in size were deleted and GLO polygons were used as the historical unit of measure.

Where a HYDRO polygon was used as the historical unit (i.e., no corresponding GLO unit), current habitat quality (with regard to anadromous salmonids) was evaluated using aerial photography, lidar, and hydro-georeferenced fish barrier data (WDFW, unpublished data) to identify apparent sources of modification and degradation (Table F.3). If degradation was apparent from these sources, the historical HYDRO polygon was copied, and the copy was classified as current (Curr) and natural modified (Nat mod), and the source of degradation was noted in the shapefile. This resulted in a matching pair of polygons (by area, one Hist/Nat, and one Curr/Nat mod), but fish density of the Curr/Nat mod polygon would later be reduced by a scaled factor depending on fish passage and estimated local water temperature. Some polygons represented man-made habitats and thus were coded as Curr/Man-made. We considered man-made ponds to be unused by anadromous salmonids.

F.1.3 Assigning Habitat Attributes to Floodplain Polygons

For each polygon, we assigned additional descriptive attributes such as EDR and subbasin names, official or popular water body names or descriptions, hierarchically stratified habitat types (Beechie et al. 1994), water type (i.e., fish or non-fish bearing, WDNR), anadromous salmonid species-stock presence or absence based on the best available information, and data source (Table F.3). We classified units as current habitat if they met one of the following criteria:

- Within 5 m of a reach that is in the spawning distribution,
- Within a mainstem subbasin and within the Watershed Science and Engineering (WSE) floodplain polygon, or

- Within the WSE floodplain polygon and associated with a reach that is within the spawning distribution.

For historical units, we used the same criteria except we used a search distance of 500 m rather than 5 m. All remaining floodplain units were classified as non-habitat.

Table F.1. List of GLO surveyor terms included in each of the four floodplain habitat types (pond, slough, lake, marsh).

Pond	Slough	Lake	Marsh
Beaver pond	Bayou channel	Alder lake	Beaver dam
Pond	Slough	Lake	Beaver dam marsh
	Tide slough		Cranberry marsh
			Marsh
			Marshy bottom
			Marshy ground
			Marshy land
			Marshy prairie
			Marshy swale
			Marshy thicket
			Prairie marsh
			Springy ground
			Wet ground
			Wet land
			Alder swamp
			Ash swamp
			Beaver dam swamp
			Beaver swamp
			Brushy swamp
			Buck brush swamp
			Cedar swamp
			Crabapple swamp
			Hardhack swamp
			Spruce swamp
			Swamp
			Swamp land
			Swamp prairie
			Swampy bottom
			Vine maple swamp

Table F.2. Description of data fields used in the QA/QC data file (filename ("Floodplain GLO note data.xls").

Field name	Description
Line FID	Identification number for each line
Sub-basin	Name of the sub-basin in which the feature is located
Year	Year of General Land Office survey
Town	Township number
Range	Range number
Section	Section number
Boundary	Section boundary that was surveyed (north, south, east, west)
Heading	Direction of survey (north, south, east, west)
Random?	Was the survey on a random line? ("Yes" if the notes referred to surveying on a random line, "No" if the notes referred to surveying a true line or made no reference to either.)
Image type	Scanned images were one of three types, map (the hand-drawn survey map), index (the index page indicating page numbers for the survey notes), or survey notes (the hand-written survey notes recorded by the surveyor)
Page #	Page number of the survey notes for this data record
Area note	Describes portion of the township surveyed: West (west boundary of the township), North (north boundary of the township), South (south boundary of the township), East (east boundary of the township), Subdiv. (surveys along the section lines)
Surveyor	Surveyor name and year of survey (surveyor name and completion date of surveys were recorded on lower left of each map page)
Polygon #	Line number, used when there was more than one feature encountered within a one-mile section survey
Dist (ch)	Distance along the section line in chains (1 chain is 66 feet)
Dist (m)	Distance along the section line in meters
Notes	Transcribed survey notes at the distance noted
Edit?	Does the feature shape or size need to be edited to match the QA/QC line and survey notes?
Change type?	Does the habitat type need to be changed based on the survey notes?
New type	Revised habitat type from the survey notes
Comments	Additional comments regarding this survey point

Table F.3. Description of data fields in the floodplain historical and current habitats shapefile (filename "Chehalis floodplain habitats.shp").

Data Field	Description
FID	Default shapefile ID number
Shape *	Default object identifier
ET_ID	Default shapefile ID number
Subwatershed	WAU subwatershed_NM in which the habitat is located
Water_Body	Tributary name based on various data sources (NHD, DNR HYDRO, WDFW, ICF)
Macrohabit	Macrohabitat connecting off-channel habitat to the main channel Chehalis River or Grays Harbor (**Sm stream**: BFW <20 m; **Lg river**: BFW >20 m; **None**: no apparent flowing water body connection)
Unit	Off-channel unit type (**marsh, pond, slough, FP channel: floodplain channel, side channel**; modified from Beechie et al. 1994)
Area_ha	Area (hectares) calculated for the polygon
Period	Time period associated with the polygon (**historic, current,** or both historic and current [**both**])
Hab_cond	Conditional status of the habitat (**natural, natural modified, or man-made**)
Watertype	Washington DNR watertype designation (**F & S**: Fish, **X & N**: No fish or unknown; only present for polygons from the DNR HYDRO data set)
Coho	Known presence (**1**) or absence (**0**) of coho salmon based on best available information (WDFW SWIFD, ICF Int'l unpublished data)
W_Stlhd	Known presence (**1**) or absence (**0**) of winter steelhead based on best available information (WDFW SWIFD)
F_Chin	Known presence (**1**) or absence (**0**) of fall Chinook salmon based on best available information (WDFW SWIFD)
Sp_Chin	Known presence (**1**) or absence (**0**) of spring Chinook salmon based on best available information (WDFW SWIFD)
Passag_Mod	If present, the type of man-made structure blocking or impeding upstream fish passage (**Block culv**: single culvert partially or fully blocking upstream fish passage in downstream reach; **Dam**: dam blocking or impeding fish passage in downstream reach(es); **Mult block struc**: multiple numbers and types of structures partially or fully block upstream fish passage in downstream reach(es))
Passag_ID	If blocking structure is present, this number refers to OBJECTID from ICF's culvert inventory shapefile

Table F.3 (cont.). Description of data fields in the floodplain historical and current habitats shapefile (filename "Chehalis floodplain habitats.shp").

Data Field	Description
Ripar_Mod	If present, indicates the degree to which riparian vegetation (mature forest) has been removed (**Deforested**: vegetation has been completely or nearly completely removed from along the margins of the polygon; **Dwnstrm ch deforest**: vegetation from a significant length of the downstream connecting stream has been removed or severely reduced; **Part deforest**: vegetation has been partially removed or damaged from along the margins of the polygon)
Gmorp_Mod	If present, indicates the degree to which channel form or channel forming processes have been apparently compromised (**Deforested**: vegetation has been completely or nearly completely removed from along the margins of the polygon; **Dwnstrm ch deforest**: vegetation from a significant length of the downstream connecting stream has been removed or severely reduced; **Part deforest**: vegetation has been partially removed or damaged from along the margins of the polygon)
Data_sourc	Data source for polygon (GLO: General Land Office http://www.blm.gov/or/landrecords/survey/ySrvy1.php, NHD: National Hydrography Dataset NHDWaterbody1710 1:24,000, WBHYDRO: Washington Department of Natural Resources DNR HYDRO 1:24,000, Hayes WDFW: Off-channel habitat data from Marc Hayes WDFW Biologist, 2011 series, Photo/lidar: Habitats identified from aerial photography and verified using various resolutions lidar data obtained from Puget Sound lidar Consortium website http://pugetsoundLIDAR.ess.washington.edu/)

F.2 Results

The largest loss of floodplain habitats was through draining of historical marshes (Figure F.2), particularly in the Black and Skookumchuck basins, and the Chehalis mainstem from the Skookumchuck confluence to the South Fork confluence (Figure F.3, Figure F.4). Floodplain pond losses were considerably less overall, and those losses were mainly in the mainstem Chehalis floodplain between Satsop and the South fork, as well as in the Black, Skookumchuck and Newaukum basins (Figure F.5). Of the remaining marshes and ponds, more than 80% have been modified through riparian degradation, physical modification, or blocked access.
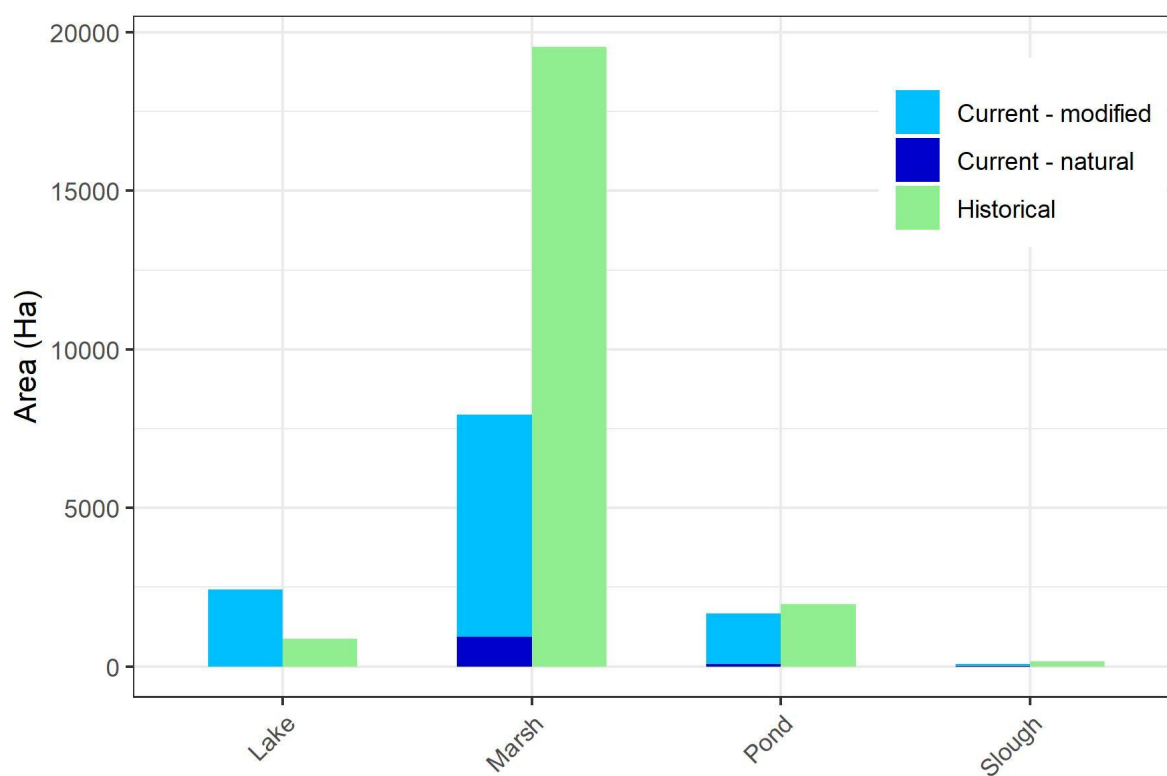
Figure F.2. Area of floodplain habitat lost and gained (Current floodplain area – historical floodplain area). Gains in area of lake and unconnected pond due in large part to impoundments (reservoirs, gravel pits, settling ponds). Losses in area of marsh are due in large part to valley draining (agriculture, development).
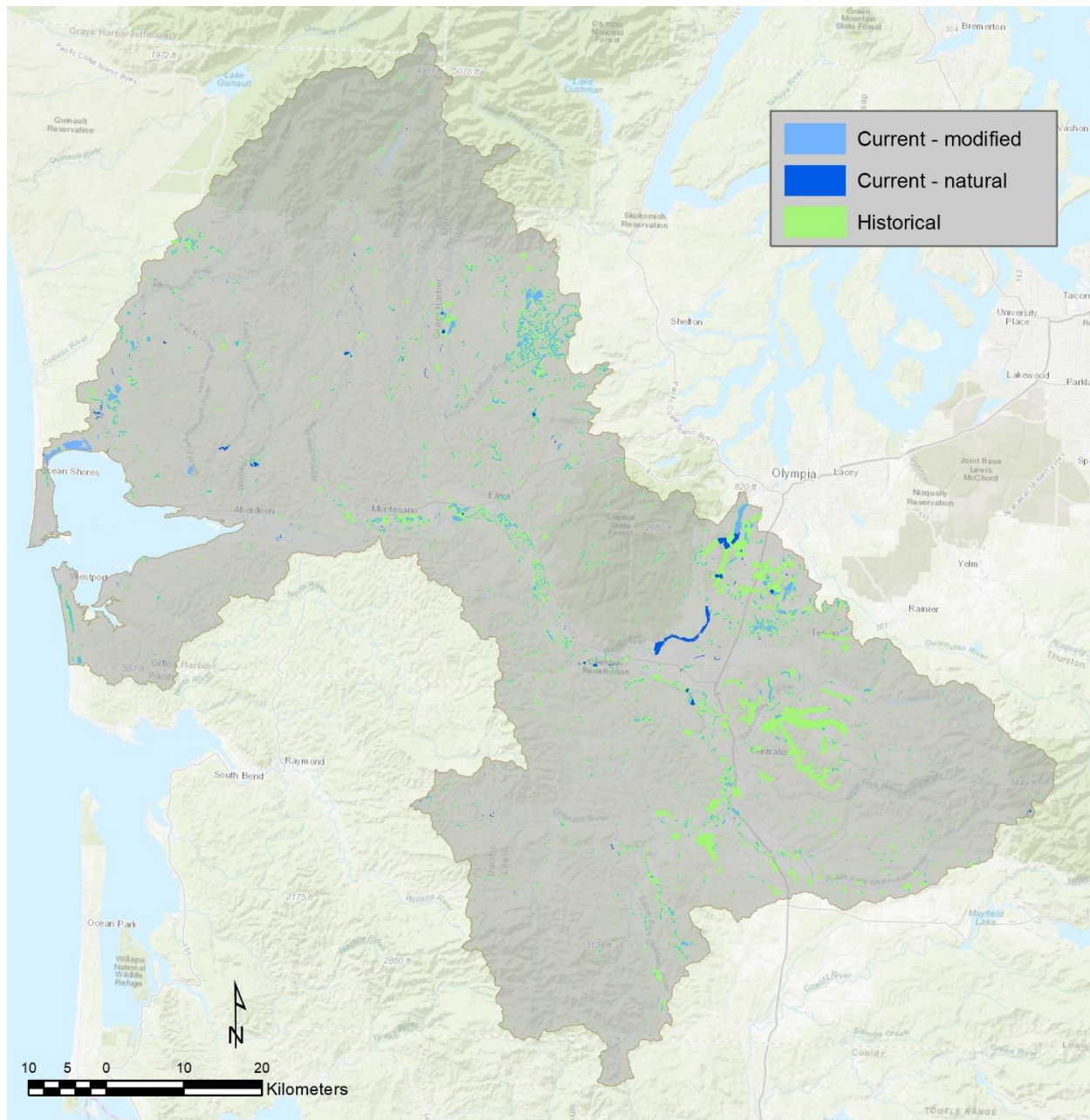
Figure F.3. Map of historical and current floodplain habitats including marsh, ponds, and lakes. Inaccessible man-made floodplain habitats are not shown.
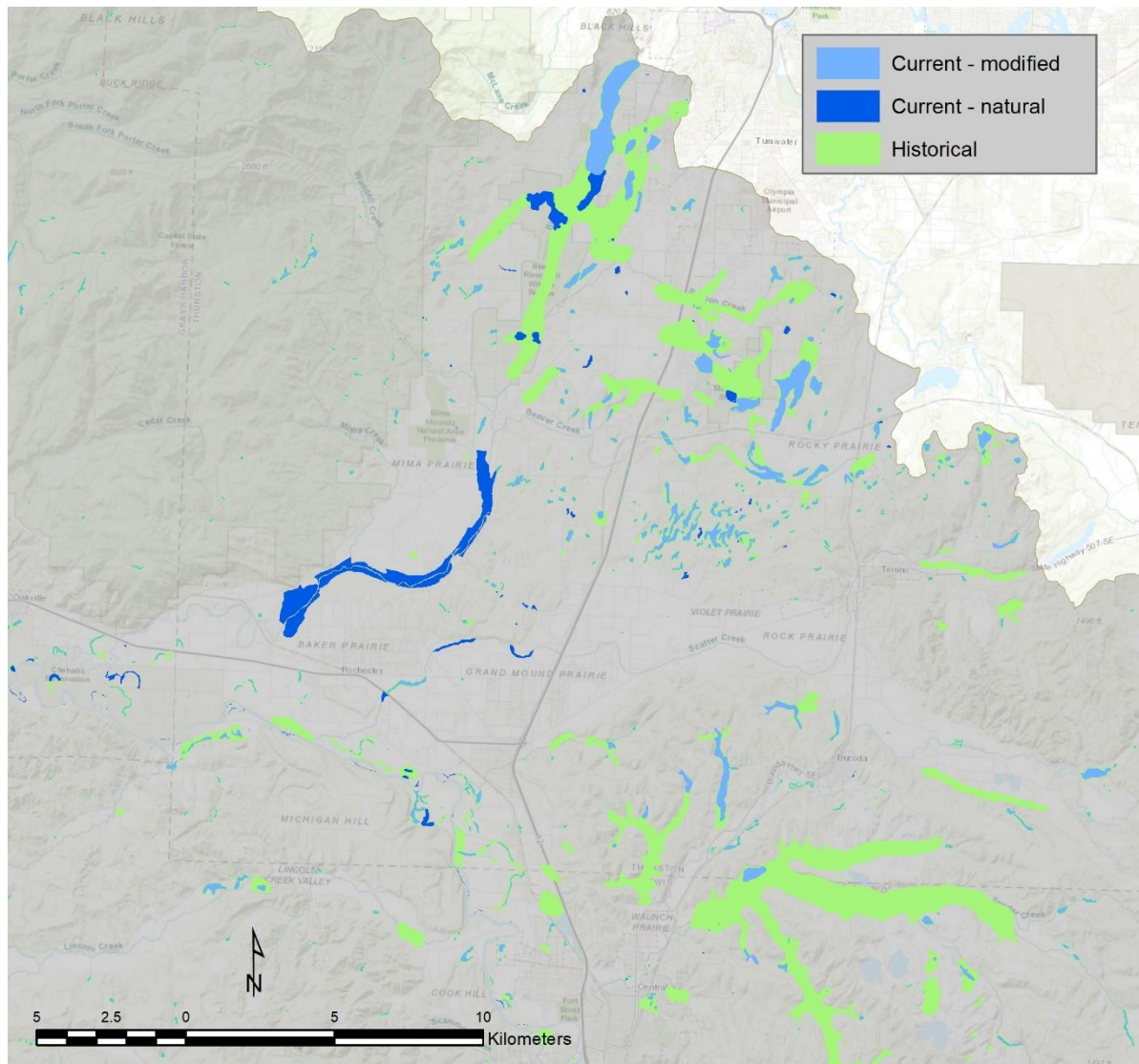
Figure F.4. Enlarged view of historical and current floodplain features in the inset region of Figure F.3.
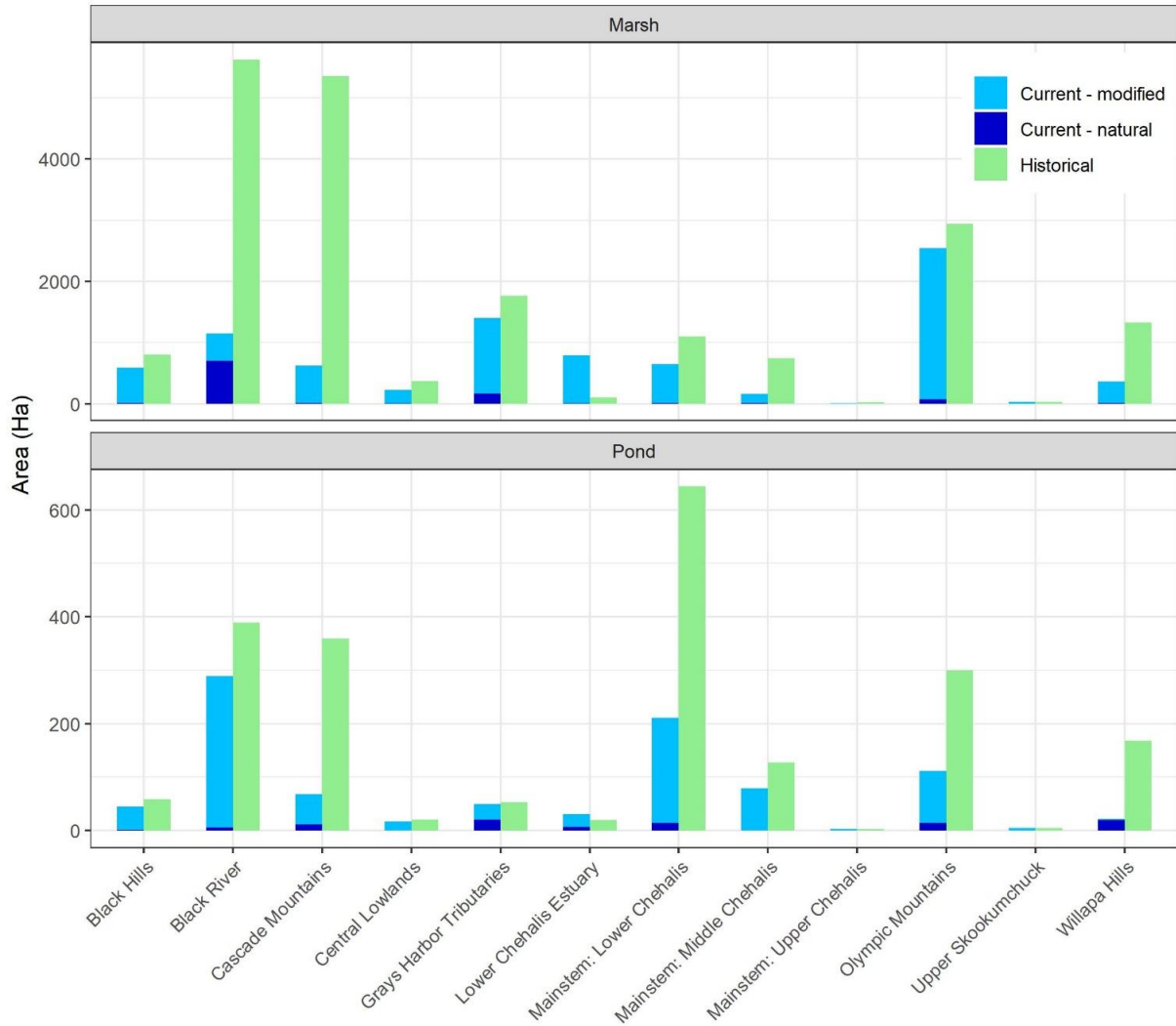
Figure F.5. Marsh and pond area by Ecological Diversity Region, highlighting the extensive marsh loss in the Black River and Cascade Mountains EDRs, as well as the pond loss in the Lower Chehalis Mainstem. Note the different y-axis scales for marsh and pond.

Appendix G. Delta Habitat Assessment

NOTE: The results of the delta habitat assessment are not currently included in the habitat analysis for the NOAA Model.

We quantified delta habitat areas within the Chehalis basin to estimate change in habitat area as well as to quantify rearing capacity for out-migrating juvenile salmonids. We estimated delta habitat areas separately for each of the six major rivers that flow into Grays Harbor: the Chehalis, Wishkah, Hoquiam, Humptulips, Elk, and Johns Rivers. We calculated capacity as a function of fish density, rearing period, and residence time, where fish density was scaled as a function of habitat quality and connectivity.

G.1 Methods

G.1.1 Habitat Classification and Delineation

To estimate estuarine habitat capacity, we first separated delta habitat from freshwater habitat within the Chehalis basin using a 50% tidal exceedance polygon, which was developed using lidar topography and NOAA tide gauges located within the basin using methods from Lanier et al. (2014). Areas within this polygon experience tidal flooding at least once every other year, based on local elevation and tidal height. We delineated the lower extent of the delta habitat where the river met the bay, with the exception of the Chehalis River and the Elk and Johns Rivers, for which we used the Hwy 101 and Hwy 105 bridges, respectively. The upper extent of each delta was defined as the upper extent of the exceedance polygon with the exception of the Chehalis River, for which used the confluence of the Chehalis and Wynoochee Rivers.

Delta habitats defined by the tidal exceedance polygon were further classified into four distinct habitat types: main channel, tidal channel, small tidal channel, and mudflat. Habitat types were chosen to represent the areas known to be used by out-migrating juvenile salmonids. Main channel habitats were defined as any large mainstem or distributary that maintained continuous river flow into the upstream end, were assumed to have a predominant downstream flow direction, and remained wetted throughout daily tidal cycles. Tidal channels were connected to the main channel or bay at the downstream end, flow direction was predominantly a function of tidal forcing, and de-watering occurred during some portion of the tidal cycle. Small tidal channels were exactly the same as tidal channel habitats, except that total channel width was equal to or less than 1 m. Mudflat habitats were defined as areas adjacent to main channel habitat or within tidal channel habitat that de-watered during the tidal cycle and were at least 40 m wide. That is, for areas adjacent to main channel habitat, the distance from the vegetated edge to the primary channel was at least 40 m, and for areas within tidal channels, the total channel width was at least 40 m wide.

We digitized habitat types in ArcGIS to quantify total available area within each type. Main channel, tidal channel and mudflat habitat types were recorded as polygon features using vegetated edges to define the boundaries and quantify area (in hectares). For mudflat

features adjacent to main channel habitats, we used a combination of vegetated edge and channel edge, where applicable, to define the total area of a particular feature. Small tidal channels were digitized as polyline features and each segment followed the centerline for each feature. Area of small tidal channels was equivalent to total segment length assuming a 1-m average width for each feature in accordance with our definition described above.

G.1.2 Current versus Historical Habitat Area

We assessed historical delta habitat area using aerial imagery and the Washington Department of Natural Resources Levee inventory GIS database. Based on the historical GLO maps, we assumed that there was no loss of main channel habitat, and therefore we restricted our analysis to tidal channel areas only. Areas that were within the tidal exceedance polygon, showed clear evidence of remnant tidal channel networks, and were behind an inventoried levee or other visible barrier were considered part of the historical delta area. Within these areas, we could not measure habitat areas using methods described above because we could not discern clear or complete channel networks after years of subsidence and disconnection from tidal inundation. Therefore, we relied on allometric relationships between total habitat area and channel area for estuarine ecosystems developed in Hood (2007). Hood (2007) found total channel surface area scaled as a power function with total marsh island area. We estimated the historical tidal channel surface area from the allometric relationships using the tidal channel areas estimated from our current habitat analysis (Figure G.1)

$$y = 0.006x^{1.3807}$$
$$R^2 = 0.8416$$
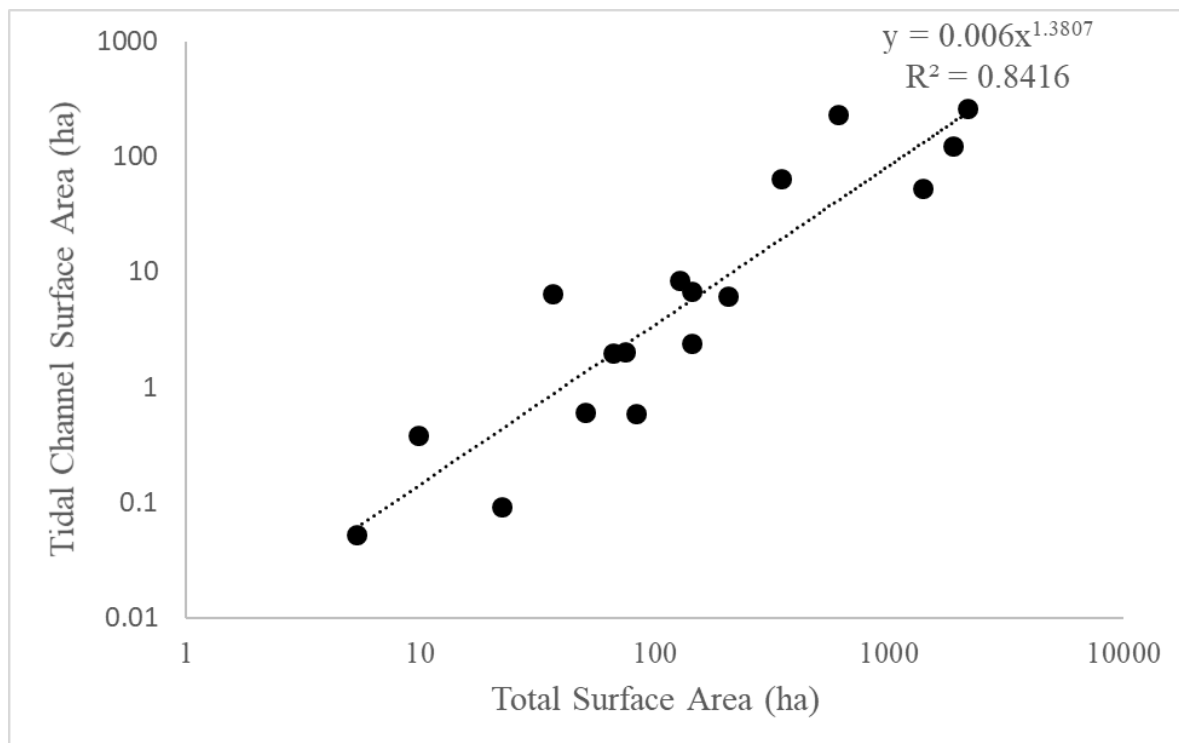
Figure G.1. Allometric relationship between tidal channel surface area and total surface area for estuary polygons in Grays Harbor river deltas.

G.2 Results

Current habitat areas by habitat type and total available habitat area varied among the six delta systems (Figure G.2). The Elk River delta had the highest overall total habitat area as well as the highest total tidal channel area (edge and mid-channel combined) among the systems. However, the Chehalis River delta had more total tidal channel edge habitat than the Elk River delta because the Elk River delta has relatively wide tidal channels and a high proportion of tidal mid-channel habitat. The lowest proportion and lowest total area of tidal channel habitat was in the Hoquiam and Wishkah deltas. Mudflat habitats were only found in the Elk River delta, yet they represented a significant proportion of the total habitat area available for the particular system.
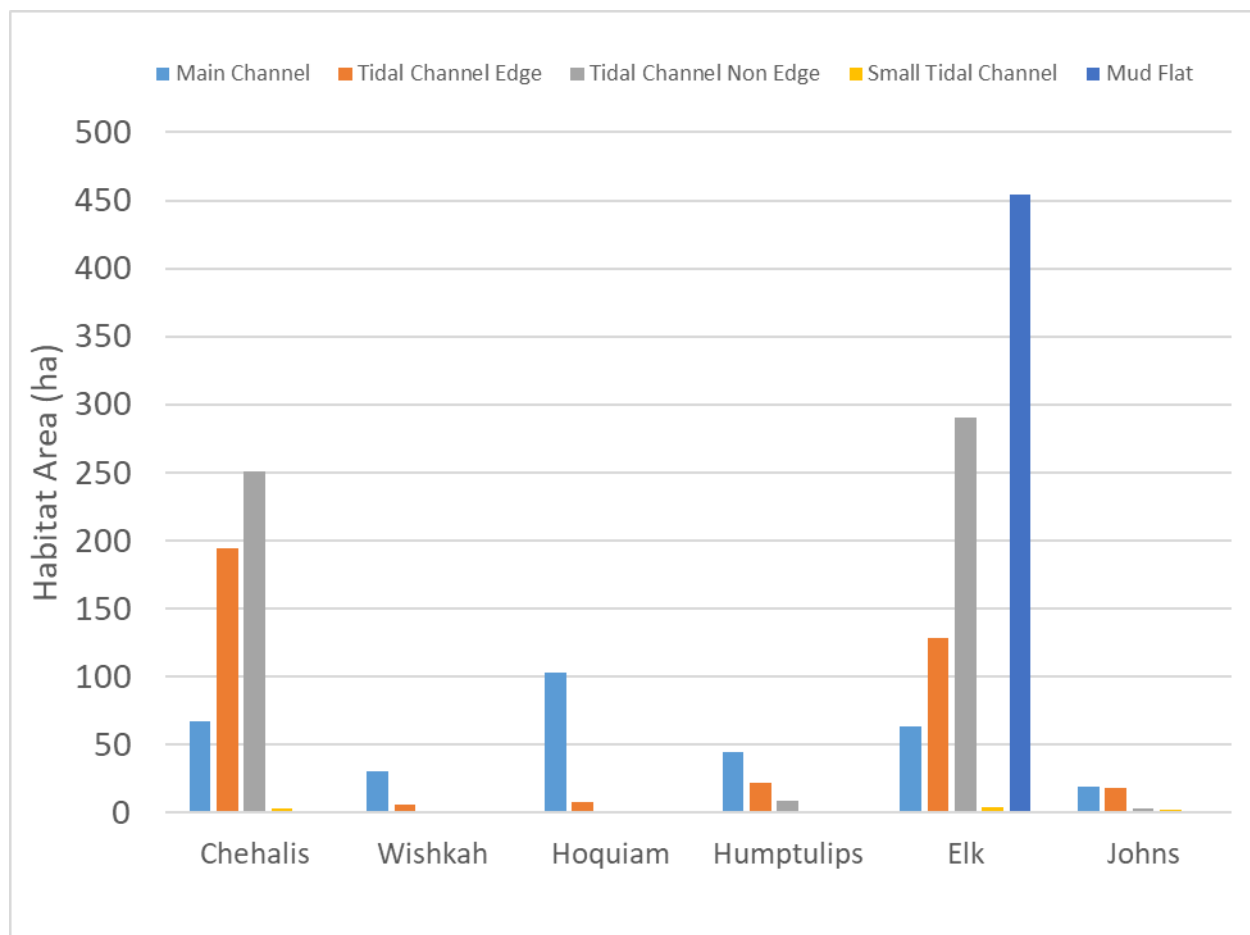
Figure G.2. Current total available habitat area (ha) by habitat type and sub-basin for delta habitats within the Chehalis basin.

Change analysis of delta habitat from historical availability to current inventory revealed relatively little change for most the of the six delta systems (Figure G.3). The Humptulips River delta was the only system where we did not identify historically available habitat area that was not accessible today. Loss of tidal channel habitat ranged between 0 and 143 ha and the average percent change was ~17% (Figure G.4). The Chehalis delta had the highest absolute total change in tidal channel habitat area. Tidal channel habitat in the Chehalis delta has been reduced by approximately 143 ha, largely due to urban development near Aberdeen. Although the Hoquiam delta had relatively little absolute total loss of tidal channel habitat (6.1 ha), the percent change was quite high compared to the other systems (Figure G.4).
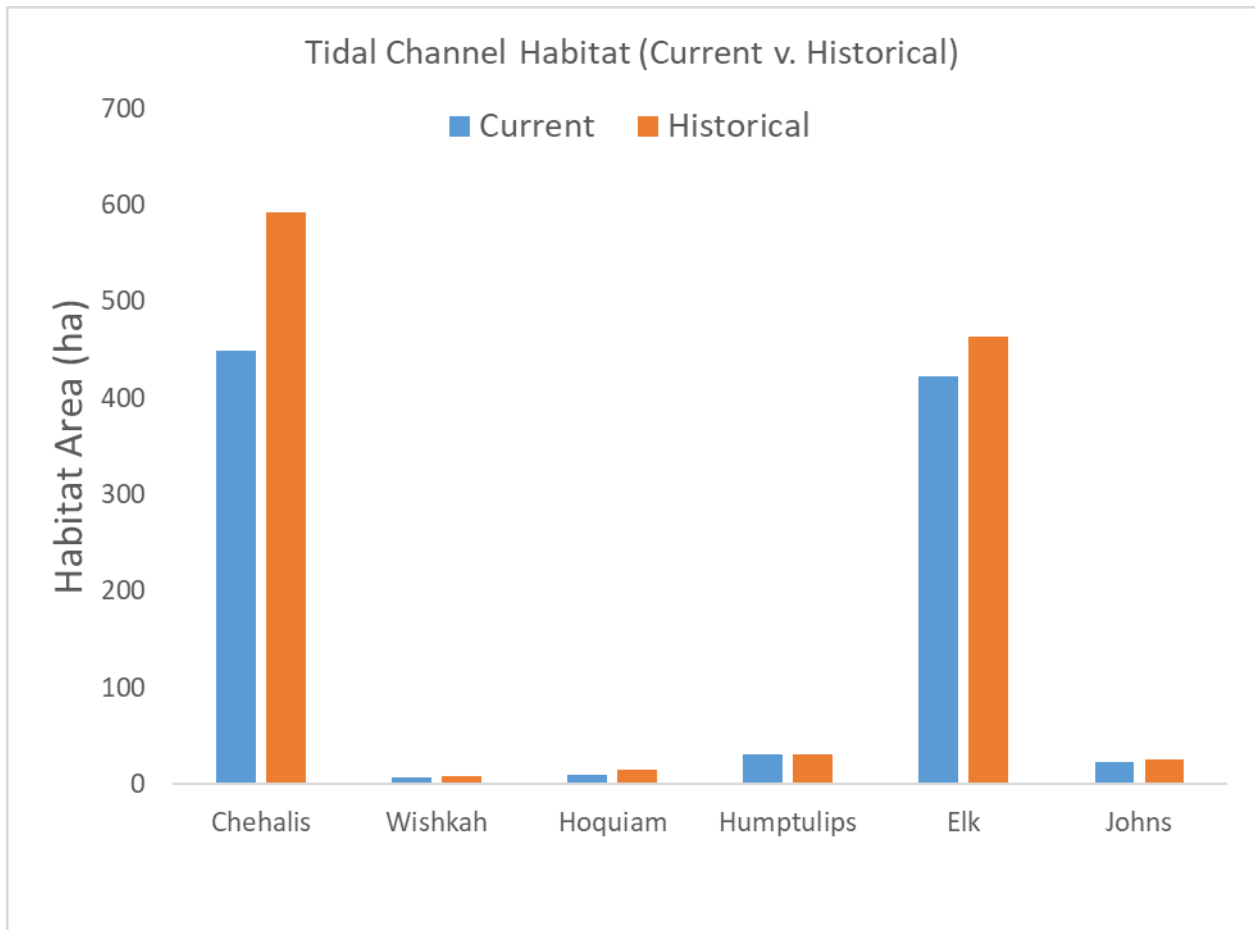
Figure G.3. Comparison of currently available and historically available tidal channel habitat by sub-basin within the Chehalis basin. Tidal channel habitat includes large and small tidal channel networks.
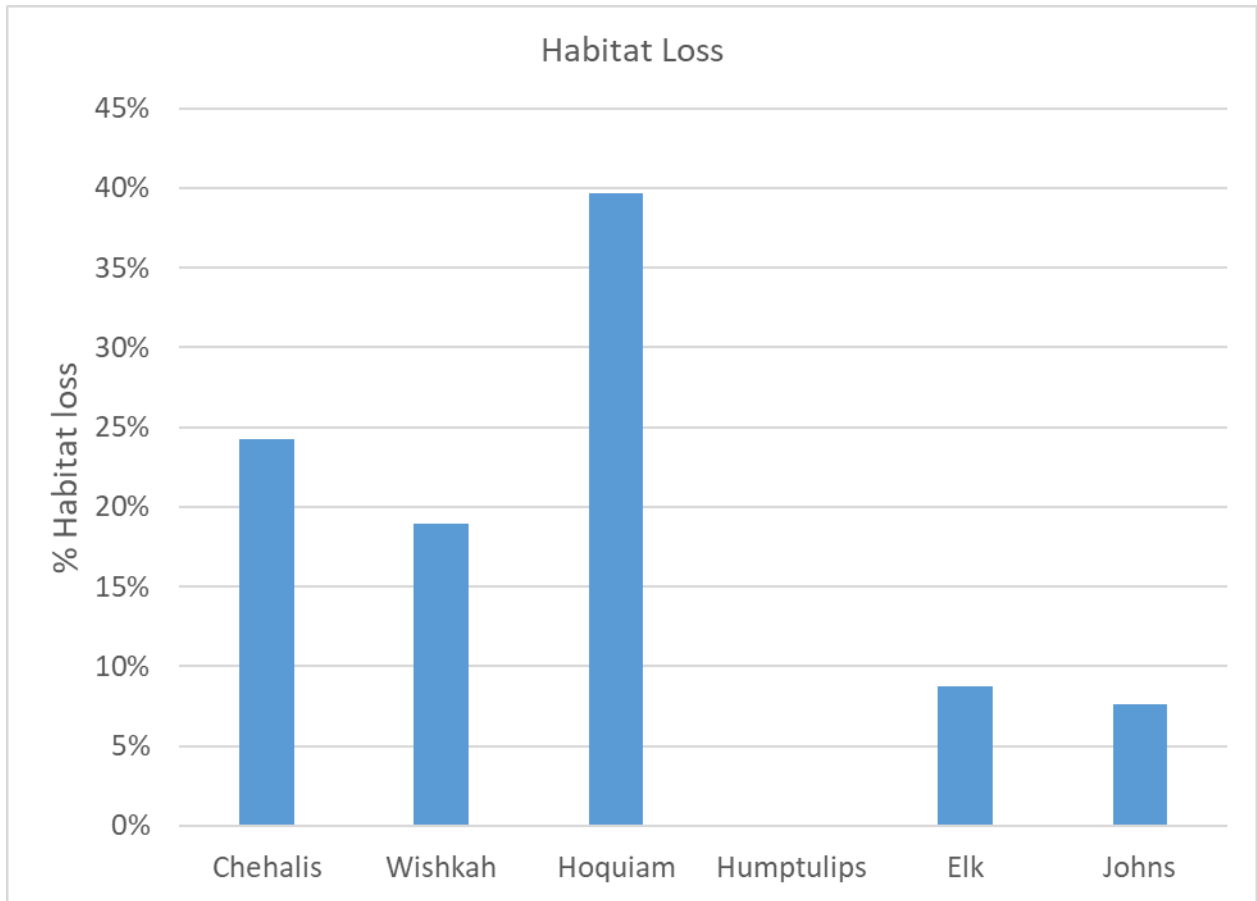
Figure G.4. Percent change in tidal channel area from historic to current conditions by sub-basin.

Appendix H. Estimating Life-Stage Capacities and Productivities

H.1 Spawning

For each species, we estimated historical and current spawning capacity in terms of number of adults and number of eggs. For coho and Chinook in small streams (bankfull width < 20 m), we estimated the species-specific egg capacities (c_{eggs}) as a function of the length of stream, redd density, and adults per redd. For each species we assume a sex ratio of 1:1 and one redd per female.

$$c_{eggs} = Stream\ length\ \times\ \frac{Redds}{km} \times fecundity$$

We used redd density values from Montgomery et al. (1999) for each channel type for Chinook and coho salmon (densities for each species and channel type listed in Section 4). For steelhead, existing redd density data for small streams were very low, and the LCM workgroup did not consider these a good representation of capacity. Therefore, for steelhead in small streams we calculate the total spawning area within each reach using the following equation:

Spawning Area = # pools × wetted width × (wetted width × 0.5)

which assumes that spawning occurs on riffles at pool tail-outs. The spawnable area is estimated by multiplying the wetted width times the length of the tail crest, which we estimated from aerial photography in large rivers to be ½ the wetted width. We use the winter wetted width in this calculation. The number of pools in each reach is calculated as:

 # pools = reach length / (pool spacing × wetted width)

where pool spacing is in units of wetted widths/pool. Conversion from the original data of pool spacing in bankfull widths per pool (Montgomery et al. 1995 and Beechie and Sibley 1997) to pool spacing in wetted widths per pool was done by dividing BFW/pool by 0.4, which is the ratio of wetted width to bankfull width from our empirical prediction equations using values for BFW < 20 m. This methodology produced the following pool spacing ratios for each slope class (<1° or > 1°) and wood abundance class (low wood or high wood):

- slope < 1° and low wood: 12.5
- slope < 1° and high wood: 6.25
- slope > 1° and low wood: 27.5
- slope > 1° and high wood: 5

In large rivers (bankfull width > 20 m) we estimated the c_{eggs} as a function of digitized spawning riffle areas from recent aerial photography and average redd area for each species.

$$c_{eggs} = \frac{(Riffle\ area)}{Redd\ area} \times fecundity$$

Redd areas and data sources for each species are listed in Section 4 of the main report.

For coho we used the average fecundity from Salo and Bayliff (1958), who reported a range from 2107 to 3629 eggs/female for North American populations. To estimate Chinook fecundity we used the average of age specific fecundities reported by Greene and Beechie (2004), which ranged from 2500 to 7500 eggs/female. For steelhead we used a fecundity of 5400 eggs per female for first-time spawners and 8000 eggs per female for repeat spawners (Stober et al. 1983, R2 Resource Consultants, Inc. 2008).

H.2 Freshwater Rearing

For each habitat type in each subbasin we estimate rearing capacity at each life stage by multiplying the total habitat area by a density of juvenile fish. The life-stage specific subbasin productivity is calculated as a weighted average of the reach-level productivities in each subbasin. Reach-specific modifiers of habitat capacity and productivity such as temperature or wood (see Appendix I) are applied prior to summing habitat areas or averaging productivities within a subbasin, but for simplicity we only describe the basic calculations of capacity and productivity in this section (i.e., without the modifiers).

H.2.1 Effect of Habitat Type and Area on Rearing Capacity

For each density dependent life stage, a single rearing capacity is calculated for each spatial unit (subbasin or mainstem unit), by summing the areas of each habitat type and multiplying each total habitat area by the type-specific density. That is, subbasin capacity is the sum of habitat unit capacities for all habitat unit types in a subbasin. For example, summer rearing habitat capacity for a habitat type (c_i) is calculated as:

$$c_i = \left(\left(\sum_{j=1}^{n} A_{ij} \right) \times d_i \right)$$

Where c_i is the capacity of one habitat type (type i), ΣA_{ij} is the sum of areas of all habitat units of that type ($j =1$ through n), and d_i is the density of fish in habitat type i in summer (densities of fish in each habitat unit type are detailed in Section 4 of the main report).

The total capacity for the summer life stage is then the sum of capacities for all habitat types:

$$c_{summer} = c_{(i=1)} + c_{(i=2)} + \cdots + c_{(i-n)}$$

For example, $c_{(i=1)}$ may be the rearing capacity of all small stream riffles in a subbasin, which is the total area of all riffles multiplied by the density of coho in riffles in summer. Similarly, $c_{(i=2)}$ may be the rearing capacity of all small stream pools in a subbasin, which is

the total area of all pools multiplied by the density of coho in pools. If $c_{(i=3)}$ is the rearing capacity of all small stream ponds in a subbasin, then c for small streams in a subbasin is:

$$c_{(small\ streams)} = c_{(riffles)} + c_{(pools)} + c_{(ponds)}$$

The total c for a subbasin also includes the rearing capacities of large river habitats

$$c_{(large\ river)} = c_{(Nat\ bank)} + c_{(Mod\ bank)} + c_{(bar)} + c_{(bkw)}$$

and floodplain habitats

$$c_{(floodplain)} = c_{(marsh)} + c_{(pond)} + c_{(side\ channel)}$$

Where $c_{(large\ river)}$ and $c_{(floodplain)}$ are comprised of the summed capacities of their respective habitat types. Hence, the total summer rearing capacity for the subbasin is

$$c_{summer} = c_{(small\ stream)} + c_{(large\ river)} + c_{(floodplain)}$$

H.2.2 Effect of Habitat Type and Area on Rearing Productivities

The life-cycle model requires a single value of productivity for each life-stage and subbasin. We use empirical or modeled productivity values (p) for each life-stage and species representing current conditions, and we estimate productivity separately for small streams, large rivers, and pond and floodplain habitats (including ponds and marshes in both small streams and floodplains). Productivities for each species and life stage are detailed in Chapter 4 of the main report. To illustrate with a simplified example, we calculate the weighted average productivity for each subbasin based on the proportion of rearing capacity in each habitat area:

$$p = (f_{ss} \times p_{ss}) + (f_{lr} \times p_{lr}) + (f_p \times p_p)$$

Where:

- p is the weighted average productivity for a life-stage and subbasin,
- f_{ss} is the proportion of rearing capacity in small streams, and p_{ss} is the productivity value applied to that proportion of the subbasin,
- f_{lr} is the proportion of rearing capacity in large rivers, and p_{lr} is the productivity value applied to that proportion of the subbasin, and
- f_p is the proportion of rearing capacity in ponds and marshes, and p_p is the productivity value applied to that proportion of the subbasin.

Note that f_{ss}, f_{lr}, and f_p sum to 1 to represent the entire spatial unit. To illustrate with a hypothetical example, if there are few coho salmon rearing in beaver ponds in winter under current conditions (5%) and most fish are rearing in small streams (55%) or large rivers (40%). The weighted average winter rearing productivity would be:

$$(0.55×0.24) + (0.40×0.24) + (0.05×0.68) = 0.26.$$

This value of 0.26 is then applied to the entire winter rearing population in that subbasin. A change in wood abundance can increase productivity in small streams (e.g., 0.24 currently to 0.40 historically, Quinn and Peterson 1996), or in large rivers when increased productivity is scaled to increased capacity (e.g., 0.24 to 0.27, McHugh et al. 2017) (see Appendix I for details). The resulting weighted average productivity change for increased wood abundance is then

$$(0.55×\mathbf{0.40}) + (0.4×\mathbf{0.27}) + (0.05×0.68) = 0.36.$$

Note that the bolded numbers have changed from the prior equation. Alternatively, if under historical conditions the proportions were 30% rearing in ponds, 30% in small streams, and 40% in large rivers, the weighted average winter rearing productivity for that subbasin would be

$$(\mathbf{0.30}×0.24) + (0.40×0.24) + (\mathbf{0.30}×0.68) = 0.37.$$

This has the effect of increasing the subbasin average productivity because a larger proportion of juvenile coho are rearing in a habitat type with a higher productivity. If both wood abundance and pond area are changed simultaneously, the weighted average productivity is then

$$(\mathbf{0.30}×\mathbf{0.40}) + (0.4×\mathbf{0.27}) + (\mathbf{0.30}×0.68) = 0.43.$$

H.3 Delta Rearing

Our goal was to develop species-specific capacity estimates for fall Chinook, spring Chinook, chum and coho salmon in the delta habitats within the Chehalis basin. We did not estimate delta capacity for steelhead since the juveniles rely very little on estuary rearing (Quinn 2005) and move rapidly through estuarine habitats (Moore et al. 2010). Chinook capacity estimates reflect only sub-yearling life history types for two reasons: 1) yearling Chinook are not known to rear or reside in estuarine/delta habitats for extended periods (i.e., similar to steelhead) and, 2) prior studies have documented very low abundance (almost non-existent) of yearling Chinook in the delta habitats (Simenstad and Eggers 1981, Sandell et al. 2014). Therefore our single combined estimate of capacity for sub-yearling Chinook represents juveniles from both fall and spring Chinook populations within the basin. Capacity per unit area within the delta is a function of daily maximum fish density (# fish/ ha at carrying capacity), mean residence time (days), and the temporal extent of the rearing period (days). Given differences in mean residence times and rearing period among species (Groot and Margolis 1991), capacity varies by species. We estimated species–specific capacity using

$$c_i = (d_i * t_i)/r_i$$

where, c_i is capacity per unit area, d is maximum daily density at carrying capacity for species i (fish/ha), t_i is the extent of the rearing period in # of days for species i, and r_i is the mean residence time in days for species i. The maximum daily density was assumed to represent the total density of fish for a particular area independent of rearing period or residence time.

Where possible, we used local data from the Chehalis basin and Grays Harbor to inform our estimates of maximum daily density, residence time and rearing period. Species-specific rearing periods in delta habitats for the Chehalis basin were taken from historical (Simenstad and Eggers 1981, Brix 1981) and recent (Sandell et al. 2014) surveys or monitoring activities in Grays Harbor and its associated delta habitats. We calculated the extent of the rearing period as the number of days fish were present in the delta based on fish counts from beach seines or fyke trap catches. Local information on maximum daily density or mean residence time was not available for the Chehalis basin delta habitats. For these attributes, we relied on information from similar large delta habitats throughout the Pacific Northwest. We substituted maximum daily sub-yearling Chinook density estimates for tidal channel habitats (0.841 fish/m^2) within the Skagit River delta (Beamer et al. 2005), a system known to operate at carrying capacity, to estimate capacity for all species of interest. We found literature values of mean residence times for each species, and compared those values to local catch curves from recent and historical survey data.

H.3.1 Scaling Delta Density Estimates Based on Habitat Quality

Estuaries provide a variety of habitat types for outmigrating juvenile salmonids, but the values of each habitat type are not equal, nor are habitats distributed uniformly across the landscape. Prior to assigning species-specific capacity estimates to each habitat area or polygon, we scaled the density estimates based on habitat quality. We assessed habitat quality using a set of variables (habitat type, depth, velocity, and vegetation) that influence how juvenile salmon are distributed within estuaries, modeled after Hendrix et al. (2014). Juvenile salmon are often found in higher densities within tidal channels compared to main channel habitats, and they prefer habitats within specific velocity (<0.2 m/s) and depth ranges (0.2 m to 1.5 m) (Beamer et al. 2005, Hendrix et al. 2014). Salmon also appear to prefer areas with vegetated banks, so we assumed non-vegetated areas (i.e., banks with urban development) were lower quality and therefore were assigned a lower maximum density value (Hendrix et al. 2014).

For the habitat type attribute, we divided habitat polygons into "main channel" or "tidal channel" (including tidal channel, small tidal channel) habitat types. Tidal channel and main channel habitats were assigned "high" and "low" quality, respectively. Empirical data for depth and velocity were not available for the deltas within the Chehalis basin, so we developed a proxy for these attributes by separating each habitat type into edge and mid-channel components. To estimate the edge habitat area for main channel and tidal channel habitats, we buffered each feature using a 10 m inside only buffer. We then calculated the total edge habitat area (ha) of each polygon feature, and subtracted edge area from the total area of the feature to get the total mid-channel area. We did not include the mid-channel component of the main channel in our analysis because we assumed that those

areas are distributary pathways for migrating fish, but not rearing habitat. The edges of both main channel and tidal channel habitats were assumed to have depth and velocity within preferred ranges, and therefore were considered "high" quality. Within tidal channels, we considered the mid-channel area to be "low" quality.

Maximum densities were scaled by habitat quality based on observed comparisons between tidal channel and main channel habitats in the Chehalis basin (Sandell et al. 2014) as well as other large river deltas (Rice et al., unpublished data). We assigned the maximum density (0.841 fish/m^2) to high-value tidal channel edge habitats, 0.5 × maximum density to non-edge tidal channel habitat, 0.25 × maximum density to vegetated main channel habitats, and 0.125 × maximum density to unvegetated main channel habitats. Mudflat habitats were assigned the same density value as unvegetated main channel habitats.

H.3.2 Scaling Capacity Estimates Based on Connectivity

Applying landscape ecology principles to estuarine research is an emerging component of estuary monitoring and restoration programs (Congleton et al. 1981, Beamer et al. 2005, Rice et al. 2014). More specifically, applying habitat connectivity measures that incorporate how the location of a particular habitat within the estuarine landscape can affect the presence or abundance of salmonids. Connectivity refers to the position in the landscape (e.g. along the upstream/downstream gradient) as well as the complexity of the channel network (i.e. the number of bifurcations passed to get to a particular habitat). Areas or habitats with higher connectivity have a higher capacity compared to location with lower connectivity (Beamer et al. 2014, Figure H.1).

We used landscape connectivity to scale the capacity (based on habitat quality assessment per above), of particular locations within each estuary following methods used in the Skagit River delta (Beamer et al. 2005). Connectivity (K) was calculated as follows,

$$ K = \frac{1}{\sum_{j=1}^{jend}\left(O_j * D_j\right)} $$

Where O_j is distributary channel order for channel segment j, D_j is distance along segment j of order O_j, j is the count (1...j_{end}) of distributary channel segments, and j_{end} is the total number of channel segments at each sample point. However, none of the delta systems in the Chehalis basin featured bifurcations where an upstream channel was divided into 2 or more downstream channels (i.e. O_j = 1 for all areas in all deltas) so the above equation was reduced to be a function of distance along the main channel. We divided the main channel within each delta into 100-m
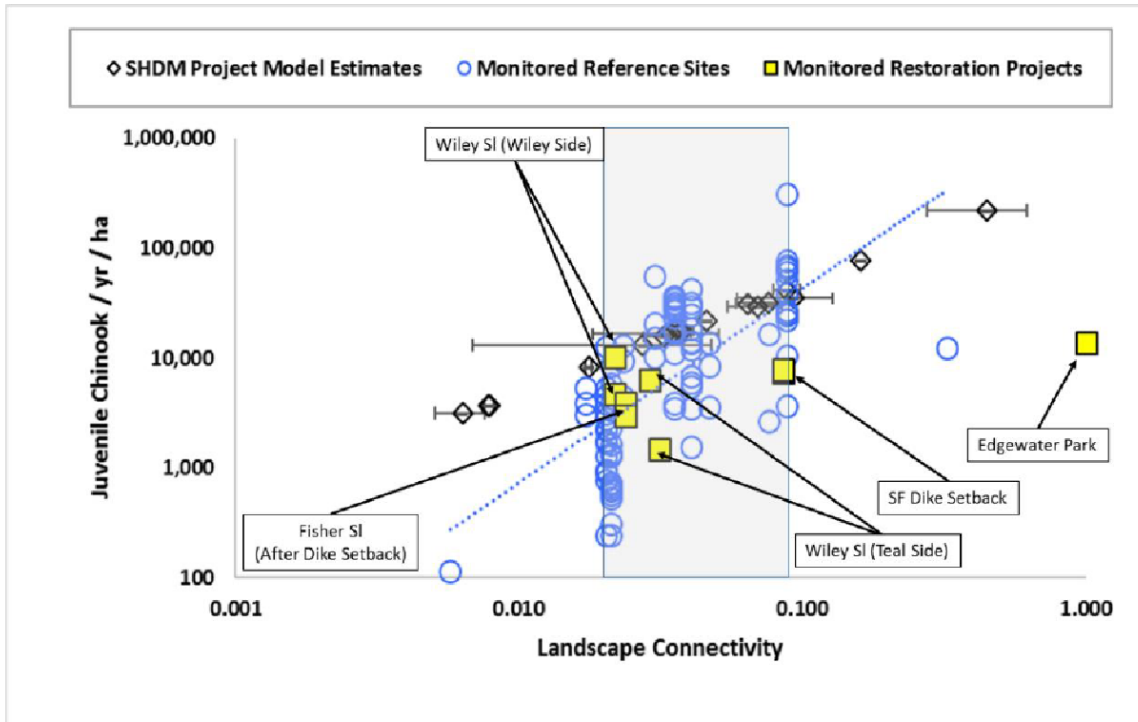
Figure H.1. Yearly capacity of juvenile Chinook salmon in the Skagit River delta as a function of landscape connectivity. Figure from Beamer et al. (2014).

sections using equally spaced points along the centerline, beginning at the upper extent of the delta. The polygon at the upper extent of each delta was given a score of 1 and all other points were scored based on their distance from the uppermost polygon along the centerline using the revised equation. Where multiple upstream channels converged to create a single downstream channel, the connectivity scores were averaged at the point of convergence and then recalculated for points downstream initiating from the value at convergence. Tidal channel, small tidal channel, and mudflat habitats were assigned a single score that matched the score where they connected to their respective main channel sections. For cases where these habitats connected between two 100-m main channel polygons they were given the higher connectivity score.

Once each polygon was assigned a connectivity score, we adjusted the capacity for each polygon based on the scaled estimates from the habitat quality assessment using the equation developed in the Skagit River delta where, the species- and habitat-specific capacities were scaled as follows;

$\ln(c) = 1.76 * \ln(K) +$ species-specific intercept

The species-specific intercepts were back-calculated from the above equation by setting K =1 and using the maximum species-specific c values as described above. Finally, total capacity is the scaled capacity estimates per unit area summed over all available habitat area within each sub-basin.

We estimated delta rearing capacity within the Chehalis basin for coho, chum, and fall and spring Chinook salmon. Species-specific theoretical maximum capacities per unit habitat area by habitat type and quality varied for Chinook, coho, and chum salmon (Table H.1). Total capacities also differed by species and among the sub-basin deltas (Table H.2). The capacities within the Chehalis River delta and the Elks River delta were the highest among the separate subbasins. The high capacities reflect not only the amount of total habitat available, but also the large proportions of tidal channel habitat available in these systems. Chum salmon had the highest total capacity among the species given their short residence time but relatively protracted presence in the delta habitats. Both Chinook and coho salmon had similar total capacity estimates, reflecting more similar rearing periods and residence times.

Table H.1. Species-specific capacity estimates per hectare for salmonids in delta habitats within the Chehalis basin. Capacity calculated from a common max daily density (8410 fish/ha) and scaled accordingly for species-specific rearing period and mean residence time and adjusted for habitat quality. Log values used to scale capacity estimates based on habitat connectivity. Note that steelhead do not have a significant estuary residency, so there is no capacity estimate.

| | | | Capacity (fish/ha/yr) | | | | | | | |
| | | | Off | | Main | | ln(Off) | | ln(Main) | |
Species	# Days present	Mean Residence Time (days)	Edge	Mid-channel	Veg	Unveg	Edge	Mid	Veg	Unveg
Chinook[a]	196	35	47,096	23,548	11,774	5,887	10.76	10.07	9.37	8.68
Coho	150	30	42,050	21,025	10,513	5,256	10.65	9.95	9.26	8.57
Chum	90	10	75,690	37,845	18,923	9,461	11.25	10.54	9.85	9.16

a. Chinook estimates are for combined fall and spring Chinook run types representing the sub-yearling life history type.

Table H.2. Total habitat area by habitat type (ha) and species-specific rearing capacity estimates (# fish/yr) for delta habitat within the Chehalis basin. Capacities divided by sub-basin and summed for total basin capacity by species.

Habitat type	Habitat area (ha)						
	Chehalis	Wishkah	Hoquiam	Humptulips	Elk	Johns	Total
Main Channel Tidal Channel	67.0	30.5	102.6	44.7	63.7	19.5	328.1
Edge Tidal Channel	194.0	6.2	8.4	21.7	128.6	18.4	377.4
Non Edge Small Tidal	251.3	0.23	0.18	8.8	290.1	3.1	553.6
Channel	3.3	0.0	0.7	0.4	4.4	2.1	10.8
Mud Flat	0.0	0.0	0.0	0.0	454.3	0.0	454.3
Total	515.6	37.0	112.0	75.5	941.1	43.0	1,724.1

Species	Rearing capacity (# fish/yr)						
	Chehalis	Wishkah	Hoquiam	Humptulips	Elk	Johns	Total
Fall/Spring Chinook	342,712	44,735	160,205	33,301	339,457	59,748	980,158
Chum	415,206	72,148	261,673	55,489	468,570	96,571	1,369,657
Coho	230,667	40,082	144,771	29,768	313,731	65,247	824,267

Appendix I. Estimating Changes in Habitat Capacity and Productivity

Changes in survival of salmonid eggs or juveniles from one life-stage to the next can be estimated based on empirical relationships between habitat characteristics and life-stage capacity or productivity. In some cases there are data available to estimate changes in capacity and productivity separately for a life stage. However, in other cases we do not have sufficient data to relate a habitat change to either a capacity or productivity change directly. In those cases, we define the functional relationship between a habitat change and capacity (or productivity), and apply that same function to productivity (or capacity). For example, we do not have data to relate summer rearing productivity to wood abundance directly, but we can estimate change in summer rearing capacity with increased wood abundance, and then estimate an equivalent increase in productivity. Similarly, we do not have data to relate summer rearing capacity to a change in temperature directly, but we can estimate a change in productivity with a change in temperature, and then apply the same function to summer rearing capacity.

Each habitat change affects one or more life stage parameters for one or more species in the NOAA model. Tables I.1 and I.2 summarize which life stage parameters are modified by each habitat factor for each species. The following sections describe the functional relationships used in the NOAA model to estimate changes in life-stage capacity or productivity for each habitat attribute.

Table I.1. Checklist of life stage capacities (c) and productivities (p) affected by each habitat factor in the habitat model and life-cycle models for coho salmon and steelhead. The value c_{egg} is egg capacity, p_{incub} is incubation productivity, c_{sr} is summer rearing capacity, p_{sr} is summer rearing productivity, c_{wr} is winter rearing capacity, and p_{wr} is winter rearing productivity.

	c_{egg}	p_{incub}	c_{sr}	p_{sr}	c_{wr}	p_{wr}
Barriers	X		X[1]	X	X[1]	X
Fine sediment		X				
Wood loading	X		X	X	X	X
Shade			X	X		
Channel length	X		X	X	X	X
Bank condition			X	X	X	X
Beaver pond area	X(neg)		X	X	X	X
Floodplain			X	X	X	X
Wood + floodplain	X		X	X	X	X

1. Effect expressed only when barrier is 100% blocking.

Table I.2. Checklist of life stage capacities (c) and productivities (p) affected by each habitat factor in the habitat model and life-cycle models for spring and fall Chinook. The value $p_{prespawn}$ is prespawn productivity, c_{egg} is egg capacity, p_{incub} is incubation productivity, c_{sub} is subyearling rearing capacity, and p_{sub} is subyearling rearing productivity.

	$p_{prespawn}$	c_{egg}	p_{incub}	c_{sub}	p_{sub}
Barriers		X		X[1]	X
Fine sediment			X		
Wood loading		X		X	X
Shade	X[2]			X	X
Channel length		X		X	X
Bank condition				X	X
Beaver pond area		X(neg)		X	X
Floodplain				X	X
Wood + floodplain		X		X	X

1. Effect expressed only when barrier is 100% blocking.
2. Spring Chinook only.

I.1 Migration Barriers

I.1.1 Barrier Effects on Spawning Capacity

We assume that a barrier reduces spawning capacity (and egg capacity) above each barrier using the passage ratings in the WDFW barrier database. For example, the spawning capacity (or egg capacity) above a barrier with a passage rating of 0.33 is given 1/3 of its full capacity. Where there are multiple barriers in sequence on a stream, the barrier passage ratings are multiplied together to further reduce spawning capacity above multiple barriers. That is, for three successive barriers with passage rating of 0.33, the egg capacity is 1/3 of capacity above the first barrier, 1/9 (0.11) of capacity above the second barrier, and 1/27 (0.04) of capacity above the third barrier.

I.1.2 Barrier Effects on Prespawn and Incubation Productivity

We weight both prespawn and incubation productivity by egg capacity, and egg capacity is affected by migration barriers. That is, when we calculate the subbasin-level average prespawn productivity we weight the reach-level productivities by egg capacity, which is reduced above each barrier using the passage rating as described in Section I.1.1. Similarly, incubation productivity for a subbasin is also calculated as the weighted average of reach-

level incubation productivities, where the weight is egg capacity. Prespawn productivity is also directly impacted by barriers using the passage rating.

I.1.3 Barrier Effects on Rearing Capacity

Rearing capacity is not affected by a barrier unless the passage rating is 0. When the passage rating is >0, we assume that some spawners can make it to that reach, and the juveniles they produce have access to the full rearing capacity. When the passage rating is 0, we assume that no spawners access that reach and no juveniles will be produced to use that habitat. Therefore, we do not include the rearing capacity of reaches above barriers with a passage rating of 0 in the total rearing capacity for a subbasin.

I.2 Beaver Dams

I.2.2 Beaver Pond Effects on Spawning Capacity

To account for inundation of spawning gravel by beaver ponds in small streams, we used a typical pond length of 25 m, which inundates 15% of the stream length in the historical condition with 6 ponds/km. Therefore, we reduced spawning habitat capacity by 15% for the historical condition in small streams to account for inundation by ponds. In the current condition with 0.55 ponds/km, we reduced spawning habitat capacity by 1.4%.

I.2.2 Beaver Pond Effects on Rearing Capacity and Productivity

Beaver ponds have strong influences on overwintering capacity and productivity of coho salmon (e.g., Pollock et al. 2004, Ogston et al. 2014), and to a lesser extent summer rearing capacity and productivity. We assumed that rearing densities of coho salmon in beaver ponds are similar under current and historical conditions, but that the area of beaver ponds was substantially greater historically (Pollock et al. 2004). For beaver ponds in small streams, we set density at 1.2 fish/m^2 in both summer and winter, which is the area-weighted average of small and large pond densities in Reeves et al. (1989) (1.8 and 0.9, respectively, with area weights estimated from Figure 4 in Pollock et al. 2004). Summer rearing productivity is set at 0.84 (Reeves et al. 1989), and is considered the same for historical and current conditions. Winter rearing productivity in beaver ponds is 0.78 (Ogston et al. 2014). To account for inundation of rearing pools and riffles by ponds, we reduced pool and riffle rearing areas by 1.4% (current condition) or 15% (historical condition).

In the spring and fall Chinook models, we found no data for densities of juvenile Chinook in ponds, so we assumed that rearing densities are the same in pools and ponds. Hence, Chinook rearing densities are 0.09 in both pools and ponds (J. Thompson, Skagit River unpublished data). By contrast, juvenile steelhead densities in beaver ponds are lower than in pools. First-year summer and winter densities are 0 and 0.03 fish/m^2 in ponds (0.63 and 0.14 in pools), and second-year summer and winter densities are 0.07 and 0.01 fish/m^2 in ponds (0.17 and 0.07 in pools) (Johnson et al. 1993).

I.3 Fine Sediment

Fine sediment affects density-independent incubation productivity in redds as a function of percent fine sediment in spawning gravels (Table 4.1.3), We model reach-level percent fine sediment <0.85 mm in spawning gravels as a function of the slope-area index and road density (Appendix C), and then model density-independent incubation productivity as a function of percent fine sediment. Incubation productivity for a subbasin is then calculated as the weighted average of reach-level incubation productivities where the weight is egg capacity. The slope-area index is an indicator of sediment transport capacity, and is the product of channel slope and drainage area. An empirical relationship between the slope-area index and percent fine sediment <0.85 mm in spawning gravels indicates that fine sediment levels are typically very high where the slope-area index is <0.05 (average of 27%, data from Mobrand Biometrics, Inc. 2003) (see Figure C.3 in Appendix C). This indicates that channels with low sediment transport capacity tend to have higher fine sediment levels regardless of road density. Where the slope area index is >0.05, we estimate fine sediment levels as a function of road density using:

$$fine\ sed = 5.74 + 2.05 * road\ density$$

where *fine sed* is percent fine sediment <0.85 mm and *road density* is in hectares of current roads per hectare of drainage area (data from the nearby Queets and Clearwater Rivers, Cederholm et al. 1982) (see Appendix C for more detail).

I.3.1 Fine Sediment Effect on Incubation Productivity

Once we estimated percent fines for each reach, we modeled incubation productivity for those reaches. Jensen et al. (2009) summarized published values of incubation productivity for four salmonid species (Chinook, coho, chum, and steelhead) and created a logistic model to relate percent fines to percent incubation productivity. Jensen et al. (2009) presented data for all four salmonid species, but there was significant overlap among species and there appeared to be little justification for using different functional relationships for each species. Therefore, we applied the published β_0 and β_1 estimates for the all-species functional relationship for each reach using the equation:

$$p_{incub} = \frac{1}{1 + e^{-(\beta_0 + \beta_1 * sed)}}$$

where p_{incub} is incubation productivity, *sed* is percent fine sediment < 0.85 mm, and β_0 and β_1 are empirically derived (β_0 = 1.989 and β_1 = -0.185, Figure I.1.1). We then averaged the reach-specific productivities for each species to generate species-specific incubation productivities for each subbasin under current conditions. Finally, we modeled historical fine sediment values to estimate historical incubation productivity (by reducing road density to zero, see Appendix C for details). This resulted in *sed* being fixed at 5.74% fines in all reaches with a *Slope*Bankfull Width* value of > 0.05, which is the intercept of the road density equation. Similar to the model of current conditions, we fixed reaches with *Slope*Bankfull Width* < 0.05 at 27.6% fines. Therefore, *p* = 0.72 under historical conditions for reaches with slope-area index >0.05, and *p* = 0.042 under historical conditions for

reaches with slope-area index <0.05. Reach-specific productivities were then averaged to generate subbasin-specific incubation productivities.
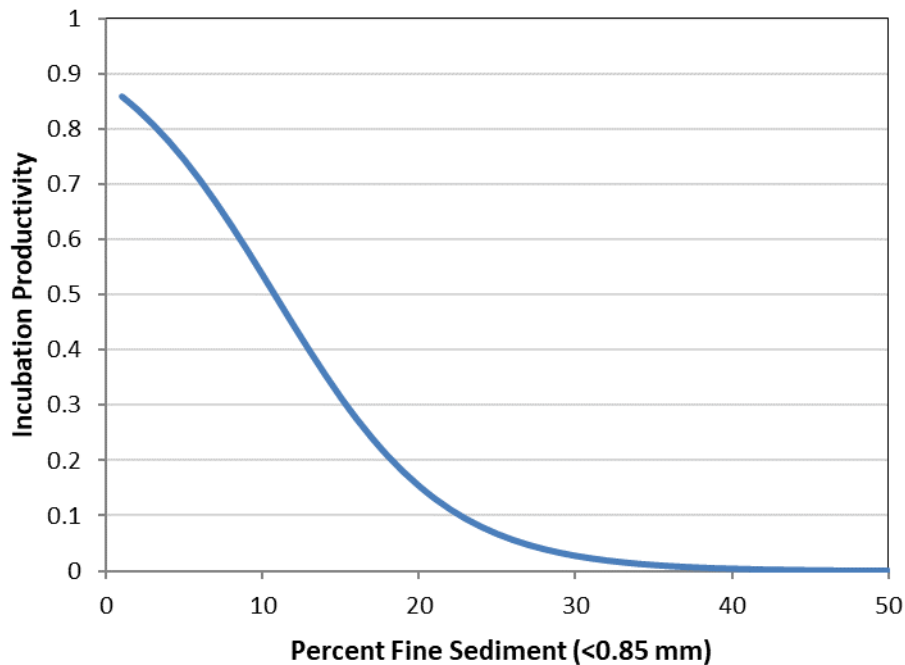

Figure I.1. Functional relationship used to calculate incubation productivity from percent fine sediment. Curve recreated from Jensen et al. (2009).

I.4 Wood Abundance

I.4.1 Wood Effect on Spawning Capacity: Small Streams

For coho salmon spawning capacity, wood abundance in small streams increases redds per km (Montgomery et al. 1999) from 85 in low-slope, low-wood (pool-riffle) channels to 274 in low-slope, high-wood (forced pool-riffle) channels, and from 12 in moderate-slope low-wood (plane bed) channels to 274 in moderate-slope, high-wood (forced pool-riffle) channels. Note that the forced pool riffle planform occurs in both low-slope and moderate-slope channels.

For spring and fall Chinook spawning capacity, historical wood abundance in small streams increases redds per km from 4.2 in low-slope, low-wood (pool-riffle) channels to 8.8 in low-slope, high-wood (forced pool-riffle) channels, and from 0 in moderate-slope low-wood (plane bed) channels to 8.8 in moderate-slope, high-wood (forced pool-riffle) channels (Montgomery et al. 1999).

For steelhead, we we did not have good redd density values in small streams. Therefore, we estimated the change in spawning capacity using the following equation to estimate change in spawning gravel area:

*Spawning Area = # pools * wetted width * (wetted width * 0.5)*

which assumes that spawning occurs on riffles at pool tail-outs. We then divided spawning area by redd area to estimate redd capacity. Additional details are in Appendix H.1.

I.4.2 Wood Effect on Spawning Capacity: Large Rivers

We found no data to support a specific percent increase in spawning gravel area as a function of wood abundance in large rivers. However, we know that in small streams with high wood abundance, bar frequency is double that of small streams with low wood abundance (Buffington and Montgomery 1999, Montgomery et al 1999). We also know that wood in large channels is mostly mobile and accumulates as bar apex or meander bend jams, which have less effect on pool and bar frequency than wood in small channels (Abbe and Montgomery 2003, Roni et al. 2017). Therefore, we assume that increased spawning capacity in large rivers is much less than the doubling in small streams, so we chose to assume that spawning capacity increases by 30% at high wood abundance in large rivers, which is intended to reflect increased spawning gravel retention and holding pool formation.

I.4.3 Wood Effect on Incubation Productivity

In theory, wood can increase gravel retention and decrease scour depth, which should increase incubation productivity. However, we currently do not have sufficient quantitative information to estimate the effectiveness of wood at reducing redd scour. For this version of the NOAA model, we have included a place-holder multiplier for increasing incubation productivity as wood increases gravel retention, but in the absence of a quantitative relationship the multiplier is currently set at 1.0 (no change in incubation productivity as wood abundance increases).

I.4.4 Wood Effect on Coho and Steelhead Summer Rearing Capacity

For summer rearing, we model an effect of wood abundance on rearing capacity through changes in pool area as a function of land cover. Therefore, the method of modeling wood effects on summer rearing capacity is the same for all species. We stratified habitat surveys conducted by WDFW by slope class and landcover, and extrapolated those values to the remaining reaches in each category (method from Beechie et al. 1994, 2001). In the Chehalis basin, low-slope reaches in agriculture and bare land have high percent pool areas relative to the estimated reference percent pool area (which is locally derived, but there are no true reference sites in the Chehalis). Therefore, habitat capacity can be as high or higher under current conditions when we assign similar fish densities. Field observations suggest that these channels are slough- or pond-like, with low densities of juvenile salmonids. However, our temperature model indicates high stream temperatures in

agriculture streams, which reduces the capacity estimates for those areas. In moderate-slope channels percent pool areas are modestly lower in the agriculture land cover class, but significantly lower in all other land cover classes. Hence, moderate slope reaches with high wood abundance (i.e., reaches assigned the reference value of percent pool area) have higher summer rearing capacity.

In large rivers, we modified summer rearing capacity for coho salmon and steelhead using an estimated increase in wood cover in edge habitats, which increases juvenile rearing densities (Beechie et al. 2005a). Based on aerial photograph observations in the nearby Queets River basin with high wood abundance, we estimated that under historical conditions approximately 5% of the habitat area would have wood cover. Juvenile salmonid data from Beamer and Henderson (1998) and Jamie Thompson (unpublished data) showed that coho salmon densities are roughly 2.5 times higher with wood cover in bar edge units and 4.2 times higher with wood cover in bank edge units than densities in these units without cover. Using a weighted average of fish densities in areas with wood and without wood under natural conditions, we estimated that weighted average densities of fish are 2% and 20% higher in bar and bank edge habitats, respectively. From these estimates, we calculated a subbasin-specific multiplier to increase coho summer rearing capacity under historical conditions, which ranged from 1.08 to 1.19. Following the same procedure for steelhead, we calculated subbasin-specific multipliers that ranged from 1.04 to 1.05.

I.4.5 Wood Effect on Coho and Steelhead Winter Rearing Capacity

For winter rearing in small streams, we used the same procedure as for summer rearing, except that we estimated that winter pool areas were 30% of summer pool areas (based on habitat surveys in the same reaches at summer and winter base flows, Beechie 1998). That is, flow velocities are higher in winter than in summer, and much more of the habitat is classified as high velocity riffles in winter than in summer. The remaining 70% of summer pool area was reclassified as riffle. We then summed the reach-level pool and riffle areas to the subbasin level, and used published rearing densities to estimate coho and steelhead winter rearing capacities in small streams.

For large river winter rearing habitat capacity, the basin-specific wood multipliers were calculated as above for summer rearing habitat and were used to increase rearing capacity under historical conditions, with subbasin specific values ranging from 1.13 to 1.20 for coho salmon and 1.06 to 1.08 for steelhead.

I.4.6 Wood Effect on Chinook Subyearling Rearing Capacity

For Chinook subyearlings in small streams, we used the same procedure as for winter rearing habitat because the highest Chinook subyearling densities are found in late winter (Beechie et al 2005a). That is, we estimated changes in pool and riffle areas in winter as a function of wood abundance, and then applied the Chinook rearing densities by habitat type (Section 4.2) to estimate change in small stream subyearling rearing capacity.

In large rivers, Chinook juvenile salmonid data from Beamer and Henderson (1998) and Jamie Thompson (unpublished data) show that juvenile Chinook salmon densities are 2.5 times higher with wood cover in bar edge units and 3.2 times higher with wood cover in bank edge units than densities in these units without cover. Based on aerial photograph observations in the nearby Queets River basin with high wood abundance, we estimated that under historical conditions approximately 5% of the habitat area would have wood cover. Using a weighted average of fish densities in areas with wood and without wood under natural conditions, we estimated that weighted average densities of fish are 3% and 16% higher in bar and bank edge habitats with natural wood abundance than in those habitats with current low wood abundance, respectively. From these estimates, we calculated subbasin-specific multipliers to increase subyearling rearing capacity under historical conditions, which ranged from 1.05 to 1.15.

I.4.7 Wood Effects on Rearing Productivity

In large rivers where empirical relationships between productivity and wood abundance were not available, we scaled summer and winter productivity increases to the increase in rearing capacity due to increased wood abundance (McHugh et al. 2017). For coho salmon, the multiplier ranges from 1.05 to 1.19 in summer, with an average of 1.13 applied to subbasins with no relationships available (i.e., in subbasins with no large river segments). In winter, the multiplier ranges from 1.20 to 1.21 in winter, with an average of 1.206 applied to subbasins with no relationships available.

For steelhead, the multiplier ranges from 1.02 to 1.05 in summer, with an average of 1.04 applied to subbasins with no relationships available (i.e., in subbasins with no large river segments). In winter, the multiplier ranges from 1.07 to 1.10 in winter, with an average of 1.08 applied to subbasins with no relationships available.

For Chinook salmon, the multiplier ranges from 1.06 to 1.15 for subyearling rearing, with an average of 1.10 applied to spring Chinook subbasins with no relationships available and an average of 1.11 applied to fall Chinook subbasins with no relationships available.

For coho salmon summer rearing productivity in small streams, we found no data relating productivity to wood abundance so we used the same multipliers as for large rivers. However, in winter we assigned a density-independent winter rearing productivity of 0.35 at low wood abundance (Ogston et al. 2014), and 0.58 at high wood abundance (based on Figure 4 in Quinn and Peterson 1996). For Chinook salmon in small streams we assumed a productivity increase similar to that for coho salmon winter rearing (multiplier of 1.67), changing juvenile Chinook rearing productivity from 0.26 to 0.43 in small streams. For steelhead, we found no data relating wood abundance to productivity in small streams for either summer or winter rearing. Therefore, for first year winter rearing we applied a multiplier of 1.67 to the summer productivity (the same ratio as winter to summer productivity for coho), and we used the large river wood multipliers for all other seasons and ages in small streams.

I.5 Floodplain Habitat

Reductions in the area of floodplain habitats that were historically available (side-channels, marshes, and ponds) reduce spawning, summer rearing, and winter rearing habitat capacities and productivities for all species of salmon. Therefore, adding floodplain habitat in the historical diagnostic scenario increases spawning and rearing capacity and productivity for all species.

I.5.1 Floodplain Habitat Effect on Spawning Capacity

Our historical scenario includes increases in side-channel length based on side channel length multipliers developed by Natural Systems Design (Tim Abbe, Susan Dickerson-Lange) and NOAA (Tim Beechie), which ranged from 0.1 to 1.5 depending on the reach and channel type (Table of multipliers in Appendix E). A multiplier of 1.5 means that historically there were 1.5 km of side channel for every km of main channel. For spawning capacity, we treat side channels as small streams, and assume that side channels had high wood abundance and high spawning capacity for all species (see also Section I.4.1 above).

I.5.2 Floodplain Habitat Effect on Rearing Capacity

For summer and winter rearing habitat capacity, we use the same added side channel length described above, and treat side channels as small streams with a wetted width of 1 m and 50% pool area. We then use the average of pool and riffle densities in summer and winter to estimate historical capacity.

Floodplain ponds and sloughs are treated as beaver ponds, and are assigned the same summer and winter rearing densities as beaver ponds for all species. Marshes are typically dry in the summer, so there is no summer rearing fish density for that habitat type. In winter, marshes are assigned species-specific rearing densities (listed in Section 4 of the main report).

I.5.3 Floodplain Habitat Effect on Rearing Productivity

Rearing productivities in side channels are the same as for small streams with high wood abundance (historical condition) or low wood abundance (current condition), as described in section I.4.7. Rearing productivities in marshes and ponds are the same as for beaver ponds, as described in I.2.2.

I.6 Temperature

Spring Chinook upstream migration productivity and coho, steelhead, and late migrant Chinook summer rearing productivity are a function of stream temperature. The input data sets for current stream temperature are from WDFW (Chehalis Thermalscape data for

tributaries) and Portland State University (PSU, mainstem from Crim Creek to Porter Creek). Temperature differences for historical and future scenarios are based on the shade and temperature model of Seixas et al. (2018) and climate change projections from NorWeST (https://www.fs.fed.us/rm/boise/AWAE/projects/NorWeST/ModeledStreamTemperatureScenarioMaps.shtml). We model effects of the 7-day average daily maximum summer stream temperature (7-DADM) for coho salmon and steelhead juveniles, and spring Chinook adults, because these fish are in freshwater during the period of high temperatures. Most spring and fall Chinook migrate to the bay prior to high temperatures in summer, and therefore we only model a June temperature effect on the late Chinook juvenile migrants. Because juvenile coho and steelhead have different thermal tolerances, we model the temperature effect with a different functional relationship for each species.

I.6.1 Temperature Effect on Spring Chinook Adult Migration and Holding Productivity

For spring Chinook upstream migration and holding, we model the life stage as density independent with productivities estimated as a function of subbasin-averaged stream temperature. The functional relationship was developed from data in the Willamette River basin, which uses the 7-day average of daily maximum (7-DADM) stream temperatures as the input temperature (Bowerman et al. 2018). The regression line shown is for points without hatchery origin spawners, where mortality increases with increasing temperature. The final equation for calculating spring Chinook prespawn productivity based on the Willamette data without hatchery fish (shown in Figure I.2) is:

$$p_{prespawn} = 1 - \frac{e^{(-9.053 + .387T)}}{1 + e^{(-9.053 + .387T)}}$$

Where T is the 7-day average of daily maximum stream temperatures. Modeled pre-spawn productivity estimates for current conditions ranged from 0.44 to 0.67 in the spring Chinook sub-basins, whereas our modeled prespawn productivity estimates for historical shade conditions ranged from 0.65 to 0.81. For reference, one empirical estimate of the current productivity is 0.58 to 0.73 based on radio tagging reported in USGS Open-File Report 2016-1158 (Liedtke et al. 2016).
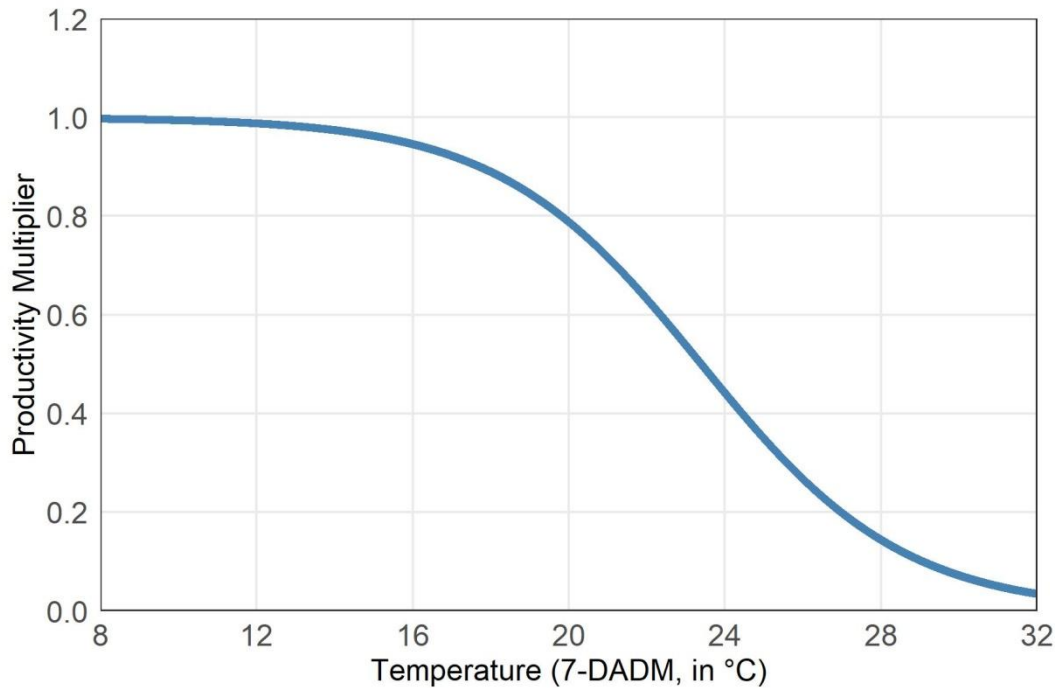
Figure I.2. Functional relationship for calculating the spring Chinook prespawn productivity multiplier based on the 7-day average daily maximum stream temperature.

I.6.2 Temperature Effect on Coho Salmon Summer Rearing Capacity and Productivity

Increasing stream temperature decreases coho salmon abundance and productivity via changes in summer rearing capacity and productivity. We estimate the productivity multiplier based on 7-day average daily maximum (7-DADM) stream temperature which decreases summer rearing productivity from its base value:

$T < 18°C$, 1

$18°C ≤ T < 24°C$, $1 - 0.17*(T - 18)$

$T ≥ 24°C$, 0

That is, at temperatures <18°C, the multiplier is 1, so there is no change in summer rearing productivity. From 18°C to 24°C, the multiplier decreases linearly from 1 to 0, and above 24°C the multiplier is 0 (Figure I.3) (based on ASEP 2014, Appendix C). We use the same multiplier for capacity that we use for productivity. We estimate historical summer rearing productivity using the same function, but the historical reach-level temperatures are based on historical shade conditions (Appendix A).

228
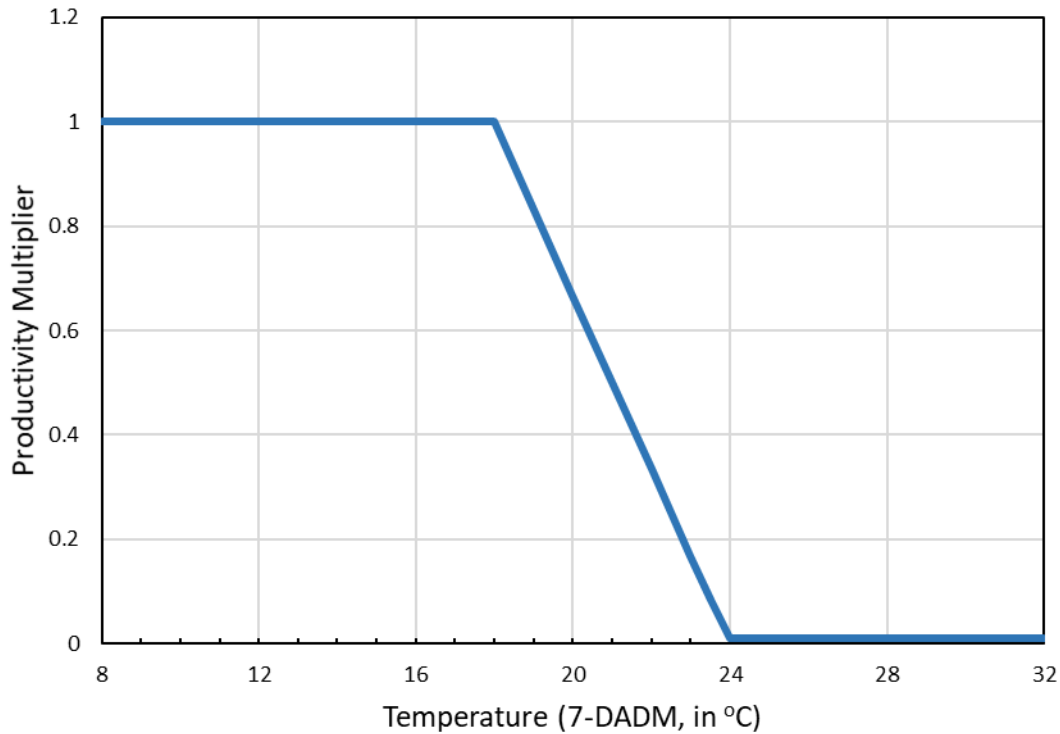
Figure I.3. Functional relationship between the summer rearing productivity multiplier and the 7-day average daily maximum stream temperature for coho salmon.

I.6.3 Temperature Effect on Steelhead Summer Rearing Capacity and Productivity

For steelhead, we use an experimentally derived relationship between juvenile steelhead survival and stream temperature (Bear et al. 2007). They exposed juvenile steelhead (110-150 mm total length) to temperatures ranging from 8°C to 30°C in two degree increments, and recorded mortality for each trial. The data and resulting regression relationship are shown in Figure I.4. The regression equation is:

$$p = \frac{97.88}{1 - e^{-((T-24.3522)/-0.5033)}}$$

where T is the 7-DADM from the temperature models. This regression produces the productivity multiplier that we use to modify summer rearing productivity for steelhead. We estimate historical summer rearing productivity using the same function, but the historical reach-level temperatures are based on historical shade conditions (Appendix A).
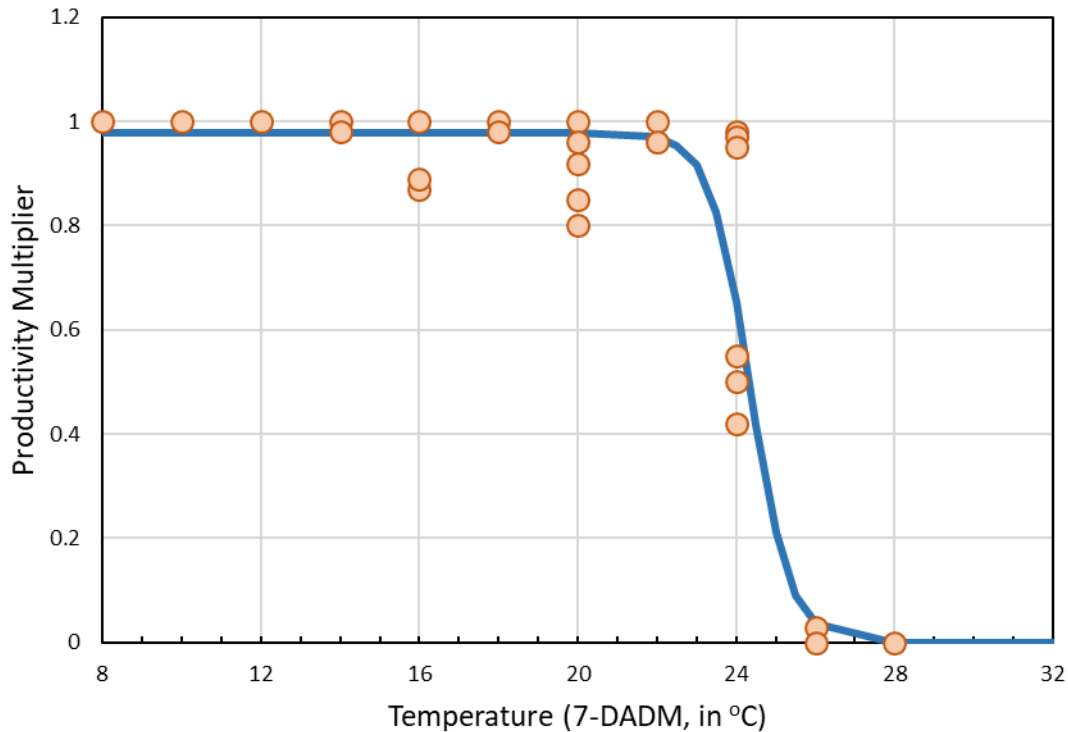
Figure I.4. Functional relationship between steelhead survival and stream temperature from laboratory experiments (orange dots, Bear et al. 2007). Points are results of experiments in Bear at al. (2007); blue line is the functional relationship for the productivity multiplier used in the steelhead life-cycle model.

I.6.4 Temperature Effect on Chinook Rearing Capacity and Productivity

For spring and fall Chinook, we use the June 1-21 average daily maximum temperature to estimate the temperature effect on productivity of juvenile Chinook parr migrating down the mainstem Chehalis in June (migration data from Winkowski and Zimmerman 2019). We use June 1-21 because that is the time period of peak outmigration (Figure I.5). Very few fish are migrating in the last week of June, so we did not include that week in the temperature calculation. Based on data from Winkowski and Zimmerman (2019) we estimate that 45% of parr are affected (red box in Figure I.5), which is the number of Chinook parr counted in the first 3 weeks in June, divided by total Chinook parr counted for the season. The functional relationship between the June 1-21 average daily maximum temperature and spring and fall Chinook outmigrant productivity multiplier (Figure I.6) is:

T < 18°C, 1

18°C ≤ T < 24°C, 1 - 0.17*(T - 18)

T ≥ 24°C, 0

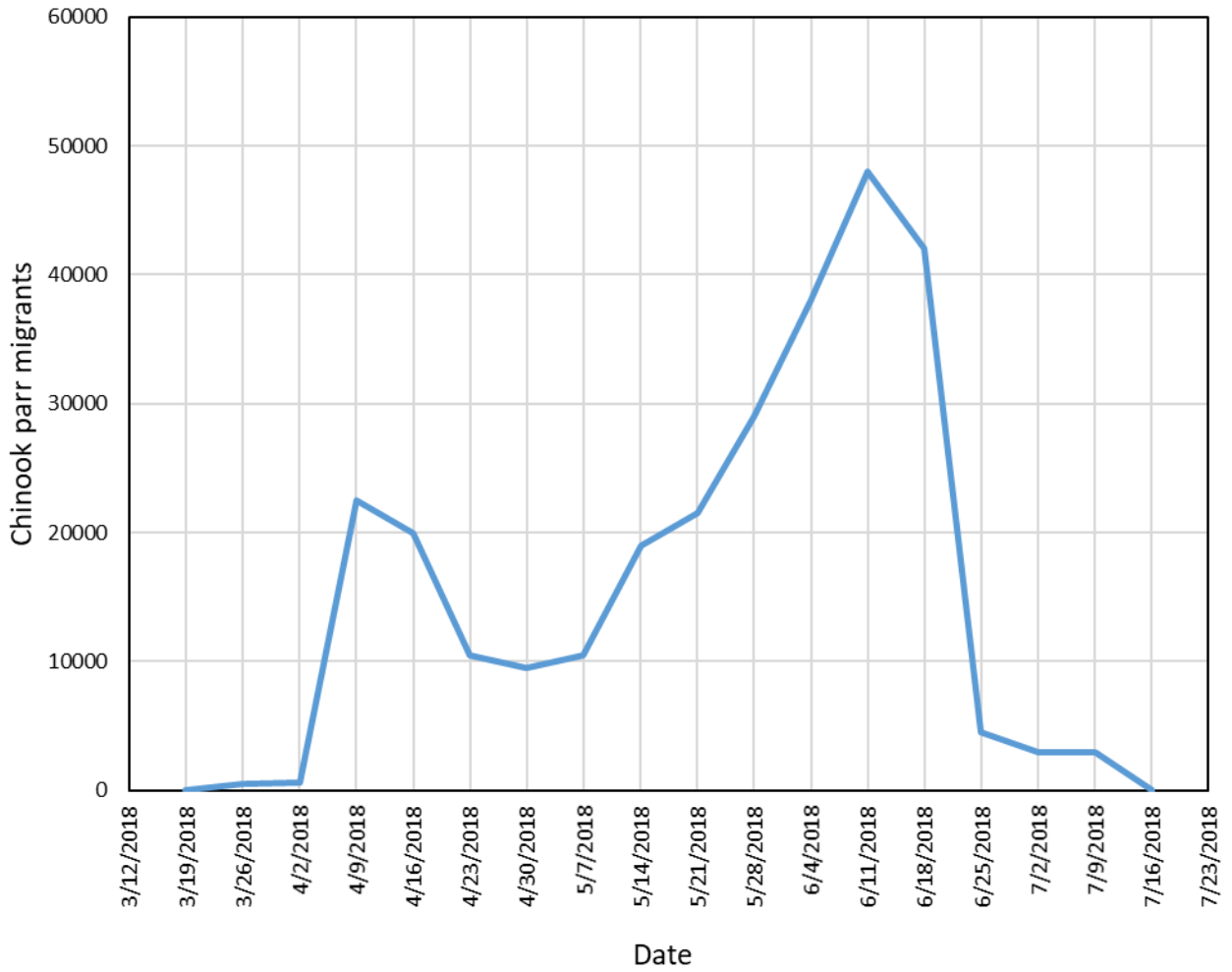This equation is applied to the 45% of juveniles that are migrating from June 1-21.

Figure I.5. Number of Chinook parr passing the mainstem Chehalis smolt trap near the Black River confluence (blue line), and time period used to calculate a stream temperature effect on parr migrant productivity (red box). Data from Winkowski and Zimmerman (2019).
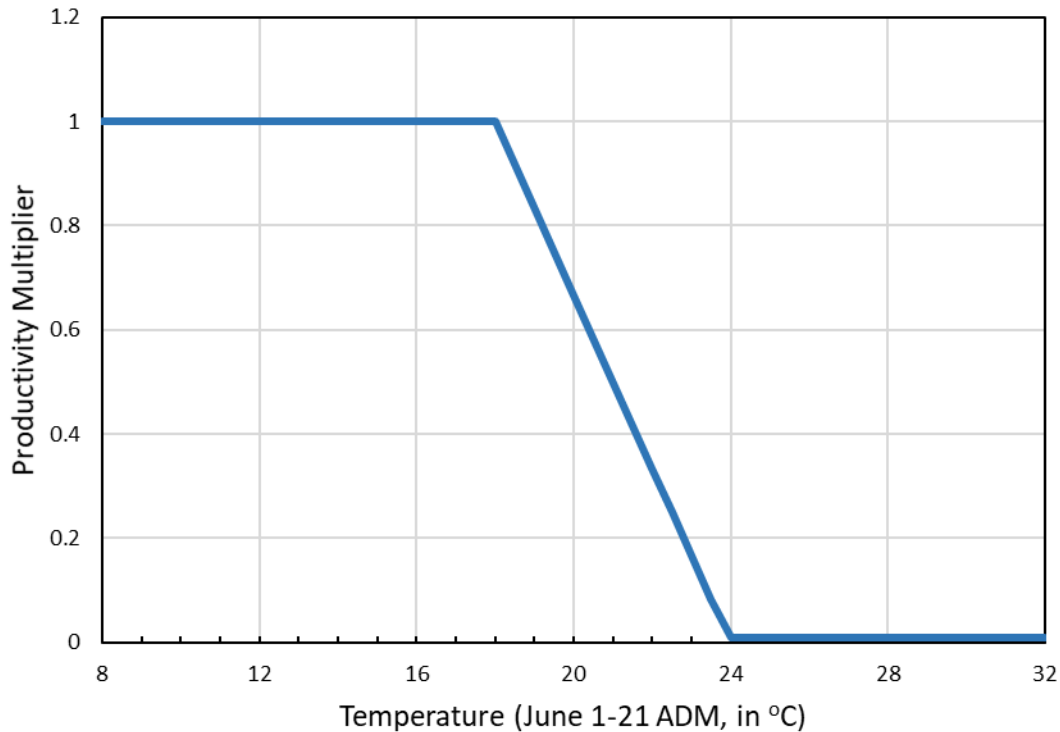
Figure I.6. Functional relationship between the outmigration productivity multiplier for spring and fall Chinook salmon and the June 1-21 average daily maximum (ADM) stream temperature.

I.7 Channel Straightening and Bank Armor

Channel straightening has reduced main channel length in the mainstem Chehalis River and a number of its larger tributaries, leading to reduced spawning and rearing capacities for all species. We estimated the difference in habitat areas between current and historical conditions using reach-specific channel length multipliers (listed in Appendix E), which increase habitat unit areas by the specified multiplier in each reach. For example, a channel length multiplier of 1.15 means that the channel was 15% longer historically, and we therefore increased habitat areas of all unit types in that reach by 15% (we assume that unit widths do not change). Rearing densities for all species remain the same in the current and historical channel length scenarios, so rearing capacity also increases by 15%. Channel length multipliers ranged from 1.0 (no change) to 1.3 (30% longer historically).

Bank armor does not affect rearing habitat areas (Appendix E), but changes the rearing densities for each species (Section 4, rearing densities from Beamer and Henderson 1998). For summer rearing, coho salmon densities are 0.54 fish/m² in natural banks and 0.20 fish/m² in riprapped banks, and for steelhead the first-year summer rearing densities are 0.32 fish/m² and 0.26 fish/m², respectively. For winter rearing, coho salmon densities are 0.054 fish/m² in natural banks and 0.05 fish/m² in riprapped banks, and for steelhead the first-year winter rearing densities are 0.21 fish/m² and 0.18 fish/m², respectively. For

spring and fall Chinook, the rearing densities are 0.68 fish/m^2 in natural banks and 0.27 fish/m^2 in riprapped banks.

I.8 Impervious Surface Effect on Coho Prespawn Productivity

The source of the impervious surface area percentages is the National Land Cover Dataset impervious surface data for 2011 (https://www.mrlc.gov/data), which is 30-m resolution gridded data with a value of percent impervious area for each cell. We calculate the current percent impervious surface area upstream of each reach using the average impervious surface area of all cells in the drainage area upstream of each reach using the flow accumulation algorithm. This average percent impervious area is then used to estimate prespawn productivity using the equation below. For historical conditions the percent impervious area is set to zero.

Prespawn mortality in coho salmon is correlated with a number of metrics indicating level of development (e.g., road density, percent impervious area) (Feist et al. 2011, 2017). The most straightforward function appears to be a linear relationship between prespawn mortality and percent impervious area (Figure 2a in Feist et al. 2011). We plotted the multi-year overall prespawn mortality for each of the six sites (Figure I.7), as well as the prespawn mortality in individual years for each site (Figure I.8). The data are fitted well with a function of:

Percent impervious area ≤66.67%: Prespawn mortality = (0.015) × (% imp. area), and

Percent impervious area >66.67%: Prespawn mortality = 1.0.

To illustrate variability in the data, Figure I.8 shows the prespawn mortality in each year at each of the six study sites, along with the same model function curve. In the NOAA model, we need to have prespawn productivity rather than mortality, so the final model functions are:

Percent impervious area ≤66.67%: Prespawn productivity = 1 – [(0.015) × (% imp. area)], and

Percent impervious area >66.67%: Prespawn productivity = 1 - 1 = 0.
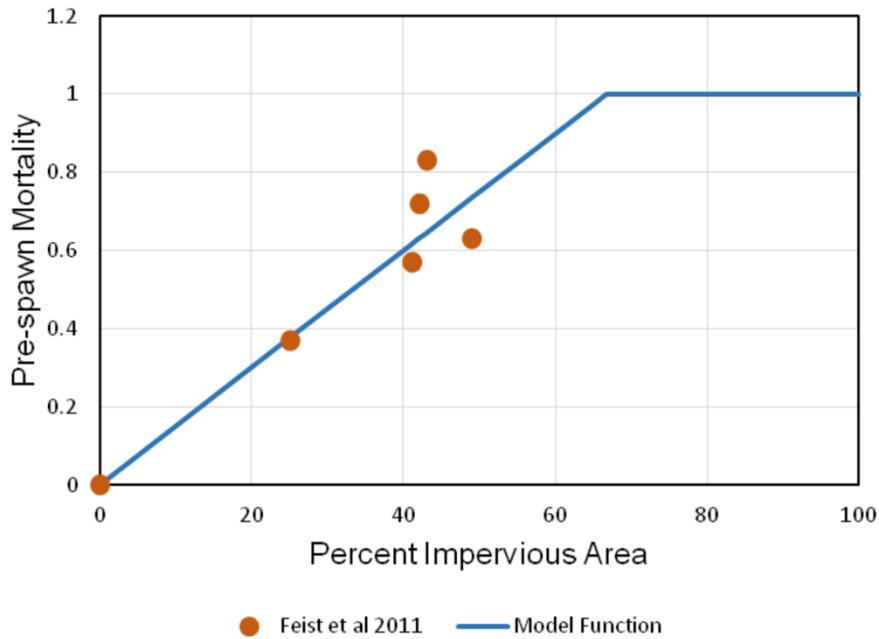
Figure I.7. Overall coho salmon prespawn mortality from Table 1 in Feist et al. 2011 plotted against percent impervious area. Blue line indicates the model function for prespawn mortality.
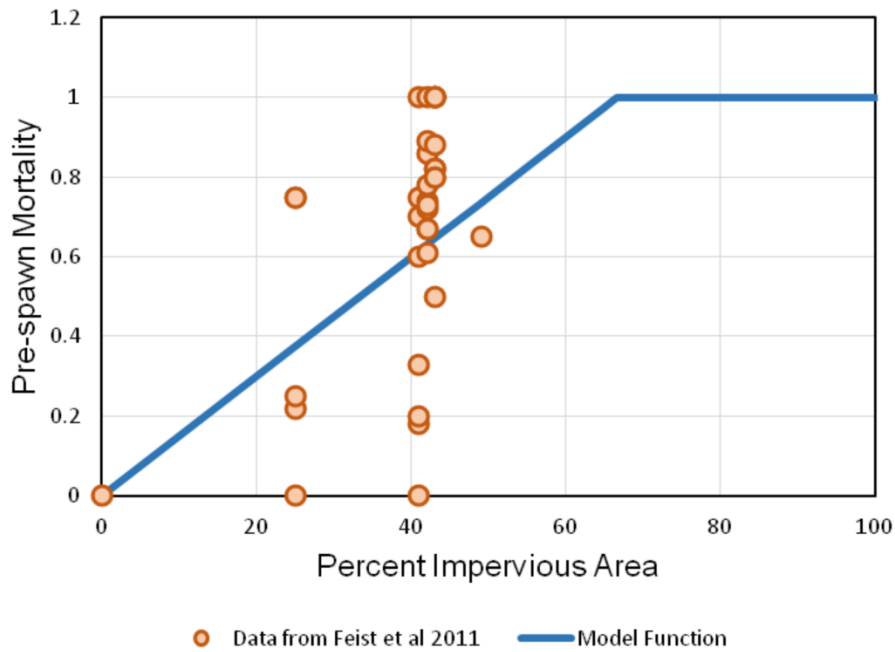

Figure I.8. Coho salmon prespawn mortality in each year at each site from Table 1 in Feist et al. 2011 plotted against percent impervious area. Blue line indicates the model function for prespawn mortality.

I.9 Peak Flow Effect on Chinook Incubation Productivity

The NOAA model has the capability of incorporating stochastic functions to influence productivity parameters from year to year, such as an effect of peak flow on incubation productivity for coho and Chinook salmon (Kinsel et al. 2007). Currently this function is turned off in the model, but it is coded and operational.

Effects of peak flows on egg to migrant fry survival have been documented in Chinook salmon in the Skagit River basin (Kinsel et al. 2007), and are presumed to reflect scour of eggs in the gravel due to the overlap in timing of floods and the incubation period. A similar effect is presumed to occur in other river basins. The data from the Skagit River basin are shown in Figure I.9, along with predicted survivals using an exponential regression relationship. Note that the recurrence interval on the x-axis is based on the Skagit River near Mount Vernon, which is low on the mainstem Skagit.

In the Chehalis basin, we rescale this relationship to create a multiplier that ranges from 1 at RI = 0 to near zero at RI = 100 (Figure I.10). The equation for the relationship is

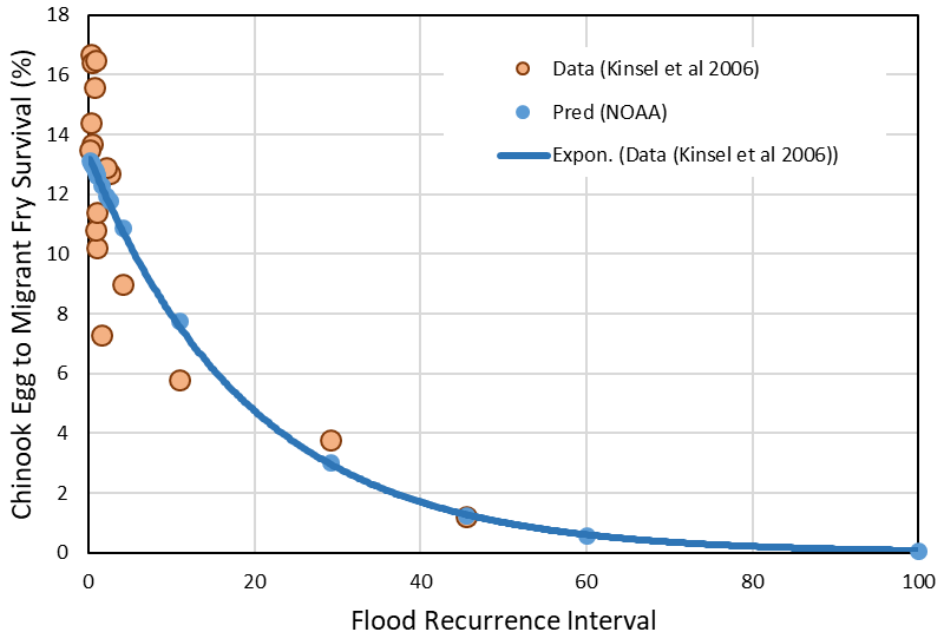$$Multiplier_{Pi} = 1.0219e^{-0.053(RI)},$$

Figure I.9. Chinook egg to migrant fry survival in the Skagit River basin from Kinsel et al. (2007). The predicted survivals using an exponential regression are shown as blue dots, and a fitted exponential curve is the heavy blue line. X-axis is for the Skagit River gage at Mount Vernon.

where *Multiplier*$_{Pi}$ is the incubation productivity multiplier and *RI* is the flood recurrence interval. In each year of the model run, the multiplier is then calculated using this function, based on the flood recurrence interval for that year. We used peak flow at the USGS gage on the Chehalis River at Porter as the index flow. Peak flows, probabilities of occurrence, and recurrence intervals were calculated using the PeakFQ USGS software (https://water.usgs.gov/software/PeakFQ/). Results for that gage are shown in Table I.3.

Table I.3. Peak flows (cfs) at USGS Gage 12031000 at Porter, with water year in which the flood occurred, probability of occurrence, and recurrence interval for each flood.

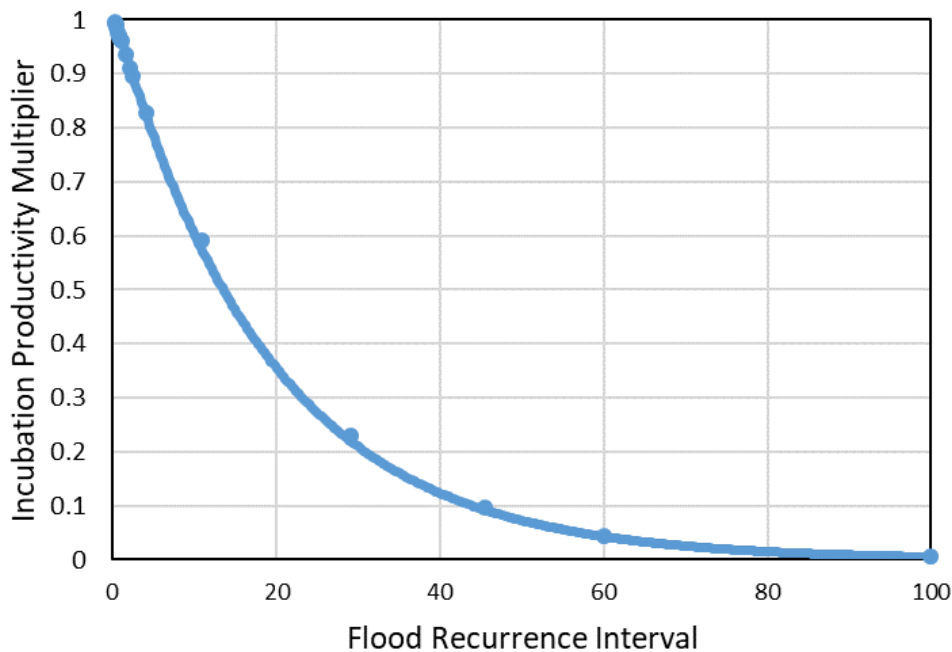| Water Year	Peak flow (cfs)	Probability of occurrence	Approximate recurrence interval (years)
1983	29,950	0.5	2
1951	45,840	0.2	5
1991	57,620	0.1	10
1987	73,900	0.04	25
1990	87,010	0.02	50
2008	101,000	0.01	100

Figure I.10. Chinook incubation productivity multiplier as a function of flood recurrence interval.

Appendix J. Modeling Future Development and Climate Change

For the restoration scenarios, we model future development as a projected change in impervious area, and climate change with increases in stream temperature, increases in peak flow, and decreases in low flow.

J.1 Future Impervious Surface Area

To estimate future impervious area, we used estimates of increased development in designated Urban Growth Areas (UGAs) combined with generalized estimates of increased development outside of UGAs in all Geospatial Units (GSUs) outside of managed forest. These estimates were provided by the Washington Department of Ecology and the Chehalis Basin Science Review Team. For GSUs outside managed forest, we were given the estimated proportion of the UGA expected to be converted to developed land by mid-century (%converted), an estimate of the intensity of development (%impervious), and the percentage of the GSU in a designated UGA (%GSUinUGA). Estimates of percent impervious area varied by expected future development class (Table J.1). The estimated additional impervious area for UGAs by mid-century *(%newimperv1$_{mid}$)* was then calculated using:

$$\%newimperv1_{mid} = \frac{\%converted}{100} \times \frac{\%impervious}{100} \times \frac{\%GSUinUGA}{100} \times 100$$

The estimated additional impervious area will be added to the current percent impervious area. For example, if a GSU currently has an impervious area of 21% and *%newimperv1$_{mid}$*= 3.5%, the mid-century impervious surface area for that GSU would be 24.5% (21% + 3.5%).

For areas outside of UGAs (but not managed forest), we used the SRT recommended estimates of 5% degradation by mid-century and 10% degradation by late-century. We interpreted these as estimates of the percent of land converted to "developed open space" (10% impervious area), for use in the equation:

$$\%newimperv2 = \frac{\%converted}{100} \times \frac{\%impervious}{100} \times \frac{100 - \%GSUinUGA}{100} \times 100$$

Table J.1. Values of percent impervious area by land cover class used in calculations of future percent impervious area.

Anticipated future land cover class	Percent impervious range in NLCD	Value used in NOAA calculation
Developed, High intensity	>80%	90%
Developed, Medium intensity	50-79%	65%
Developed, Low intensity	20-49%	35%
Developed, Open space	<20%	10%

For GSUs with no UGA, the equations for added impervious area then become:

$$\%newimperv2_{mid} = \frac{5}{100} \times \frac{10}{100} \times \frac{100 - 0}{100} \times 100 = 0.5\%$$

and

$$\%newimperv2_{late} = \frac{10}{100} \times \frac{10}{100} \times \frac{100 - 0}{100} \times 100 = 1\%$$

In GSUs partly covered by a UGA, the estimated future added impervious area in mid-century is $\%inewimperv1_{mid}$ plus

$$\%newimperv2_{mid} = \frac{5}{100} \times \frac{10}{100} \times \frac{100 - \%GSUinUGA}{100} \times 100$$

In late-century, the future added impervious area is $\%inewimperv1_{mid}$ plus

$$\%newimperv2_{late} = \frac{10}{100} \times \frac{10}{100} \times \frac{100 - \%GSUinUGA}{100} \times 100$$

Note that there are no available GSU-specific estimates of development for late-century, so the late century estimate inside a UGA is the same as for mid-century ($\%inewimperv1_{mid}$).

The highest estimated values for mid-century are 11.8% additional impervious surface area in the Tidal Zone GSU and 9.3% in the Skookumchuck to Black GSU. Four GSUs have additional impervious surface area values between 1.3% and 3.6%, and all of the remaining GSUs have estimated added impervious area of 1% or less. For comparison, a retrospective analysis of change in percent developed area in Puget Sound found that the added impervious area averaged less than 1% over the 22 year period from 1986 to 2008 (right column of Table 1 in Bartz et al. 2015). However, within floodplains in specific river basins, the change in impervious area was as high as 2.5%, and basins with higher percent developed area in 1986 generally had higher rates of increase in developed area over the 22 years. These results appear to be broadly consistent with the estimates of future increases in impervious area for the Chehalis by mid-century, which has a similar time span (~22 years) to that of the Puget Sound analysis. However, the Puget Sound study used larger spatial units than we use in the Chehalis, and analyzed change in the area of the developed land cover class rather than change in impervious area. Therefore, it is not possible to make a direct comparison of the rates of change between the two locations.

J.2 Future Stream Temperature

Future stream temperatures are modeled as a function of climate change effects, shade effects, and floodplain connectivity effects.

J.2.1 Climate Change Effects

The climate change component of the restoration scenarios includes estimated increases in stream temperature from the NorWeST stream temperature datasets (Isaak et al. 2017), which are estimated from the A1B emissions scenario in IPCC (2013). In Figure 7 of Isaak et al. (2017) the projected increase is +1°C in August average daily average (ADA) by mid-century (by 2030-2059, midpoint 2045) and +2°C by late century (2070-2099, midpoint 2085). However, data from the interactive NorWeST map in the Chehalis basin (https://usfs.maps.arcgis.com/apps/webappviewer/index.html?id=bf3ff38068964700a1f278eb9a940dce) suggest increases of +1.4°C by 2045 and +2.4°C by 2085. These projected temperature increases specific to the Chehalis basin are 0.4°C to 0.6°C less than the earlier estimates we had been using (Isaak et al. 2011).

The baseline period for the new NorWeST estimates is 1993-2011 (midpoint 2002), but the new Chehalis Thermalscape data are based on temperature data from 2014-2016, which are considerably closer to 2045 and 2085 than the NorWeST baseline midpoint date of 2002. Therefore, we adjusted (prorated) the temperature changes to account for a change in the baseline year from 2002 to 2015. This is to avoid adding the 2002-2015 portion of the temperature increase to the 2015 temperature. The proration indicates that the estimated temperature increases should be 70% of the published estimate for 2045 and 84% of the published estimate for 2085 when using the Thermalscape data. The percentages are calculated by dividing the revised year range by the original year range:

Mid century:
$$70\% = \frac{2045 - 2015}{2045 - 2002} = \frac{30}{43}$$

Late century:
$$84\% = \frac{2085 - 2015}{2085 - 2002} = \frac{70}{83}$$

Prorated temperature increases for mid- and late-century are shown in Table J.2, using both low and high estimated temperature increases. The proration suggests that temperature increases should be 0.7°C to 1.0°C for mid-century and 1.7°C to 2.0°C for late-century. We used the high end of the range of temperature increases in the restoration scenarios.

We converted the climate-change related increases in the August ADA to the equivalent changes in the 7-DADM, and Jun1-21 ADM, using the slopes from the regression equations above:

Δ7-DADM = 1.02 (ΔAugustADA), and

Table J.2. Prorated increases in the August ADA for mid- and late-century to adjust for differences in baseline dates for current temperature estimates, using both low and high estimated temperature increases. The low temperature increase estimate is from Figure 7 in Isaak et al. (2017), and the high estimate is from the NorWeST interactive map.

Baseline year	2045		2085	
	Temperature increase low	Temperature increase high	Temperature increase low	Temperature increase high
2002	1.0°C	1.4°C	2.0°C	2.4°C
2015 (prorated)	0.7°C	1.0°C	1.7°C	2.0°C

ΔJun1-21ADM = 0.96 (ΔAugustADA).

J.2.2 Riparian Shade Effects

Riparian restoration can decrease temperature due to increased shade, and in some cases offset or exceed the climate-change induced temperature increase. Using a tree growth function, we modeled future tree heights in one-year time increments. At each time step, we calculated tree height using the modeled age and canopy opening angle from tree height. We then use the change in canopy opening angle to calculate the change in water temperature (7-DADM) due to increased shade from current conditions to 2045 and 2085, and then convert the modeled change in 7-DADM to a change in Jun1-21ADM using the slopes from the regression equation as above for historical temperature:

ΔJun1-21ADM = 0.98 (Δ7DADM).

J.2.3 Floodplain Connectivity Effects

Connected floodplains can have high rates of hyporheic exchange through gravel and bars and the floodplain, potentially reducing stream temperature and creating local thermal refugia (Arrigoni et al. 2008, Poole et al. 2008). One study in the Willamette River projected that reconnecting a floodplain corridor roughly 425 m wide would decrease temperature by 2°C (Seedang et al. 2008). For the NOAA model we assumed that a typical restored width would be closer to 210 m (~700 feet), and that the maximum temperature decrease through floodplain reconnection would be 1°C on the 7DADM. For reference, the ASRP assumes a floodplain/riparian restoration corridor of 1000 feet on large rivers, 600 feet on medium rivers and 200 feet on small streams. After calculating the change in 7-DADM, we convert the modeled change in 7-DADM to a change in Jun1-21ADM using the slopes from regression equations:

ΔJun1-21 ADM = 0.98 (Δ7DADM).

J.2.4 Net Future Temperature Change

The reach-level future temperatures for 2045 and 2085 are then calculated as the current temperature, plus the increase due to climate change, minus the decreases due to increased shade and floodplain reconnection.

Notably, much of the basin (~65%) has riparian conditions that are similar to the reference condition tree heights (i.e., there are tall, mature trees in the riparian zone, especially in managed forest areas). Therefore, in those areas the projected temperature change is equal to or close to the projected climate change increase. There are relatively few areas where there are extremely poor shade conditions currently, but in those areas planting and growth of trees can reduce the modeled stream temperature by as much as -6°C by 2085 without climate change, or a net change of -4°C when coupled with the climate change increase of +2°C.

J.3 Future Stream Flows

Mauger et al. (2016) modeled future changes in flows in the Chehalis River basin using the Variable Infiltration Capacity (VIC) and Distributed Hydrologic Soil Vegetation Model (DHSVM) hydrologic models. We focused on future climate conditions based on two future emissions scenarios, or Representative Concentration Pathways (RCPs): the low (RCP 4.5) and high (RCP 8.5) emissions scenarios. The older mid-range scenario (A1B) did not extend beyond 2070, so there are no late-century model results for a moderate-emissions scenario. Note that emissions scenarios in Mauger et al. (2016) set the mid-century period at 2040-2069 (midpoint of 2055), rather than at 2030-2059 (midpoint 2045) as used in other studies we rely on (e.g., Isaak et al. 2017) (Figure J.1). The late-century time period in Mauger et al. (2016) is the same as that used in other studies (2070-2099, midpoint 2085). We used projected changes in the 7-day average low flow with a 10-year recurrence interval (7Q10) to indicate change in summer low flow and created a regression between recurrence interval and percent change from current to estimate future peak flows. The Isaak data were used for temperature changes (see preceding section).
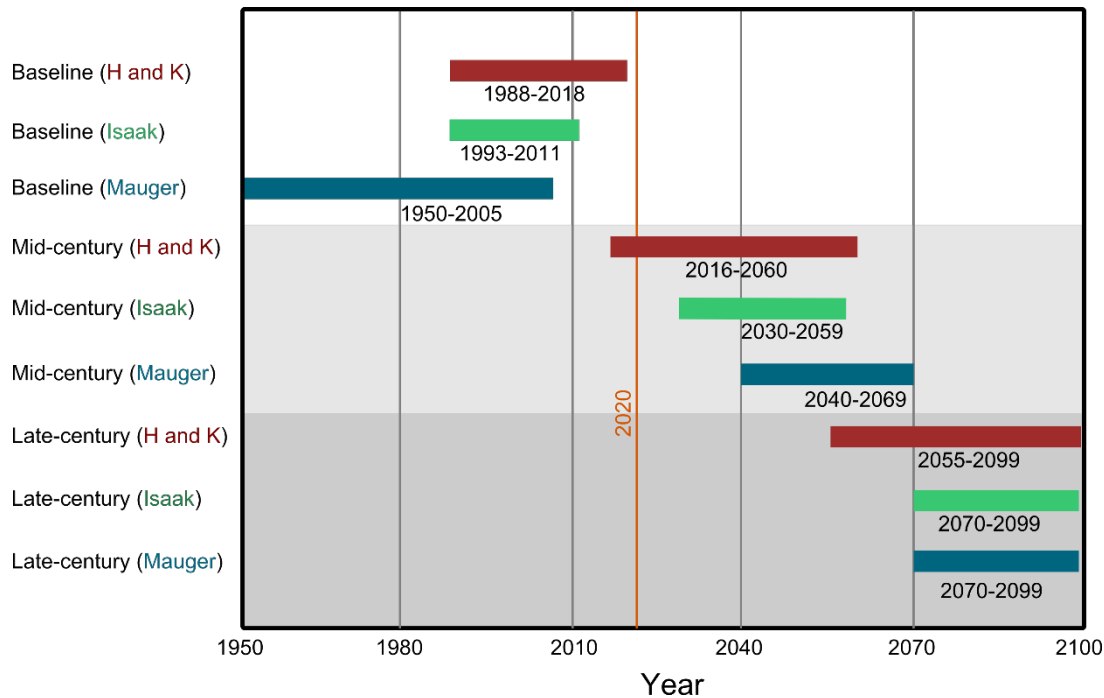
Figure J.1. Comparison of year ranges used in baseline periods and future periods for estimating potential climate change effects on stream temperature, peak flows, and low flows. "H and K" refers to the Anchor QEA memo on estimated flow changes authored by Hill and Karpack (2019), "Isaak" refers to the temperature change analysis in Isaak et al. (2017), and "Mauger" refers to the peak and low flow changes in Mauger et al. (2016).

J.3.1 Low Flows

For changes in low flows, we used projected changes in the 7Q10 at the eight bias-corrected stations in rainfall-dominated parts of the basin and the three bias-corrected stations in the snowmelt-dominated part of the basin (Mauger et al. 2016). We averaged percent changes in low flow across all stations and both models in each hydrologic regime to estimate change in low flows for future scenarios. The average projected change in the 7Q10 by mid-century under RCP 4.5 for rain-dominated portions of the basin was -11% (range from -12% to -26% with DHSVM and +1% to -14% with VIC) (Table J.3). Under RCP 8.5, the average projected change was -10% (range from -10% to -27% with DHSVM and +2% to -15% with VIC). For the snowmelt portion of the basin, the average projected change in the 7Q10 by mid-century under RCP 4.5 was -41% (range from -47% to -66% with DHSVM and -19% to -27% with VIC). Under RCP 8.5, the projected change was -43% (range from -48% to -70% with DHSVM and -17% to -31% with VIC).

The average projected change in the 7Q10 by late-century under RCP 4.5 for rain-dominated portions of the basin was -8% (range from -9% to -21% with DHSVM and +4% to -13% with VIC). Under RCP 8.5, the average projected change was -10% (range from -5% to -28% with DHSVM and +3% to -17% with VIC). For the snowmelt portion of the basin,

Table J.3. Projected average percent changes in 7Q10 low flow by future time period, hydrologic regime, and emissions scenario; average values for each hydrologic model separately are in parentheses. Average value for rainfall dominated is calculated from eight stations and both models (16 total values) for each emissions scenario, and the average value for each model is calculated from the eight stations and one model (8 total values each) for each emissions scenario. Average values are calculated similarly from the three snowmelt dominated stations (6 total values for the average across models, and 3 total values each for each model separately).

| Regime/Emissions Scenario | Future Time Period | |
	Mid-century (2055)	Late-century (2085)
Rainfall dominated		
RCP 4.5 (low emissions)	-11%	-8%
	(DHSVM: -18%, VIC: -5%)	(DHSVM: -14%, VIC: -3%)
RCP 8.5 (high emissions)	-10%	-10%
	(DHSVM: -18%, VIC: -3%)	(DHSVM: -15%, VIC: -6%)
Snowmelt dominated		
RCP 4.5 (low emissions)	-41%	-44%
	(DHSVM: -58%, VIC: -24%)	(DHSVM: -62%, VIC: -25%)
RCP 8.5 (high emissions)	-43%	-52%
	(DHSVM: -61%, VIC: -25%)	(DHSVM: -71%, VIC: -34%)

projected change in the 7Q10 by late-century under RCP 4.5 was -44% (range from -51% to -71% with DHSVM and -23% to -27% with VIC), and -52% under RCP 8.5 (range from -61% to -79% with DHSVM and -32% to -37% with VIC).

It is notable that there are very small differences between emissions scenarios and between the mid-and late-century time periods. There were much larger differences between models and between hydrologic regimes. Because we had no basis for choosing one hydrologic model over the other (neither model was calibrated in the study of Mauger et al. (2016) due to funding and time constraints), we averaged the differences between models for our future projections.

Although there were much larger decreases projected for snowmelt systems, we chose to use -10% as the future flow change for both time periods and all reaches, because the snowmelt regime is limited to a very small portion of the Chehalis basin. Therefore, our low flow change estimates may underestimate decreases in low flow in parts of the Humptulips, Wynoochee, and West Fork Satsop Rivers, which have their sources in the Olympic Mountains.

It is worth noting that the percentage change is calculated from a baseline period of 1970-1999 (midpoint 1985), but we did not adjust the percent changes to account for the baseline midpoint being >30 years old. We are currently half-way between the baseline midpoint and the mid-century midpoint (1985 and 2055, respectively), and 35% of the way between the baseline midpoint and the late-century midpoint (1985 and 2085, respectively).

To translate low flow changes into changes in wetted width, we used the same equations used by ICF for the EDT model, based on methods described in the October 14, 2019 memorandum from McMullen et al. to Merri Martz. In that analysis, there were two width equations, one for confined channels and one for unconfined channels:

Confined: $Q = 0.004984 \times w^{2.299}$,

Unconfined: $Q = 0.06811 \times w^{1.767}$,

where Q is discharge in cubic feet per second and w is wetted width in feet. We rearranged both equations to estimate change in width as a function of change in discharge:

Confined channels: $w = (Q/0.004984)^{0.435}$

Unconfined channels: $w = (Q/0.06811)^{0.567}$

Because the percent change in discharge is constant across all channel sizes (-10%), the rearranged equations can be reduced to

Confined channels: $w_{future}/w_{current} = (0.9)^{0.435} = 0.96$

Unconfined channels: $w_{future}/w_{current} = (0.9)^{0.567} = 0.94$

That is, the change in wetted width with a -10% change in discharge is -4% for confined channels and -6% for unconfined channels. Because the estimated changes are similar between confined and unconfined channels, we calculated future wetted width as 95% of current wetted width for all reaches (-5% for all reaches). These values are consistent with those used for EDT (based on Figure 5 in October 14, 2019 memorandum from McMullen et al. to Merri Martz). For comparison, a -20% change in discharge (late century average across both hydrologic regimes and models) would produce a -9% to -12% change in wetted width, and a -48% change in discharge (late century, snowmelt average of both hydrologic models) would produce a -25% to -31% change in wetted width.

J.3.2 Peak Flows

For future peak flows, the memorandum from Adam Hill (Anchor QEA) and Larry Karpack (Watershed Science and Engineering) to Andrea McNamara Doyle and Chrissy Baily (Office of Chehalis Basin) dated May 6, 2019 recommended a 12% peak flow increase for mid-century and 26% for late century. Notably, the year ranges for both time periods differ from those of all other studies we rely on. They used 2016-2060 for mid-century and 2055-2099 for late-century (Figure J.1).

For this study, we reanalyzed data from Mauger et al. 2016, who set the mid-century period at 2040-2069 (midpoint of 2055) and the late-century time period at 2070-2099 (midpoint 2085). As with the low flow projections, we used the average of both the VIC and DHSVM model run data for each time period (mid- and late-century) and emission scenario (RCP 4.5 and RCP 8.5). For this analysis we needed an index site to represent the flow magnitude of the entire basin. We used the data from the Chehalis near Porter USGS gage

(#12031000) site as it represented the site lowest on the mainstem with a consistent period of record. The average projected change in peak flow for mid century is +25% for RCP 4.5 and +36% for RCP 8.5. The average projected change for late century is +27% for RCP 4.5 and +32% for RCP 8.5.

To model the impact of peak flows, we use a stochastic function to generate a time series of flows and associated changes in rearing survivals. Therefore we needed to generate estimates of percent change in flow across a range of peak flows. We used the average bias-corrected results from the VIC and DHSVM models to construct regressions for mid and late century under both the RCP 4.5 and RCP 8.5 emissions scenarios (Figure J.2). Each of the four regressions was used to scale current flow data to a future scenario. This work is scheduled to be completed by summer of 2020 for Phase 2 of the ASRP.

We log transformed the predictor variable for each regression such that

$$\Delta Q = \beta_0 + \beta_1 \ln(RI)$$

where ΔQ is the percent change in flow, RI is the recurrence interval of a given flow, and β_0 and β_1 are the regression coefficients. The results of the four regressions are summarized in Table J.4.

Table J.4. Parameter estimates for the regressions models of the four future peak flow scenarios

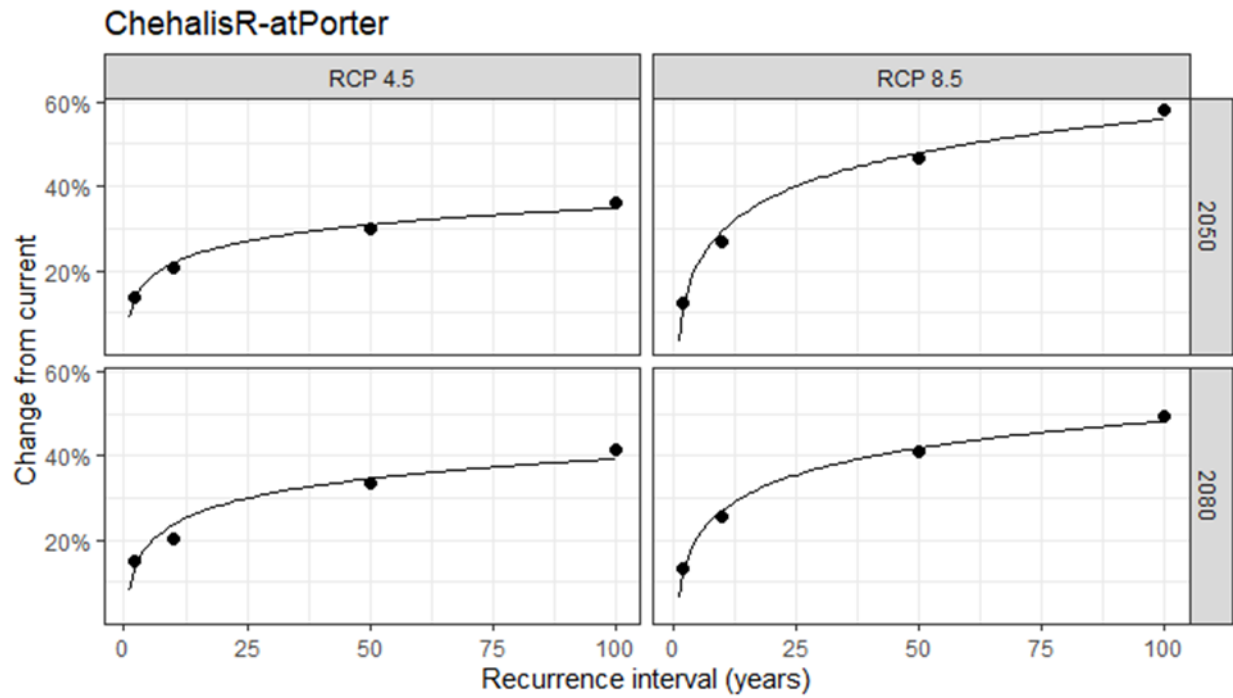| Emission Scenario	Future Time Period	Parameter Estimates	
		β_0	β_1
RCP 4.5	Mid-Century	0.087	0.057
RCP 8.5	Mid-Century	0.029	0.115
RCP 4.5	Late-Century	0.082	0.067
RCP 8.5	Late-Century	0.061	0.091

Figure J.2. Regressions used to calculate the percent change in flow across the range of recurrence intervals. Each data point represents the average of the VIC and DHSVM model outputs. A separate regression was created for each emission scenario and time period combination.

Appendix K. Study Area

The Chehalis River drains portions of the Willapa Hills, the Cascade Mountains, and the Olympic Mountains, flowing into Grays Harbor (Figure K.1). The drainage area of the Chehalis River is 6,889 km² (2,660 mi²), including the tributaries to Grays Harbor (Humptulips,

Figure K.1. Map of the Chehalis River basin showing major water bodies, tributaries, cities, towns, highways, and mountain ranges.

Wishkah, Hoquiam, Elk, and Johns Rivers). The mainstem Chehalis River drains a portion of the low-elevation Willapa Hills in the southern portion of the basin. The river flows north, then east, joined by the South Fork and Newaukum Rivers, and then north again near the town of Chehalis. From Centralia the river flows northwest, along this portion being joined by the Skookumchuck River, Scatter Creek, the Black River, and Cloquallum Creek. At Elma the river turns to flow west toward Grays Harbor, along this stretch joined by the Satsop and Wynoochee Rivers.

K.1 Geology, Precipitation and Land Use

The basin is underlain by marine basalts and sedimentary rocks, uplifted onto the west coast of North America as the Juan de Fuca plate is subducted beneath the North America plate (Figure K.2). The Puget Lobe ice sheet occupied a small portion of the basin ~16,000 years ago near
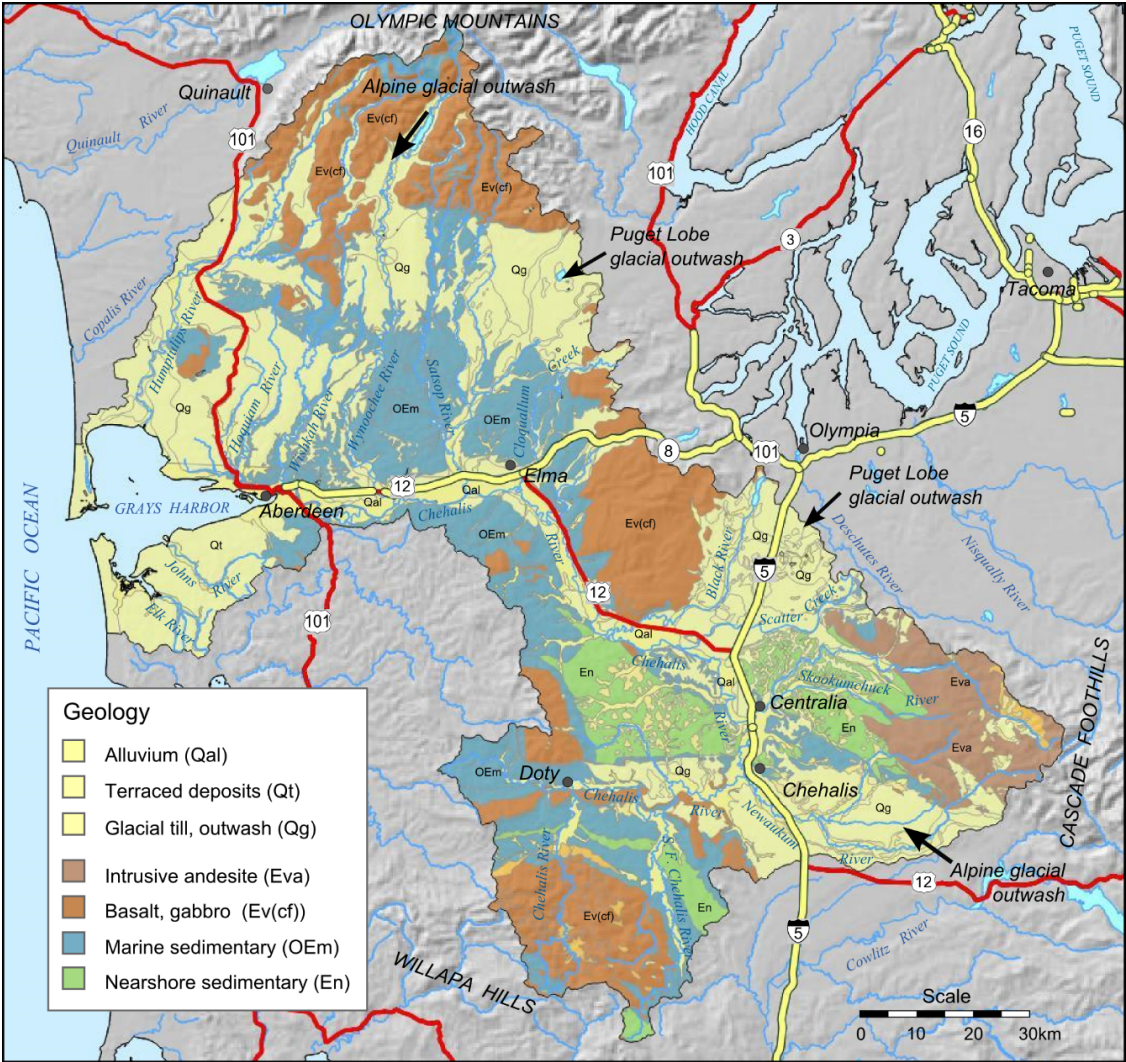

Figure K.2. Geologic map of the Chehalis River basin. (Data from www.geography.wa.gov, "geologic_unit_poly_100k.shp").

Grand Mound, and pro-glacial rivers flowing into lower Chehalis River deposited thick glacial outwash deposits in the Black River and East Fork Satsop River Valleys (Gendaszek 2011). Alpine glaciers from the Cascade Mountains deposited till and outwash deposits in the Newaukum Valley and along the middle Chehalis River, while alpine glaciers from the Olympic Mountains deposited till and outwash across much of the Humptulips, Wishkah, and Wynoochee River basins (Gendaszek 2011).

Annual rainfall in much of the basin is less than 100 in/yr (250 cm/yr) (PRISM Climate Group, http://www.prism.oregonstate.edu/normals) (Figure K.3), and because the southern ¾ of the basin is at relatively low elevation the Chehalis River has a rainfall-dominated hydrograph. The upper Humptulips, Wynoochee, and Satsop Rivers are at higher elevations in the Olympic Mountains, with annual rainfall between 100 and 275 in/yr (250-700 cm/yr). These rivers have transitional to snowmelt-dominated hydrographs. Due to the extensive glacial outwash deposits, groundwater-surface water interactions are significant in portions of the Chehalis River, but the net gain in ground water is relatively small (study conducted in the middle Chehalis between the Newaukum and Black Rivers, Gendaszek 2011).
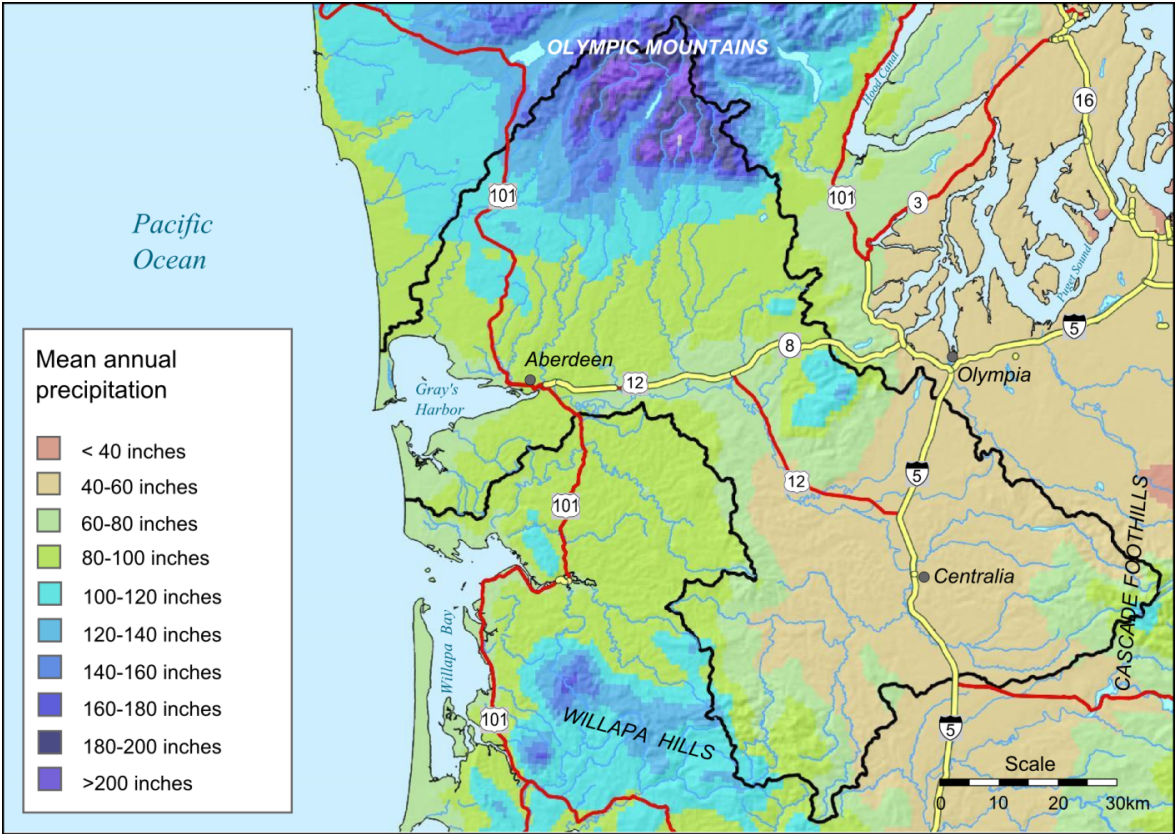

Figure K.3. Mean annual precipitation in the Chehalis River basin (Data from the PRISM Climate Group, http://www.prism.oregonstate.edu/normals, PRISM_ppt_30yr_normal_800mM2_annual_bil.tif").

A limited number of tree species comprise floodplain, shoreline, and delta vegetation in the study area, which is part of the Pacific Coastal Forest extending from Northern California to Alaska. Dominant species include red alder (*Alnus rubra*), black cottonwood (*Populus trichocarpa*), Sitka spruce (*Picea sitchensis*), western hemlock (*Tsuga heterophylla*), western red cedar (*Thuja plicata*), Douglas-fir (*Pseudotsuga menziesii*), and big leaf maple (*Acer macrophyllum*) (Franklin and Dyrness, 1973). The general successional pattern is from hardwood to conifer, with young patches occupied by colonizing species such as alder and cottonwood and old patches occupied by climax species such as Sitka spruce, western hemlock, and western red cedar (Crocker and Major, 1955; Fonda, 1974; Henderson et al., 1989).

Most of the Chehalis River basin is in commercial forest lands, with a smaller proportion in state and federal forest land (Figure K.4). Agricultural lands are concentrated in the low elevation portions of the Black, Skookumchuck, and Newaukum Rivers. Developed lands are somewhat more scattered in the basin, although the majority of developed lands are in the mainstem Chehalis floodplain, Black River basin, and Newaukum River basin.
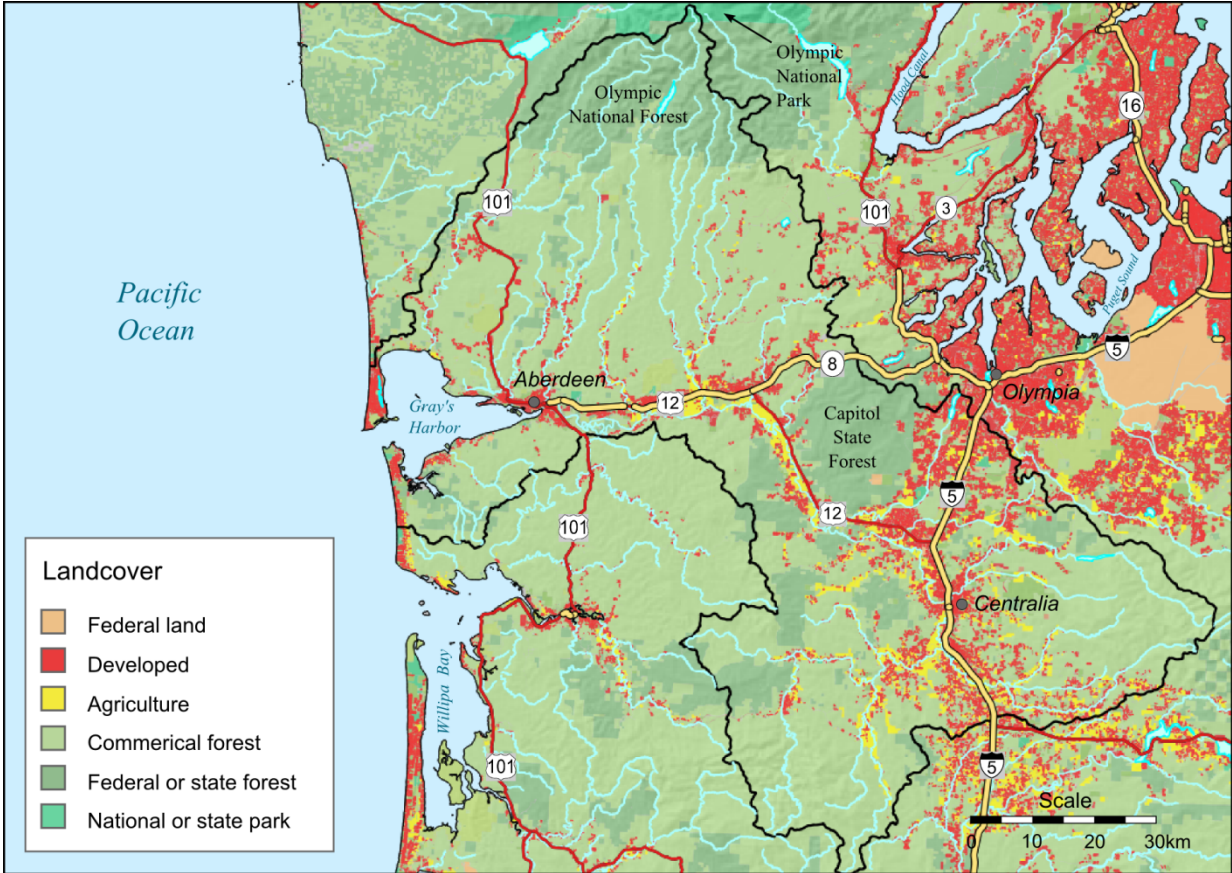

Figure K.4. Landcover map of the Chehalis River basin. (Data from www.geography.wa.gov, "landuse10.shp").

K.2 Overview of Salmon and Steelhead Life Histories

Aquatic species of interest in the ASRP restoration planning effort include salmonids, non-salmonid fishes, and amphibians. Five species of salmon and steelhead are found in the Chehalis River basin: Chinook salmon (*Oncorhynchus tshawytscha*), coho salmon (*O. kisutch*), chum salmon (*O. keta*), pink salmon (*O. gorbuscha*), and steelhead (*O. mykiss*). For this study, we focus on the key species of interest in the basin for life cycle modeling: Chinook salmon (spring and fall runs), coho salmon, steelhead, and chum salmon (pink salmon are not addressed in the ASRP). Restoration benefits for other fish and non-fish species have been qualitatively evaluated in a prior assessment (ASRP 2014) and other efforts, and are not addressed further here.

Chehalis River Chinook salmon are classified broadly as either fall run (later spawn timing and mostly sub-yearling outmigrants), and spring run (earlier spawn timing and mostly sub-yearling outmigrants). Returning adults of the fall runs enter the Chehalis River from September to mid-November and typically spawn in October and November (Myers et al. 1998). Fry emerge from the gravel from February to June. Most Chinook salmon fry migrate downstream as sub-yearlings over a period of several months, using primarily edge and backwater habitats on their seaward migration (Beechie et al. 2005a). Sub-yearlings then utilize the delta and nearshore, and most sub-yearlings reach Grays Harbor between June and October. For the spring runs, adults return between late March and mid-July, and spawning occurs in September and October (Myers et al. 1998). Juvenile outmigrants rear in rivers to their first spring before migrating to salt water, and adults rear at sea for two to five years before returning to spawn.

Coho salmon enter the Chehalis River from late October to early December, and spawn from November to February (Weitkamp et al. 1995). Most juveniles rear in freshwater for about 18 months, and leave as smolts in April and May. In small streams in summer (bankfull width <20m), age 0 coho salmon generally rear in pool habitats (Bisson et al. 1988), but in winter they occupy stream pools and riffles at low densities and ponds or off-channel habitats at higher densities (Brown and Hartman 1988). In larger rivers (bankfull width >20m), age 0 juveniles occupy bank edge and backwater habitats in both summer and winter (Beechie et al. 2005a). However, they generally occupy velocities <45 cm/s with wood or plant cover in summer, but in winter they occupy velocities <15cm/s and are most commonly associated with wood cover (Beechie et al. 2005a). They spend approximately one year at sea and spawn in their 3rd year (Weitkamp et al. 1995; WDFW unpublished data).

Adult spawning steelhead enter the Chehalis River between December (historically November) and April, and spawn from February through June (Busby et al. 1996). In the Chehalis River Basin most juveniles rear in fresh water for 2 years and become outmigrating smolts. In small streams, juvenile steelhead do not exhibit strong habitat preferences, although there is a slight preference for low velocity backwater pools at age 0 (Bisson et al. 1988). In large rivers, age-0 juveniles occupy a wide range of edge habitat types and velocity classes in summer, but in winter they choose bank edge habitats with velocities <0.45 m/s (Beechie et al. 2005a). Age-1 juveniles focus on bank edge habitats in

both summer and winter, although velocity preferences are unclear (Beechie et al. 2005a). Age at first spawning is typically 4 or 5 years for Chehalis River steelhead, and respawners are typically 5 to 7 years old (Busby et al. 1996).

Appendix L. Record of Model Changes in the Life-Cycle Model Workgroup

Table L1. Record of NOAA Model revisions for the Life-Cycle Model Workgroup during 2018 and 2019. Date is the month in which the change was made, and the model version lists the model development version in which the change was first included. The table is organized into eight categories of changes: Input data, landscape-habitat conditions, habitat-LCM functions – coho salmon, habitat-LCM functions – spring and fall Chinook, habitat-LCM functions – steelhead, ASRP restoration scenarios, and model outputs.

Question or suggested change	Revision or response	Date	Model Version
Input data			
Source of passage ratings (barrier data)	We use the same migration barrier data that ICF uses in EDT (from WDFW and modified by ICF).	Oct 2018	V3
Fish distribution source	We use the same fish distribution data that ICF uses in EDT (from WDFW and modified by ICF).	Oct 2018	V3
Stream temperature source	We use the same current temperature data that ICF uses in EDT (from PSU and modified by ICF).	Oct 2018	V3
Change to EDT stream widths	Changed input data to use EDT stream widths (data from ICF)	March 2019	V7
Water quality not included? (e.g., nitrogen & fertilizers, fire retardants, stormwater, etc.)	These are not part of the model scope.	No change	NA
Why isn't sediment from non-forest roads (ditch runoff), or from agriculture (instream grazing, farm to stream edge) not included?	We did not have data to quantify this relationship. However, we added some detail to the description that the low slope reaches that have naturally high fine sediment, which are mostly in agricultural areas. Also, we note that the riparian assessment indicates that most riparian areas have at least a narrow buffer. Many studies indicate that vegetated buffers of 15 feet wide or more are sufficient to filter out more than 70% of fine sediment (see review by Sather, NK and CW May, 2008, Riparian Buffer Zones in the interior Columbia River basin: a review of best available science. Battelle, PNWD-3817).	No change	NA
Add new riparian data for added reaches in new fish distributions	After changing the fish distributions we needed to update stream reaches that did not have riparian measurements. New reaches were added to the riparian data set.	May 2019	V10
Add new WDFW stream temperatures	Brought in the new current August mean temperatures from WDFW. Created conversion equations to calculate 7-DADM, Jun1-21ADM, and Jul1-Sept15 ADA temperatures for the model	Sept 2019	V12

Table L1 (cont.). Record of NOAA Model revisions during 2018 and 2019.

Question or suggested change	Revision or response	Date	Model Version
Landscape-habitat conditions			
Influence of wood on gravel retention (wood effect)	The model includes measurements of riffle areas from aerial photography, which reflect loss of gravel (especially in bedrock areas). We have added a multiplier for increased spawning gravel area with increased wood loading (currently set at 1.3 for historical wood loading in large rivers).	Added 2018	V3
Add new multipliers for large river channel length	Same multipliers used by EDT, developed by NSD and NOAA.	August 2018	V3
Add new multipliers for floodplain side channel length	Same multipliers used by EDT, developed by NSD and NOAA.	August 2018	V3
Channel incision has caused significant losses to channel length. Wood placement should address changes in alluvial channels, off channel habitats, instream overwinter habitat.	This is correct, and is modeled as restoring either channel length or floodplain reconnection.	No change needed	NA
Should food supplies be considered? Large woody debris for example provides cover and significant amounts of terrestrial insects	The model directly relates wood loading to productivity (density independent survival) and capacity based on empirical relationships between wood and survival (e.g., Quinn and Peterson 1996), which presumably encompasses effects of habitat structure, cover, and food.	No change needed	NA
Review pool-riffle data sources being used; consider use of wood-pool relationships from outside Chehalis system.	We checked this and the values from local data are in fact similar to our other studies for moderate slope and steep channels, with the exception of the agriculture value which is higher than in other places. Our field tour suggests that those channels do in fact have high percentages of slow water habitat. These areas tend to have high temperature currently, so fish densities and productivity tend to be lower under current conditions as a function of temperature. We did not adjust pool areas.	No change needed	NA
Add temperature reduction with floodplain reconnection	Added up to 1°C temperature reduction with floodplain reconnection, based on Seedang et al. 2008.	Sept 2019	V12

Table L1 (cont.). Record of NOAA Model revisions during 2018 and 2019.

Question or suggested change	Revision or response	Date	Model Version
Habitat-LCM functions – Coho Salmon			
Change winter capacity estimate for coho salmon	Per Lestelle recommendation: Changed winter densities to match those of Nickelson 1998.	July 2018	V3
Summer temperature influence on coho summer rearing capacity in addition to survival	We use the same function as for survival changes.	August 2018	V3
Add fry colonization stage for coho salmon	Stage added August 2018.	August 2018	V3
Wood effect on large river spawning capacity (all species)	Multiplier currently set at 1.3 for high wood loading. In small streams, the model already addressed influence of wood on spawner density in small streams using empirical estimates of spawners/km under low and high wood loading.	Oct 2018	V3
Wood effect on egg-to-fry survival (all species)	Multiplier currently set at 1 for high wood loading, pending input from SRT on potential values.	Oct 2018	V3
Coho migration patterns	We have added movement of coho salmon between sub-basins and the main stem prior to summer rearing and again prior to winter rearing. This results in migrant fry occupying the mainstem prior to summer rearing (there are virtually no spawners in the mainstem, so few or no natal mainstem fry), and migrant parr occupying the mainstem prior to winter rearing.	Added 2018	V3
Check backwater densities for coho salmon in winter	No change. We reviewed these and kept the existing densities with approval of Larry Lestelle. We use a value of 0.06 fish/m^2 in large river backwaters based on data from Beamer and Henderson (1998), and reanalyzed in Beechie et al. (2005a). These data are only from large river reaches (bankfull width >50 m). We apply these data only to large river reaches in the Chehalis to maintain consistency between the source data and sites to which they are applied. Nickelson (1998) found densities in backwaters to be ~0.25 to 0.5 fish/m^2, although it is not clear how large the streams were at the sample sites (n = 16, streams ranged from 2nd to 6th order according to the paper). Backwater pools in small streams in our Chehalis model have an assigned winter coho density of 0.4 fish/m^2, which is more similar to that of Nickelson (1998).	No change	V4

Table L1 (cont.). Record of NOAA Model revisions during 2018 and 2019.

Question or suggested change	Revision or response	Date	Model Version
Should barriers also affect productivity of pre-spawning adults in addition to spawning capacity above barriers?	We brought this question to the SRT and it was agreed to include an effect on productivity. Subsequently revised to use average productivity across reaches weighted by egg capacity.	Feb 2019	V4
Add current beaver pond area	We used beaver dam counts and surveyed stream lengths from Wampler et al. 1993 and got an average density of 0.6 ponds/km. For comparison, our historical estimate is 6 ponds/km. We noted that 8% of the stream length already has ponds and marshes in our data set, so reduced the current pond density number to 0.55 ponds/km to avoid "double counting" of pond habitat.	Feb 2019	V5
Weight subbasin egg to fry survival by egg capacity	Completed	March 2019	V5
Limit downstream distribution of spring migrants	Spring redistribution now moves fish down to the mainstem, and they stay in the reach they enter. In the fall redistribution, fish that reach the mainstem are distributed evenly through all mainstem reaches downstream of the entry point.	March 2019	V5
Should more mainstem habitat be accessible in current condition?	Yes, revised using the EDT current condition polygon to select floodplain habitat polygons that are accessible.	March 2019	V7
Assign mainstem temperature to adjacent floodplain polygons	Done	March 2019	V7
Should pre-spawn productivity vary spatially as a function of land use?	Percent impervious area is calculated by flow accumulation on the NLCD impervious area dataset, and then translated to prespawn mortality using an empirical function based on data in Feist et al. (2011).	March 2019	V8
Flood scour effect on egg-to-fry survival	Added stochastic effect of floods on scour.	May 2018	V9
Add future development for coho prespawn mortality	Future development is now in the model. It affects future prespawn productivity for coho in the ASRP scenarios.	May 2018	V9

Table L1 (cont.). Record of NOAA Model revisions during 2018 and 2019.

Question or suggested change	Revision or response	Date	Model Version
Why is movement restricted to downstream areas? Isn't there also some movement upstream?	Movement within subbasins or within the mainstem can be upstream or downstream or lateral (where floodplain habitat exists). We model migration of juvenile coho from sub-basins downstream to the mainstem, and fish are allowed to access floodplain habitats adjacent to reaches they occupy. We do not have movement of fish upstream, except as needed to access floodplain habitats.	No change	NA
Why didn't we use riffle area change in small streams as a function of wood to modify spawning capacity, rather than using redd densities from Montgomery et al. (1999)?	No change. Our observations in the Chehalis basin indicate that a large percentage of riffle areas in small streams are plane-bed channels with little or no spawning gravel (i.e., riffle area ≠ spawning gravel area). Montgomery et al. (1999) showed that spawning density is inversely related to pool spacing, and that both coho and Chinook rarely spawn in plane-bed reaches (little or no wood). The relationship between spawner density and pool spacing suggests that there is more suitable spawning gravel and/or more suitable holding habitat in proximity to spawning habitat where there are more pools. Pool spacing is known to be a function of wood abundance (Montgomery et al. 1995, Beechie and Sibley 1997), so we assume that high spawning density at high pool abundance is driven by wood-induced habitat changes. That is, we assume that spawning capacity is highest at high wood abundance, and we use the empirical changes in redd density with changing wood abundance to estimate changes in spawning capacity.	No change	NA
Revise coho densities and productivities	Updated to 95th percentile of densities for large river. Updated productivities to high end of the range for most data sets.	January 2020	V13
Habitat-LCM functions – Spring and Fall Chinook			
Temperature effect on pre-spawn survival for spring Chinook	Function revised in Nov 2018 after import of new temperature data. Now use temperature function from Honea at al. (2009).	Nov 2018	V3
Investigate why the subbasin above the dam site has high spawner abundance relative to observations	We found a gap in the temperature data that led to high prespawn productivity estimates. Correcting the data error produces a more realistic spawner abundance for the upper Chehalis above the dam site.	March 2019	V7

Table L1 (cont.). Record of NOAA Model revisions during 2018 and 2019.

Question or suggested change	Revision or response	Date	Model Version
Spring Chinook migration patterns	We model density dependent movement of fry from subbasins to the main stem during natal subbasin fry colonization, and also density dependent movement of fry to the delta-bay during mainstem fry colonization. This results in three groups of outmigrants, natal basin sub-yearlings, mainstem sub-yearlings, and fry migrants. Fish that move to the mainstem are evenly distributed to segments downstream of the entry point, so that a migrant group experiences the average condition of all segments in the mainstem.	April 2019	V8
Investigate why the Skookumchuck subbasin has low spawner abundance relative to observations	Percent fines appeared to be too high, leading to lower than expected egg-to-fry survival. Adjusted road density above the dam (set to zero) and Skookumchuck now has highest N_{eq}.	April 2019	V8
Add temperature effect on late outmigrants	Currently we apply a June 7DADM mortality to 10% of subyearling migrants (not to fry migrants, which we assume are out of the basin by June). Need to discuss what percentage is most appropriate.	April 2019	V8
Add temperature effect on late outmigrants	Added function to have the June 7-DADM temperature affect subyearling migrants (not fry migrants since we assume they are in the bay by June). 10% of subyearling migrants are affected (need data).	May 2019	V8
Revised temperature effect on late outmigrants	Revised function to have the June 1-21 temperature affect subyearling migrants. Revised percent of subyearling migrants affected to 45% based on trap data in Winkowski and Zimmerman (2019).	May 2019	V9
Vary percent spring/fall by sub-basin	Newaukum, Skookumchuck and South Fork Chehalis are the only three subbasins which have escapement totals for both spring and fall chinook in the WDFW data set. For these subbasins we used the percent of total chinook escapement accounted for by both spring and fall Chinook. For the other Subbasins, excluding the mainstem, we used the mean of the Newaukum, Skookumchuck and South Fork Chehalis percentages (spr = 0.3454204, fall = 0.6545796). For mainstem subbasins, we used the original .81/.19 split assuming fall fry are coming in from other subbasins.	May 2019	V9
Change date range for prespawning temperature (spring Chinook)	We now use the average daily maximum temperature from Jul 1-Aug 31 instead of Jul 1 –Sept 30 (per recommendation of the LCM work group).	May 2019	V9

258

Table L1 (cont.). Record of NOAA Model revisions during 2018 and 2019.

Question or suggested change	Revision or response	Date	Model Version
Adjust bay survival	Adjusted bay survival so SAR and fry:parr ratios are within observed range.	May 2019	V9
Explain clearly how movement and rearing timing is structured in the model	Created new figures to illustrate density dependent movement and relationship between tributary and mainstem spawning and rearing.	April 2019	NA
Find solution to the 'flipping' problem	We discovered that the flipping problem was created by moving fish from a density-independent stage to a density-dependent stage. The problem was solved by keeping fry migrants and subyearling migrants separate in the model, with fry experiencing only density-independent rearing productivity.	June 2019	V10
Modify solution to flipping problem to include migration Chinook downstream	First iteration was to model redistribution of all Chinook fry stayers after week 1 throughout the natal subbasin and all downstream reaches (similar to the code as used in the fall redistribution for coho).	June 2019	V10
Give all Chinook parr 12weeks total rearing in the basin	We no longer have shorter rearing periods for juveniles rearing closer to the delta.	July 2019	V11
Remove negative Cn values	When P_n is < 1, the back-calculated Cn value is negative. Revised so that both values are 0 in output tables.	July 2019	V11
Revise Chinook SAR	Revised Chinook SAR based on analysis of Queets R data. Bay survival for subyearlings back-calculated so that Chinook SAR is 2% for subyearling outmigrants. Then bay survival back-calculated for fry migrants so that percent fry migrants in spring Chinook adult returns is ~5%.	July 2019	V12
Revise Spring Chinook prespawn temperature function	Revised the Spring Chinook prespawn temperature function using the published relationship in Bowerman et al. (2018), which is based on observations in the Willamette River using the 7DADM temperature.	October 2019	V13
Revise Chinook densities and productivities	Updated to 95th percentile of densities for large river. Updated productivities to high end of the range for most data sets.	January 2020	V13

Table L1 (cont.). Record of NOAA Model revisions during 2018 and 2019.

Question or suggested change	Revision or response	Date	Model Version
Habitat-LCM functions – Steelhead			
Revised year 2 juvenile rearing densities (second summer and winter in freshwater)	Based on WDFW data from Newaukum River.	Feb 2019	V4
Add effect of temperature on steelhead rearing	Estimated temperature effect uses functional relationship based on Bear et al. (2007).	Feb 2019	V4
Additional revision of densities and productivities	Densities and productivities were updated again and documented in the LCM report.	June 2019	V10
Revise percentage of steelhead outmigrants leaving basin at age- 1	Revised so that percent of age 1 outmigrants in returning adults is ~10%.	July 2019	V11
Code steelhead movement	Revised steelhead movement code so that no age-1 fish are leaving subbasins with drainage area > 450 km^2 (Satsop, Humptulips, Wynoochee), 20% of age-1 fish leave subbasins with drainage area between 150-450 km^2 (Newaukum, Black, S. F. Chehalis, Skookumchuck, Wishkah, Hoquiam, Cloquallum, Chehalis Above Crim, Upper Skookumchuck, Elk Creek), and 50% of age-1 fish leave subbasins with drainage area < 150 km^2 (smaller than Elk Creek).	July 2019	V12
Revise smolt ages to include age-3 smolts	Revised based on data in adult returns indicating the most smolts surviving the ocean were age-2 and age-3.	November 2019	V13
Revise small stream spawning densities	Revised to estimate spawning gravel area first, and then estimate spawning capacity based on redd area.	November 2019	V13
Update fecundity	Fecundity updated to 5,400 for maiden spawners and 8,000 for respawners.	November 2019	V13
Update summer rearing productivities	Updated summer rearing productivities from 0.27 value for age-0 summer rearing to 0.47, and to 0.7 for age-1+ and age-2+ summer rearing.	November 2019	V13
Add steelhead rearing densities to the center of large river reaches	For steelhead, we use a mid-channel density of 5% of the natural bank density for the first year, and 28% of the natural bank density for the second and third year (based on Skagit R data from Beamer and Henderson 1998). For C hinook, we apply a density of 0.3% of the natural bank density. For coho and chum we apply a density of 0 to the mid-channel area.	December 2019	V13

Table L1 (cont.). Record of NOAA Model revisions during 2018 and 2019.

Question or suggested change	Revision or response	Date	Model Version
Revise steelhead densities for multiple habitat types	Update densities: 1st summer, Mid-channel = 0.016, SS riffle = 0.48, SC riffle = 0.48. 1st winter, Mid-channel = 0.011, SS riffle = 0.09, SC riffle = 0.09. 2nd and 3rd summer, Mid-channel = 0.017, SS riffle = 0.06, SC riffle = 0.06. 2nd and 3rd winter, Mid-channel = 0.011, SS riffle = stays the same, SC riffle = stays the same.	December 2019	V13
Revise use of wood multipliers for steelhead rearing	We decided that the 1.67 would be applied only to the first winter. All summers and the 2nd and 3rd winter will get the large river wood multiplier for steelhead (since we had no data for 2nd and 3rd winter).	December 2019	V13
Revise steelhead densities and productivities	Updated to 95th percentile of densities for large river and mean + one standard error for small streams. Updated productivities to high end of the range for most data sets.	January 2020	V13
Habitat-LCM functions – Chum Salmon			
Add chum model	Chum model added, and calibrated to recent run size observations.	November 2019	V13
ASRP restoration Scenarios			
Code in selection of restoration GSUs and actions	Developed code for selecting restoration GSUs and specific actions within GSUs per the ASRP restoration action spreadsheet developed for the ASRP (approved by the SRT).	June 2019	V10
Revise modeling of all restoration actions	Reviewed ASRP scenario assumptions with Merri Martz, Neala Kendall, and Emelie McKain, and revised restoration modeling code accordingly.	June 2019	V10
Bug fix for GSUs designated primary creek only	The model was not applying wood and floodplain restoration in subbasins designated as primary creek only; the bug fix solves the problem.	July 2019	V11
Model outputs			
Consideration should be given to reporting resilience, the productivity-determined capacity to sustain mortality as a result of changes in productivity and capacity.	We've added calculation of intrinsic productivity and cumulative capacity by fitting a Beverton-Holt curve to model outputs of recruits per spawner.	Late 2018	V3
Consider output of results at subbasin scale	We now output results at both EDR and subbasin scales.	Late 2018	V3

Table L1 (cont.). Record of NOAA Model revisions during 2018 and 2019.

Question or suggested change	Revision or response	Date	Model Version
For P_n, try plotting the stock-recruit curve rather than estimating via weighting	This was completed, but result is not satisfactory for Chinook because the R-S outputs take the hockey form that drives the number of fry migrants.	Late 2018	V3
For P_n, estimate slope at origin only	Revised approach estimates slope at the origin of the R-S curve by running one fish through one generation in the model. The number produced is P_n.	June 2019	V10
Update sensitivity analysis	Revised outputs to include all freshwater life stages.	Sept 2019	V12
Remove recent run size from output plots	Removed.	November 2019	V13
Quasi-extinction thresholds	These will not be included at this time.	NA	NA
Hatchery effects	These will not be included.	NA	NA